Evaluating the effects of dengue virus and iminosugar treatment on cellular unfolded protein response and redox homeostasis



Nilanka Perera

St Peter's College

University of Oxford

Michaelmas term 2019

Submitted for the degree of Doctor of Philosophy

Evaluating the effects of dengue virus and iminosugar treatment on cellular unfolded protein response and redox homeostasis

Dengue virus (DENV) infections cause significant morbidity worldwide. The complex host-viral interactions affecting viral replication and the host immune response result in variable disease severity in affected individuals. This thesis focuses on two such host responses implicated in DENV pathogenesis; unfolded protein response (UPR) and oxidative stress. DENV preferentially activated the proviral and pro-inflammatory IRE1α-XBP1 arm of the UPR in monocyte-derived macrophages *in vitro*. Investigation of redox homeostasis revealed induction of reactive oxygen species and increase in total antioxidant capacity in DENV-infected macrophages. Further evaluation of peripheral blood mononuclear cells during early DENV-infection revealed increased XBP1s and reduced DDIT3 and HSPA5 transcripts in affected individuals who later developed severe dengue disease. Proteomics performed on the cell lysates revealed upregulation of the IRE1-mediated UPR pathway and differential expression of several protein markers in individuals who developed severe disease compared to non-severe disease potentially providing a foundation to develop markers of DENV disease severity.

Iminosugars are broad spectrum antivirals targeting host ER glucosidases causing antiviral effects against DENV. The effects of iminosugars have not previously been studied in DENV-infected dendritic cells. The percentage of infected cells and secretion of DENV were reduced in dendritic cells treated with three DNJ-derived iminosugars in a dose-dependent manner. The specific infectivity was reduced at iminosugar doses exceeding 3.16 μM which inhibited α-glucosidase I. Furthermore, DENV-induced TNFα levels were reduced with iminosugar treatment. Evaluation of the UPR in DENV-infected and 2THO-DNJ treated macrophages revealed a reduction in XBP1s levels compared to untreated cells and an increase in EDEM1

and ERDJ4 transcripts. However, the UPR was not required for the antiviral or anti-inflammatory effects of the iminosugar 2THO-DNJ. ROS levels and antioxidant capacity were also reduced in DENV-infected macrophages following treatment with 2THO-DNJ and MON-DNJ.

Overall, this thesis describes the role of the UPR and oxidative stress in DENV infection and the effect of iminosugars on these host responses.

Acknowledgements

The three years in the Zitzmann lab was one of the most memorable periods in my life with many wonderful people leaving footprints and memories. There are many to thank for making me feel at home and welcoming me into this lab.

Nicole has been a great supervisor and a mentor. It wouldn't have been possible to achieve this much without her continuous encouragement and confidence. I am ever grateful for her for letting me divulge into areas of my interest and having faith in all the work. I am also thankful to Jo for teaching basic techniques and introducing me to the world of virology and having patience throughout. Transition from a clinical environment into a laboratory setup is never easy. It is worse having to learn everything from scratch but still make science work during the limited time available. Thank you Steve and Michelle for making that transition smooth for me. The two proteomic kings, Abhinav and Bevin have been the perfect office mates; giving advice when I ran into trouble and also for doing all the mass spec work for Chapter 6 with such enthusiasm. Basement crew: Snezana, JL and Dom were always available to chat through, talk science and share tears. Thank you guys for being such wonderful friends. All good times spent in the lab and outside work with the Johann, Mario and Beatrice will be remembered forever. A special note for a friend who shared the difficult and good times and made the gloomy Oxford a cheerful place: Juli. Thank you for being the great friend you are.

I would also like to thank Raymond Dwek, who has been an inspiring figure to look up to. All science chats over coffee will be fondly remembered.

A DPhil in Oxford would not have been a reality if not for the Commonwealth funding, St Peter's college for accepting me and everyone else in Sri Lanka who helped me in achieving this. I fondly remember all my teachers in school and university who shaped me.

It would not be complete unless I acknowledge another awesome mentor, Neelika. Thank you again for getting me to do a PhD, introducing to Nicole and all the help given throughout.

Family has always been my strength. My parents have been guiding and supporting me silently. None of this would have been possible without their inspiration. Thank you dear Amma and Thatta: I am forever grateful for all you have done for me. And my brothers for all the good times together and for giving a lending hand whenever needed.

Finally, Dil, who has shared my life for the past 15 years and supported throughout my crazy and sometimes ambitious decisions. Thank you for having faith during my journey. You were one of the few people who believed that I will pull this through. Thank you for sharing ups and downs of my life!

Statement of authorship

The experiments described in this thesis were performed by myself of Nicole Zitzmann's laboratory, Oxford Glycobiology Institute except in the following circumstances.

The free oligosaccharide (FOS) analysis of iminosugar treated and DENV-infected monocyte-derived dendritic cells described in chapter 4, Figure 4.7 (page 63) was performed by Juliane Brun of Zitzmann laboratory as acknowledged.

The tandem mass tag (TMT) mass spectrometry described in chapter 6 and acknowledged in chapter 3.10.7 (page 45) was performed by Dr Abhinav kumar of Zitzmann laboratory. Samples were collected, prepared and processed by myself for this experiment.

Contents

List of abbreviations xii

List of figures xv

List of tables xviii

Chapter I

Introduction

1.1 Dengue virus infection 2
1.1.1. Dengue disease burden 2
1.1.2 Vaccines 2
1.1.3 Dengue disease pathogenesis 3

1.2 Unfolded protein response 7
1.2.1 The UPR and its pathways of activation 8
1.2.2 The role of the UPR in facilitating viral replication in DENV infection 11
1.2.3 The role of the UPR in DENV-induced inflammation 13

1.3 Reactive oxygen species (ROS) in DENV infection 18

1.4 Iminosugars 20

Chapter II

Research questions and aims of the thesis

2.1 Research questions 28
2.2 Aims of the thesis 29

Chapter III

Materials and Methods

3.1 Cell culture and virus 31
3.1.1. Peripheral blood mononuclear cell (PBMC) separation 31
3.1.2 Differentiation of monocytes to MDMΦ and DC 31
3.1.3 Cell lines and culture 32
3.1.4 Growth of DENV stocks 33
3.1.5 In vitro DENV infection and drug treatment 33

3.2 Viral quantification 33
3.2.1 Plaque assays 33
3.2.2 Viral RNA extraction and quantification 35
3.2.3 Immunofluorescence to detect DENV envelope protein 36
3.2.4 Flow cytometry for DENV NS3 37

3.3 Iminosugars, UPR inhibitors and cytotoxicity assay 37
3.3.1 Iminosugar stocks 37

3.3.2 UPR inhibitors 38
3.3.3 Cytotoxicity assay 38

3.4 Phenotyping MDMΦ and DCs by flow cytometry 39

3.5 Functional TNFα and IFNα measurement 39
3.6 Western blotting 40
3.6.1 Western blot 40
3.6.2 Antibodies 41

3.7 Reactive oxygen species and antioxidant levels 42
3.7.1 Detection of reactive oxygen species (ROS) by flow cytometry 42
3.7.2 Antioxidant capacity measurement 42

3.8 Measurement of cellular mRNA levels by qRT-PCR 43

3.9 Free oligosaccharide analysis (FOS) 43

3.10 Fieldwork experiments 44
3.10.1 Recruitment of study participants and ethical considerations 44
3.10.2 Isolation of PBMCs 45
3.10.3 Generating cDNA from PBMCs for qRT-PCR 46
3.10.4 Quantification of the UPR transcripts by qRT-PCR 46
3.10.5 Measurement of viral load in serum 47
3.10.6 Dengue rapid NS1 detection and measurement of DENV-specific IgM antibodies in serum 48
3.10.7 Proteomics analysis of cell lysates 49

Chapter IV

The antiviral effect of iminosugars in primary monocyte-derived dendritic cells

4.1 Introduction 53

4.2 Results: 56
4.2.1 Phenotype of differentiated Mo-DCs 56
4.2.2. Immature DCs are susceptible to in vitro DENV infection 56
4.2.3 Iminosugars have minimal cytotoxicity in primary imDCs 57
4.2.4 DNJ-derived iminosugar treatment reduced the percentage of infection of imDCs, secretion of DENV and reduced specific infectivity of the secreted virus 60
4.2.5 DNJ-based iminosugars reduce DENV-induced functional TNα levels in a dose-dependent manner 63
4.2.6. ER α-glucosidase I inhibition by the DNJ-derived iminosugars potentiates the anti-viral effect and reduces DENV-induced TNFα levels 63

4.3 Discussion 66

Chapter V

The effect of 2THO-DNJ on DENV-induced unfolded protein response

5.1 Introduction 71

5.2 Results 75
5.2.1 The unfolded protein response in DENV-infected macrophages 75
5.2.2. The Effect of 2THO-DNJ treatment on DENV-induced UPR 82
5.2.3. The effect of chemical inhibition of PERK and IRE1α pathways on 2THO-DNJ induced antiviral effects 89
5.2.4 The effect of PERK and IRE1 pathway inhibition on TNFα and IFNα levels in the presence of 2THO-DNJ 90
5.2.5. 2THO-DNJ treatment produces a different UPR signature in DENV-infected THP-1 cells compared to primary macrophages 92

5.3 Discussion 95

Chapter VI

Identification of novel markers of dengue disease severity in a patient cohort

6.1 Introduction 104

6.2 Results 108
6.2.1. Phase I: Identification of UPR markers by qRT-PCR in PBMCs of dengue fever patients 114
6.2.2. Phase II: Identification of protein markers of disease severity in the PBMCs of dengue patients 127

6.3 Discussion
6.3.1 UPR chaperones identified as markers of severe dengue disease 133
6.3.2 Non-UPR proteins differentially expressed in DHF 136

Chapter VII

The effect of iminosugar treatment on DENV-induced oxidative stress and antioxidant levels

7.1 Introduction 142

7.2 Results 143

7.3 Discussion 146

Chapter VIII

Conclusions & Future work

8.1 Overview 149

8.2 Limitations 152

8.2 Future work 154

Appendix 1 156

Appendix 2 158

Appendix 3 161

Appendix 4 184

References 186

List of abbreviations

2THO-DNJ	N-8′-(2″-tetrahydrofuranyl)-octyl-deoxynojirimycin
ADE	Antibody-dependent enhancement
αGluI	α-glucosidase I
αGluII	α-glucosidase II
ARE	Antioxidant response element
ATF4	Activated transcription factor 4
ATF6	Activating transcription factor 6
ATG5	Autophagy related 5
CD 14	Cluster of differentiation 14
CHOP	CCAAT-enhancer-binding protein homologous protein
DC SIGN	Dendritic cell-specific intercellular adhesion molecule-3-grabbing non-integrin
DENV	Dengue virus
DGJ	1-deoxygalactonojirimycin
DHF	Dengue haemorrhagic fever
DNJ	1-deoxynorjirimycin
EDEM1	ER degradation-enhancing alpha-mannosidase-like protein 1
eIF2α	Eukaryotic translation initiation factor 2α
ER	Endoplasmic reticulum
ERAD	ER associated degradation
ERDJ4	ER-localized DNAJ4
GADD34	Growth arrest and DNA damage-inducible protein
GCN2	General control nonderepressible-2-kinase
GM-CSF	Granulocyte colony stimulating factor

GRP78	78 KD glucose regulated-protein
GSK3β	Glycogen synthase kinase 3β
HCV	Hepatitis C virus
IFIT1	Interferon-induced protein with tetratricopeptide repeats 1
IFN	Interferon
IL-10	Interleukin-10
IL-1β	Interleukin 1β
IL-6	Interleukin-6
iPSC	Induced pleuripotent stem cells
IRE1	Inositol requiring kinase 1
IRF3	Interferon regulatory factor 3
JEV	Japanese encephalitis virus
JNK	c-Jun N-terminal kinase
LPS	Lipopolysaccharide
MAP kinases	Mitogen activated protein kinases
MDMΦ	Monocyte-derived macrophages
Mo-DCs	Monocyte-derived dendritic cells
*N*B-DNJ	*N*-butyl-deoxynojirimycin
NF-κB	Nuclear factor kappa B
NLRP3	Nod-like receptor protein 3
NOX-2	NADPH oxidase 2
Nrf2	Nuclear factor erythroid 2-related factor 2
PBMC	Peripheral blood mononuclear cell
PCV	Packed cell volume
PDI	Protein disulphide isomerase
PERK	PKR-like ER kinase

PKR	Protein kinase R
qRT-PCR	Quantitative reverse transcription polymerase chain reaction
RANTES	Regulated on Activation, Normal T cell Expressed and Secreted
RIDD	Regulated IRE1 dependent-decay pathway
RIG-I	Retinoic acid inducible gene-I
ROS	Reactive oxygen species
SOCS3	Suppressors of cytokine signalling 3
TAC	Total antioxidant capacity
TLR	Toll like receptors
TMT	Tandem mass tag
TNFα	Tumour necrosis factor α
TRAIL	TNF-related apoptosis inducing ligand
WNV	West Nile virus
XBP1	X-box binding protein 1

List of figures

1.1	Activation of UPR pathways in response to ER stress and manipulation of UPR by DENV	10
1.2	The role of UPR in potentiating the inflammatory cascade induced by viral infection.	14
1.3	Iminosugar derivatives of Castanospermine, DNJ and DGJ	21
1.4	*N*-glycoprotein processing in the ER	24
4.1	An illustration of the iminosugars used for the experiments	57
4.2	Phenotyping data of monocyte-derived macrophages and dendritic cells.	58
4.3	Susceptibility to DENV infection and the TNFα response in imDCs	59
4.4	Percentage infection of DENV-infected imDCs following iminosugar treatment.	60
4.5	Secretion of DENV and the specific infectivity of secreted virus from iminosugar treated imDCs	62
4.6	Functional TNF-α levels in imDCs treated with iminosugars	64
4.7	FOS levels in DENV-infected and iminosugar treated imDCs	65
5.1	Activation of UPR pathways in response to ER stress.	74
5.2	Activation of the PERK-eIF2α-ATF4 pathway in primary macrophages	77
5.3	Activation of IRE1α-XBP1 in DENV-infected primary macrophages	79
5.4	The effect of chemical inhibition of UPR arms on DENV secretion and secretion of TNFα and IFNα.	81
5.5	The effect of 2THO-DNJ treatment on PERK-eIF2α-ATF4 pathway	83
5.6	The effect of 2THO-DNJ treatment on the IRE1α-XBP1 pathway in DENV infection	85
5.7	The effect of 2THO-DNJ treatment on EDEM1 and ERDJ4 gene expression in DENV infection	86

5.8	The effect of αGluII and αGluI inhibition by 2THO-DNJ on IRE1α-XBP1 pathway activation	88
5.9	The effect of 2THO-DNJ treatment on Tm and DTT-induced XBP1 splicing	88
5.10	The effect of chemical inhibition of PERK and IRE1α pathways on 2THO-DNJ induced antiviral activity	89
5.11	The effect of chemical inhibition of PERK and IRE1 pathways on 2THO-DNJ mediated TNFα and IFNα.	91
5.12	The effect of chemical inhibition of PERK and IRE1 pathways and 2THO-DNJ on LPS-induced TNFα.	92
5.13	The effect of 2THO-DNJ on IRE1α-XBP1 pathway activation in THP-1 macrophages	94
6.1	A schematic presentation of Phase I of the study	111
6.2	A schematic presentation of Phase II of the study	113
6.3	Expression levels of XBP1s and ATF4 transcripts in PBMCs of patients with dengue fever	117
6.4	Expression levels of DDIT3 and HSPA5 transcripts in PBMCs of patients with dengue fever	118
6.5	Serum viral load measured by qRT-PCR in patients with dengue fever	119
6.6	Correlation of UPR transcripts in PBMCs with the platelet count on admission.	121
6.7	Correlation of UPR transcripts in PBMCs with the lowest platelet count	122
6.8	Correlation of the UPR transcripts in PBMCs with the white cell count (WCC) on admission	123
6.9	Correlation of the UPR transcripts in PBMCs with the lowest white cell count	124
6.10	Correlation of UPR transcripts in PBMCs with the PCV on admission.	125
6.11	Correlation of the UPR transcripts in PBMCs with the highest PCV	126
6.12	Pathways differentially regulated in dengue infected PBMCs compared to healthy controls.	129
6.13	Pathways differentially regulated in severe dengue patient PBMCs compared to non-severe dengue PBMCs	132

6.14	Expression of SAMHD1 and PRG2 proteins in the PBMC lysates	138
7.1	Reactive oxygen species and total antioxidant capacity in DENV-infected monocyte-derived macrophages	143
7.2	Reactive oxygen species in DENV-infected and iminosugar-treated monocyte-derived macrophages	144
7.3	TAC in DENV-infected and iminosugar-treated monocyte-derived macrophages	145

List of tables

3.1	The constituents of RIPA buffer	40
3.2	The constituents of transfer buffer	41
3.3	The constituents of stripping buffer	41
3.4	Taqman primers and probes used for the quantification of cellular mRNA	43
3.5	Components of the reverse transcription reaction	46
3.6	The primers/probes used for the qRT-PCR experiments	47
3.7	DENV primers used for quantifying viral load by qRT-PCR	47
3.8	DENV probes used in the qRT-PCR reaction to identify the serotype and quantify viral load	48
4.1	Antiviral activity and cytotoxicity of iminosugars in imDCs and MDMΦ	61
4.2	Selectivity index of iminosugars in imDCs and MDMΦ	61
6.1	The baseline characteristics and investigation results in patients recruited to the Phase I study	115
6.2	Diagnosis of dengue fever in patients recruited to the study	116
6.3	The top 20 differentially expressed proteins in dengue-infected PBMCs	123
6.4	Top 20 differentially regulated proteins in dengue haemorrhagic fever (DHF) compared to dengue fever (DF)	126

I

Introduction

1.1 Dengue virus infection

1.1.1. Dengue disease burden

Dengue virus (DENV) causes a reemerging arthropod borne viral infection transmitted by the *Aedes* mosquito. Approximately one third of the global population is at risk of infection from this *Flavivirus* which poses a significant health burden [3]. Disease estimates vary and a report published in 2013 by Bhatt et al. suggested that there are approximately 390 million infections occurring per year with 96 million having apparent manifestations [4]. More recent studies estimate 50-100 million apparent dengue infections occurring per year [5, 6]. From nine countries being affected in 1970, DENV has spread across continents to be endemic in more than 100 countries [7]. In addition to an increase in the number of cases worldwide, DENV has resulted in explosive outbreaks in endemic countries causing significant morbidity and mortality. DENV serotypes 1-4 cause symptoms ranging from asymptomatic illness to severe haemorrhagic fever and death. Severe dengue disease is characterized by increased vascular permeability leading to hypovolaemic shock and multi-organ failure [8].

1.1.2 Vaccines

There have been significant advances in vaccine development against DENV, but the process has been slow and difficult [9]. One of the challenges for the development of an effective vaccine has been the difficulty in inducing effective protective immunity to all four antigenically distinct DENV serotypes [9]. In addition, the complex immune response to dengue infection and the necessity to avoid cross-reactive antibody mediated disease enhancement has posed further challenges. The first DENV vaccine that become available was the CYD-TDV (Dengvaxia by Sanofi Pasteur) which was recommended by the World Health Organization (WHO) to be used in areas with seroprevalence >70%[10]. The overall efficacy of the vaccine for symptomatic disease was 60%. Efficacy was 66% for those 9 years or older

and 45% for those less than 9 years of age [9, 11]. A major concern was the increase in hospitalization of children aged 2-5 years of age following vaccination compared to unvaccinated children [12]. This has caused concern over the use of the CYD-TDV in most countries. Further vaccines such as the Takeda tetravalent dengue vaccine have completed Phase II and recruitment is currently ongoing for Phase III in several Latin American and South Asian countries [13]. An attenuated tetravalent lyophilized vaccine by the United States National Institutes of Health and National Institute of Allergy and Infectious Diseases has completed Phase I and II and is currently undergoing a Phase III evaluation [9]. Although development of a DENV vaccine has been slow, designing a DENV specific antiviral has been even more challenging, and none exists to date.

1.1.3 Dengue disease pathogenesis

Viruses are obligate intracellular parasites and depend on the host cellular machinery for assembly of their virions [14]. The DENV virion comprises of a spherical structure containing a single strand positive sense RNA genome of approximately 11 kb in length and an endoplasmic reticulum (ER) derived host membrane envelope in which are embedded virally encoded envelope glycoproteins [3]. DENV enters target cells such as monocytes, dendritic cells (DC) and macrophages by receptor-mediated endocytosis. Although a specific receptor has not been identified yet, many candidate receptors have been implicated in DENV entry including dendritic cell-specific intercellular adhesion molecule-3-grabbing non-integrin (DC-SIGN; CD209), heparan sulfate, lipopolysaccharide receptor CD14, heat shock proteins 70 and 90, GRP78 and mannose receptor [15, 16]. The viral RNA which has a single open reading frame is translated into a single polyprotein which is further cleaved co- and post-translationally in the ER by viral and host proteases into 3 structural (core, C; pre-membrane, prM; and envelope, E) and 7 non-structural proteins (NS1, NS2A, NS2B, NS3, NS4A, NS4B and NS5) [17, 18]. DENV replicates in virus-induced organelle-like membrane structures derived from the ER referred to as replication factories [14]. The immature virions are

transported via the *trans*-Golgi network which results in the cleavage of prM into M by the host cell protease furin to produce mature virions. These virions are secreted from the cell via exocytosis [18]. The mature virions have a smooth marble-like structure while immature virions have a spiky appearance [19]. This furin-mediated cleavage is mostly incomplete resulting in a mixed population of secreted mature and immature virions to be secreted. The degree of maturity displayed by DENV virions also determines the type of cell that can be infected due to the variable expression of receptors on the cell surfaces and the variable ability of certain antibodies to bind to immature versus mature viral envelopes [19].

DENV infections have variable manifestations and disease severity. Pathogenesis of severe manifestations is still poorly understood and the variable presentation is presumed to be due to complex host-viral interactions modulating viral replication and the host immune response. The clinical course can be divided into three phases; febrile phase, critical phase and convalescence. The early febrile phase denotes the viraemic phase during which patients develop fever, myalgia and other symptoms of a viral illness commonly associated with thrombocytopaenia. The majority of infected people will go into convalescence with resolution of fever (defervescence) and improvement of clinical and laboratory parameters. A minority of the infected population develop severe disease characterized by increased vascular permeability leading to accumulation of fluid in the pleural and peritoneal cavities and intravascular fluid depletion causing shock, multi-organ failure, coagulopathy and death. These severe manifestations occur when the fever subsides and coincides with an excessive upregulation of cytokines, sometimes referred to as cytokine storm. This transient phase of fluid leakage is known as the critical phase which lasts approximately 48 hours before reaching recovery.

The WHO (World Health Organization) published guidelines on case detection and

classification of dengue initially in 1975 based on data of Thai children. This was revised in 1988 and 1997 [20]. Patients with suspected dengue disease was classified into dengue fever (DF), dengue haemorrhagic fever (DHF) and dengue shock syndrome (DSS). DHF was defined as fever with haemorrhagic tendency, thrombocytopaenia and evidence of plasma leakage due to increased vascular permeability. Patients who developed weak and rapid pulse, narrow pulse pressure, hypotension, cold clammy skin and restlessness were grouped in to DSS. Based on the largest prospective study, the dengue and control (DENCO) study, WHO proposed the most recent classification of dengue fever patients in to severe dengue (SD), dengue with warning signs and dengue without warning signs [21]. Severe dengue is defined as patients with any one of the following; (a) severe plasma leakage with shock and/or fluid accumulation with respiratory distress, (b) severe bleeding, (c) severe organ impairment [21]. There has been many discussions and criticism about each classification. Some experts believe that the use of several clinical manifestations as criteria to identify severe dengue disease divert the attention from vascular leakage which is the main cause for mortality inn dengue (reviewed in [22]). As such, the classification of DF and DHF based on the 1997 criteria will be adopted in this thesis.

The exact mechanism of endothelial dysfunction in severe DENV is not clearly understood. However, many mediators such as cytokines (tumour necrosis factor α [TNFα], interleukin-1β [IL-1β], IL-6, IL-10), mast cell products (vascular endothelial growth factor, tryptase, chymase, histamine), lipid mediators (platelet activating factor, phospholipase-A2) and angiopoietin 1/2 have been implicated in affecting the endothelial barrier (reviewed in [23]). In addition, immune factors, viral factors and host responses influence the outcome of DENV infection [24].

Prior exposure to DENV infection has been found to sometimes increase disease severity if

patients are subsequently infected by a different serotype. This worse outcome from a secondary or subsequent infection is hypothesized to be at least partly due to antibody-dependent enhancement (ADE) and/or T-cell mediated original antigenic sin. ADE initially proposed by Halstead *et al* after observing severe dengue manifestations in infants exposed to maternal antibodies, suggests that idiosyncratic Fc receptor signalling results in an increased infected cell mass and a heightened inflammatory response [25]. Cross-reactive heterologous antibodies produced in response to a previously encountered serotype different to the one currently causing the infection, fail to neutralize the DENV antigens but facilitate uptake of the virus via Fc receptors leading to a worse outcome in secondary dengue infection [24-26]. However, it is also important to note that the antibody: virus ratio plays a role in determining ADE and not all patients with secondary infection will develop severe dengue manifestations [26]. This is attributed to the biology of the Fc receptor and a narrow range of antibody concentrations predisposing to severe dengue disease. Also, some patients are known to produce IgG antibodies with high affinity for Fc receptor facilitating viral uptake [27]. Finally, an increased viral uptake leads to increased production of the vasoactive substances mentioned above and caspase-dependent apoptosis of mast cells [28]. The enhancement of virus-mediated effects in secondary infection is also partly attributed to T-cells. The role of T-cells in severe dengue manifestations has been studied extensively [29-31]. It is proposed that CD4+ and CD8+ memory T-cells from a previous infection proliferate rapidly following a secondary dengue infection increasing the production of inflammatory mediators. Cross-reactive memory T-cells which expand during the heterologous secondary infection have poor affinity for the second DENV serotype and do not have the ability to eliminate the virus as efficiently as high affinity naïve T cells [28]. Therefore, virus elimination is affected while increasing the production of inflammatory mediators [25, 26, 30]. DENV NS3 and NS5 have been implicated in generating T-cell responses. In addition, DENV NS1 antigen [23] as well as antibodies against NS1 have been associated with severe disease manifestations

[32]. It is also worth noting that primary infections can lead to severe disease, and that not all factors contributing to dengue pathogenesis are known. The ability to distinguish between individuals likely to develop severe disease from non-severe disease during early DENV infection would greatly help clinicians to triage patients. In addition, it would reduce the healthcare burden by preventing admissions of patients who otherwise can be managed in an outpatient setting.

Host responses such as the UPR, lipid droplets, autophagy, ubiquitin-proteasome system and oxidative stress also play a role in dengue pathogenesis [17, 18, 33, 34]. Overall, it is clear that virus-host interactions play a crucial role in determining the outcome from DENV infection. This thesis focuses on two such host responses during DENV infection that are less well studied, namely, the unfolded protein response (UPR) and the redox response.

1.2 Unfolded protein response

DENV utilizes the host cellular machinery, in particular the ER, for the production of viral proteins [35]. ER stress caused by DENV infection mounts a pro cell-survival cellular reaction known as the UPR [17, 36, 37]. This cascade of events, important not just in viral but also bacterial and non-pathogenic adverse conditions, maintains cell survival and facilitates eradication of the virus [38]. The UPR has complex interactions with the cellular autophagy machinery, apoptosis mediators, innate immunity and pro-inflammatory reactions [33, 39]. To overcome this hostile host cell environment, DENV selectively modifies these host processes to enhance viral replication and has the ability to evade host innate immunity. As such, host-viral interactions play an important role in deciding the fate of the infection in affected individuals. Our understanding of the highly complex intersection of and interplay between the UPR, induction and effector mechanisms of innate immunity and autophagy with the DENV life cycle in human host cells is continuously evolving. It is important to explore the role of the UPR and its multiple cellular effects during DENV infection for a better

understanding of the pathophysiology following infection, and to explore potential early markers of subsequent disease severity.

1.2.1 The UPR and its pathways of activation

The UPR is a host cellular reaction which counteracts and alleviates ER stress. Viral or bacterial infections, changes in cellular redox status, changes in calcium homeostasis and nutrient starvation all cause accumulation of unfolded and misfolded proteins which exceed the capacity of ER protein handling [38, 40]. This results in ER stress which leads to activation of the UPR for cell survival. Once activated, the ensuing cascade of events results in attenuated mRNA translation which limits protein load in the ER, an increase in the ER protein folding capacity and ER associated degradation (ERAD) of misfolded proteins. However, increased synthesis of ER chaperones BiP/GRP78, GRP94, protein disulphide isomerase (PDI) and CCAAT-enhancer-binding protein homologous protein (CHOP/*GADD135*) amidst inhibition of global protein production, highlights the specificity of this process [36]. Furthermore, activation of the UPR potentiates the host antiviral response creating an inflammatory milieu [35, 38]. Inability of these mechanisms to restore cellular homeostasis results in apoptosis.

The UPR initiation molecules, inositol requiring kinase 1 (IRE1 or *ERN1*), PKR-like ER kinase (PERK or *EIF2AK3*) and activating transcription factor 6 (ATF6) reside in the ER membrane and are maintained in an inactive state by the folding chaperone immunoglobulin heavy-chain binding protein (BiP/GRP78) [38] (Figure 1.1). BiP, a member of the Hsp70 chaperone family is an inhibitory regulator of the three ER-membrane sensors and is bound to the lumenal domains of these molecules. When ER stress occurs, BiP is competitively sequestered by misfolded proteins in the ER and released from the initiation molecules. This triggers homodimerisation and phosphorylation of IRE1 and PERK with subsequent activation of the downstream signaling cascades [38]. Other potential mechanisms of activation are direct

sensing of misfolded proteins by IRE1 [41] and dissociation of the stable BiP-ATF6 complex by an undefined mechanism [42].

IRE1 has a stress sensing ER-lumenal N-terminus and an effector C-terminal tail (protein kinase domain and RNase domain) in the cytoplasm [36, 43]. Activation of IRE1 cleaves X-box binding protein 1 (XBP1) mRNA [36, 44, 45], activates the regulated IRE1 dependent-decay pathway (RIDD) and promotes expansion of the ER membrane [45]. Activation of c-Jun N-terminal kinase (JNK) and the effect of IRE1 on apoptosis is shown in Figure 1A [38, 46-48]. PERK phosphorylates eIF2α, which inhibits global protein translation except that of the activated transcription factor 4 (ATF4) reading frame (Figure 1.1b).

ATF4 is a transcription factor which regulates amino acid metabolism, oxidative stress and modulates expression of ER chaperones and foldases [45]. Phosphorylation and activation of eIF2α by protein kinase R (PKR), general control nonderepressible-2-kinase (GCN2) and heme-regulated eIF2α kinase are alternative pathways of eIF2α activation. Activated ATF6 is cleaved to produce the activated transcription factor ATF6p50 which translocates to the nucleus to regulate the expression of genes in the ERAD pathway [49]. Overlap of the branches of the UPR is demonstrated by activation of XBP1 by ATF6, enhancing the pro-survival factors and upregulation of ER chaperones [50]. Both ATF6 and IRE1-XBP1s (spliced XBP1) cascades independently and in combination help to relieve ER protein burden by enhancing ERAD. Low level ER stress is presumed to be handled by the ATF6 pathway, medium to high levels by both ATF6 and IRE1-XBP1 and extremely high levels by multiple rounds of activation of the XBP1 cycle [50]. However, prolonged ER stress results in activation of the cell death pathways.

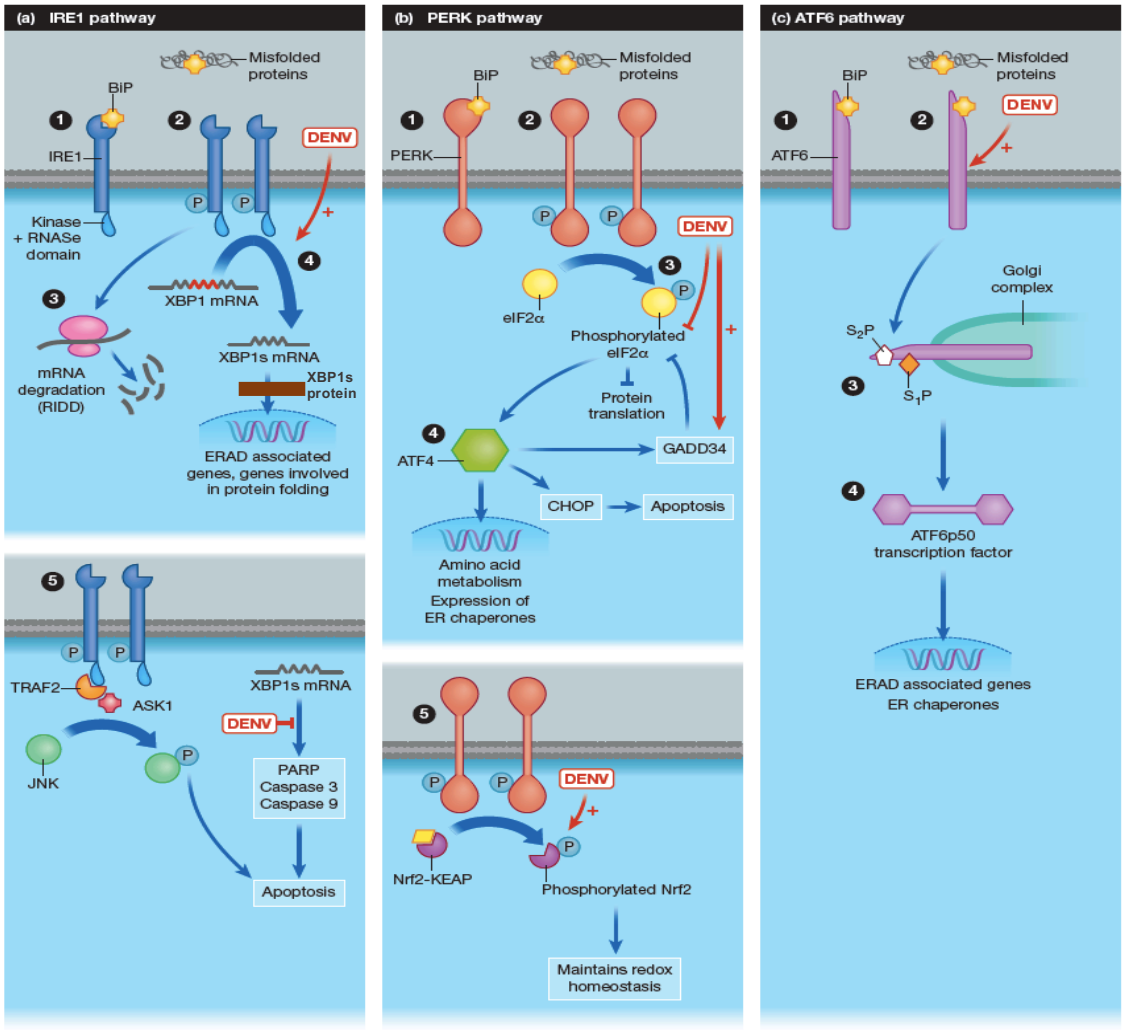

Figure 1.1. Activation of UPR pathways in response to ER stress and manipulation of UPR by DENV. (A) IRE1 pathway; (1) IRE1 is kept in an inactive state by BiP. (2) Dissociation of BiP results in dimerization and trans-autophosphorylation (by the kinase domain) of IRE1 which activates the RNase domain. (3) RIDD: The RNAse domain causes degradation of several mRNA and microRNA (e.g. mir17). (4) The IRE1 RNase segment cleaves XBP1mRNA transcript to produce the multifunctional transcriptional factor, XBP1s. XBP1s activates ERAD associated genes to degrade misfolded proteins and genes promoting protein folding. DENV induces activation of the IRE1-XBP1 pathway. (5) IRE1 recruits TNF receptor associated factor 2 (TRAF2) and apoptosis signal-regulating kinase-1(ASK1) which activates JNK to induce apoptosis. XBP1s activates caspase 3, 9 and poly(ADP-ribose) polymerase PARP to promote apoptosis if ER stress persists. This activation is blocked by DENV. **(B) PERK pathway; (**1) PERK is kept in an inactive state by BiP. (2) Once dissociated from BiP, PERK dimerizes and autophosphorylates to activate its kinase activity. (3) Activated PERK catalyzes phosphorylation of eukaryotic translation initiation factor 2α (eIF2α) which inhibits protein translation. DENV transiently activates and then inhibits eIF2α activation to overcome protein translation attenuation. (4) ATF4 induced by eIF2α, induces activation of C/EBP homologous protein (CHOP) and growth arrest and DNA damage inducible 34 (GADD34) which mediates apoptosis. GADD34 dephosphorylates eIF2α to maintain a negative feedback. DENV promotes GADD34 induced eIF2α inhibition. (5) Phosphorylation of nuclear factor (erythroid-derived 2 factor)-related factor (Nrf2) by PERK dissociates it from the cytoskeletal anchor, Kelch-like ECH-associated protein (KEAP1) to translocate into the nucleus. Nrf2 induces genes with an antioxidant response element (ARE) to maintain redox homeostasis. DENV induces phosphorylation and nuclear translocation of Nrf2. **(C) ATF6 pathway;** (1) ATF6 is maintained in an inactive state by BiP. (2) Dissociation of BiP from ATF6 uncovers the Golgi localization signal. DENV induces activation of ATF6. (3) The N-terminus of ATF6 is cleaved by site 1 and site 2 proteases (S1P and S2P). (4) Cleaved and activated transcription factor ATF6p50 translocates to the nucleus to induce genes associated with ERAD and ER chaperones. Arrows in the diagram represent positive effects while blocked lines represent inhibition. Effects of DENV on the UPR are shown in red.

1.2.2. The role of the UPR in facilitating viral replication in DENV infection

Increased production of viral proteins in dengue infection leads to accumulation of unfolded and misfolded proteins in the ER [35]. This results in ER stress and thus activation of the UPR as a host response. The ensuing cascade of events decribed above relieves ER stress, determines cell survival and mounts an inflammatory response to eliminate the virus. DENV, similar to many other viruses, manipulates the host UPR pathways to enhance its survival . This section describes how DENV facilitates viral protein production and inhibits apoptosis to ensure enhanced viral replication.

Dengue infection induces all three arms of the UPR [46, 51, 52]. Activation of this host response is observed in immune [52] and non-immune cells [46, 51, 53] infected with DENV. Activation of the UPR is time dependent [46] and also virus strain and serotype specific [51]. The PERK arm is activated early in DENV infection followed by IRE1-XBP1 in mid-infection and ATF6 later in the infection [46]. Serotype specific differences in UPR activation are seen in dengue infected A549 cells and similarly in ADE infection of THP-1 monocytic cells [51, 54]. DENV 1 and 3 serotypes cause a stronger induction of BiP, phosphorylation of eIF2α, and higher growth arrest and DNA damage-inducible protein (GADD34) and CHOP mRNA levels than DENV 1 and 4 [54]. In addition, ADE infection of monocytes using different strains of DENV 2 clinical isolates (Indonesian outbreak) showed higher levels of BiP, CHOP and GADD34 levels with strains causing severe disease [54]. Fast replicating viral strains demonstrated higher ER stress. This suggests a possible role for UPR in DENV pathogenesis and severity.

Activation of the PERK arm is antiviral due to attenuation of protein translation. Pena *et al.* demonstrated that DENV transiently activated PERK-dependent eIF2α phosphorylation at 6 hours post-infection which then reversed with DENV causing suppression of eIF2α activation therafter. DENV ensures continous production of its proteins and facilitates virion production

by rapidly reversing PERK activation (Figure 1B). This is presumed to be due to an increased expression of GADD34, which acts in a feedback loop to inhibit further phosphorylation of eIF2α [55]. Pharmacological activation of the PERK-arm (via nuclear transporter 4-HPR) or removing the GADD34 mediated dephosphorylation of eIF2α (using Salubrinal) result in significant inhibition of DENV viral replication [35, 56]. It is apparent that DENV modulates the PERK pathway to overcome translation attenuation for survival, and pharmacological upregulation of this process results in enhanced antiviral activity.

Infection with DENV activates the IRE1-XBP1 pathway and a subset of XBP1-activated genes involved in ERAD which helps to alleviate ER stress [53]. XBP1 pathway activation is induced by ER associated DENV glycoproteins (prM, E, NS1) and smaller hydrophobic ER anchored proteins (NS2A, NS2B, NS4B). In addition, DENV is able to inhibit apoptosis mediators downstream of IRE1-XBP1 (Figure 1A) which results in increased cell survival and enhanced viral replication [46]. Inhibition of XBP1 using siRNA, in conjunction with DENV infection, resulted in reduced ER expansion, increased cytopathic effects of the virus and increased levels of the apoptosis marker pro-caspase 3 [53]. This is further evidence that activation of the IRE1-XBP1 pathway in dengue infection protects the cells against apoptosis, and alleviates ER stress contributing to DENV pathogenesis. In a study by Huang *et al*., Japanese encephalitis virus (JEV) virus secretion and cellular viral RNA load was not changed in BHK-21 cells by inhibiting the RNase activity of IRE1α [57]. The JEV infection activated this pathway, inducing pro-apoptotic markers CHOP and caspase-3 and splicing of XBP1, which were inhibited by both RNase and JNK inhibitors [58]. Interestingly, investigation of the IRE1α-XBP1 pathway in hepatitis C virus (HCV) infection by Tardif *et al*. revealed that XBP1s trans-activating activity was suppressed by the virus despite an increased splicing of XBP1, resulting in inhibition of transcription of ER degradation-enhancing alpha-mannosidase-like protein 1 (EDEM1). The reduced EDEM-mediated ERAD of the viral proteins was essential for the

expression of HCV viral proteins and persistence in hepatocytes [59]. A similar effect was seen during West Nile virus (WNV) infection of Vero cells. XBP1s was increased 10-fold by the virus infection but the increase in EDEM1 transcripts was observed to be only 3-fold from untreated cells [60]. Interestingly, transfection of the cells with GFP and viral non-structural protein fusion constructs revealed that WNV NS4A and NS4B proteins were responsible for the XBP1 activation which did not increase EDEM1 transcripts in these cells [60]. However, in a study by Saeed et al., HCV infection of 293T cells resulted in upregulation of EDEM1 transcripts and increased degradation of HCV envelope proteins due to ubiquitylation [61]. Knockdown of EDEM by siRNA resulted in increased HCV production. Given the contradictory data observed in studies, further data is needed to better understand the role of EDEM1 in DENV pathogenesis.

1.2.3. The role of the UPR in DENV induced inflammation

Viral infections induce a potent inflammatory response in infected immune cells. A complex network activates type 1 interferons (IFN) and other antiviral mediators to eradicate the offending virus and limit viral disseminaton [62]. Pro-inflammatory mediators such as TNFα, IL-6, IL-8 and RANTES (Regulated on Activation, Normal T cell Expressed and Secreted) recruit other cell types, induce oxidative stress and contribute to inflammation [63]. In addition, several cell death pathways are activated in the infected cells to limit infection. Viral components are detected by toll like receptors (TLR) and cytoplasmic helicases [63-65]. The ensuing cascade of events [66, 67] is shown schematically in Figure 1.2.

DENV, similar to many viruses, activates signaling pathways leading to production of antiviral mediators. These pro-inflammatory cytokines and chemokines aid eradication of DENV. Evasion of these defenses by DENV results in enhanced viral replication. Simultaneously, overexpression of these mediators can cause harm to the host [63, 68] and

possibly contribute to the cytokine storm which is thought to be associated with increased vascular permeability seen in severe dengue disease. The UPR is an important mediator of virus induced inflammatory signaling [39]. However, the role of the UPR in DENV mediated inflammation is under-investigated. The literature supporting this area is complicated to interpret due to the different cell systems used and the pathways investigated. I bring together what is currently understood to summarize for the field how interactions between DENV and the UPR can affect, with both pro- and antiviral outcomes, innate immune pathways such as IFNα/β, NF-κB, IRF3 and TNF-α.

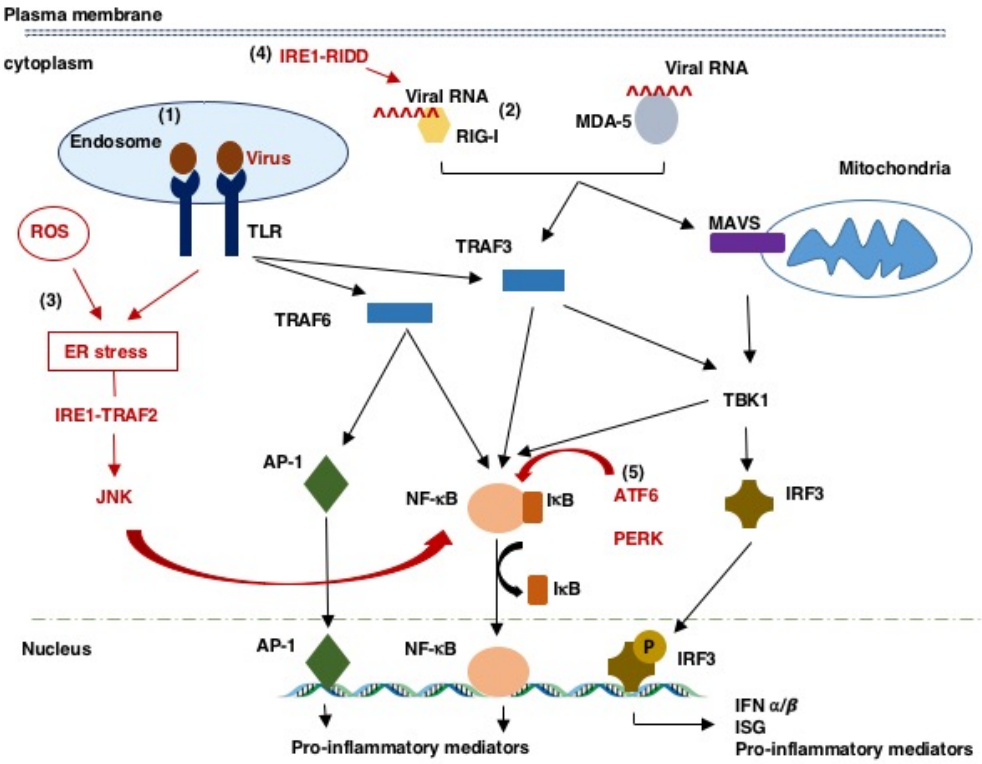

Figure 1.2. The role of UPR in potentiating the inflammatory cascade induced by viral infection. (1) Viral RNA is recognized by toll-like receptors (TLR) following endosomal acidification, leading to enhanced TNF receptor associated factor (TRAF) 3 and 6 signalling. Activation and nuclear translocation of activator protein-1(AP-1), nuclear factor kappa B (NF-kB) and interferon regulatory factor 3 (IRF3), by TRAF3 and TRAF6 result in production of interferon stimulated genes (ISG), IFN-α/$\boldsymbol{\beta}$ and pro-inflammatory mediators. (2) Cytoplasmic dsRNA is detected by retinoic acid-inducible gene I (RIG-I) and melanoma differentiation-associated protein 5 (MDA-5) which act synergistically with TLR to generate a type 1 IFN response. RIG-I triggers mitochondrial antiviral signaling protein (MAVS) and TRAF3 activation of TANK-binding kinase 1 (TBK1). TBK1 phosphorylates IRF3 and NF-kB to activate downstream inflammatory pathways. Secreted IFN-α/$\boldsymbol{\beta}$ acts on the infected cells in an autocrine fashion and on adjacent uninfected cells in a paracrine fashion to activate antiviral responses and resist infection. (3) ER stress induced by reactive oxygen species (ROS), TLR signalling and misfolded proteins in the ER, activates the IRE1 pathway to phosphorylate JNK. JNK activates NF-kB. (4) The IRE1-RIDD pathway activates RIG-I signalling and the downstream activation of inflammatory mediators. (5) The PERK pathway and ATF6 activate NF-kB to induce pro-inflammatory mediators. The effect of UPR mediators on the inflammatory cascade is shown in red.

In addition and prior to viral protein production in the ER, viral infection also induces ER stress via TLR signaling. This results in activation of the IRE1 pathway leading to splicing of XBP1 (Figure 1A). XBP1s is crucial in inducing the production of TNFα, interferon-β (IFNβ) and IL-6 in macrophages following TLR stimulation [69, 70]. Macrophages deficient in XBP1 have an impaired cytokine response to viral infection [69]. In addition, IRE1 is able to increase IL-1β directly by inducing glycogen synthase kinase 3β (GSK3β) [70]. The IRE1-TRAF2 complex activates JNK (Figure 1A) and recruits IKK to induce NF-κB activation [71](Figure 1.2). Translational activation of retinoic acid inducible gene-I (RIG-I) by the IRE1-RIDD pathway further activates NF-κB induced inflammation [72](Figure 1.2). Activation of the PERK pathway and the subsequent attenuation of protein translation increases the ratio of NF-κB/IκB resulting in increased NF-κB activity [73]. Both JNK and NF-κB lead to induction of cytokines and inflammatory mediators. ER stress potentiates induction of TNFα, IL-1, IL-6 and chemokines such as CXCL1 and CXCL2. ATF6 also plays a role in activating NF-κB [49](Figure 1.2).

Activation of the UPR by VER-155008 (VER) treatment in DENV infection activates innate immune factors such as PKR, IRF3, IL-1β and NF-κB [35]. VER causes pharmacological inhibition of GRP78 (BiP) and the enhanced innate immune activation achieved by upregulation of IRE1, PERK and ATF6 results in increased DENV clearance. This suggests that the UPR can potentiate innate immune responses in DENV to facilitate viral clearance.

A critical antiviral mechanism against DENV is the type 1 IFN response. Patients with severe disease have lower serum IFNα levels and suppression of ISG during early DENV infection, which highlights the role of type 1 IFN in dengue pathogenesis [74-76]. Similar to many viruses, DENV has developed strategies to evade IFN activation, signaling and effector mechanisms. DENV inhibits IFN induction and its signaling pathways to facilitate its replication and survival [66]. Both TLR induced inflammatory pathways and RIG-I/MDA-5 induced pathways are inhibited by DENV in an attempt to reduce type 1 IFN and cytokine production [62, 67, 77]. Autophagy is a process by which cytoplasmic materials and organelles are sequestered in a double membrane vesicle and degraded [78]. Activation of autophagy maintains cellular homeostasis in addition to preventing cell death during streses such as starvation and viral infection. It is known that DENV-induced autophagy could help infected cells avoid apoptosis and thus maintain viral replication [79]. One host response exploited by DENV to evade innate immunity is the UPR-autophagy pathway. The role of UPR-autophagy in suppressing innate immunity is well studied in infection with HCV, a *Hepacivirus* belonging to *Flaviviridae* family. Activation of the UPR is required for upregulating autophagy in HCV infected cells and this activation significantly reduces the HCV pathogen-associated molecular pattern (PAMP)-mediated cytoplasmic RIG-I signaling. RIG-I activation leads to phosphorylation, dimerization and nuclear translocation of IRF-3 (Figure 1.2) which induces IFNβ promoter activation. Ke *et al.* demonstrated that UPR-autophagy mediators (CHOP, ATG5, LC3B, IRE1, PERK, ATF6) negatively regulated HCV PAMP-mediated IFNβ mRNA

levels and IFNβ promoter activation. Interference with the UPR-autophagy pathway by stable gene knockdown (ATG5 and CHOP gene silencing) in human hepatoma cells led to increased IFNβ promoter activation and IFNβ mRNA levels in HCV. Furthermore, IFN mediated downstream signaling detected by IFNα stimulated interferon stimulated gene response element (ISRE) promoter activity and interferon-induced protein with tetratricopeptide repeats 1 (IFIT1/ISG56) expression was upregulated in ATG5 and CHOP gene knockdown cells in HCV infection [80]. In the same study, the authors showed that the negative effect of UPR-autophagy on innate immune reponses is not limited to HCV but extended to DENV. IFNβ promoter activity and ISG56 expression was enhanced in cells following ATG5 and CHOP gene silencing and in *Atg5-/-* mouse embryonic fibroblasts in DENV infection [81]. It is evident that UPR-autophagy plays a crucial role in inhibiting type 1 IFN activation and its downstream signaling cascades in DENV infection. Further investigation of the role of UPR-autophagy pathway in DENV mediated inflammation is useful as repression of this cascade is an attractive antiviral therapeutic option.

DENV infection induces production of pro-inflammatory mediators, such as TNFα, implicated in causing severe disease [82, 83]. Activation of the PERK arm of the UPR in DENV infection was recently shown to upregulate nuclear factor erythroid 2-related factor 2 (Nrf2)-CLEC5A mediated TNFα production [84]. Pharmacological inhibition of Nrf2 *in vivo* results in reduced TNFα production in the brain of DENV-infected mice and a better clinical outcome.

The UPR has complex interactions with the anti-inflammatory and pro-inflammatory cascades during DENV infection. Manipulation of induction of UPR pathways during DENV infection shows that they can mediate supression and induction of innate immune and inflammatory pathways, affecting both viral replication and immunopathology. Further

investigation of these interactions would lead to a better understanding of DENV pathogenesis and help explore antiviral therapeutic targets.

1.3 Reactive Oxygen Species (ROS) in DENV infection

Another important cellular response implicated in DENV pathogenesis is oxidative stress. DENV infection, similar to other viruses, induces free radical formation in infected cells [65]. This is attributed to an interaction of viral proteins with mitochondrial components during infection [63]. Olagnier *et al*. showed that accumulation of intracellular ROS in DENV-infected monocyte-derived dendritic cells (Mo-DCs) was NADPH oxidase 2 (NOX)-dependent and these reactive species were required to produce an effective innate antiviral and pro-inflammatory signaling in the cell [65]. The production of ROS is likely to contribute to viral clearance by activating inflammatory cascades and these results suggest that ROS are important second messengers during DENV-infection. While ROS-mediated inflammasome activation is helpful to clear the virus, excessive oxidative stress could pose detrimental effects due to oxidative damage to lipid membranes, proteins and DNA, ultimately leading to apoptosis. Counteracting antioxidant defense mechanisms help to mitigate ROS-induced damage by clearing free radicals or reducing production of ROS. The main antioxidants are glutathione peroxidase, catalase, superoxide dismutase and thioredoxin reductase [85]. Nrf2 is an important antioxidant mediator in the cell which once activated, binds to the antioxidant response element (ARE) in the nucleus to induce transcripts necessary to combat the ROS challenge [65]. As such, the redox homeostasis plays an important role in determining the outcome from DENV-infection. This is reflected in the unfavourable balance of oxidative stress and compensatory antioxidant mechanisms seen in severe dengue disease patients. Lipid peroxidation products and other markers of oxidative stress are higher in patients with severe dengue disease than non-severe dengue [86-88]. In addition, total antioxidant capacity was found to be lower in patients with severe DENV compared to non-severe DENV [89]

suggesting the important role of redox status in dengue disease pathogenesis.

There is crosstalk between UPR and cellular oxidative stress pathways during viral infections. Viral infections induce NOX2 production, a super-oxide generating enzyme which forms ROS. This oxidative stress causes accumulation of misfolded and unfolded proteins resulting in ER stress and activation of the UPR. ROS are essential for XBP1 induced cytokine production [49]. Concomitant activation of TLR and UPR pathways has the potential to amplify the cytokine response and determine cell survival during viral infections. Therefore, the effect of DENV and iminosugar treatment on redox status will be evaluated in detail in this thesis.

Cellular ROS are predominantly generated by mitochondrial respiration [90]. In addition to the mitochondrial electron transport chain, NADPH oxidases, the cytochrome P450 system, xanthine oxidases, cyclooxygenases and lipoxygenases also contribute to ROS generation [85, 90]. The superoxide anion ($O_2^{\bullet -}$) generated in the mitochondria is converted to H_2O_2 by superoxide dismutase and H_2O_2 diffuses out into the cytoplasm to be further converted to the hydroxyl radical ($OH^{\bullet}$) in the presence of iron. The $O_2^{\bullet -}$ also generates other reactive metabolites such as peroxynitrile (ONOO), hypochlorous acid (HOCl) and singlet oxygen ($^1O_2$) and all these reactive products are collectively known as ROS [85].

DENV-infection activates a ROS-dependent pro-inflammatory cascade in liver cells [91] and Mo-DCs [65]. ROS production in DENV-infected dendritic cells is NOX-dependent and previous studies suggest that the innate immune response and the pro-inflammatory responses depend on the redox status of the cell [65]. The antiviral responses (STAT1, IRF3, IFIT1, IκBα, RIG-1) and the inflammatory cytokines and chemokines were all reduced by inhibiting NOX activity [65]. ROS production by monocytes in response to Nod-like receptor protein 3 (NLRP3) activators mediates ROS-dependent transcriptional activation of NF-κB

and activated protein-1 (AP-1) via mitogen activated protein kinases (MAP-kinases) leading to pro-inflammatory mediator production (reviewed in [90]). In addition, production of ROS in endothelial cells by DENV-infection was worsened by circulating TNFα which contributed to severe haemorrhage in a DENV mouse model [92].

1.4 Iminosugars

Iminosugars are small molecule monosaccharide mimetics which possess a nitrogen atom in place of the endocyclic oxygen [1]. They were initially discovered as natural products of plants and bacteria [93]. The lead natural occurring glucose mimetic iminosugars are castanospermine and 1-deoxynorjirimycin (DNJ) (Figure 1.3). Iminosugars have the ability to inhibit many hydrolytic enzymes in the cell including α-glucosidases important for *N*-linked glycosylation, glucosyltransferases and Golgi α-mannosidases (Indoli-zidine D-swainsonine) in a cell [94-96] Despite being known for many years, the advancement of these first generation iminosugars to the clinic has been hampered by inadequate potency and reduced selectivity [94]. However, two drugs which have progressed to clinical use are *N*-hydroxyethyl DNJ (Miglitol) approved since 1996 for Type 2 diabetes mellitus [97] and *N*-butyl-deoxynojirimycin (Miglustat, *N*B-DNJ) for type 1 Gauchers's disease and Niemann-Pick C disease [98].

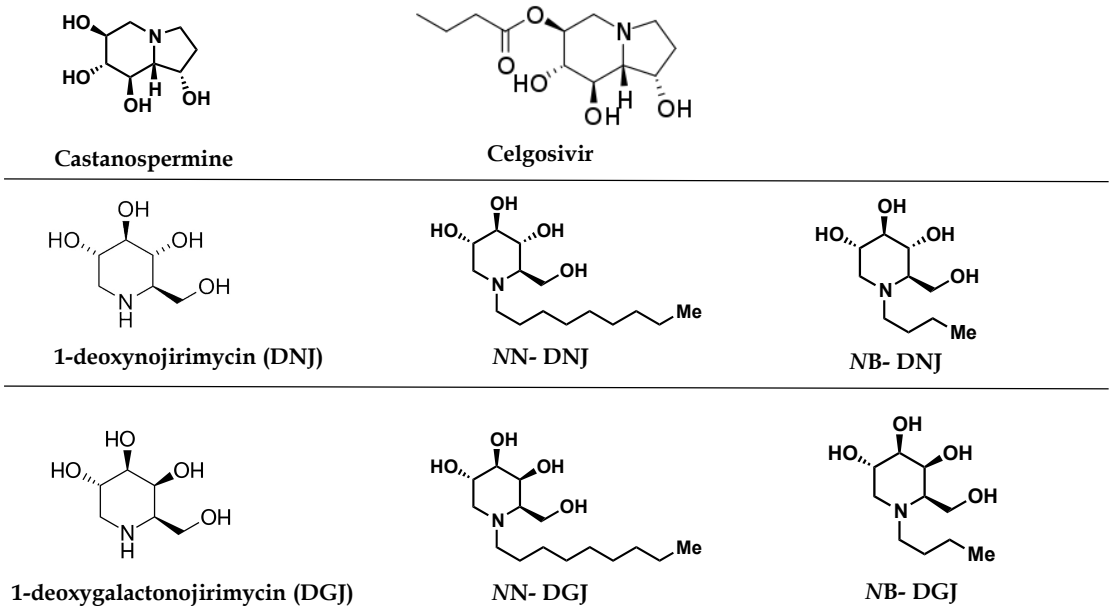

Figure 1.3: Iminosugar derivatives of castanospermine, DNJ and DGJ. This figure show Celgosivir derived from castanospermine, *N*N-DNJ and *N*B-DNJ derived from DNJ and the iminosugars with a galactose stereochemistry (*N*N-DGJ and *N*B-DGJ derived from deoxygalactonojirimycin, DGJ). Adapted from Sayce et al. [1].

In addition to these uses, iminosugars have been tested for their broad-spectrum antiviral effects. Enveloped viruses rely on the protein folding machinery of the ER for proper folding and formation of the three dimensional structure of their glycoproteins, which is necessary for their function and/or secretion [99]. Preassembled 14-sugar residue N-glycan precursors are added to newly forming polypeptides in the ER [100, 101]. The terminal glucose residues of these N-glycans are then sequentially trimmed by the host ER α-glucosidases I and II to allow the mono-glucosylated glycoproteins to interact with the ER folding chaperones calnexin and calreticulin (Figure 1.3). The effect of iminosugar treatment on the host protein folding machinery which is required for morphogenesis of enveloped viruses, results in antiviral activity against a broad spectrum of viruses and also avoids development of virus induced resistance. Antiviral activity of iminosugars has been demonstrated against DENV [1, 101-103], Japanese encephalitis virus (JEV) [101], hepatitis B [104, 105], hepatitis C [106],

influenza virus [107] and human immunodeficiency virus (HIV) [108] amongst others. Both bicyclic iminosugars (castanospermine and Celgosivir) and monocyclic iminosugars (DNJ and its derivatives) inhibit α-glucosidases in the ER [94]. In addition, certain iminosugars such as long alkylchain (with four or more C atoms in their sidechains) the DNJ- and DGJ-derivatives inhibit ceramide-specific glucosyltransferase preventing accumulation of glycosphingolipids in lysosomal storage diseases [95]. The effect on glucosidases was found to be responsible for the antiviral effect against DENV [1]. Iminosugars with galactose stereochemistry such as *N*N-DGJ and *N*B-DGJ which affect glycolipid processing but do not inhibit the glucosidases, do not elicit antiviral activity against DENV [1]. Therefore, these DGJ-derivatives provide a good control for the experiments evaluating the mechanism of iminosugar antiviral activity.

DENV has four glycoproteins: envelope (E), pre-membrane (prM), NS1 and NS4B [1]. Correct folding of at least some of these glycoproteins requires interaction with the membrane bound calnexin and soluble calreticulin [96]. ER α-glucosidase inhibitors such as iminosugars prevent formation of the mono-glucosylated form of these glycoproteins, thereby preventing their interaction with calnexin/calreticulin. Iminosugar treatment will therefore lead to the misfolding of those glycoproteins which rely on interaction with calnexin/calreticulin to fold properly. Accumulation of misfolded proteins in the ER activates ER associated degradation (ERAD) pathways which divert these proteins to the cytosol to be hydrolyzed by the proteasome [99]. Previous data show that treatment with DNJ-derived iminosugars reduced DENV virus secretion from primary macrophages [1, 102, 109]. In addition, treatment with iminosugars was shown to increase survival of DENV-infected mice [102, 109, 110]. These initially promising results paved the way for Celgosivir and M*O*N-DNJ to enter clinical trials [111, 112]. The phase 1b trial of Celgosivir in DENV infection showed that the drug was safe and well-tolerated but a significant difference was not seen in the virological log reduction or

fever in the treatment group compared to placebo group [111]. Treatment group received 400 mg Celgosivir loading followed by 200 mg twice daily for a total of 9 doses. The authors did not find significant differences in the haematological parameters or time to serum NS1 clearance. Close scrutiny of the trial reveals many pitfalls. Firstly, the end points studied were related to viraemia and symptoms that occur during the febrile phase. The hallmark of severe DENV is fluid leakage and any antiviral treatment should be able to prevent or minimize patients developing these severe manifestations. CELADEN trial was not designed to investigate patients with severe dengue. Secondly, the number of recruited participants were only 50 (24 received Celgosivir and 26 received placebo). The power has been calculated to have a mean virological log reduction of 0.7 in the treatment group. This number would not have given adequate power to investigate the patients developing severe dengue. At the same time, numbers needed to identify a difference in patients developing fluid leakage would be massive. This is not feasible in such a trial and pose problems in recruitment of such a large number. The multiple ascending dose phase 1b clinical trial of iminosugar MON-DNJ to evaluate the safety profile and pharmacokinetics was started in 2016 with 5 cohorts of healthy subjects receiving the drug from 30mg TID onwards. This study was terminated early following the first cohort of subjects as the product development was halted due to business reasons [112]. One serious adverse event was noted (haemorrhoids).

Development of an antiviral for dengue is difficult. Patients present to healthcare facilities once they are symptomatic and after development of fever. The peak viraemia would coincide with these symptoms and the immunological manifestations would occur later. To try and treat patients early on the disease is difficult and treatment after symptoms manifest in them might be too late to tackle the viraemia. A disease modifying drug designed to alter the immunological response or vascular permeability would be an ideal candidate in this situation.

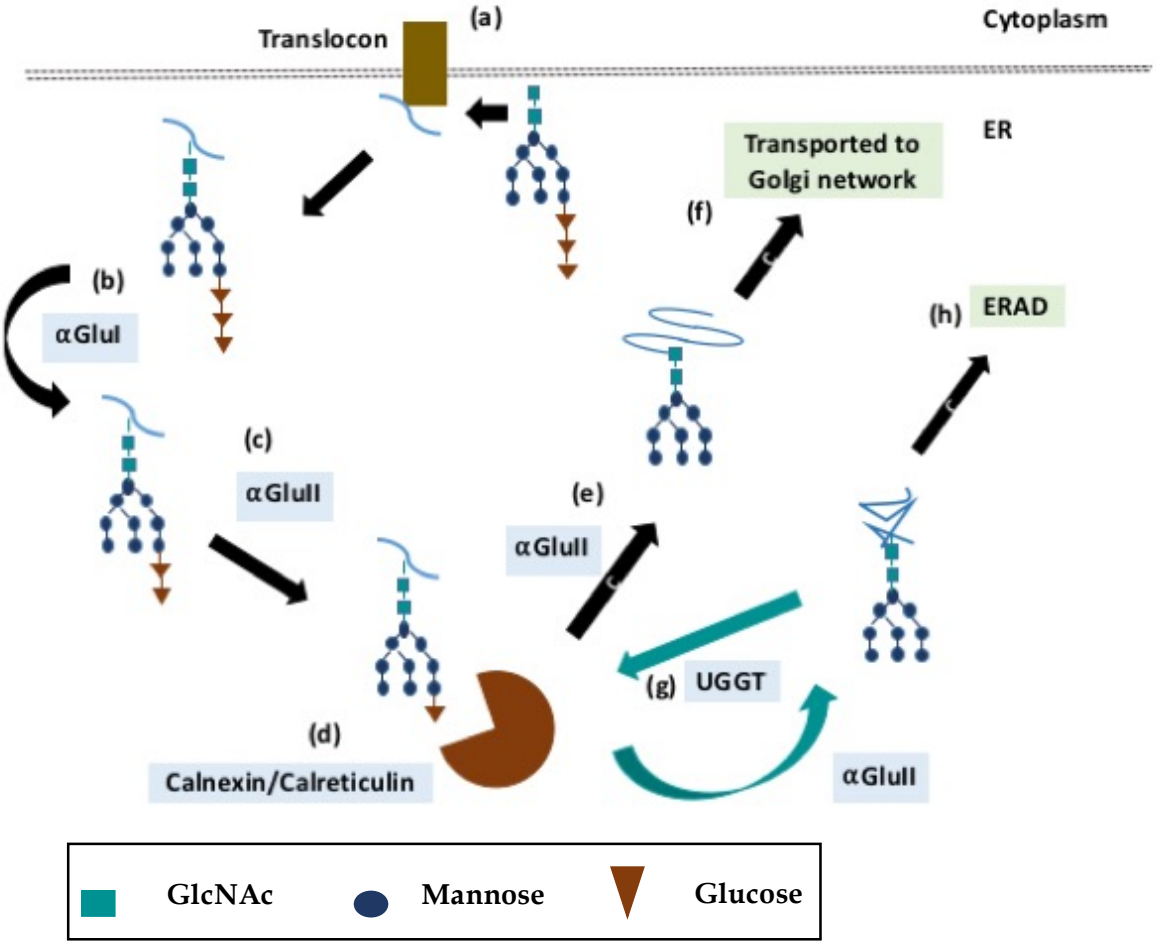

Figure 1.4: ***N*-glycoprotein processing in the ER.** Processing of the N-linked glycans and interaction with the calnexin cycle is shown. (a) A dolichol-P-P linked oligosaccharide ($Glc_3Man_9GlcNAc_2$) is transferred to the nascent polypeptide by oligosaccharide transferase (OST). (b) A glucose residue is cleaved by α-glucosidase I (αGluI). (c) A second glucose residue is cleaved by α-glucosidase II (αGluII). (d) Monoglucosylated glycans interact with calnexin/calreticulin lectins to achieve proper protein folding. (e) The terminal glucose is removed by αGluII. (f) Proteins that are properly folded will be diverted to the golgi network for secretion, (g) Misfolded proteins wil have a glucose added by UDP glucose: glycoprotein glucosyltransferase (UGGT) to allow interaction with calnexin for anoyther attempt at folding. (h) Terminally misfolded proteins will be diverted to ERAD for degradation. Adapted from Andrew Sayce (2014) [2].

The pathogenesis of DENV is revolved around production of many inflammatory mediators coinciding with the development of critical phase. As such, an effective antiviral against DENV is required to curb the excessive inflammatory mediator induced effects to prevent or reduce the endothelial dysfunction. The effect of iminosugar treatment on the inflammatory cascade is of interest in this regard. Previous published data suggest a reduction of multiple inflammatory mediators in DENV-infected mice following treatment with 2THO-DNJ (UV-12) [113]. Interestingly, M*O*N-DNJ treatment of DENV-infected and lipopolysaccharide (LPS)-treated macrophages resulted in reduction of secreted TNFα and IFNα levels suggesting an anti-inflammatory effect of these drugs [2]. The mechanism of this anti-inflammatory effect is not clear. A transcriptomic analysis of DENV–infected and M*O*N-DNJ treated macrophages was performed previously in our lab by Dr Andrew Sayce to identify possible pathways differentially regulated in these cells [2]. Results revealed dampening of the inflammatory pathways by iminosugar treatment and up-regulation of the host UPR pathways at 6 hours and 24 hours post-infection. The Nrf2 mediated antioxidant pathways were also up-regulated following M*O*N-DNJ treatment. Given the complex interactions of the UPR and ROS/antioxidant cascades with the inflammatory pathways, evaluating the effect of iminosugars on these host responses could help understand the mechanisms of the anti-inflammatory effect of this drug. It would be important to identify and understand the effects of these iminosugars on the diverse host and viral induced responses to exploit clinical uses of these drugs in DENV infection and non-DENV conditions. In addition, better understanding of the iminosugar effects on host responses would help to plan clinical evaluation studies better.

This thesis focuses on evaluating the effects of 2THO-DNJ on the UPR and the redox response in DENV-infected primary monocyte-derived macrophages. In addition, the antiviral effects

of an array of DNJ-derived iminosugars were tested in primary monocyte-derived dendritic cells for the first time.

II

Research questions & Aims of the thesis

2.1 Research questions

a) Iminosugars have been tested in different cell culture models. The main cells of interest in a clinical infection include monocytes, macrophages and dendritic cells. The antiviral effects of iminosugars have not been tested before in primary monocyte-derived dendritic cells. Therefore, the first question was whether DNJ-derived iminosugars elicit antiviral effects and reduce DENV-mediated TNFα secretion in dendritic cells.

b) The main question investigated in this thesis was whether 2THO-DNJ, a long alkylchain derivative of the iminosugar DNJ, had any effects on the host UPR and ROS/antioxidant levels during DENV infection. I selected these specific pathways for further investigation based on results of a large transcriptomics study conducted by a previous DPhil student in the Zitzmann lab (Dr Andrew Sayce), which suggested a putative link between the dampening of the inflammatory cascade and activation of the UPR and Nrf2-mediated antioxidant pathways in DENV infection. Experiments discussed in this thesis were performed in primary monocyte-derived macrophages to evaluate the effects of 2THO-DNJ on cellular UPR/redox homeostasis and to understand whether the changes identified were required for the antiviral and anti-inflammatory effects observed with iminosugar treatment.

c) The third question was whether the UPR is differentially regulated in patients with severe disease manifestations and to evaluate the possibility of using these markers to predict disease severity. To this end, the *in vitro* results were expanded to a clinical study to identify UPR and non-UPR markers that could be potentially used as markers of DENV disease severity in early dengue infection.

2.2 Aims of the thesis:

Chapter 4 of this thesis aims to evaluate the antiviral effects of three DNJ-derived iminosugars in DENV-infected primary monocyte-derived dendritic cells for the first time. In addition, the effect of these iminosugars on DENV-induced TNFα levels were identified. A DGJ derivative was used as a control in these experiments to understand the effect of α-glucosidase inhibition in mediating these effects. FOS levels were performed in DENV-infected and iminosugar treated dendritic cells to identify the ability of these iminosugars to inhibit α-glucosidase I and II.

The main question of the effect of 2THO-DNJ treatment on the cellular UPR was evaluated in Chapter 5. The IRE1α-XBP1 and PERK-ATF4 pathways were investigated to identify how DENV infection affect these pathways in primary monocyte-derived macrophages and the effect of iminosugar treatment was identified. Chemical inhibitors were used to further understand the role of these pathways in mediating the antiviral and anti-inflammatory effects of 2THO-DNJ.

The effect of DENV infection and iminosugar treatment on cellular oxidative stress and the total antioxidant capacity will be evaluated in detail and presented in chapter 7.

Finally, a clinical study is presented in chapter 6 which attempts to identify UPR related and non-related markers of dengue disease severity. Patient samples during early dengue infection were used to identify transcripts and proteins differentially expressed in those who developed severe disease later in the course of illness compared to those developing non-severe manifestations.

III

Materials and Methods

3.1 Cell culture and virus

3.1.1 Peripheral blood mononuclear cell (PBMC) separation

Human PBMCs were isolated from buffy coats (NHS Blood and Transport, Ethical approval ref no 09/H0606/3) by a Ficoll gradient centrifugation method. All donors remained anonymous and an alphabetical code was assigned to refer to the samples for processing and experiments. In brief, buffy coats were diluted 1:1 with phosphate-buffered saline (PBS) and overlaid on Ficoll-Paque™ PLUS (GE Healthcare). PBMCs were isolated following centrifugation and allowed to adhere to 2% gelatin-(Sigma) coated tissue culture plates for 90 min at 37^0C. Non-adherent cells were washed off in RPMI-1640 media (Gibco) and attached monocytes were further incubated in X-VIVO™ 10 media (Lonza) supplemented with 1% autologous plasma for 18 hours at 37^0C, 5% CO_2. Monocytes were detached by incubation with cold PBS + 5 mM EDTA followed by vigorous pipetting and cultured in specific media supplemented with growth factors to differentiate into macrophages (MDMΦ) or dendritic cells (DCs).

3.1.2 Differentiation of monocytes to MDMΦ and DCs

Monocytes were differentiated into partially mature MDMΦ by culturing in X-VIVO™ 10 media supplemented with recombinant human interleukin-4 (IL-4, Peprotech) 25 ng/ml for 3 days at 37^0 C, 5% CO_2. Differentiation to DCs was achieved by culturing in RPMI-1640 media with 10% heat inactivated foetal bovine serum (HI FBS, Life Technologies) supplemented with 50 ng/ml IL-4 and 100 ng/ml granulocyte colony stimulating factor (GM-CSF, Peprotech) for 4 days to obtain immature DCs (imDCs). Media was changed 4 days later and monocytes were incubated in fresh media containing IL-4 and GM-CSF for a further 2 days then treated with *Salmonella enterica* lipopolysaccharide (LPS, Sigma) for 48 hours to differentiate monocytes

into mature DCs (mDCs). Expression of surface markers was analysed by flow cytometry to confirm the phenotype as described in Chapter 3.4.

3.1.3 Cell lines and culture

Cell lines used in this thesis include the C6/36 mosquito cell line (a gift from US Armed Forces Research Institute of Medical Sciences, Thailand [AFRIMS]), *Macaca mulatta* kidney cells (LLC-MK2, a gift from Armed Forces Research Institute of Medical Sciences, Thailand [AFRIMS]), THP-1 human monocytic cell line (a gift from Fernando Martinez Estrada, Oxford), HEK-Blue™ TNF-α cells (Invivogen) and HEK-Blue ™ IFN-α/β cells (Invivogen). C6/36 cells were cultured in Leibovitz L15 medium (Gibco) supplemented with 10% HI FBS, 100 U/ml penicillin and 0.1 mg/ml streptomycin (Sigma) at 28^0C and without CO_2. LLC-MK2 cells were cultured in Medium 199 (Gibco) supplemented with 10% HI FBS, 100 U/ml penicillin and 0.1 mg/ml streptomycin at 37^0C, 5% CO_2. THP-1 cells were cultured in suspension in RPMI-1640 media supplemented with 10% HI FBS, 100 U/ml penicillin and 0.1 mg/ml streptomycin at 37^0C, 5% CO_2. THP-1 monocytes were differentiated to macrophages by culturing in media supplemented with 100 ng/ml of phorbol 12-myristate 13-acetate (PMA, Sigma) for 72 hours and culturing for a further 24 hours in fresh media devoid of PMA. HEK-Blue™ TNFα ells and HEK-Blue ™ IFN-α/β cells were grown in Dulbecco's Modified Eagle Medium (DMEM, Gibco) containing 4.5 g/L glucose and 2 mM L-glutamine at 37^0C, 5% CO_2. Medium was supplemented with 10% HI FBS, 100 μg/mL normocin (Invivogen), 100 U/ml penicillin and 0.1 mg/ml streptomycin. Cells were selected in medium supplemented with cell type specific antibiotics until harvested for experiments. Selection medium for HEK-Blue™ TNFα reporter cells included growth media (as above) with 100 μg/mL zeocin (Invivogen) and 1 μg/mL puromycin (Invivogen) antibiotics. HEK-Blue ™ IFN-α/β reporter cells were selected in growth medium supplemented with 100 μg/mL zeocin and 30 μg/mL blasticidin (Invivogen).

3.1.4 Growth of DENV stocks

DENV serotype 2, strain 16681 (a gift from G. Screaton, University of Oxford, UK) was propagated in C6/36 cells. Virus was concentrated from C6/36 supernatant and precipitated using 10% weight per unit volume (w/v) poly(ethylene glycol) M_n 6000 (Sigma) and 0.6% sodium chloride (Sigma) overnight at 4^0C. The virus was collected by centrifugation at 3750 rpm at 4^0C for 45 min. The pellet was resuspended in Leibovitz L15 media and stored at -80^0C until further use.

3.1.5 *In vitro* DENV infection and drug treatment

Infection of MDMΦ, DCs and THP-1 cells was carried out as follows. The virus was diluted in respective media to have virus plaque forming units (pfu) at a specific multiplicity of infection (MOI). Virus was added to cells, seeded in the plates or flasks and left to attach, for 90 min rocking at room temperature. After this period, virus was removed and replaced with media with or without the drugs and the cells cultured at 37^0 C, 5% CO_2.

3.2 Viral quantification

3.2.1 Plaque assays

Infectious DENV was measured by plaquing the virus containing supernatant on naïve LLC-MK2 cells. LLC-MK2 cells were seeded at a concentration of $1.7x10^5$ cells/ml in 12 well plates at 2 ml/well. Cells were allowed to adhere and grow overnight to form a monolayer. Medium was aspirated and cells were washed once in Hanks' balanced salt solution (HBSS) prior to adding serial dilutions of virus in minimal essential media (MEM) supplemented with 10% HI FBS. Virus was incubated on the cells for 90 min, rocking at room temperature, before aspirating the virus and adding the 1st overlay (for composition see below) and 1.8% agarose (1:1 dilution) mixture. Cells were cultured for 5 days at 37^0 C, 5% CO_2. Neutral red (720 μL from a 6 g/L solution) was added to the 2nd overlay (for composition see below) and agarose

(1:1 dilution) mixture and added to the cells on day 5 after virus infection and cells were cultured overnight. Plaques were counted on the next day and calculated as below:

Plaque forming units/ml (pfu/ml) = n x 10 x dilution factor

n - number of plaques

Composition of the overlays used for plaque assays:

1st overlay:

50ml	Hank's balanced salt solution stock A
50ml	Hank's balanced salt solution stock B
10ml	100x MEM vitamin solution (Thermofisher)
10ml	50x MEM amino acid solution (Thermofisher)
50ml	Heat inactivated (57^0 C) FCS
6ml	L-glutamine
20ml	7.5% $NaHCO_3$, *p*H=8.2
10ml	100 U/ml penicillin and 0.1 mg/ml streptomycin
294ml	deionized water
500ml	Total and adjust for *p*H to 8.2

2nd overlay:

50ml	Hank's balanced salt solution stock A
50ml	Hank's balanced salt solution stock B
10ml	100x MEM vitamin solution (Thermofisher)
10ml	50x MEM amino acid solution (Thermofisher)
6ml	L-glutamine
10ml	100 U/ml penicillin and 0.1 mg/ml streptomycin
364ml	deionized water
500ml	Total and adjust pH to 6.3

Hank's balanced salt solution stock A consisted of 160 g NaCl, 8 g KCl, 2 g $MgSO_4.7H_20$, 2.8 g $CaCl_2.2H_20$ in one litre of deionized water. Hank's balanced salt solution stock B consisted of 1.2 g Na_2HPO_4, 1.2 g KH_2PO_4 and 20 g of glucose in one litre of deionized water.

3.2.2 Viral RNA extraction and quantification

Viral RNA was extracted from cell culture supernatant using the Directzol RNA mini prep kit (Zymo research) in experiments described in chapter IV according to the manufacturer's instructions. QiaAmp Viral RNA mini kit (Qiagen) was used to extract RNA from cell culture supernatant in experiments described in chapter V. A one-step quantitative reverse transcription polymerase chain reaction (qRT-PCR) for DENV NS5 was performed using the Thermoscientific Verso one–step RT qPCR kit or Luna Universal one-step RT qPCR kit (New England BioLabs). Genome copies were quantified by a thermo-start DNA Taq polymerase to enable Taq-mediated release of fluorescently labelled dyes from a DENV-2 NS5 specific probe as described in the literature [1, 114]. All samples were run in technical duplicates and compared to a standard curve of high titre viral RNA isolated from C6/36 grown DENV-2. The qRT-PCR was performed in an Applied Biosystems 7500 Fast Real-Time PCR System.

Primer sequences for DENV-2 NS5:

Forward primer: 3′ primer (ACAAGTCGAACAACCTGGTCC)

Reverse primer: 3′ primer (GCCGCACCATTGGTCTTCTC)

FAM-TAMRA NS5 qRT probe sequence:

(6FAM)CCAGTGGAATCATGGGAGGAAATCCCA(TAM)

Verso one-step RT qPCR kit protocol:

The primers, probe, ROX dye (passive reference dye), RT enhancer, Verso enzyme mix and the 2x 1-step qPCR mix was used with 2 μL volume of total template RNA in a final 20 μL reaction. Samples were run at 48^0 C for 30 min (reverse transcription), 95^0 C for 15 min (initial denaturation) followed by 40 cycles of 95^0C for 15 seconds, 55^0C for 60 seconds and 60^0C for 25 seconds before reading the plate.

Luna Universal one-step RT qPCR kit protocol:

Luna Universal Probe One-step reaction mix (1:2 dilution) and Luna WarmStart RT Enzyme Mix (1:20 dilution) were combined with a final concentration of 0.4 μM primers and 0.2 μM FAM-TAMRA probe to have a 20 μL reaction. Template total RNA 2 μL was added to the reaction and the samples were run at 55^0 C for 10 minutes (reverse transcription), 95^0C for 60 seconds (initial denaturation) followed by 40 cycles of 95^0C for 10 seconds, 55^0C for 60 seconds and 60^0C for 25 seconds before reading the plate.

3.2.3 Immunofluorescence to detect DENV envelope protein

Cells were seeded in a 24-well tissue culture plate containing sterilised, acid-etched glass coverslips. Following infection and drug treatment as described in section 3.1.5, supernatants were aspirated and cells were washed once in PBS. The cells were fixed by adding 4% paraformaldehyde in PBS for 15 min at 4°C. Cells were washed in PBS and then permeabilised for 15 minutes at room temperature in 0.5% (v/v) Triton X-100 in PBS (Tx100/PBS). Primary antibody against DENV2 envelope (clone 3H5, mouse IgG1, purified from ATCC hybridoma HB-46) was added in Tx100/PBS at a concentration of 10 μg/ml and the cells were incubated at room temperature for 50 min. Following two further PBS washes, cells were incubated with Alexa 488-anti-mouse secondary antibody (Molecular Probes) at 10 μg/ml for 50 min at room temperature. Cells were washed twice in PBS and then mounted with Vecta-Shield mounting

medium (Vector Laboratories Inc) containing DAPI (4',6-diamidino-2-phenylindole) for staining of nuclei. After drying at room temperature, slides were imaged on a Nikon Eclipse TE200-U fluorescent microscope such that at least 500 cells were imaged and scored for infection for each technical replicate.

3.2.4 Flow cytometry for DENV NS3

The cells were seeded in 12-well tissue culture plates and infected with DENV 16681, MOI 1 for a specified time in the experiment in the presence or absence of iminosugars. The cells were lifted by scraping using a rubber blade cell scraper and blocked in fluorescence activated cell sorting (FACS) block (PBS with 0.5%w/v BSA, 5mM EDTA and 5% v/v heat inactivated normal human plasma) for 15 min at 4^0 C. Subsequently, cells were fixed in 4% paraformaldehyde and permeabilised using 0.5% Triton-X 100. The cells were stained with the anti-DENV NS3 antibody (GeneTex) at a concentration of 5 μg/ml for 1 hour at 4^0C. Cells were washed twice and incubated with 2 μg/ml anti-mouse secondary antibody conjugated to phycoerythrin (PE) for 1 hour at 4^0C prior to washing and re-suspending the cells in FACS buffer (PBS with 0.5%w/v BSA, 5mM EDTA). Flow cytometry acquisition was performed using a FACS Calibur (Beckton Dickinson), gated for non-debris cells. A minimum of 10,000 gated events were identified and results were analysed by FlowJo V10 software. The NS3 positive cells were identified by gating on the cells having higher fluorescent intensity in the infected samples compared to the isotype and the uninfected controls. The infected population was expressed as a % from the total gated population.

3.3 Iminosugars, UPR inhibitors and cytotoxicity assay

3.3.1 Iminosugar stocks

Iminosugars used in this thesis include *N*N-DNJ (*N*-nonyl deoxynojirimycin), *N*N-DGJ (***N*-nonyl-**deoxygalactonojirimycin), 2THO-DNJ (8-tetrahydrofuranyl-octyl-DNJ, E*O*O-DNJ (*N*-

(8′-ethoxyoctyl)- deoxynojirimycin) and M*O*N-DNJ (*N*9-methoxynonyl-DNJ). *N*N-DNJ was a gift from Oxford GlycoSciences Ltd. and *N*N-DGJ was purchased from Toronto Research Chemicals. 2THO-DNJ (8-tetrahydrofuranyl-octyl-DNJ) was kindly given to us by Emergent BioSolutions Ltd. and E*O*O-DNJ was from J.L. Kiappes (Oxford Glycobiology Institute). *N*N-DNJ and *N*N-DGJ were dissolved in dimethyl sulfoxide (DMSO) or water. 2THO-DNJ was dissolved in water. E*O*O-DNJ and M*O*N-DNJ were dissolved in DMSO.

3.3.2 UPR inhibitors

Chemical inhibition of the PERK-eIF2α arm of the unfolded protein response (UPR) was achieved by treating cells with the cell permeable kinase inhibitor GSK2606414 (Calbiochem) dissolved in DMSO. Working stocks were dissolved in cell culture media and stored at -20^{0}C. The IRE1-XBP1 arm of the UPR was inhibited by using the endonuclease inhibitor 4μ8c (Calbiochem) dissolved in DMSO and stored at -20^{0}C.

3.3.3 Cytotoxicity assay

Cytotoxicity of iminosugars and other drugs was assessed by assaying for metabolic activity using a CellTiter 96® AQ_{ueous} One Solution Cell Proliferation Assay (Promega) as per the manufacturer's instructions. A 20 μL of the solution containing the electron coupling reagent (phenazine ethosulfate) and the tetrazolium compound [3-(4,5-dimethyl-2-yl)-5-(3-carboxymethoxyphenyl)-2-(4-sulfophenyl)-2H-tetrazolium; MTS] was added to cells seeded in a 96-well plate in 100 μl medium. Samples were incubated for 1-4 hours (37° C, 5% CO_2) and the absorbance was measured at 490 nm (A_{490}) on a SpectraMax M5 microplate reader (Molecular Devices). Absorbance was normalised to untreated controls after subtracting the blank reading.

3.4 Phenotyping MDMΦ and DCs by flow cytometry

Monocytes (one day after isolation), MDMΦ ± IL-4 (3 days after isolation), immature DCs (4 days after isolation) and mature DCs (8 days after isolation) were scraped from the flasks, washed in cold PBS, re-suspended in FACS block and placed on ice for 30 min. Fc block (BD Biosciences) was used during phenotyping of mature DCs to reduce non-specific binding. Cells were stained with primary antibody for 45 min on ice. 10 μg/ml anti-DC-SIGN (R&D) and 10 μg/ml anti-CD86 (BioLegend) antibodies were compared to 10 μg/ml IgG2b (R&D) isotype antibody. 50 μg/ml anti-CD14 (R&D), 20 μg/ml anti-CD16 (BioLegend), 10 μg/well anti-CD83 (BioLegend) and 20 μg/ml anti-MR antibodies (clone 3.29.B1; a gift from Luisa Martinez-Pomares, University of Nottingham) were compared to 50 μg/ml IgG1 (clone D1.3) isotype control. Cells were re-suspended in 2 μg/ml secondary antibody (PE-Goat anti-mouse IgG (F(ab')2 (eBioscience)) after two washes with FACS buffer and kept on ice for 45 min. Cells were subjected to two further washes before re-suspending in FACS buffer. Data was collected using a FACS Calibur machine (BD) with approximately 10,000 gated cells per population and analysed by CellQuest software. Histograms were used to determine the expression of these surface receptors compared to the isotype control.

3.5 Functional TNFα and IFNα measurement

Functional tumour necrosis factor α (TNFα) levels and interferon α (IFNα) levels were measured using HEK-Blue™ reporter cells. Stimulation of these cells by TNFα or IFNα results in activation of the NF-κB inducible promoter and production of secreted alkaline phosphatase (SEAP). The levels of SEAP were detected using QUANTI-Blue™ following the change of colour to blue which is quantified by reading the OD at 620-655nm. A standard curve of TNFα and IFNα was used to calculate the functional cytokine levels in the cell culture supernatant. All samples were done in technical triplicates.

3.6 Western blotting

3.6.1 Western blot

Cell lysates were prepared in RIPA buffer supplemented with complete EDTA free protease inhibitor tablets (Roche) and fresh phosphatase inhibitor (Sigma). Cell culture supernatant was removed and cells were washed twice in ice cold PBS. Cells were either scraped and centrifuged and the cell pellet was re-suspended in RIPA buffer (for THP-1 cells) or cells were scraped and lysed on the plate in RIPA buffer for MDMΦ. The cell lysate was placed on ice for 20 min then centrifuged at 12000 g for 30 min. The supernatant was collected and stored at -80^0 C until further use. An equal volume was loaded for running the SDS page gel. The lysates were mixed with loading buffer (1:4) and reducing agent (1:10) followed by heating at 95^0 C for 5 min. The samples were loaded onto a 4-12% Bis Tris gel and run in MES buffer (low molecular weight proteins) for 35 min or MOPS buffer (high molecular weight proteins) for 50 min.

Table 3.1: The constituents of RIPA buffer (pH 7.4)

Component	Concentration
Tris HCL	25mM
NaCl	150mM
NP-40	1%
Sodium deoxycholate	1%
SDS	0.1%
Water to dissolve	

Transfer of proteins:

Proteins were transferred to a PVDF membrane by a semi-dry method at 125 mA for 50 min using a semi-dry blotter (BioRad). The membrane was blocked in 5% w/v dried skimmed milk dissolved in TBS-T (TBS + 0.1% Tween 20) for 1 hour at room temperature. Subsequently, the membrane was washed and incubated with the primary antibody dissolved in 5% BSA

(bovine serum albumin) in TBS-T overnight at 4^0C. The membrane was washed three times in TBS-T and incubated with the respective secondary antibody conjugated to horse radish peroxidase (HRP) for 1 hour at room temperature. After probing with the antibodies, the membrane was washed three times in TBS-T followed by addition of Amersham ECL Prime western blotting detection reagent (Life Sciences) for 5 min. Chemiluminescence was detected by exposing under a Fuji LAS 1000 camera. The membranes were stripped in mild stripping buffer heated to 40^0C and washed three times before re-probing with further antibodies. Actin was used as the house keeping protein and the membranes were probed after stripping as described before.

Table 3.2: The constituents of transfer buffer

Component	Amount
Trisbase	24mM
Glycine	192mM
Methanol	20%
Dissolved in ultra-pure water	

Table 3.3: The constituents of stripping buffer

Component	Amount
Glycine	15g
SDS	1g
Tween-20	20ml
Dissolved in 1L of ultra-pure water	
pH 2.2	

3.6.2 Antibodies

The following antibodies were used for western blotting. Anti-PERK rabbit monoclonal antibody 1:1000 (Cell Signalling #5683), anti-eIF2α rabbit monoclonal antibody 1:1000 (Cell Signalling, #9722), anti-phospho-eIF2α (Ser51) rabbit monoclonal antibody 1:750 (Cell

Signalling, #9721), anti-ATF-4 (D4B8) rabbit monoclonal antibody 1:750 (#11815), anti-XBP-1s rabbit monoclonal antibody 1:1000 (clone D2C1F, Cell Signalling, #12782), anti-β-actin mouse monoclonal antibody 1:2500 (clone C4, Santa Cruz, #sc-47778), anti-rabbit HRP-linked antibody 1:10000 (Abcam, #ab6112) and anti-mouse HRP-linked antibody 1:10000 (Sigma).

3.7 Reactive oxygen species and antioxidant levels

3.7.1 Detection of reactive oxygen species (ROS) by flow cytometry

CellROX^{R} Green (Thermofisher) dye was used to detect ROS production in cells by flow cytometry. Briefly, supernatants from cells were aspirated and 5 μM CellROX diluted in PBS was added to cells and incubated at 37^{0} C for 30 min. Cells were washed twice in PBS and scraped in FACS buffer. Cells were centrifuged, resuspended in 4% paraformaldehyde and placed on ice for 15 min for fixing. Cells were then pelleted and washed once before resuspending in FACS buffer for analysis using the FL1 filter in the FACS Calibur. Cells were gated to remove debris and the mean fluorescence intensity was compared between the treatment conditions. A minimum of 5000 gated events was analysed.

3.7.2 Antioxidant capacity measurement

Antioxidant capacity in the whole cell lysates was measured using an antioxidant assay kit (Sigma) according to the manufacturer's instructions. Briefly, cells ($3x10^{6}$ cells per sample) were scraped from 6-well tissue culture plates in 1 x assay buffer and lysed by multiple freeze thaw cycles. The lysates were centrifuged at 12,000 x g for 15 min at 4^{0} C. The samples were stored at -80^{0} C until further use. The assay was performed in a 96-well plate with each sample in triplicate. Trolox, a water soluble vitamin E analogue was used as the standard to quantify antioxidant capacity. A standard curve was generated and the antioxidant level was calculated based on the average absorbance of the samples measured at 405 nm.

3.8 Measurement of cellular mRNA levels by qRT-PCR

Quantification of the mRNA levels of genes of interest was achieved by a one-step qRT-PCR assay using the Verso one-step PCR kit (Applied Biosystems). Total cellular RNA was extracted using the Qiagen RNeasy mini kit (Qiagen) according to the manufacturer's instructions. Briefly, cells were lysed in the plate by adding the lysis buffer (supplemented with 1% β-mercaptoethanol). Ethanol was added in an equal volume to the lysate and the lysate was applied to a spin column. Following repeated centrifugation steps and washing of the spin column, RNA was eluted in 30 μL of nuclease-free water. A multiplex qRT-PCR was performed to quantify the genes of interest using Taqman gene expression assays (Table 3.4) and RPLP2 as the house keeping gene. RPLP2 gene was used as this was seen to be least affected by dengue infection and iminosugar treatment in macrophages compared to conventional housekeeping genes (GAPDH, Actin). The plate was analysed in a 7500 Fast Real-Time PCR System (Applied Biosystems) and the gene expression levels were expressed as a fold change calculated by the ΔΔCt method [115]

Table 3.4: Taqman primers and probes used for the quantification of cellular mRNA

Gene of interest	Gene ID (Gene expression assays)	Dilution
sXBP1	Hs 03929085_g1 (FAM)	1:20
TXBP1	Hs 00231936_m1 (FAM)	1:20
ATF4	Hs 00909569_g1 (FAM)	1:20
RPLP2	Hs 01115128_gH (VIC)	1:60

3.9 Free oligosaccharide analysis (FOS)

Free oligosaccharides (FOS) accumulate due to inhibition of the ER α-glucosidases and quantification of the exact type of FOS provides an indication of αGluI and αGluII inhibition *in vitro*. The DCs were seeded in a 6-well plate and either not infected or infected with DENV2 at MOI 1 and treated with 0.3, 3.16, 31.6μM concentrations of iminosugars or left untreated. After 48 hours post-infection, the supernatant was removed and the cells were lysed in 0.5%

Triton to inactivate DENV and access the intracellular oligosaccharides. The cell lysates were further diluted in deionised water and analysed by normal phase (NP)-HPLC for detection of FOS [116]. For enzymatic determination of individual GlcNAc- and galactose-terminating FOS species, samples were subjected to digestion with β-galactosidase at 50 U/ml at 37 °C overnight to remove the terminal galactose residues. Peak area was used to assess molar quantity in comparison to standards of known identity and quantity. All FOS values were normalised based on the protein concentration.

3.10 Fieldwork experiments

3.10.1 Recruitment of study participants and ethical considerations

The fieldwork experiments were carried out in Sri Lanka from 01/07/2018- 25/08/2018. The study participants were recruited by myself from the outpatient department and the wards based at the Infectious Disease Hospital (IDH) at Colombo, Sri Lanka. The criteria for inclusion in the study were a history of fever lasting less than 72 hours. Patients less than 18 years of age were excluded due to complexities involved in obtaining consent. In addition, pregnant patients were also excluded due to diverse factors affecting the course of illness. An initial screening was done to identify patients having high likelihood of viral fever compared to those having other illnesses. This included asking questions and checking their investigations to identify patients having fever suggestive of dengue fever. The SD Bioline dengue rapid NS1 kit (Abbott) was used to identify patients with a high likelihood of having dengue fever. Due to the sensitivity of the NS1 kit being approximately 62%[117], the samples from NS1 negative patients were collected and used for downstream analysis if the clinical course was suggestive of dengue fever with detectable dengue virus in serum by qRT-PCR. The research was explained to the participants and written consent was obtained at recruitment. After obtaining their consent, blood samples were taken at admission and defervescence (24 hours after fever subsided). A 5 ml blood sample was collected into a

heparinised container for PBMC isolation and 2 ml of blood was collected to a plain tube for separating serum. All participants had the right to withdraw from the research during the study period. Clinical data were obtained from the bed-head tickets and samples were processed either at the Centre for Dengue Research, University of Sri Jayewardenepura or the Oxford Glycobiology Institute, University of Oxford. Healthy volunteers were recruited to generate samples to be used as controls. The methodology is further explained in detail in chapter VI.

The study was approved by the Oxford Tropical Research Ethics Committee (OxTREC 16/18) and the Ethics Review committee (ERC 01/18), University of Sri Jayewardenepura, Sri Lanka prior to the commencement of recruitment.

3.10.2 Isolation of PBMCs

The PBMCs were isolated by a gradient centrifugation method as described in 3.1.1. Whole blood (5 ml) was collected to a heparinised 15 ml falcon tube and transported at room temperature for PBMC isolation within 4 hours. Blood was diluted 1:1 in sterile PBS and overlayed slowly onto 5 ml of Lymphoprep (Stem cell technologies). The sample was centrifuged at 2000 rpm (900g), room temperature, with the brake off for 20 min. The PBMC layer was aspirated using a sterile pasteur pipette and transferred to a new tube. Ice cold PBS was added to the cells and they were centrifuged at 1500 rpm (500g), brake on low, 4^0C for 10 min. The supernatant was discarded and the cell pellet was resupended in 1x red cell lysis buffer (BioLegend) and incubated at 4^0C for 5 min to remove any red cells. The 10x lysis buffer was diluted 10 times in deionized water to prepare the working solution. The lysis buffer was removed by adding 14 ml PBS and centrifuged at 960 rpm (200g) for 10 min at 4^0 C, with the brake on high. Cells were washed once in PBS and counted to use 1-2x10^6 cells for generating cDNA using the Taqman Gene Expression Cells-Ct kit (Thermofisher).

3.10.3 Generating cDNA from PBMCs for qRT-PCR

Following isolation of the PBMCs, the cell pellet containing 1-2x10^6 cells was lysed in 50 µL lysis buffer in the Taqman Gene expression cells-Ct kit. Briefly, DNAse 1 was added to the lysis buffer at a 1:100 dilution and the cells lysed in 50 µL of lysis buffer and incubated at room temperature for 5 min. The stop solution was added at 5 µL per sample and incubated at room temperature for 2 min to inactivate the lysis reaction. The generated lysates were used in the reverse transcription reaction (lysates constituted 30% of the volume of the reaction) to produce 2 reactions of 75 µL of cDNA per sample as given below.

Table 3.5: Components of the reverse transcription reaction

Component	Volume per reaction (µL)
2x RT buffer	37.5
20x RT enzyme mix	3.75
Nuclease-free water	11.25
Lysate	22.5
Total	**75**

Samples were run in a thermal cycler at 37^{0}C for 60 min (reverse transcription) followed by 95^{0}C for 5 min to inactivate the reverse transcription reaction and held at 4^{0}C. The cDNA prepared from the reverse transcription reactions were stored at -80^{0}c until further analysis.

3.10.4 Quantification of the UPR transcripts by qRT-PCR

A multiplex qRT-PCR was performed using Taqman gene expression assays for the target genes of interest and RPLP2 as the housekeeping gene. Briefly, the primers/probe for the target gene and primers/probe for RPLP2 was added to 16 µL of Taqman gene expression master mix which was combined with 4 µL of cDNA for the qRT-PCR reaction.

Table 3.6: The primers/probes used for the qRT-PCR experiments

Genes of interest	Gene ID (Gene expression assays)	Dilution
sXBP1	Hs 03929085_g1 (FAM)	1:20
DDIT3 (CHOP)	Hs 99999172_m1 (FAM)	1:20
HSPA5 (BiP)	Hs 00946084_g1 (FAM)	1:20
ATF4	Hs 00909569_g1 (FAM)	1:20
EDEM1	Hs 00976004_m1 (FAM)	1:20
ATF6	Hs 00232586_m1 (FAM)	1:20
NFE2L2	Hs 00232352_m1 (FAM)	1:20
RPLP2	Hs 01115128_gH (VIC)	1:50

All samples were run in duplicate in an Applied Biosystems 7500 real-time PCR system and the fold change of the gene of interest was calculated by the ΔΔCt method. A sample from a healthy donor was used as the reference sample.

3.10.5 Measurement of viral load in serum

The DENV serotype was identified and the viral load was measured by a multiplex qRT-PCR using four different Taqman primers and dual labelled probes for the four serotypes. All probes were labelled with the QSY quencher.

Table 3.7: DENV primers used for quantifying viral load by qRT-PCR

Target	Forward primer (5′-3′)	Reverse primer (5′-3′)
DENV 1 (NS5)	CAAAAGGAAGTCGYGCAATA	CTGAGTGAATTCTCTCTRCTRAAC
DENV 2 (E)	CAGGYTATGGCACYGTCACGAT	CCATYTGCAGCARCACCATCTC
DENV 3 (prM)	GGACTRGACACACGCACYC	CATGTCTCTACCTTCTCGACTTGYCT
DENV 4 (prM)	TTGTCCTAATGATGCTRGTCG	TCCACCYGAGACTCCTTCCA

Table 3.8: DENV probes used in the qRT-PCR reaction to identify the serotype and quantify viral load

Serotype	Probe sequence	Reporter dye
DENV 1	CATGTGGYTGGGAGCRCGC	JUN
DENV 2	CTCYCCRAGAACRGGCCTCGACTTCAA	ABY
DENV 3	ACCTGGATGTCGGCTGAAGGAGCTTG	FAM
DENV 4	TYCCTACYCCTACGCATCGCATTCCG	VIC

Firstly, RNA extraction was performed using the QiaAmp viral RNA mini kit (Qiagen) using 140 μL of serum according to the manufacturer's instructions. The extracted RNA was reverse transcribed to cDNA using the high capacity cDNA reverse transcription kit (Thermofisher). Following reverse transcription, 2 μL of cDNA was used in a 20 μL qRT-PCR reaction which constituted 10 μL Taqman multiplex mastermix (Thermofisher), 900 nM of each primer and 250 nM of each probe to amplify and measure DENV copies. The standard curve was generated by a mixture of gBlock DNA fragments (Appendix 1) similar to the sequences amplified in the PCR reaction and the viral load in the sample was calculated using the standard curve.

3.10.6 Dengue rapid NS1 detection and measurement of DENV-specific IgM antibodies in serum

The dengue NS1 antigen was detected in whole blood of the participants. This was performed using the SD Bioline dengue rapid NS1 kit (Abbott) in the acute fever samples collected from the participants. Briefly, 3 drops of whole blood were added to the NS1 detector paper strip and the results read after 5-7 minutes of incubation at room temperature. The test was considered positive when both the control and test lines appeared on the strip.

DENV-specific IgM antibodies were quantified in serum using the Panbio dengue IgM capture ELISA (Abbott) according to the manufacturer's instructions. Serum was diluted in

1:100 using the assay diluent provided with the kit and 100 µL was added to the immunocapture microplates coated with anti-human IgM antibodies and incubated for 1 hour at 37^0C. The peroxidase labelled anti-dengue antibodies were mixed with the DENV antigens provided in the kit and the antigen-antibody mixture was added to the microplate after removing serum and washing thoroughly. The plate was incubated for 1 hour at 37^0C and tetramethylbenzidine (TMB) substrate was added to the wells after several washes. The plate was incubated at room temperature for 10 min and the reaction was stopped by adding the stop solution. The absorbance was read in an ELISA plate reader at 450 nm. The positive and the negative controls were used for validation purposes and the cut-off control was used to calculate the IgM concentration in Panbio units. A sample/cut-off ratio ≥ 1.1 was considered positive while a value <0.8 was interpreted as negative.

3.10.7 Proteomics analysis of cell lysates

PBMC cell lysates were produced by resuspending the cell pellets in RIPA buffer (Table 3.1) supplemented with protease inhibitor (Roche) and phosphatase inhibitor (sigma) and incubating at 4^0C for 20 min. The lysates were centrifuged at 12,000g for 10 min and the supernatant collected for experiments. The lysates were subjected to quantification of protein levels by the Pierce BCA protein assay kit (Thermofisher). Tandem mass tagging (TMT) mass spectrometry was performed on 10 selected samples (2 healthy, 4 DF and 4 DHF donors) by using equal amounts of proteins. Further normalisation was performed by determining the peptide concentrations of the samples using the Pierce quantitative colorimetric peptide assay (Thermofisher) and TMT labelling was performed and run on the Mass spectrometer to identify differentially expressed peptides in the samples. Mass spectrometry experiment was performed by Dr Abhinav Kumar of Zitzmann lab.

IV

The antiviral effect of iminosugars in primary monocyte-derived dendritic cells

Dendritic cells (DCs) are important targets for DENV infection and they play a significant role in the immune response against early dengue infection. The antiviral effects of iminosugars against DENV have been described previously in monocyte-derived macrophages. Given the important role played by DCs in innate immune defense against DENV, the antiviral effects of three deoxynojirimycin (DNJ) derivatives and a

deoxygalactonojirimycin (DGJ) control was evaluated in DENV-infected primary human monocyte-derived DCs. This chapter demonstrates that iminosugar derivatives of DNJ, but not DGJ, elicit antiviral activity in DENV-infected monocyte- derived DCs similar to that observed in macrophages. The iminosugars *N*N-DNJ, E*O*O-DNJ and 2THO-DNJ reduced the percentage of infected cells and inhibited the secretion of DENV in a dose dependent manner. The ER α-glucosidase I inhibition by DNJ containing iminosugars was determined by quantification of the free oligosaccharides for the first time in primary DCs. ER α-glucosidase I inhibition by doses exceeding 3.16 μM of these drugs correlated with reduction in specific infectivity of secreted virus and reduction in DENV-induced TNFα secretion in DCs. Following these results, 2THO-DNJ was selected as the candidate drug to continue the experiments in this thesis.

4.1 Introduction

Dendritic cells (DCs) play a crucial role in combating infection by diverse pathogens [118-120]. DCs are potent antigen presenting cells (APCs) and they are called 'mobile sentinels' that bring together the antigens and naïve T and B lymphocytes in the lymphoid organs [121]. This is in addition to their ability to directly control infections [122]. DCs originate in the bone marrow from a common monocyte-DC precursor [123] to form the main conventional/classical DC population (cDC) and the circulating plasmacytoid DCs (pDC) [120]. The cDCs are found in both lymphoid and non-lymphoid organs and are potent stimulators of naïve T cells [122]. The cDCs have the ability to present endogenous as well as exogenous antigens to T cells via the major histocompatibility complex [122]. The pDCs circulate in the blood and reside in the spleen, liver and bone marrow. They have a robust type 1 interferon response to toll-like receptor (TLR) stimulation in addition to their function of activating and recruiting natural killer (NK) cells [124]. Thus DCs link the innate and adaptive immune networks to produce an efficient antimicrobial response. DCs are also derived from the circulating monocytes in the presence of inflammatory stimuli [118, 122, 125]. These constitute the Mo-DC and TNFα producing and iNOS producing (Tip)-DCs [125-127]. The macrophages and DCs constitute the mononuclear phagocytic system (MPS) which recognises pathogenic antigens and scavenges them in addition to producing an inflammatory response against invading organisms [123, 125]. This common goal is achieved because of the significant heterogeneity in their phenotype, tissue localization, proliferative potential and distinct function [121, 125, 128].

DENV preferentially infects mononuclear phagocytic cells such as monocytes, macrophages and DCs [129]. Immature DCs (imDC) are the most susceptible primary cell for mosquito-derived DENV infection compared to macrophages and mature DCs [130]. The C-type lectin CD209/DC-SIGN expressed on DCs binds to DENV E protein and acts as a co-receptor to

facilitate viral entry [131-133]. DCs in the skin are one of the earliest cells to be infected following a clinical DENV infection or injection of the virus to skin [120, 132]. Resident cDCs and macrophages in the dermis are infected early followed by monocytes and Mo-DCs [120]. DENV tropism changes in the presence of antibodies and macrophages become more susceptible than DCs due to the ability of the macrophages to support antibody-dependent enhancement (ADE) [130, 131].

Many cytokines and chemokines have been implicated in the pathogenesis of severe dengue manifestations [29, 134, 135]. Among these, TNFα secreted by activated T cells [136, 137], monocytes [138] and dendritic cells [139] has been identified as an important mediator in the development of severe disease. Patients with dengue haemorrhagic fever (DHF) and dengue shock syndrome (DSS) have higher levels of serum TNFα compared to dengue fever (DF) patients during the febrile phase and critical phase [140-142]. *In vitro* studies also reveal that secreted TNFα from DENV-infected immune cells leads to fluid leakage by activating the vascular endothelial cells [138]. In addition to the direct permeability enhancing effect, TNFα activates the coagulation cascade [133], induces production of vasoactive substances such as IL-6 from endothelial cells , production of platelet activating factor, vasoactive leukotriene and thromboxane production [138]. Treatment by an anti- TNFα monoclonal antibody prevents vascular leakage *in vitro [138]* and *in vivo* in mice [143]. Ho *et al*. showed that monocyte-derived DCs produce TNFα and IFNα in response to DENV-infection *in vitro* [139]. Therefore, TNFα was studied in the context of iminosugar treatment of DENV-infected monocyte-derived DCs in the following experiments.

Iminosugars that inhibit ER α-glucosidases have broad antiviral properties due to altering N-glycosylation processing in the ER as described in detail in chapter 1. The antiviral effects of iminosugars in DENV-infected monocyte-derived macrophages has been described before [1,

144]. However, the effects on DCs are not known and it is important to identify whether the observed effects of iminosugars are cell type specific or applicable to other immune cells during a DENV infection. Given the important role played by DCs in DENV pathogenesis, the antiviral effects of DNJ-derived iminosugars were evaluated in DENV-infected imDCs. In addition, the effect on DENV-induced secretion of functional TNFα was evaluated and will be discussed in this chapter. Three DNJ-derived iminosugars with different alkyl chain compositions were studied. The drug *N*N-DNJ, which has been modified from DNJ to have an *N*-alkylated nine carbon side chain, has been studied extensively against many viruses including DENV, hepatitis B virus (HBV) and bovine viral diarrhoea virus (BVDV) [145]. The drug 2THO-DNJ has a tetrahydrofuran ring in the chain while E*O*O-DNJ has an oxygen atom in the alkylating chain (Figure 4.1). Addition of an oxygen molecule and the tetrahydrofuran ring to the DNJ moiety in E*O*O-DNJ, M*O*N-DNJ and 2THO-DNJ has resulted in reduced drug-induced toxicity while improving the antiviral efficacy. The different chemical compositions of these drugs are of interest when studying the antiviral effects and the effect on DENV-induced cytokine response. Therefore, the drugs *N*N-DNJ, E*O*O-DNJ and 2THO-DNJ were studied in this chapter. The galactose analogue containing DGJ-derivative, *N*N-DGJ was used as a control in these experiments as an iminosugar which lacks the ability to inhibit α-glucosidases.

4.2 Results:

4.2.1 Phenotype of differentiated Mo-DCs

Primary monocytes were differentiated and cultured into Mo-DCs as described in previous literature and further explained in chapter 3 [146]. Briefly, the monocytes isolated from buffy coats were incubated for 4 days in the presence of IL-4 and GM-CSF to produce imDCs. DCs arranged in clusters at full differentiation and exhibited dendrites when observed under a microscope. Flow cytometry analysis of the differentiated Mo-DCs (both imDCs and matDC) showed increased expression of CD83, CD86, DC-SIGN and mannose receptor (MR) compared to day 1 monocytes and 3 day differentiated monocyte-derived macrophages (MDMΦ). Both DC populations had lower expression of the myeloid marker CD14 (Figure 4.2) than the monocytes and MDMΦ.

4.2.2. Immature DCs are susceptible to *in vitro* DENV infection

Mature DCs are known to be less susceptible to DENV infection than imDCs [132]. Similar findings were observed in our lab in mature DCs compared to the other immune cells (data not shown). Previous literature also suggests that imDCs do not support ADE in DENV infection [131, 132]. Therefore, we proceeded to investigate DENV infection of imDCs in a non-ADE setting. The differentiated imDCs were susceptible to DENV infection and expressed DENV envelope protein (as detected with monoclonal antibody 3H5) following *in vitro* infection by the DENV2 strain 16681 (Figure 4.3a). Approximately 30% (±5.5) cells were infected at 48 hrs after an *in vitro* infection at a multiplicity of infection (MOI) of 1 (data pooled from cells from 2 donors). The imDCs secreted infectious virus which was detected in the cell culture supernatant by plaque assay. The imDCs also secreted TNFα in response to DENV infection and the level of this cytokine was measured by a functional assay (Figure 4.3b).

4.2.3 Iminosugars have minimal cytotoxicity in primary imDCs

After establishing that imDCs were susceptible to DENV infection, the effect of iminosugars were evaluated in this context. The DENV-infected imDCs were treated with the three DNJ-derived iminosugars (2THO-DNJ, E*O*O-DNJ and *N*N-DNJ) and the DGJ-based iminosugar, *N*N-DGJ. The iminosugar *N*N-DNJ is known to reduce the percentage of DENV infection in MDMΦ and reduce secretion of virus in a dose-dependent manner [102]. However, none of these iminosugars have been evaluated in a primary DC model. First, the cytotoxicity of these iminosugars in imDCs was determined. Iminosugars with an oxygen atom in the *N*-substituent (2THO-DNJ and E*O*O-DNJ) had minimal cytotoxicity in DCs (Table 4.1). *N*N-DGJ had variable cytotoxicity in imDCs with 82.83% (SD 31.67%) viability at 100 μM. All the iminosugars were used within the non-toxic range (less than the dose which corresponds to CC_{10}) for further experiments. *N*N-DGJ was used at concentrations not exceeding 31.6 μM, while all other iminosugars were used up to 100 μM.

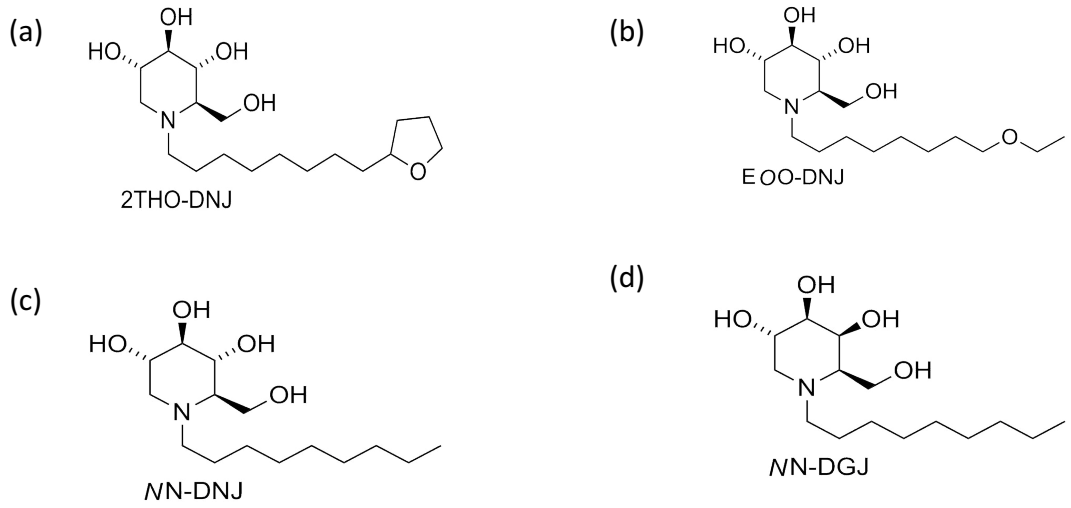

Figure 4.1: An illustration of the iminosugars used for the experiments. DNJ derivatives are: (a) 2THO-DNJ (8-tetrahydrofuranyl -octyl –DNJ), (b) E*O*O-DNJ (*N*- (8'-ethoxyoctyl)- deoxynojirimycin) and (C) *N*N-DNJ (*N*-(n-Nonyl)-deoxygalactonojirimycin). The DGJ derivative is (d) NN-DGJ (*N*-(n-Nonyl)- deoxygalactonojirimycin).

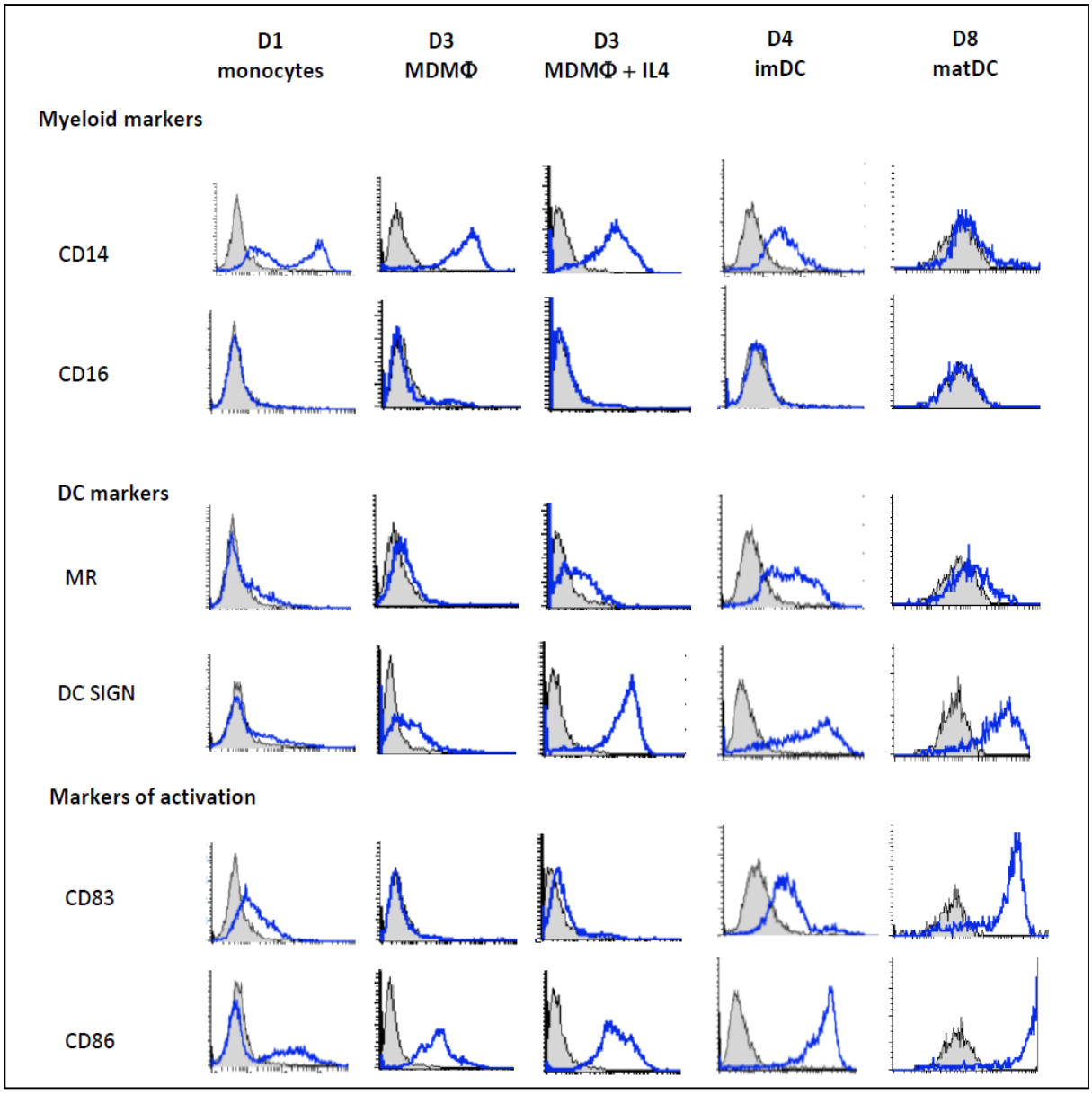

Figure 4.2: Phenotyping data of monocyte-derived macrophages and dendritic cells. Monocytes were isolated from buffy coats as described in methods (chapter 3.1) and differentiated into macrophages (D3), immature DC (D4) or mature DC (D8). The differentiation protocol is described in detail in the methods section (chapter 3.2). D1 monocytes, D3 macrophages ± IL4, D4 immature DCs and D8 mature DCs were stained using antibodies to detect 6 different surface markers (CD14, CD16, mannose receptor, DC-SIGN, CD83 and CD86). Cells were subjected to flow cytometry and the above histograms demonstrate the expression of these surface markers (in blue) compared to the isotype controls (grey filled). The Y axis represents the number of events and the X axis the fluorescence intensity. These are representative histograms from 2 independent experiments.

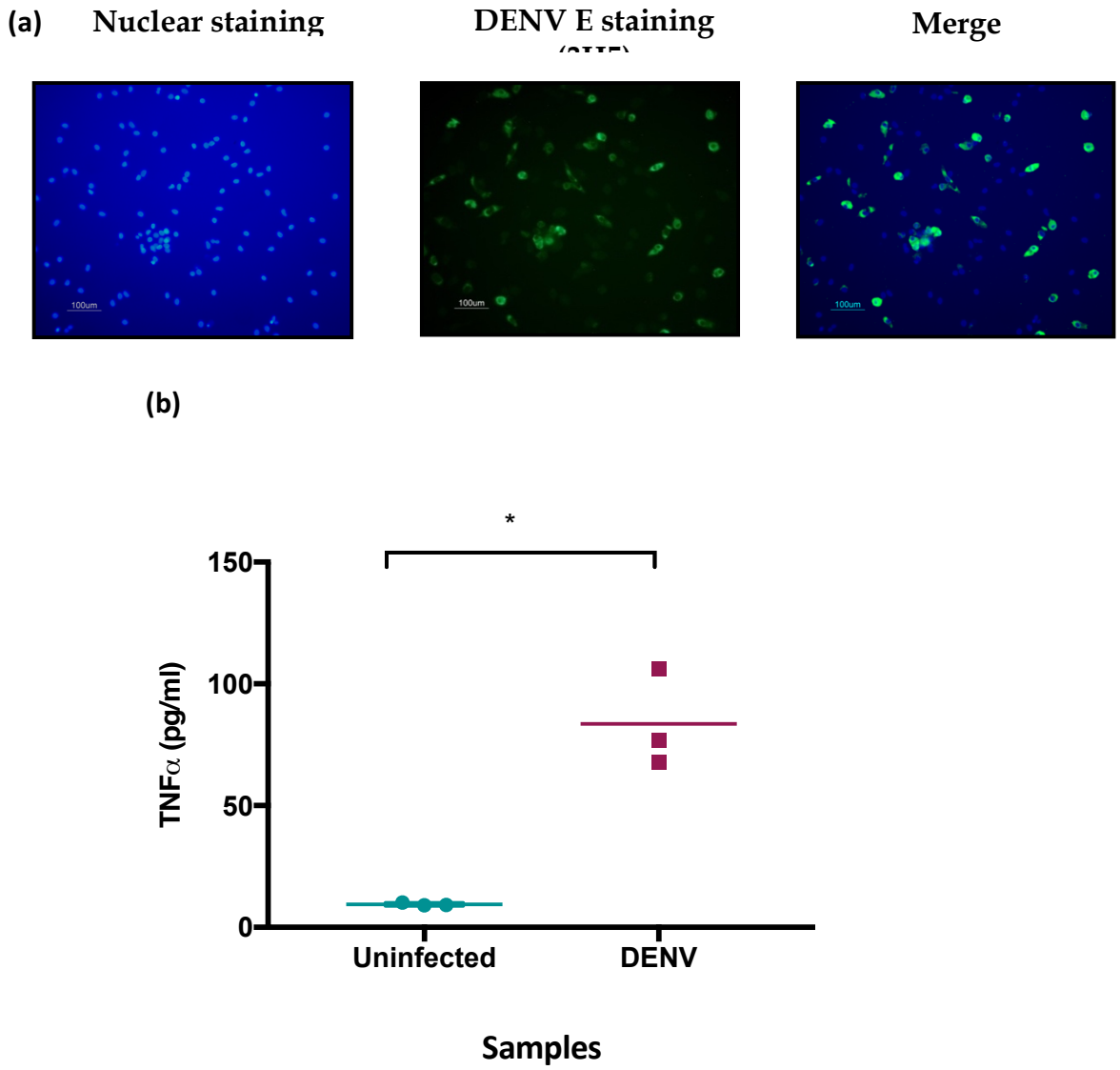

Figure 4.3: Susceptibility to DENV infection and the TNFα response in imDCs. (a) The imDCs were susceptible to DENV infection and expressed the envelope protein detected by the 3H5 antibody (green) by immunofluorescence. Nuclei are stained by DAPI (blue). (b) TNFα was secreted in response to DENV infection by imDCs (cells from n = 3 donors) and detected by a HEK-Blue™ reporter assay.

4.2.4 DNJ-derived iminosugar treatment reduced the percentage of infection of imDCs, secretion of DENV and reduced specific infectivity of the secreted virus

Immunofluorescence performed on DENV-infected imDCs revealed that the percentage of infection reduced in a dose-dependent manner following DNJ-derived iminosugar treatment. The percentage of infection reached a plateau at doses exceeding 3.16μM- 10μM and the maximum reduction observed was 70-75% compared to untreated cells (Figure 4.4).

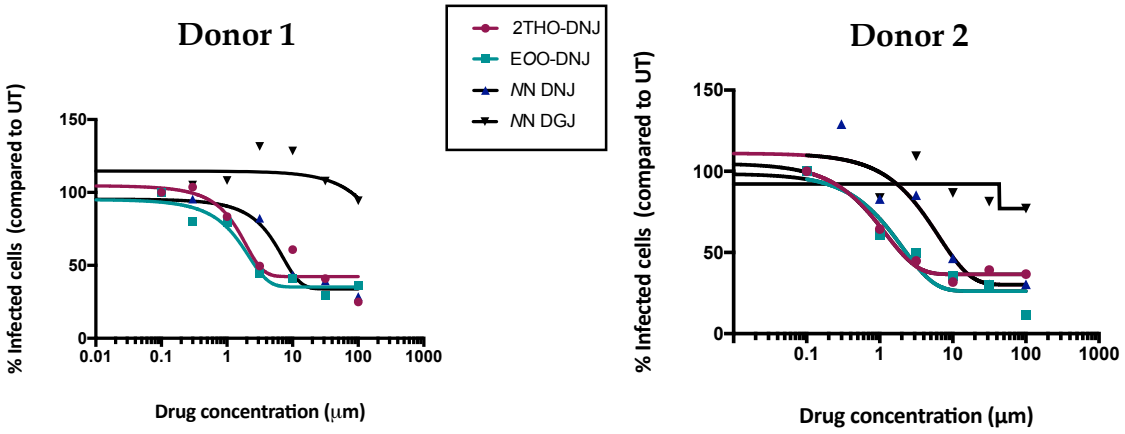

Figure 4.4: Percentage infection of DENV-infected imDCs following iminosugar treatment. The imDCs were infected with DENV at MOI 1 and treated with iminosugars for 48 hrs. Infected cells were identified by immunofluorescence using an antibody against the DENV envelope protein (3H5). The percentage of infection was normalised to the iminosugar untreated sample. Data represent analysis of 2 independent experiments. Values denote mean..

Next the infectious virus released from DENV-infected imDCs was quantified by a plaque assay and the total secreted viral genome copies were measured by qRT-PCR. Treatment with the DNJ-derived iminosugars resulted in reduction of both total genome copies and infectious virus levels suggesting that these drugs reduced virus output (Figure 4.5a-b). However, it is important to note that this reduction of secreted virus could be due to the drugs' effect on virus replication and assembly. This has been a separate question to answer in the context of iminosugar treatment. In addition, calculation of the specific infectivity (infectious virus in pfu/total viral genome copies) revealed an added effect on the infectivity at doses exceeding

10μM of iminosugars (Figure 4.5c). In contrast, *N*N-DGJ did not affect the secretion of DENV from imDCs.

Table 4.1: Antiviral activity and cytotoxicity of iminosugars in imDCs and MDMΦ

Drug	imDC			MDMΦ		
	IC_{50},μM [a](n)[b]	**IC_{90},μM [c] (n)**	**CC_{50},μM[d](n)**	**IC_{50}, μM (n)**	**IC_{90}, μM(n)**	**CC_{50},μM (n)**
2THO-DNJ	1.6± 0.8 (3)	4.7± 1.1 (3)	443 (1)	4.4±2.2 (5)[e]	23.5±14.7(5)[e]	476±6 (2)[e]
EOO-DNJ	3.1± 1.3 (3)	15.4 ± 10 (3)	>1000 (2)	9.8 (2)[f]	55.8 (2)[f]	
***N*N DNJ**	3.3± 1.5 (3)	10.1± 2.2 (3)	479±211 (2)	0.9±0.4 (4)[g]	8.0±4.1 (3)[g]	317 (1)
***N*N DGJ**	ND	ND	351±385 (2)	ND	ND	796±113 (2)

[a] IC_{50} and [c]IC_{90} indicate the concentration of iminosugar which inhibits infectious virus secretion by 50% and 90% respectively.

[b] n indicates the number of donors tested.

ND is not detected due to the absence of antiviral effects.

[d] CC_{50} indicates the concentration of the drug at which the viability of the cells is 50%.

[e] data from Beatrice Tyrrell (personal communication)

[f] data from Michelle Hill and JL Kiappes (personal communication)

[g] data from Miller *et al.* (21)

Table 4.2: Selectivity index of iminosugars in imDCs and MDMΦ

Drug	imDC (SI)	MDMΦ (SI)
2THO-DNJ	276.87	108.18
EOO-DNJ	>322.58	NA
*N*N DNJ	145.15	352.22
*N*N DGJ	ND	ND

Selectivity index (SI) was calculated as follows: SI1 = CC_{50}/IC_{50}

SI was not detected for NN-DGJ due to lack of antiviral activity

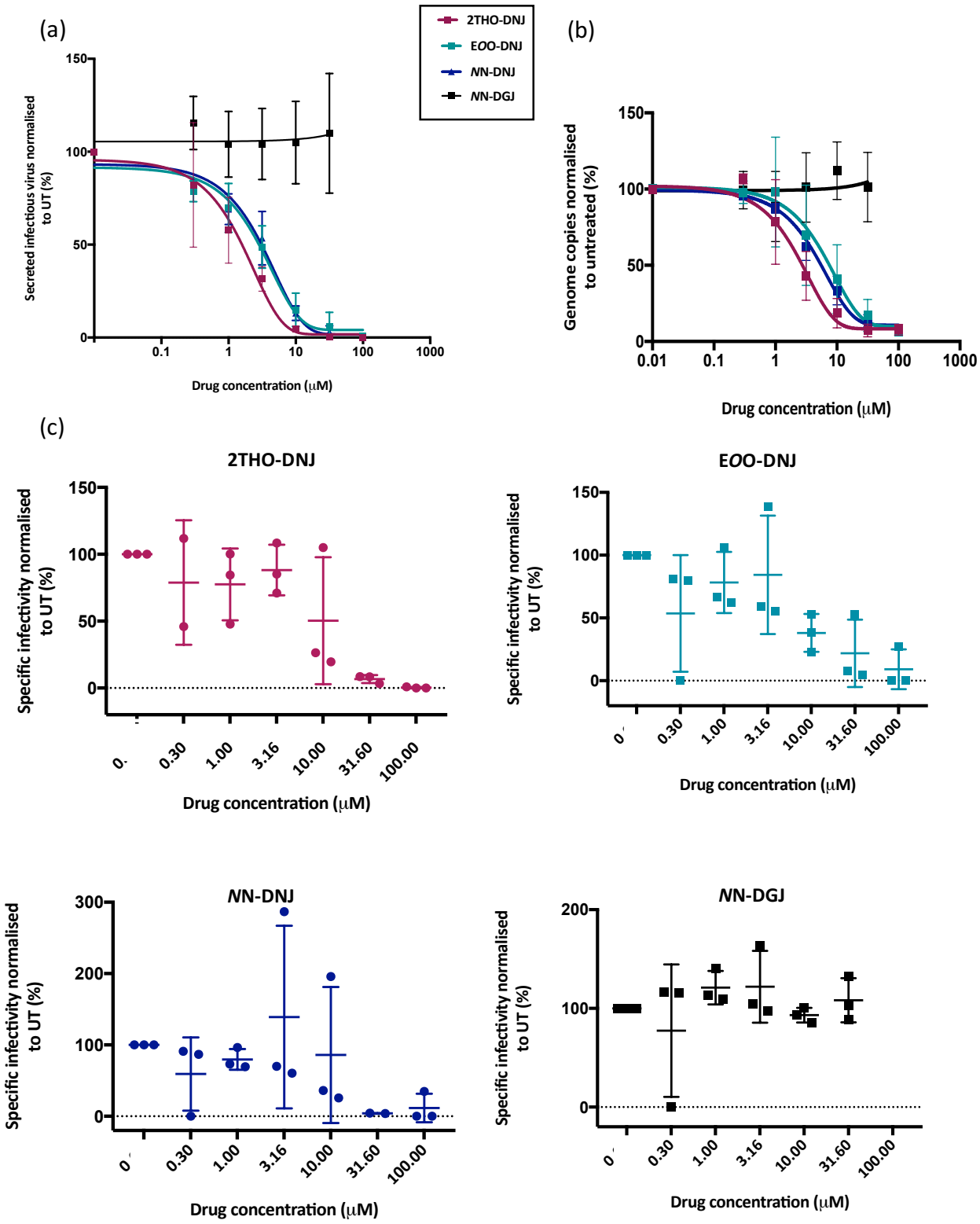

Figure 4.5: Secretion of DENV and the specific infectivity of secreted virus from iminosugar treated imDCs. (a) Infectious virus secreted from DENV-infected and iminosugar treated imDCs was quantified by a plaque assay. (b) Total DENV genome copies secreted by the imDCs following iminosugar treatment is shown in this figure. (c) Specific infectivity of the secreted virus was calculated in iminosugar treated DENV-infected imDCs. All data are normalised to the untreated (UT) control. These figures show data derived from 3 independent experiments. Values represent Mean±SEM.

4.2.5 DNJ-based iminosugars reduce DENV-induced functional TNFα levels in a dose-dependent manner

The imDCs secrete TNFα in response to DENV infection as shown above (Figure 4.3). Given the important role of this cytokine in DENV pathogenesis, we evaluated the effect of iminosugar treatment on TNFα secretion. Iminosugars affect protein folding and subsequent ER quality control. It is possible that any misfolded TNFα secreted could be detected by an ELISA assay but still fail to elicit an adequate function in the affected cells. Therefore, a functional assay was used to quantify TNFα levels in the cell supernatant. Results revealed that DNJ-derived iminosugars reduced functional TNFα levels in a dose-dependent manner (Figure 4.6). The levels were significantly reduced at concentrations exceeding 31.6μM. *N*N-DGJ treatment reduced functional TNFα levels at doses of 10μM without having a significant effect at 31.6 μM treatment. This effect was seen despite not having any antiviral effect from *N*N-DGJ treatment on DENV-infected imDCs.

4.2.6 ER α-glucosidase I inhibition by the DNJ-derived iminosugars potentiates the anti-viral effect and reduces DENV-induced TNFα levels

Following the observation of a reduction in specific infectivity of DENV by DNJ-derived iminosugars at high doses of treatment and the inhibitory effect on secreted TNFα levels, the α-glucosidase inhibition doses of the iminosugars were identified. All iminosugars were tested at 0.3 μM, 3.16 μM and 31.6 μM; the 100 μM dose was avoided due to the toxicity of *N*N-DGJ at that dose. Accumulation of $Glc_1Man_4GlcNAc_1$ species occurs due to α-glucosidase II inhibition and $Glc_3Man_5GlcNAc_1$ species can be detected following α-glucosidase I inhibition [116]. Measurement of FOS derived from DENV-infected imDCs treated with the imonosugars by NP-HPLC revealed that 2THO-DNJ, E*O*O-DNJ and *N*N-DNJ inhibited α-glucosidase II (αGluII) at doses starting from 0.3 μM which corresponded to the reduction in virus secretion seen with these drugs (Figure 4.7).

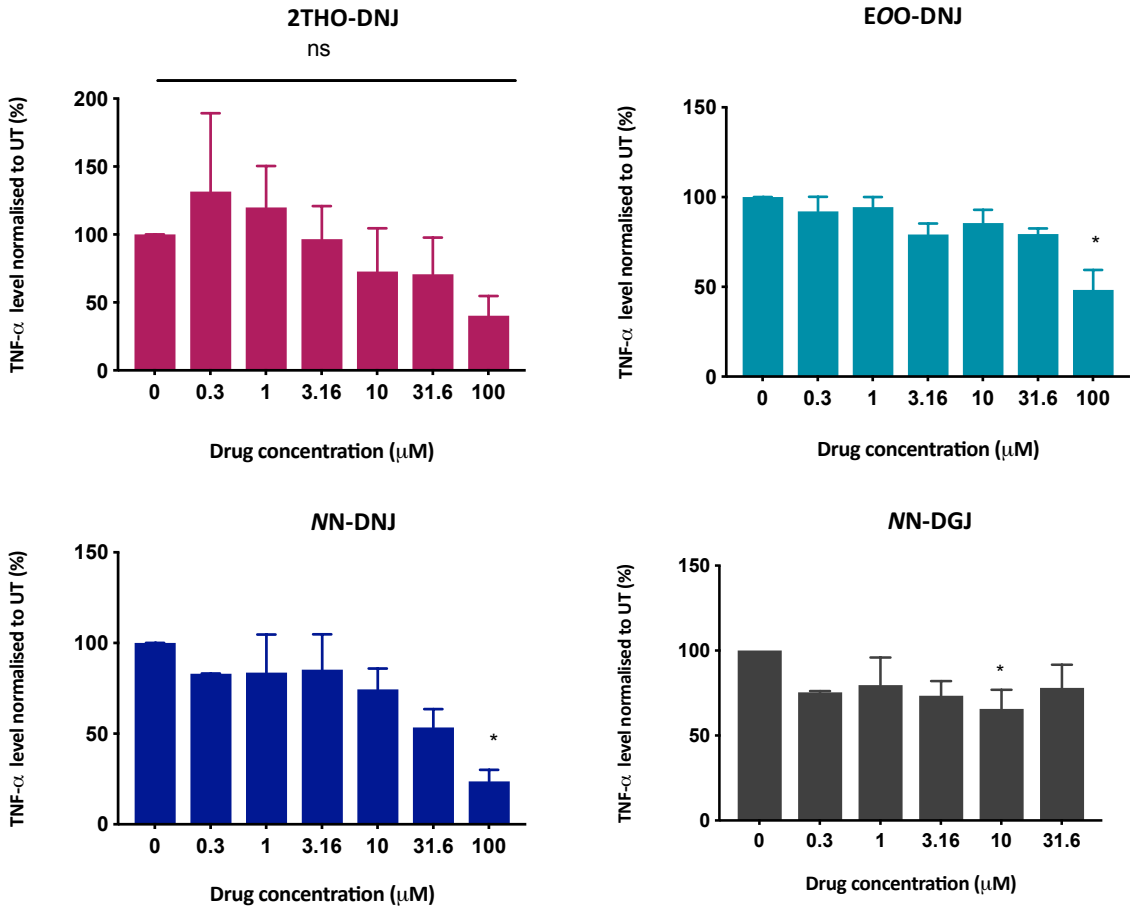

Figure 4.6: Functional TNF-α levels in imDCs treated with iminosugars. The imDCs were infected with DENV and treated with a dose titration of iminosugars. Cell culture supernatant was harvested at 48hrs p.i and evaluated for functional TNF-α levels by a reporter assay. All data are normalised to the untreated (UT) DENV-infected control. These figures show data derived from 3 independent experiments. Values represent Mean±SEM. *p<0.05.

The inhibition of α-glucosidase I (αGluI) occurred at 31.6 μM of the DNJ-derived iminosugar treatment at which stage the secretion of virus was reduced to a minimal. The reduction of the specific infectivity of secreted virus became apparent at concentrations where αGluI was inhibited and the reduction in the functional TNFα levels were also seen at these concentrations. Although αGluII inhibition is sufficient to reduce viral secretion from imDCs, these data suggest that αGluI inhibition could have an additive effect on the antiviral activity and also affect TNFα levels in DENV-infection.

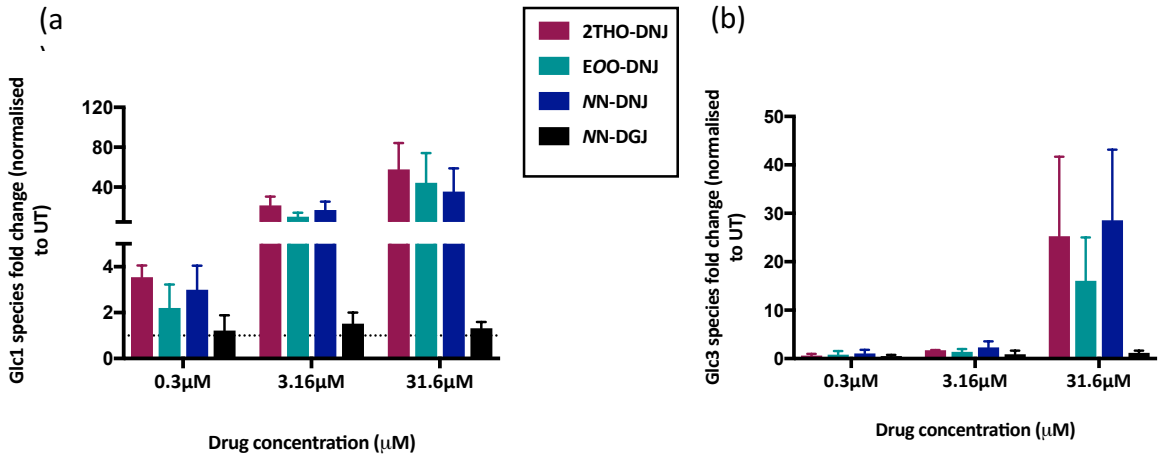

Figure 4.7: FOS levels in DENV-infected and iminosugar treated imDCs. The imDCs were infected with DENV and treated with 0.3μM, 3.16μM and 31.6μM of iminosugar. Cells were harvested at 48hrs p.i and analysed for FOS levels by NP-HPLC. (a) Glc1 species (α-glucosidase II inhibition) and (b) Glc3 species (α-glucosidase I inhibition) are shown. All data are normalised to the untreated (UT) control. These figures show data derived from 3 independent experiments. Values represent Mean±SEM. *p<0.05, **p<0.01, ***p<0.001, ****p<0.0001. NP-HPLC was performed by Juliane Brun.

4.3 Discussion:

The antiviral effects of several DNJ-derived iminosugars have been evaluated in DENV-infected primary macrophages previously [1]. Here, the evaluation of a panel of iminosugars derived from DNJ revealed similar antiviral effects in monocyte-derived imDCs. The drugs used caused minimal cytotoxicity in imDCs and comparison of the antiviral efficacy of these drugs in imDCs revealed that 2THO-DNJ (IC_{50} 1.6 μM) was more potent than *N*N-DNJ (IC_{50} 3.3 μM) and E*O*O-DNJ (IC_{50} 3.1 μM). This was different to data derived from MDMΦ where *N*N-DNJ had lower IC_{50} values than 2THO-DNJ (0.9 μM vs 4.4 μM) suggesting that cell type specific differences in antiviral efficacy exist. *N*N-DGJ did not elicit antiviral effects, consistent with previous literature [1] and the absence of α-glucosidase inhibition by *N*N-DGJ treatment in DCs, further supports that the iminosugars achieve antiviral effects by ER α-glucosidase inhibition rather than glycolipid processing inhibition.

Inhibition of αGluII by the DNJ-derived iminosugars is sufficient to induce antiviral effects in imDCs as shown previously for T*O*P-DNJ, a selective αGluII inhibitor [144]. However, key differences were observed in the antiviral effects elicited by doses inhibiting only αGluII compared to doses at which both α-glucosidases were inhibited. These DNJ-derived drugs reduced expression of viral envelope (DENV E) protein at doses inhibiting αGluII. A dose dependent reduction was seen in the percentage of cells expressing DENV E protein, in addition to a reduction in virus secretion, with increasing iminosugar concentration. The percentage of infection did not reduce to zero but plateaued with increase in iminosugar treatment and it is apparent that cells are still infected with DENV at higher doses of the drug treatment inhibiting αGluI. This is quite interesting given the fact that the secretion of DENV is negligible at these drug doses suggesting that the infected cells express viral envelope protein but are unable to release fully assembled virion particles that could be detected by a qRT-PCR against NS5 genome nor induce infectivity in a plaque assay. It is also possible that

E protein of infected cells persist longer before degradation in these cells. Inhibition of αGluI in addition to αGluII at higher doses of iminosugar treatment significantly reduced virus secretion from imDCs despite not reducing the percentage of infected cells further. Furthermore, secreted virus, albeit minimal had significantly lower infective potential as seen by the reduction in specific infectivity at doses of drugs that inhibited αGluI. Iminosugars were previously thought to have insignificant effects on specific infectivity of secreted DENV[1]. This was contrary to data seen in human immunodeficiency virus (HIV) infection when treated by *N*B-DNJ in which the drug reduced infectivity of secreted virus without reducing viral output [147]. However, findings on imDCs suggest that DNJ-derived iminosugars have a dual effect and the drugs significantly reduce DENV secretion at all doses of treatment while reducing specific infectivity at doses inhibiting αGluI.

The functional TNFα assay reveals a reduction in this cytokine following high-dose treatment of the DNJ-derived iminosugars. The observed 30-40% reduction of TNFα levels seen with *N*N-DGJ treatment is independent of any antiviral effects and it is difficult to explain the reason for this observation. FOS analysis confirms that *N*N-DGJ treatment does not inhibit the α-glucosidases at any doses used in these experiments suggesting that TNFα reduction is due to an α-glucosidase independent effect and perhaps due to a yet unidentified mechanism. Drug was not toxic at doses less than 100 μM and drug toxicity could well be excluded as the cause for the reduction in TNFα. Future experiments to understand any effects of *N*N-DGJ on inflammatory signalling cascades leading to reduced TNFα secretion will be helpful to answer this question.

The additive antiviral effects observed at iminosugar doses exceeding 3.16 μM correspond to αGluI inhibition and the results from this chapter suggest that αGluI inhibition potentiates the antiviral effects of iminosugar treatment by reducing secretion of virus and reducing

infectivity of particles released from the cells. In addition, αGluI inhibition corresponded to the reduced TNFα levels observed with iminosugar treatment. These data suggest that αGluI inhibition by iminosugars is important for its antiviral effects and the anti-TNFα effect against DENV infection. Following these findings, 2THO-DNJ was selected as the candidate drug to continue with all other experiments described in this thesis.

Although the antiviral effects of iminosugars and toxicity on imDCs provide important data on the action of these drugs, human infection is complex and many other factors could potentially influence the overall effect of these drugs. As such, care should be taken when extrapolating *in vitro* findings to human clinical infections.

V

The effect of 2THO-DNJ on the DENV-induced unfolded protein response

The unfolded protein response (UPR) and ER stress play a significant role in determining the outcome of viral infection. DENV modulates this host response to its advantage. There are no data available on the effect of DENV infection on the UPR in primary cells and no data on the effect of DNJ-derived iminosugars on this DENV-induced response. Results described in this chapter in a primary macrophage cell culture model revealed that DENV activates the IRE1α-XBP1 pathway preferentially over the PERK arm. Chemical inhibition of the IRE1α endonuclease activity produced an antiviral effect and reduced the secretion

of TNFα and IFNα levels. Treatment with 2THO-DNJ attenuated the activation of the IRE1α-XBP1 pathway as evidenced by reduced XBP1s levels suggesting that the drug dampens excessive activation of the IRE1α-XBP1 arm in DENV-infection. This effect was also seen in response to other non-replicating ER stress inducers and treatment with 2THO-DNJ significantly increased transcription of ERAD-associated chaperones. PERK-eIF2α-ATF4 pathway inhibition resulted in reduced TNFα levels without a significant effect on antiviral activity. Treatment with 2THO-DNJ activated the PERK-eIF2α-ATF4 pathway in DENV infection. Results in this chapter revealed that 2THO-DNJ treatment in the absence of DENV-infection does not induce a significant UPR response. Further evaluation of the effect of 2THO-DNJ revealed that the drug does not rely on the UPR for its antiviral or TNFα and IFNα reducing effect.

5.1 Introduction

The cellular ER machinery is indispensable for protein synthesis and secretion, lipid biogenesis, carbohydrate metabolism and calcium storage in a cell [148]. Co- and post-translational modification and folding of proteins occurs in the ER, which co-ordinates secretion of proteins together with the Golgi and trans-Golgi network as described in detail in chapter 1. It is not surprising that viruses hijack this complex network and factory to synthesize viral proteins. The high turnover of pathogen-derived and host proteins during viral infections induces a protein burden on the ER. Cells have evolved a counteracting response against this ER stress in an attempt to evade cell death by facilitating protein folding, attenuating protein translation and increasing ER-associated protein degradation (ERAD). This "unfolded protein response" (UPR) is initiated by three transmembrane proteins residing in the ER which activate a cascade of downstream signaling events summarized in Figure 5.1 and described in chapter 1. The UPR is activated by many DNA viruses such as herpes simplex virus (HSV) [149, 150], cytomegalovirus (CMV) [151], human papilloma virus [152], adeno virus [153] and RNA viruses including Japanese encephalitis virus (JEV) [154], hepatitis C virus [81, 155], West Nile virus [156] and influenza A virus [157]. DENV infection is known to activate the UPR and use this response to its advantage [33]. Studies reveal activation of the UPR in a DENV infected human fibrosarcoma cell line [46], THP-1 and U937 monocytic cell lines [52, 54], A549 human alveolar epithelial cell line [51] and HepG2 human hepatocyte cell line [158]. While studies claim that DENV activates all three arms of the UPR pathway [51], findings also support limited activation of some of these signaling cascades [46, 159]. Activation of the PERK arm of the UPR results in phosphorylation of eIF2α which attenuates translation of mRNA in an attempt to reduce ER protein burden. It is perhaps of no surprise therefore that DENV inhibits the phosphorylation of eIF2α to continue viral protein production [46]. This is presumed to be achieved by activating GADD34 which counteracts

phosphorylation of eIF2α [51]. A similar mechanism is observed in HSV infection where the virus protein $\gamma_1$34.5 forms a complex with protein phosphatase 1α (PP1α) to inhibit eIF2α phosphorylation and thereby inhibit its activation [160]. Human CMV infection limits phosphorylated eIF2α (p-eIF2α) to overcome translation attenuation during infection and CMV also reduces ATF6 activation [151]. In addition, the IRE1α-XBP1 pathway was observed to be activated by CMV despite not activating the downstream ERAD-associated transcript, ER degradation-enhancing alpha-mannosidase like protein (EDEM) in this study. These studies provide evidence on how viruses manipulate the UPR by selectively activating proviral mechanisms to facilitate replication and persistence.

Use of different cell culture models might contribute to the different findings observed in studies evaluating the UPR activation in DENV-infection and highlight the importance of using relevant cell lines for a better understanding and interpretation of research findings. In addition, the neoplastic nature of available cell lines in itself increases the protein turnover and alters cell signaling pathways which could mask virally induced effects. There is no data available in DENV-infected primary cells. Monocytes, dendritic cells and macrophages provide a major reservoir for viral replication during a human clinical infection [130]. The resulting activation of host responses in these cells contributes to the outcome of the disease. Although any *in vitro* model would have its own drawbacks, primary monocyte-derived cells represent a better *ex vivo* model to study DENV-induced host responses. This chapter attempts to fill this gap in the available literature and discusses the modulation of the PERK and IRE1α pathways by DENV in primary monocyte-derived macrophages.

Iminosugars inhibit ER α-glucosidases and interfere with glucose trimming which affects folding of *N*-glycosylated proteins. Use of such glucose mimetics in DENV-infection is

believed to misfold DENV proteins which could potentially activate the UPR due to ER stress. It is intriguing to evaluate the UPR during iminosugar treatment and DENV-infection given the complex modulation of this host process by the virus *per se*. There are many questions: *Does treatment with an iminosugar increase or decrease ER stress and the UPR? Does this activation or inhibition help to reduce virus secretion as observed with iminosugar treatment? Could this change in the UPR contribute to the TNFα and IFNα reduction observed with iminosugar treatment?* Rathore *et al*. reported activation of the UPR by Celgosivir, a castanospermine-derived iminosugar in DENV-infected THP-1 cells [161]. However, there are no reports on the effects of DNJ-derived iminosugars in DENV-infection in primary immune cells. Previous data from the lab in mice suggested that Celgosivir and the DNJ-derived iminosugar MON-DNJ could modulate host responses differently [2]. Therefore, this thesis chapter provides a comprehensive analysis of the IRE1α-XBP1 and PERK-eIF2α-ATF4 pathways in DENV infection and evaluates the effect of the iminosugar 2THO-DNJ on this response in primary monocyte-derived macrophages. This is the first study evaluating this host response in primary cells following DENV infection.

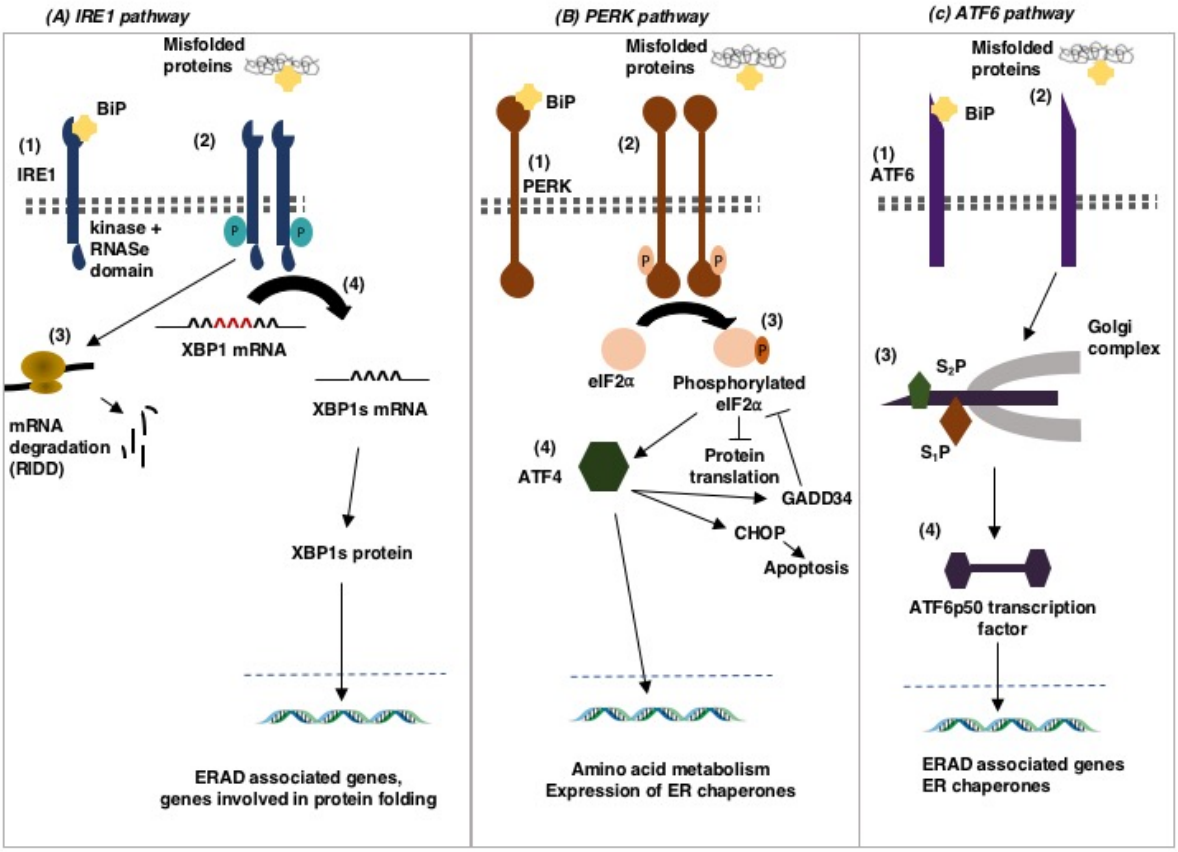

Figure 5.1: Activation of UPR pathways in response to ER stress.(A) IRE1 pathway; (1) IRE1 is kept in an inactive state by BiP. (2) Dissociation of BiP results in dimerization and trans-autophosphorylation (by the kinase domain) of IRE1 which activates the RNase domain. (3) RIDD: The RNAse domain causes degradation of several mRNA and microRNA (e.g. mir17). (4) The IRE1 RNase segment cleaves XBP1mRNA transcript to produce the multifunctional transcriptional factor, XBP1s. XBP1s activates ERAD associated genes to degrade misfolded proteins and genes promoting protein folding. **(B) PERK pathway; (**1) PERK is kept in an inactive state by BiP. (2) Once dissociated from BiP, PERK dimerizes and auto-phosphorylates to activate its kinase activity. (3) Activated PERK catalyzes phosphorylation of eukaryotic translation initiation factor 2α (eIF2α) which inhibits protein translation. (4) ATF4 induced by eIF2α, induces activation of C/EBP homologous protein (CHOP) and growth arrest and DNA damage inducible 34 (GADD34) which mediates apoptosis. GADD34 dephosphorylates eIF2α to maintain a negative feedback. **(C) ATF6 pathway;** (1) ATF6 is maintained in an inactive state by BiP. (2) Dissociation of BiP uncovers the Golgi localization signal of ATF6. (3) The N-terminus of ATF6 is cleaved by site 1 and site 2 proteases (S1P and S2P). (4) Cleaved and activated transcription factor ATF6p50 translocates to the nucleus to induce genes associated with ERAD and ER chaperones. Arrows in the diagram represent positive effects while blocked lines represent inhibition.

5.2 Results

5.2.1 The unfolded protein response in DENV-infected macrophages

The experiments were conducted in primary monocyte-derived macrophages. For experiments requiring larger number of cells, such as time course experiments, an immune cell line (THP-1 cells) was used due to feasibility. The THP-1 monocytes have been derived from a patient with acute monocytic leukaemia. These cells were differentiated to macrophages by treating with PMA for 72 hours. This differentiation results in greater susceptibility to virus infection and upregulation of CD14 and Toll-like receptors (TLRs) [162]. Differentiation and infectivity of THP-1 macrophages were optimized prior to experiments. Tunicamycin (Tm) which inhibits N-linked glycosylation causing ER stress and activation of the UPR, was used as a positive control. Tm The two arms of the UPR were studied in THP-1 macrophages from 3 hours post-infection (p.i.) to 72 hours p.i. to identify the best time point to investigate these pathways. The results showed that the PERK arm was not significantly activated by DENV in THP-1 macrophages during infection (Appendix 2, Figure S1) and the IRE1α-XBP1 arm was activated with an increase in XBP1s and XBP1t in THP-1 cells (Appendix 2, Figure S1).

Activation of the PERK arm of the UPR results in auto-phosphorylation of PERK protein and phosphorylation of eIF2α. The p-eIF2α attenuates protein translation but selectively translates proteins such as activating transcription factor 4 (ATF4). Western blots were performed at each time point to look at the effect of DENV on three proteins in the PERK pathway (Figure 5.2a). Phosphorylated PERK (pPERK) protein could not be detected due to the lack of a good antibody against human pPERK. A non-significant increase in ATF4 protein was seen across cells from three donors at 12 hours p.i. compared to the uninfected control (Figure 5.2). The ATF4 protein level was reduced back to baseline by 24 hours suggesting that DENV induced PERK-eIF2α-ATF4 activation was transient and minimal.

Tm treatment increased ATF4 protein 2-fold from the untreated control. This is shown in figure 5.3. However, the PERK arm activation in primary macrophages to even Tm was minimal. However, it is possible that even a minimal increase in the protein level could have a significant effect on its downstream targets. The ATF4 mRNA levels did not change following DENV-infection at 6 hours or 12 hours p.i. Tm treatment increased ATF4 mRNA levels by 2-fold from untreated control similar to the protein response (figure 5.3). The protein levels detected by western blot suggested that the activated downstream proteins of the PERK pathway were low in levels in macrophage cell lysates even during DENV-infection. This data is consistent with results from Pena *et al*. who suggested that DENV infection suppresses the eIF2α phosphorylation to overcome the inhibition of protein translation [46]. The ATF4 levels measured by densitometry of the western blots in infected primary macrophages was not significantly higher than in the uninfected control which questions the relevance of this pathway during DENV infection in macrophages.

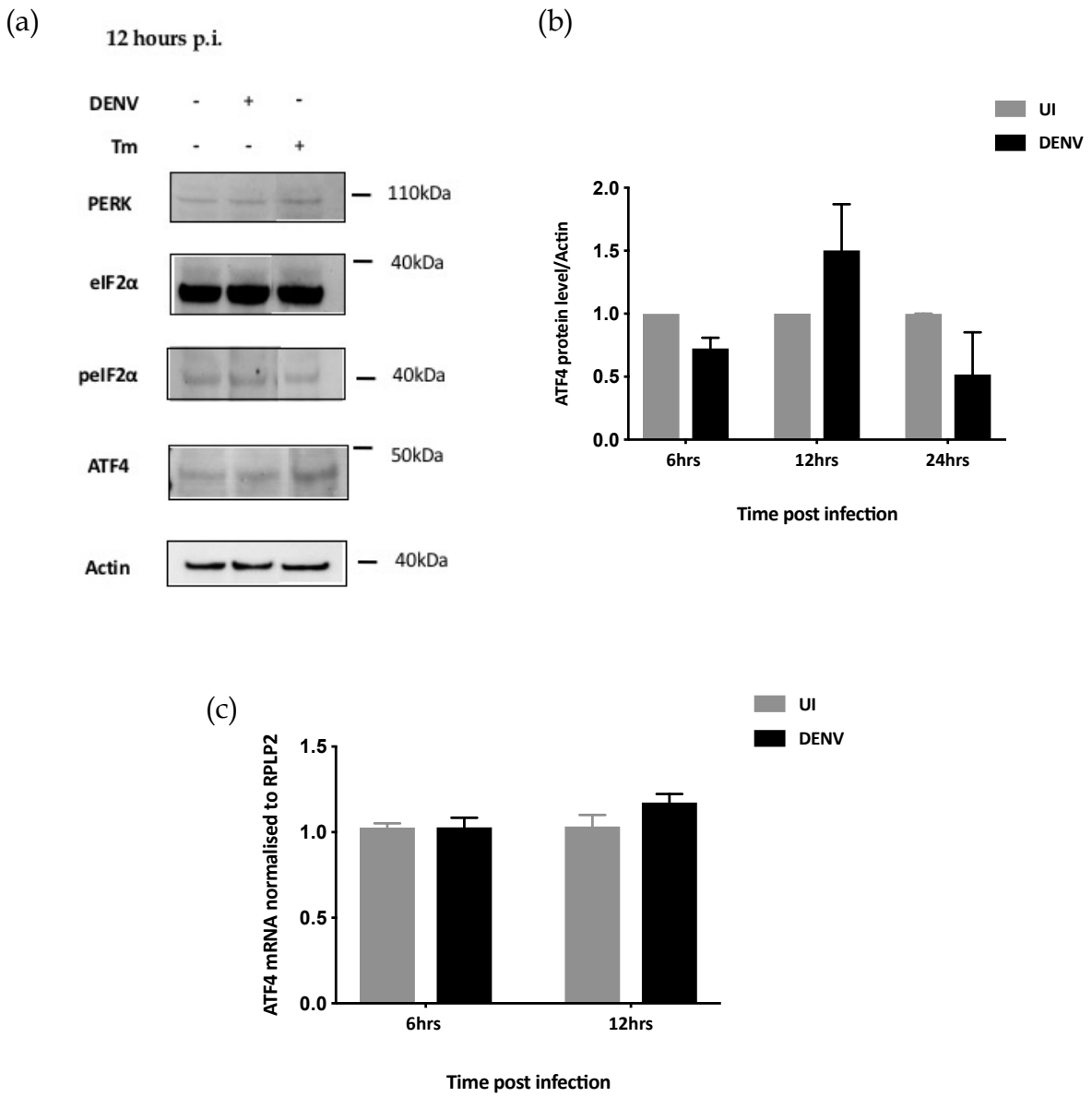

Figure 5.2. Activation of the PERK-eIF2α-ATF4 pathway in primary macrophages. Primary macrophages were infected with DENV (MOI 1), uninfected or treated with 1μg/ml Tm for 6 hours. (a) Western blots were performed on cell lysates for PERK, peIF2α and ATF4. Actin was used as the housekeeping control. A representative blot at 12 hours p.i. is given. (b) Densitometry was used to quantify protein bands in western blots in DENV-infected macrophages at 6 (n=2), 12 (n=3) and 24 (n=2) hours p.i. and pooled data shown in the figure. (c) qRT-PCR was performed to quantify ATF4 mRNA levels in macrophages at 6 and 12 hours p.i. (n=3). All values represent mean and error bars represent standard error of the mean, n denotes the number of donors.

The IRE1α-XBP1 pathway activation results in the splicing of 26bp from the XBP1 mRNA to yield the XBP1 spliced (XBP1s) mRNA. Quantification of cellular RNA using qRT-PCR in primary macrophages revealed that this pathway is activated at 48 hours p.i. with a significant increase in both total XBP1 (XBP1t) and XBP1s levels (Figure 5.3). The greater increase in splicing of the XBP1 mRNA resulted in an increased ratio of XBP1s/XBP1t in macrophages during DENV infection. This was different to the response observed with Tm treatment which did not increase XBP1t levels significantly but led to increased splicing activity. The level of XBP1s production in response to DENV infection was similar to that of Tm activation which suggests that the IRE1-XBP1 pathway is strongly activated by DENV in primary macrophages. In addition, the IRE1α-XBP1 pathway activation was seen at 48 hours p.i., i.e. later than the PERK pathway which was marginally activated at 12 hours p.i. in primary macrophages consistent with previous literature from Pena *et al.* performed in human fibrosarcoma cells [46].

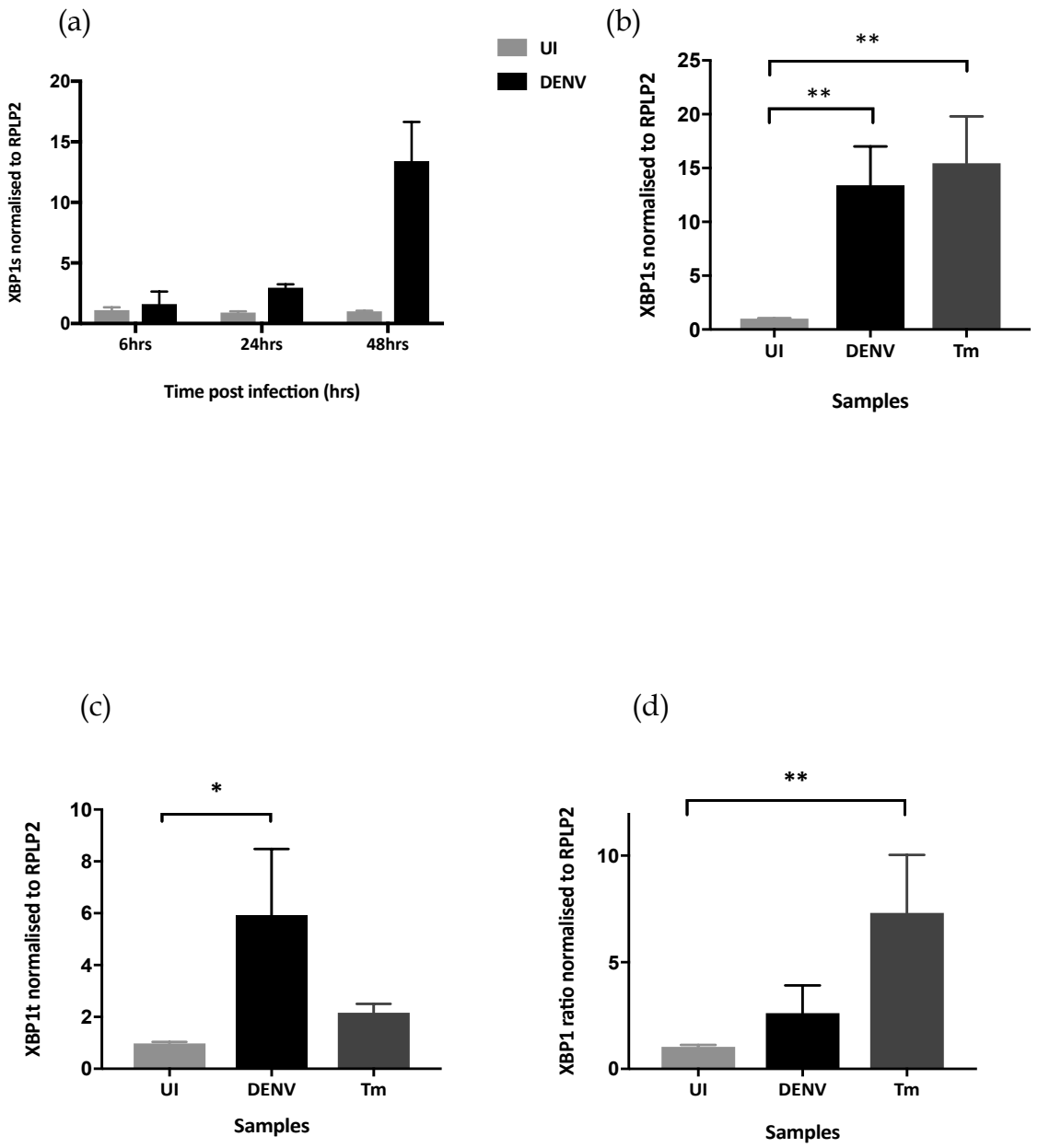

Figure 5.3. Activation of IRE1α-XBP1 in DENV-infected primary macrophages. Primary macrophages were infected with DENV (MOI 1), uninfected or treated with Tm 1μg/ml for 6 hours. qRT-PCR was performed to quantify sXBP1 and XBP1t RNA levels normalised to RPLP2 RNA. (a) XBP1s levels in DENV-infected macrophages at 6 (n=2), 24 (n=2), and 48 (n=3) hours p.i.; (b) XBP1s levels 48 hours p.i. in macrophages (n=3); (c) XBP1t levels 48 hours p.i. in macrophages (n=3); (d) XBP1s/XBP1t ratio at 48 hours p.i. (n=3). Mean values are given in the figures and error bars represent standard error of the mean. Data were analysed by one-way ANOVA. *$p<0.05$, **$p<0.01$

Given the significant activation of the IRE1α-XBP1 pathway by DENV-infection, it was intriguing to see the effect of this pathway on viral secretion and cytokine response. An endonuclease inhibitor, 4μ8c was used to inhibit IRE1α induced splicing of XBP1 and for

comparison with effects of the PERK pathway, GSK2606414, a kinase inhibitor, was used to inhibit PERK mediated phosphorylation. These two inhibitors of the UPR were used within a non-toxic concentration range to examine the effect on virus secretion and secretion of TNFα and IFNα from primary macrophages. Different regimes of using the inhibitors were studied. Pre-treatment with the inhibitors prior to DENV infection resulted in a rebound activation of the pathways during DENV replication (data not shown). Therefore, cells were treated with the inhibitor during DENV infection at the viral binding and entry stages and also during subsequent incubation with media to achieve maximum inhibition. The maximum non-toxic dose of 4μ8c was determined to be 40 μM which inhibited DENV-induced XBP1s by 30% (Appendix 2, Figure S2) and the inhibitor GSK2606414 was used at 1 μM for these experiments. The results showed that the secretion of total viral genome copies as well as infectious virus was significantly reduced by chemical inhibition of the IRE1α pathway (Figure 5.5). There was no significant reduction in secretion of total or infectious virus when the PERK pathway was inhibited. These findings suggest that the IRE1α-XBP1 activation that occurs in the presence of DENV is proviral in primary macrophages.

The effect of UPR pathway inhibition on the cytokine response to DENV infection was studied by quantifying secreted TNFα and IFNα levels in cell culture supernatant. Both TNFα and IFNα levels were significantly reduced by 4μ8c treatment (Figure 5.4 d-e). Treatment with GSK2606414 reduced DENV-induced TNFα levels but did not affect IFNα levels significantly. These data suggest that the IRE1α-XBP1 activation that occurs in response to DENV-infection creates a proviral milieu and increases TNFα cytokine secretion and IFNα secretion from primary macrophages. The DENV- induced PERK arm activation, although minimal, seems to increase TNFα levels in response to DENV-infection which was reduced following GSK2606414 treatment. This effect on TNFα is

likely to be independent of its effect on viral secretion.

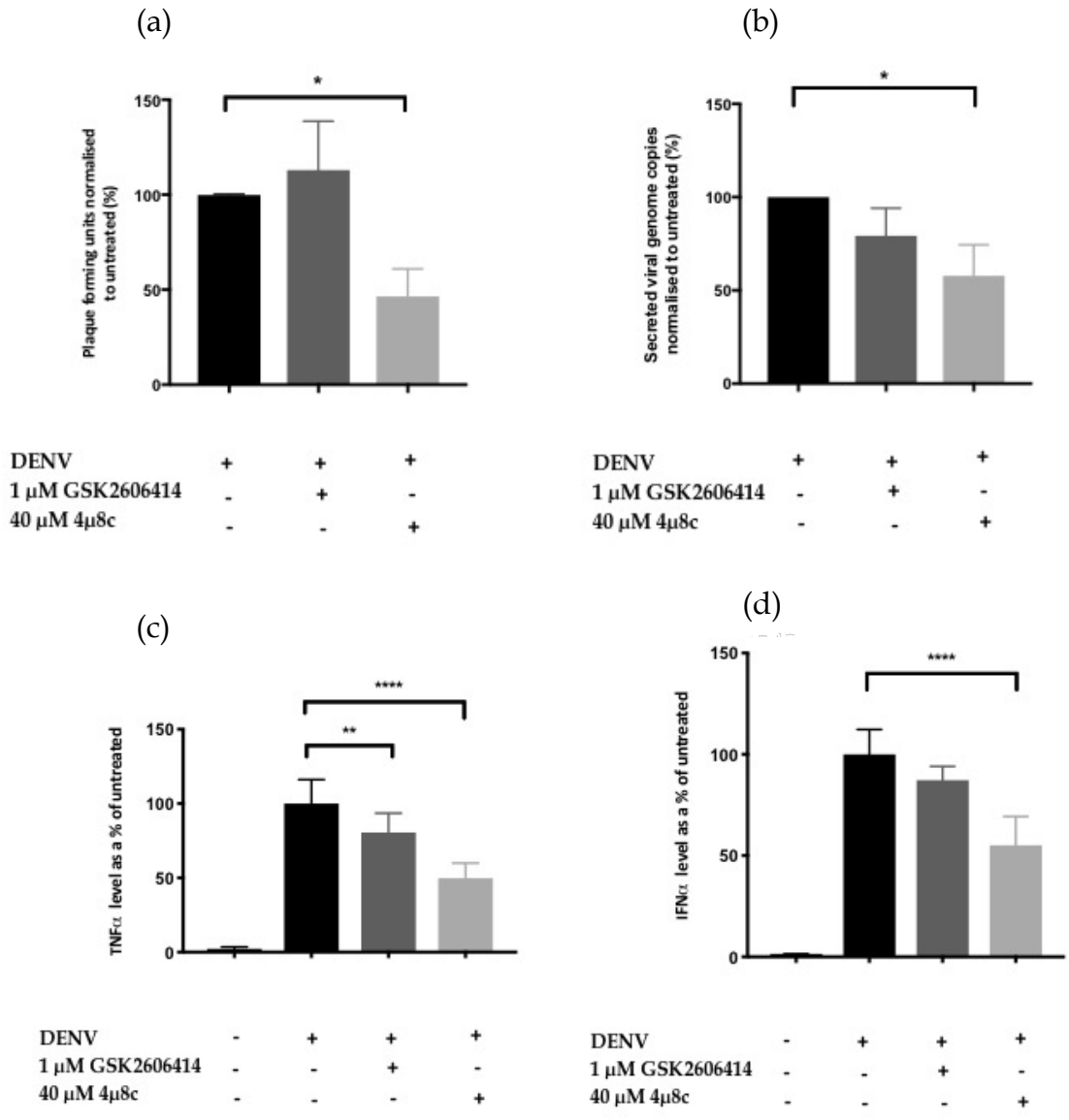

Figure 5.4. The effect of chemical inhibition of UPR arms on DENV secretion and secretion of TNFα and IFNα. Primary macrophages were infected with DENV (MOI 1) in the presence or absence of 1 μM GSK2606414 or 40 μM 4μ8c for 48 hours. (a) Secreted infectious virus was measured by plaque assay, (b) total secreted viral genome copies detected by qRT-PCR, (c) secreted functional TNFα levels measured in the cell culture supernatant and (d) secreted functional IFNα measured by a functional assay. All data represent pooled values from 3 independent experiments. Data represent mean and the error bars denote standard error of the mean. Data were analysed by one-way ANOVA. *p<0.05, **p<0.01, ****p<0.0001.

5.2.2. The Effect of 2THO-DNJ treatment on DENV-induced UPR

After identifying the UPR response to DENV infection in primary macrophages, the effect of 2THO-DNJ treatment was studied at 12 hours p.i. This time point was selected because the maximum increase of ATF4 levels by DENV was observed at this time (Figure 5.2). Evaluation of the PERK-eIF2α-ATF4 proteins by western blot revealed minimal changes in these proteins following either DENV infection or treatment with 2THO-DNJ (Figure 5.5a). Treatment with the stress inducer Tm increased ATF4 mRNA levels (Figure 5.5c-d) and also increased the ATF4 protein levels (Figure 5.5b). Treatment with the compound 2THO-DNJ increased ATF4 mRNA levels and the ATF4 protein in DENV infected cells. An increase in ATF4 mRNA level was seen in uninfected 2THO-DNJ-treated cells although the ATF4 protein did not change significantly in those cells. The results show a slight but non-significant increase in the ATF4 protein level following 2THO-DNJ treatment. However, even a minor increase in the protein levels of these mediators could still produce a significant effect in target organs. Overall, the results suggest that DENV does not activate the PERK pathway and that 2THO-DNJ seems to increase ATF4 mRNA and protein levels in DENV-infected cells.

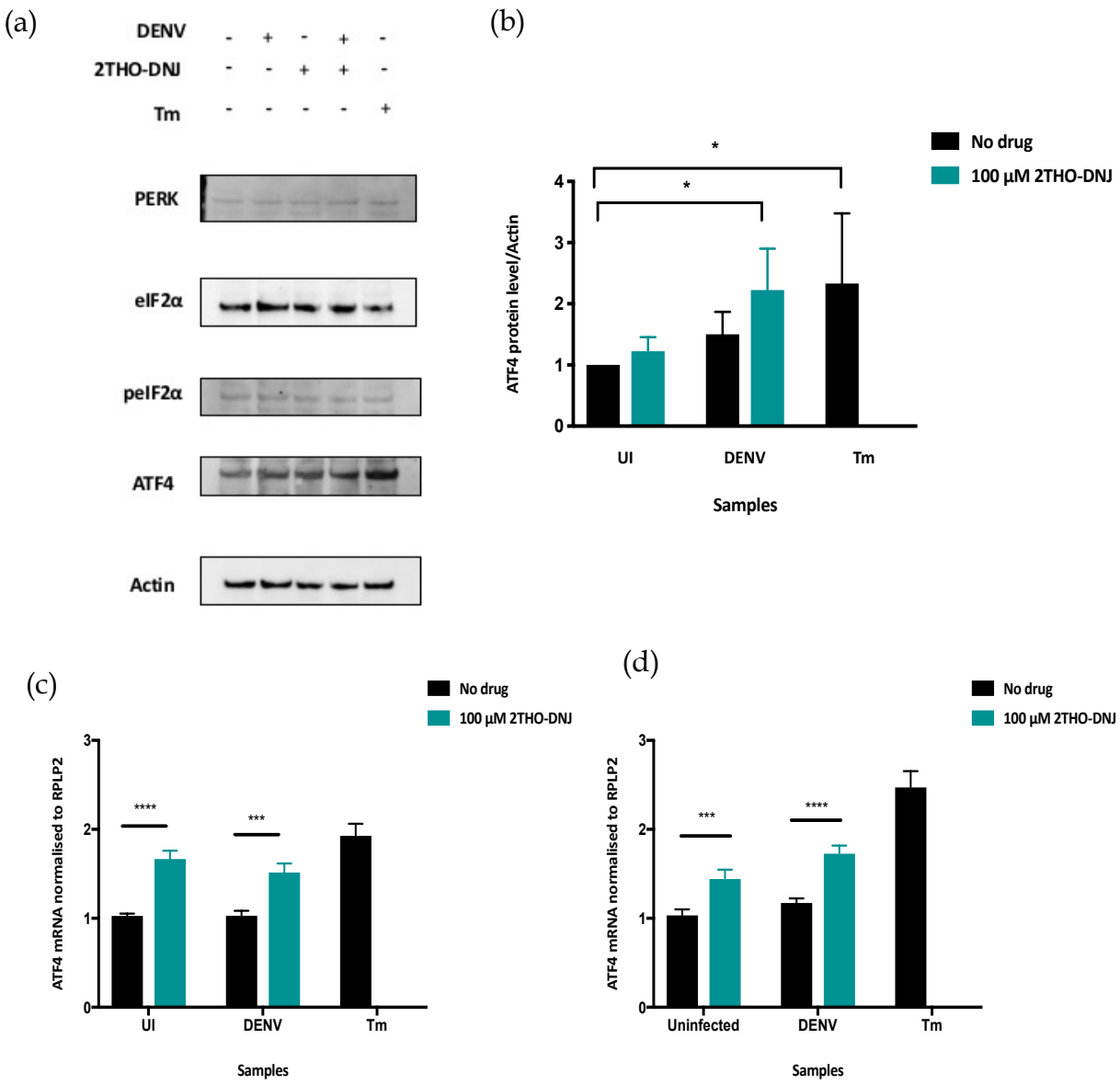

Figure 5.5. The effect of 2THO-DNJ treatment on PERK-eIF2α-ATF4 pathway. Primary macrophages were infected with DENV at MOI 1 and treated or untreated with 2THO-DNJ 100 μM for 12 hours p.i. Positive control was 1 μg/ml Tm for 6 hours. (a) Western blot image is a representative blot showing the expression of PERK, eIF2α, ATF4 proteins. (b) Densitometry values of ATF4 protein expression normalised to actin protein. (c) ATF4 mRNA levels at 6 hours p.i, (d) ATF4 mRNA levels at 12 hours p.i. quantified by qRT-PCR. All values represent the mean of 3 independent experiments and the error bars show standard error of the mean. Analysed by 2-way ANOVA. *$p<0.05$, ***$p<0.001$, ****$p<0.0001$.

In contrast, the IRE1α-XBP1 pathway was activated strongly by DENV in primary macrophages. This was achieved by increasing XBP1t levels and also by specifically increasing splicing of unspliced XBP1 to XBP1s at 48 hours p.i. as evidenced by the XBP1s/XBP1t ratio exceeding one. 2THO-DNJ treatment reduced this heightened activation significantly (Figure 5.6). Both XBP1t levels and XBP1s levels were reduced by 2THO-DNJ treatment following DENV infection, which was likely achieved by a reduction in XBP1t mRNA levels and as a consequence, XBP1s levels (Figure 5.6). This was reflected in the ratio of XBP1 mRNA (Figure 5.6c). There was no significant change seen in the IRE1α-XBP1 pathway (activated transcription factor XBP1s), upon treatment of uninfected cells by the compound 2THO-DNJ suggesting that the iminosugar does not increase this arm of the UPR in uninfected cells.

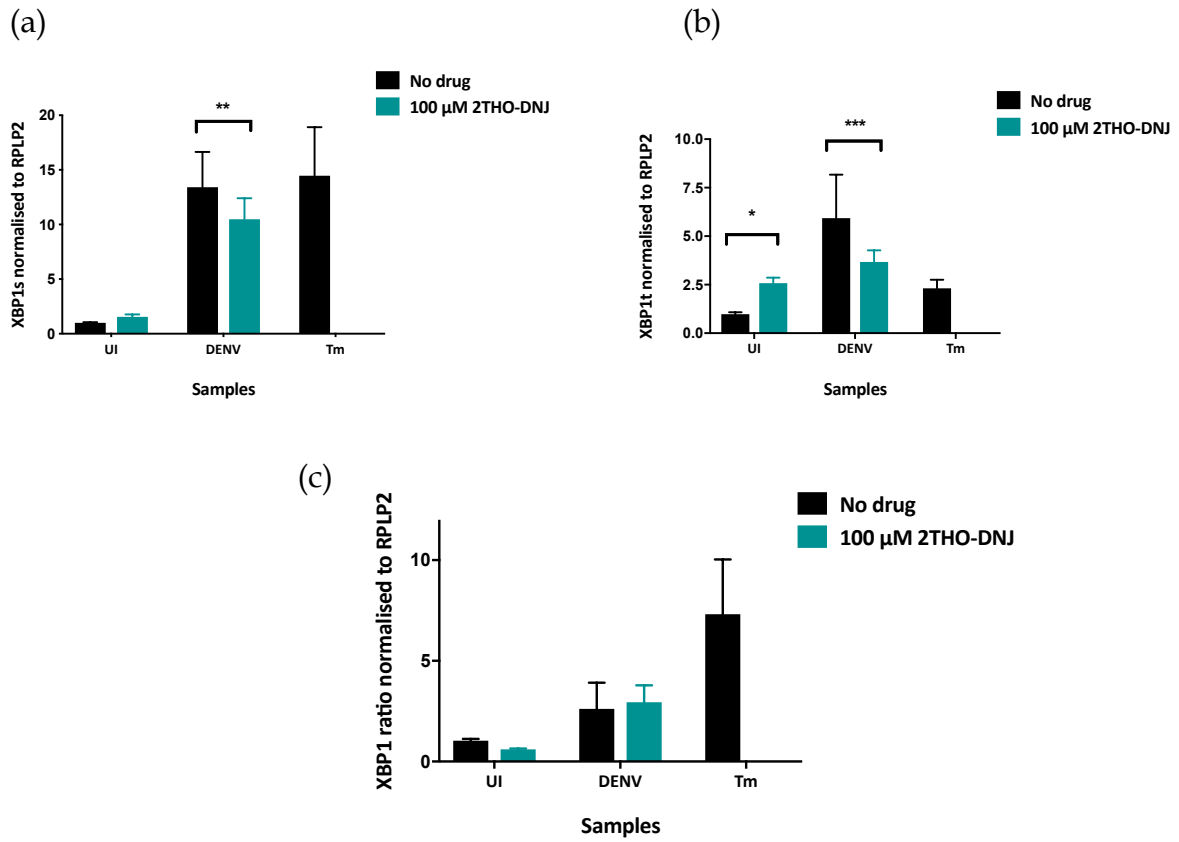

Figure 5.6. The effect of 2THO-DNJ treatment on the IRE1α-XBP1 pathway in DENV infection. Primary macrophages were infected with DENV at MOI 1 and left untreated or were treated with 100 µM 2THO-DNJ for 48 hours p.i.. Positive control was 1 µg/ml Tm for 6 hours. Transcripts were measured by qRT-PCR and normalised to the RPLP2 control. (a) XBP1s levels, (b) XBP1t levels and (c) XBP1s/XBP1t ratio are shown. All transcripts are given normalised to the RPLP2 control. All values represent mean of 3 independent experiments and the error bars denote standard error of the mean. Analysed by 2-way ANOVA, *$p<0.05$, **$p<0.01$, ***$p<0.001$.

Activated XBP1s protein increases the transcription of ERAD-associated genes. The levels of EDEM1 and ER-localized DNAJ4 (ERDJ4) mRNA levels were analyzed at 48 hours p.i. (Figure 5.7). 2THO-DNJ significantly increased both EDEM1 and ERDJ4 levels in both DENV-infected and uninfected cells suggesting an increase in ERAD. DENV infection also increased both ERDJ4 and EDEM1, with a stronger effect seen for ERDJ4 transcripts. It is interesting that DENV activates ERAD mechanisms downstream of the XBP1 arm which

could lead to clearance of any misfolded proteins including those of viral origin. This increase in ERAD by the 2THO-DNJ could potentially be the reason for reduced XBP1s levels seen with 2THO-DNJ treatment in DENV-infected macrophages due to reduction in ER stress.

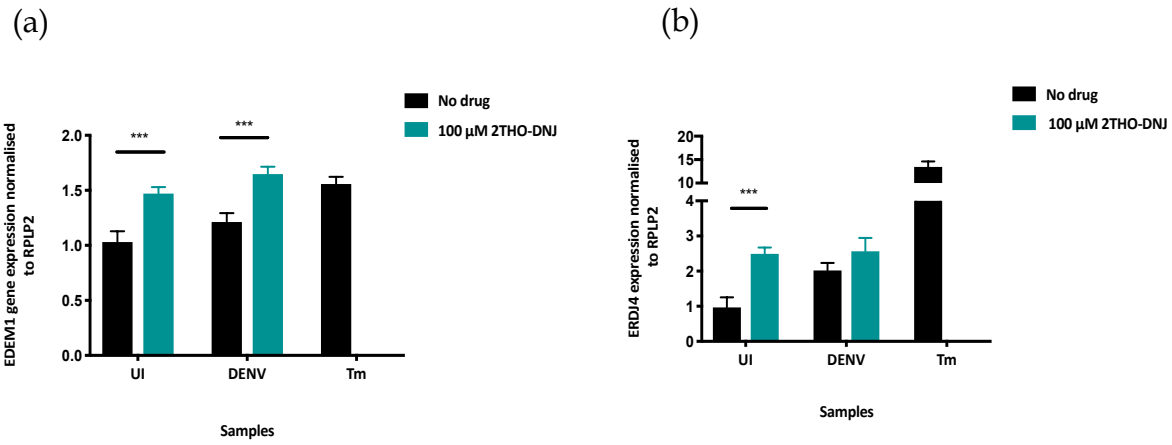

Figure 5.7. The effect of 2THO-DNJ treatment on EDEM1 and ERDJ4 gene expression in DENV infection. Primary macrophages were infected with DENV at MOI 1 and left untreated or treated with 100 µM 2THO-DNJ for 48 hours p.i.. Positive control was 1 µg/ml Tm for 6 hours. Transcripts were measured by qRT-PCR and normalised to RPLP2 control. (a) EDEM1 levels, (b) ERDJ4 levels are given. All values represent mean of 3 independent experiments and the error bars denote standard error of the mean. Analysed by 2-way ANOVA, ****p<0.001*.

The dose of 2THO-DNJ used in these experiments was 100 μM which inhibits both αGluII and αGluI [163]. A dose of the compound which inhibits αGluII exclusively (10 μM) [163] was also used to identify the effect on XBP1 splicing. Reduction of XBP1s levels was observed with 100 μM 2THO-DNJ treatment of DENV-infected primary macrophages and not with 10 μM 2THO-DNJ treatment (Figure 5.8a). The XBP1t levels were reduced in DENV-infected cells by both 10 μM and 100 μM 2THO-DNJ treatment (Figure 5.8b) and the XBP1s/XBP1t ratio was unchanged in 10 μM treatment in DENV-infection (Figure 5.8c). The reduction of the activated factor XBP1s by 100 μM 2THO-DNJ could also reflect lower ER stress and thus a reduced UPR activation at 100 μM than at 10 μM due to a more pronounced antiviral effect at this dose.

The lower levels of virus secreted in the presence of 100 μM 2THO-DNJ, in comparison with 10 μM 2THO-DNJ treatment (personal communication and Figure 5.9), could result in reduced numbers of additional macrophages being infected following multiple rounds of replication at 48 hours compared to untreated cells. Therefore, the effect of 2THO-DNJ treatment on other non-replicating ER stress inducers were studied to understand whether 2THO-DNJ reduced overall IRE1α-XBP1 activation during ER stress in primary macrophages. The primary macrophages were treated with the stress inducers Tm and dithiothreitol (DTT) in the presence or absence of 2THO-DNJ treatment. 2THO-DNJ reduced XBP1s in Tm and 5 mM DTT treatment while it did not significantly affect XBP1s levels at lower levels of stress seen following 1.25 mM DTT treatment (Figure 5.8).

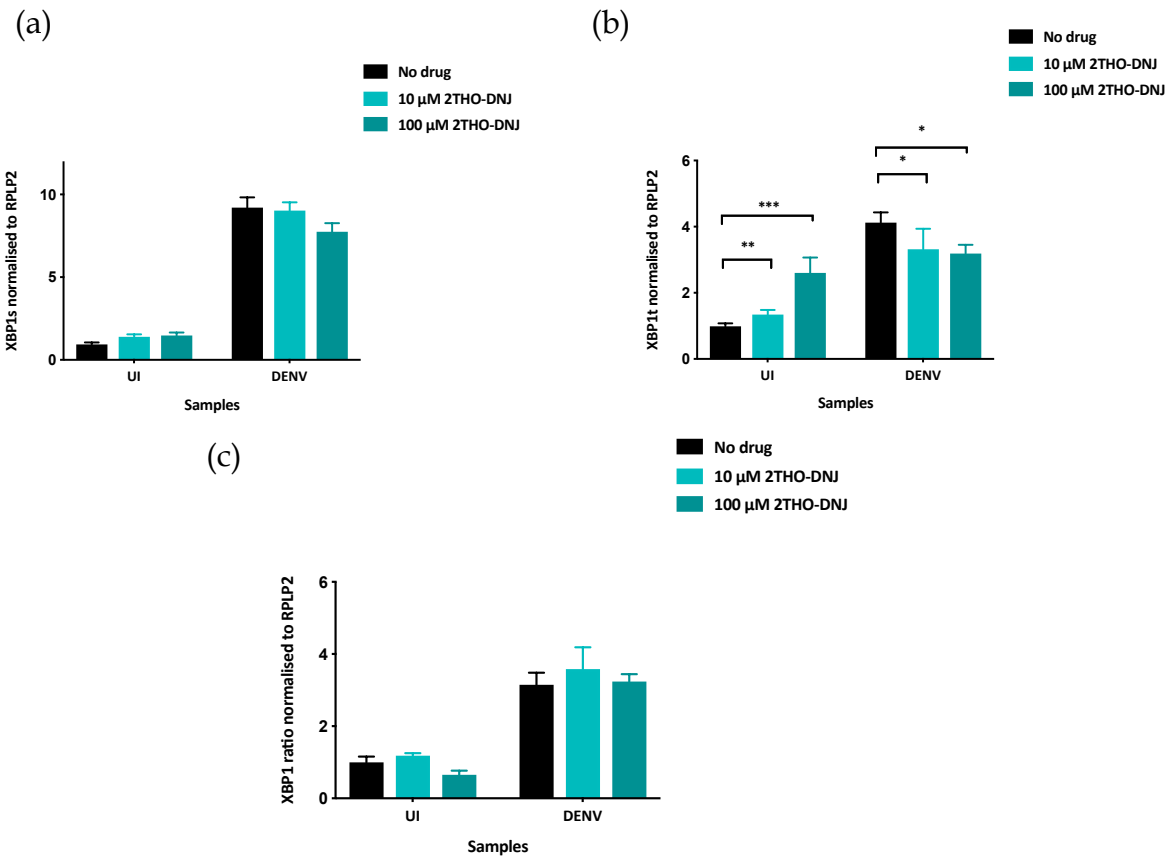

Figure 5.8. The effect of αGluII and αGluI inhibition by 2THO-DNJ on IRE1α-XBP1 pathway activation. Primary macrophages were infected with DENV, MOI 1 and left untreated or treated with 10 µM or 100 µM 2THO-DNJ for 48 hours. Data represent values from 3 independent experiments. Figures show (a) levels of XBP1s normalised to RPLP2, (b) XBP1t levels normalised to RPLP2 and (c) XBP1s/XBP1t ratio. Values represent mean and the error bars show standard error of the mean. Analysed by 2-way ANOVA. *$p<0.05$, **$p<0.01$, ***$p<0.001$.

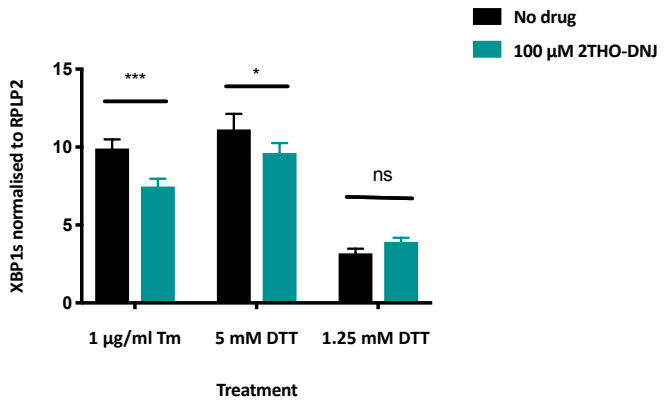

Figure 5.9. The effect of 2THO-DNJ treatment on Tm and DTT-induced XBP1 splicing. Primary macrophages were treated with Tm and DTT in the presence or absence of 100 µM 2THO-DNJ for 6 hours. XBP1s levels were measured by qRT-PCR. The values represent mean and standard error of the mean of 3 independent experiments. Analysed by 2-way ANOVA, *$p<0.05$, ***$p<0.001$.

5.2.3 The effect of chemical inhibition of PERK and IRE1α pathways on 2THO-DNJ induced antiviral effects

The effect of chemical UPR inhibition was investigated in the context of 2THO-DNJ treatment in DENV infection. As shown earlier in this thesis, PERK pathway inhibition in primary macrophages did not cause a reduction in the infectious virus release following infection with DENV (Figure 5.4b-c) and 2THO-DNJ treatment at both doses of 10 μM and 100 μM resulted in significantly ($p<0.0001$) reduced infectious virus secretion (Figure 5.9). Inhibition of the endonuclease activity of IRE1α resulted in significantly reduced secretion of DENV from macrophages and additional treatment of 2THO-DNJ caused further reduction of virus secretion and infectivity (Figure 5.9). The reduction of virus secretion by 2THO-DNJ despite inactivation of PERK and IRE1α-XBP1 pathways suggest that the compound does not require these two pathways for its antiviral effects.

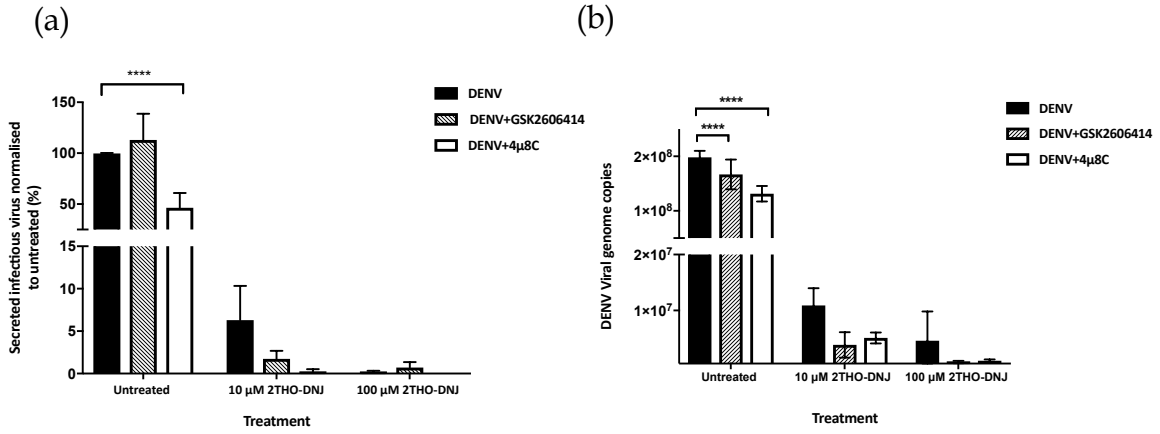

Figure 5.10. The effect of chemical inhibition of PERK and IRE1α pathways on 2THO-DNJ induced antiviral activity. Primary macrophages were infected with DENV, MOI 1 and left untreated or treated with 100 μM 2THO-DNJ for 48 hours and left untreated or treated with 1 μM GSK2606414 or 40 μM 4μ8c. Figures show (a) secreted infectious virus in supernatant measured by plaque assay and (b) secreted total viral genome copies measured by qRT-PCR. Values represent mean of 3 independent experiments and the error bars show standard error of the mean. Analysed by two-way ANOVA. ***p<0.01*, *****p<0.0001.*

5.2.4 The effect of PERK and IRE1 pathway inhibition on TNFα and IFNα levels in the presence of 2THO-DNJ

The TNFα and IFNα levels were significantly reduced following 100 μM 2THO-DNJ treatment of DENV-infected macrophages (Figure 5.11a-b). Inhibition of the IRE1α pathway resulted in a reduction of TNFα and IFNα levels in DENV infection and PERK inhibition did not have a significant effect (Figure 5.11c-d). Addition of 100 μM 2THO-DNJ in the presence of an IRE1α pathway inhibitor resulted in a significant reduction of TNFα and IFNα levels in comparison to no UPR pathway inhibitor (ie. iminosugar alone) suggesting that the effect was due to the inhibitor of the IRE1α arm. There seems to be an interaction between the PERK pathway and 2THO-DNJ in reducing TNFα and IFNα levels. However, the ability of 2THO-DNJ to reduce these mediators despite inhibition of the IRE1α and PERK arms suggest that 2THO-DNJ does not require activation of these pathways for the TNFα and IFNα reducing effect.

To clarify the role of the PERK and IRE1α arms of the UPR in the cytokine response, the effect of chemical inhibitors of these two arms on TNFα induction by a non-replicating PAMP was investigated. Treatment of macrophages with 100 μM 2THO-DNJ significantly reduced LPS-induced TNFα levels (Figure 5.12). The ability of the iminosugar to reduce this cytokine induced by LPS treatment supports the hypothesis that 2THO-DNJ has the ability to reduce TNFα independent of its antiviral effects. However, PERK and IRE1α pathway inhibition during LPS treatment did not alter the TNFα levels significantly and 2THO-DNJ seems to mediate its effect independent of the UPR. Overall, these data suggest that the ability of 2THO-DNJ to reduce TNFα and IFNα does not require the UPR.

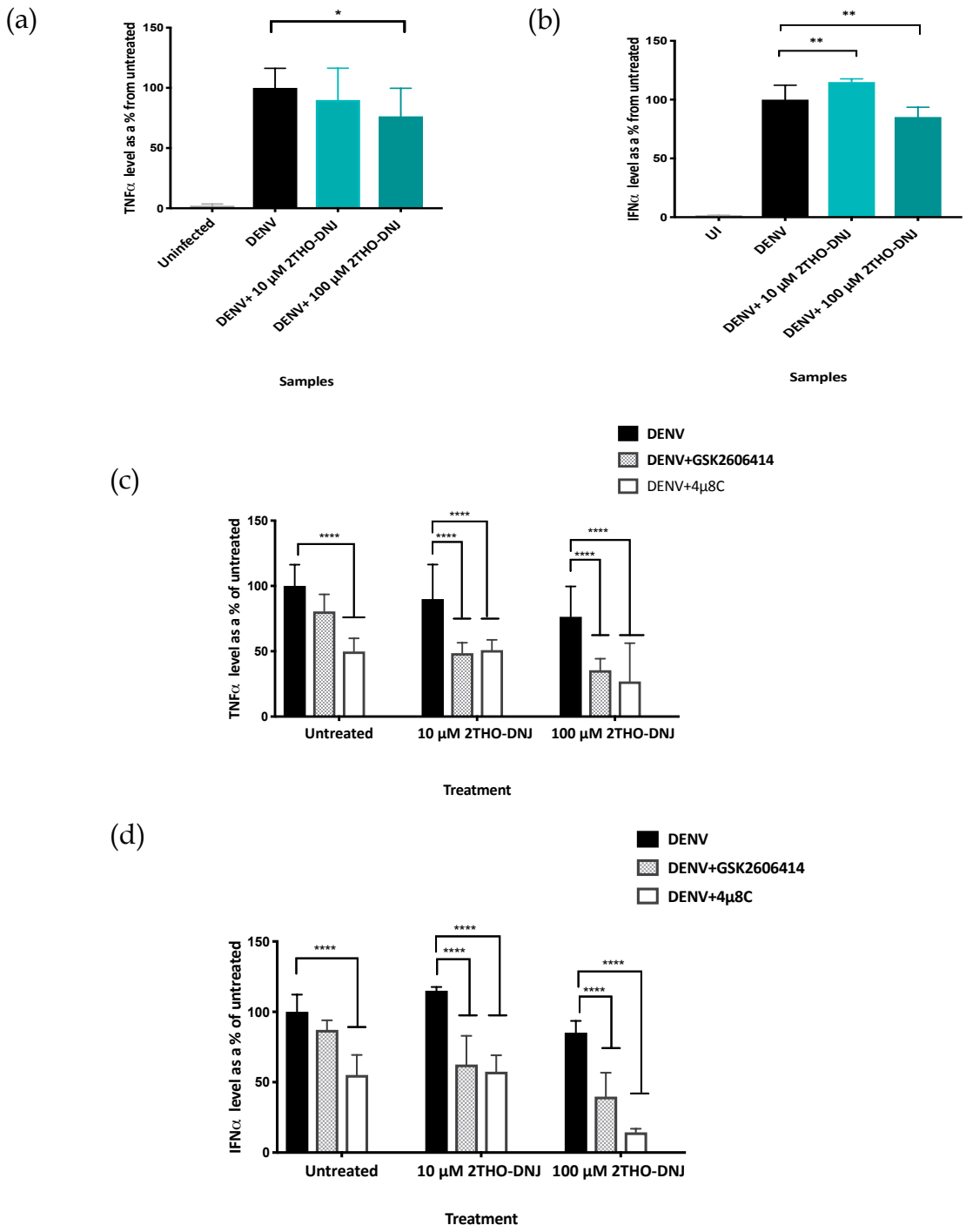

Figure 5.11. The effect of chemical inhibition of PERK and IRE1 pathways on 2THO-DNJ mediated TNFα and IFNα. Primary macrophages were infected with DENV, MOI 1 and untreated or treated with 100 µM 2THO-DNJ for 48 hours and treated or untreated with 1 µM GSK2606414 and 40 µM 4µ8c. Figures show (a) secreted functional TNFα levels following 2THO-DNJ treatment (n=3), (b) secreted functional IFNα levels following 2THO-DNJ treatment (n=2), (c) TNFα levels following 2THO-DNJ and UPR inhibitor treatment (n=3) and (d) IFNα levels following 2THO-DNJ and UPR inhibitor treatment (n=2). Values represent mean of independent donors (n) and the error bars show standard error of the mean. Analysed by two-way ANOVA. *$p<0.05$, **$p<0.01$, ****$p<0.0001$.

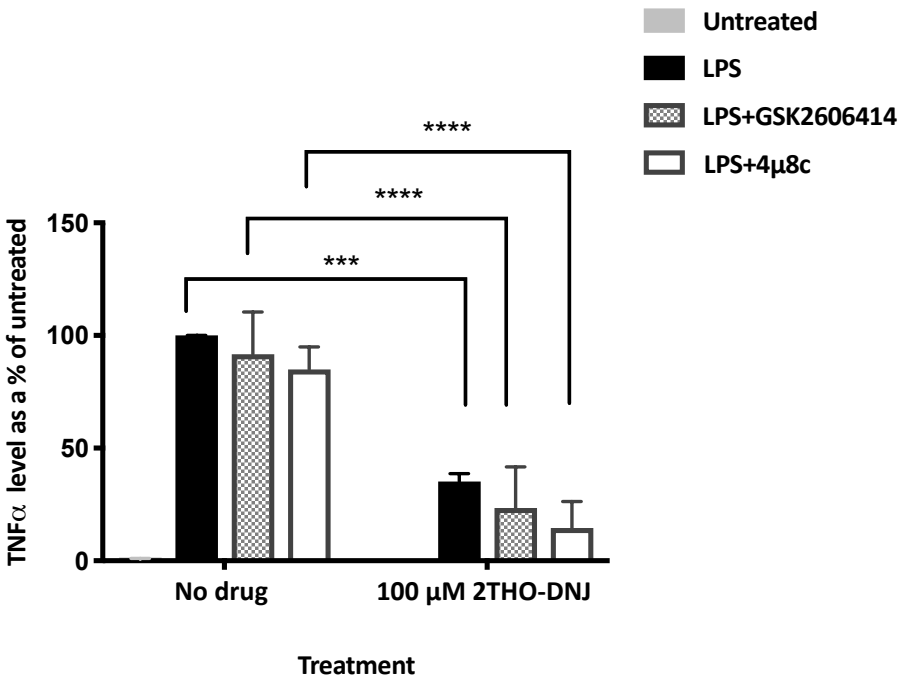

Figure 5.12. The effect of chemical inhibition of PERK and IRE1 pathways and 2THO-DNJ on LPS-induced TNFα. Primary macrophages were treated with 100 ng/ml LPS MOI 1 and left untreated or treated with 100 μM 2THO-DNJ for 6 hours and left untreated or treated with 1 μM GSK2606414 and 40 μM 4μ8c. Values represent mean of 3 independent experiments and the error bars show standard error of the mean. Analysed by two-way ANOVA. ****p<0.001*, *****p<0.0001.*

5.2.5. 2THO-DNJ treatment produces a different UPR signature in DENV-infected THP-1 cells compared to primary macrophages

Several differences were observed in the activation of IRE1α-XBP1 pathway in the THP-1 cell line compared to the response seen in primary macrophages. Unlike with primary macrophages, the THP-1 cells produced an increased XBP1s level in uninfected 2THO-DNJ treated cells, indicating IRE1α-XBP1 activation by 2THO-DNJ in the THP-1 cell line (Figure 5.13). The levels of XBP1s were significantly higher in 2THO-DNJ treated THP-1 cells, than in untreated cells, at multiple time points (Figure 5.13) irrespective of DENV-infection. However, treatment of primary macrophages with 2THO-DNJ did not elicit a significant activation of the PERK or IRE1α-XBP1 arm in the absence of infection (Figures 5.5 and 5.6) suggesting that 2THO-DNJ does not induce ER stress in basal state resting primary cells. The increases in the XBP1 levels in THP-1 cells were predominantly driven

by an increase in XBPt without a significant increase in the XBP1s: XBP1t ratio. The degree of XBP1 activation by the virus in THP-1 cells was weaker compared to the activation seen in primary cells (as measured by changes in the XBP1s) suggesting that UPR activation could be cell-type specific. This further highlights the need to select an appropriate cell culture model for investigating the UPR in dengue infection.

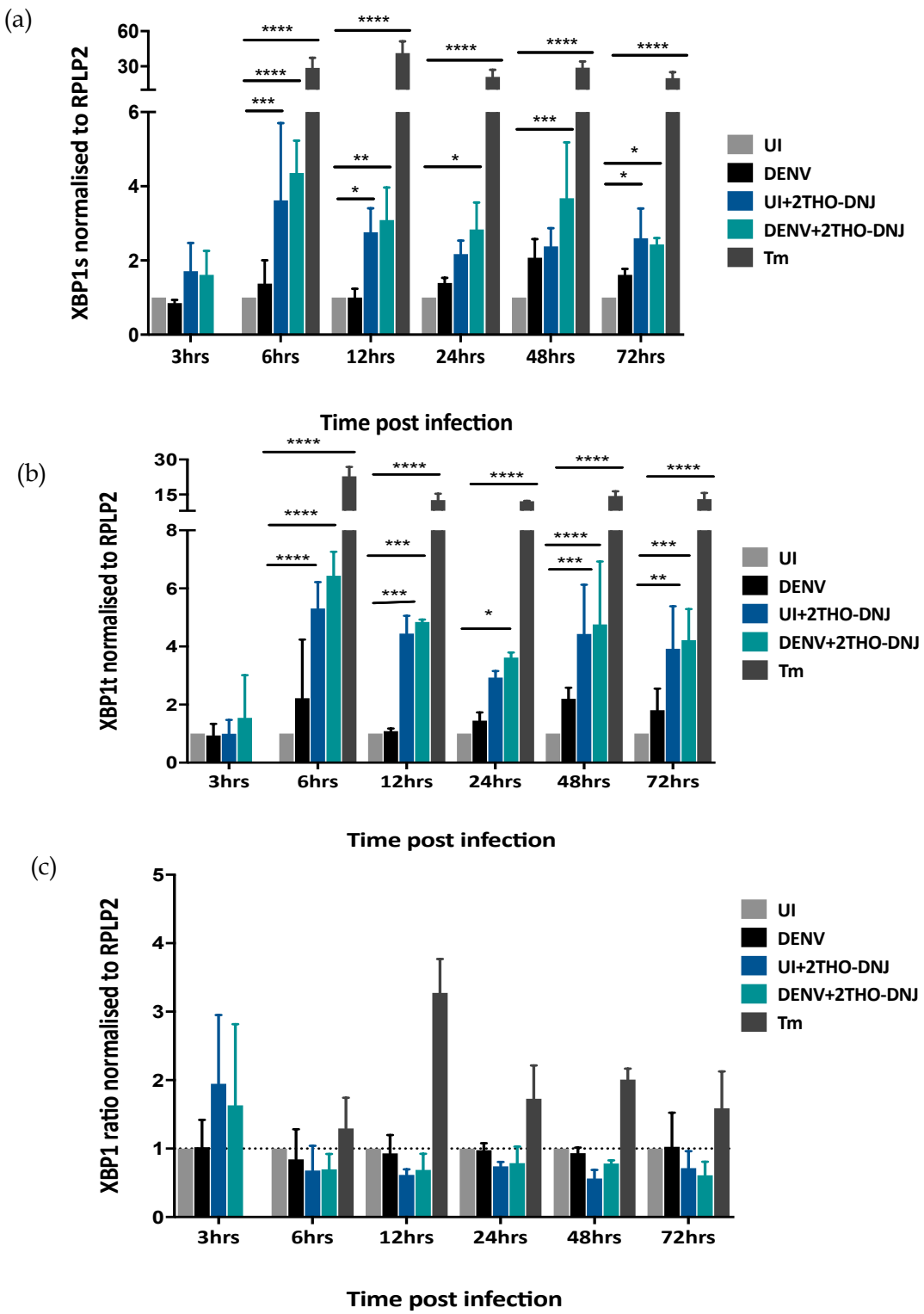

Figure 5.13. The effect of 2THO-DNJ on IRE1α-XBP1 pathway activation in THP-1 macrophages. THP-1 macrophages were infected with DENV, MOI 5 and left untreated or treated with 100 μM 2THO-DNJ for 48 hours. The figure shows (a) XBP1s transcripts, (b) XBP1t transcripts and (c) the XBP1s:XBP1t ratio. All transcripts were normalised to the RPLP2 housekeeping gene and given as a fold change from the untreated control. Values represent mean of 3 independent experiments and the error bars show standard error of the mean. Statistical significance measured by 2-way ANOVA and compared to UI sample at each time point. *p<0.05, **p<0.01, ***p<0.001, ****p<0.0001

5.3 Discussion

ER stress and the UPR have gained much interest over the last few years in the context of viral infections and non-viral conditions [18, 34, 164]. The complex networks and crosstalk between many key cellular elements hamper better understanding of this host response. The UPR was thought to be an antiviral response produced by the cells to combat invading infections. However, recent evidence suggests that this host response could well be hijacked by the viruses to have a favourable outcome for the virus (reviewed in [33]). DENV utilizes the ER and its machinery for folding of its proteins during viral assembly. A previous study by Rathore *et al*. revealed that Celgosivir activated the UPR and increased expression of ERAD genes [161]. The UPR transcripts were evaluated in this study. However, the protein levels were not evaluated and the study was done in THP-1 cells which is a leukaemic cell line. The UPR cascade activation is different in immortal cell lines such as THP-1 cells compared to primary immune cells as described in this chapter. Therefore, it is important to understand the effects of iminosugars in DENV-infected primary immune cells. The data presented in this chapter were obtained in primary human immune cells and confirm the contradictory observations that UPR in fact is proviral in the presence of virus and promotes virus-induced inflammatory cytokine production. Treatment with the compound 2THO-DNJ upregulated the PERK arm of the UPR but attenuated the strongly DENV-induced IRE1α-XBP1 activation. The PERK and IRE1α arms of the UPR were evaluated in this chapter due to the availability of chemical inhibitors of these pathways. Use of these inhibitors allowed a better understanding of the inflammatory and antiviral effects of these cascades.

DENV activates IRE1α-XBP1 pathway of the UPR

Chronic ER stress increases the oligomerization state of IRE1α which hyperactivates the endonuclease to induce splicing of XBP1 [49]. DENV activated the IRE1α-XBP1 pathway

at 48 hours p.i. in primary macrophages which supports previous literature of activating these UPR arms in a time-dependent manner [46]. XBP1t levels increased in response to infection as well as XBP1s levels with a XBP1s:XBP1t ratio exceeding one which suggests that DENV increased IRE1α endonuclease-mediated splicing of the XBP1 in addition to increasing the total amount of available substrate for the enzyme activity. This resulted in a significantly higher XBP1s level following DENV infection compared to uninfected cells. This was in contrast to the ER stress inducer, Tm which increased XBP1t levels marginally with a much increased XBP1s:XBP1t ratio. IRE1α-JNK induced apoptosis has been extensively studied and the IRE1α regulation of ER stress induced cell death has been characterized (reviewed in [165]). IRE1α-JNK pathway activation has been linked to activation of DENV-induced autophagy which subsequently increases viral replication [159]. But non-apoptotic functions of the IRE1α pathway are less well established [165]. The role of the IRE1α-XBP1 pathway on viral replication or secretion has been documented in non-DENV viruses as described in great detail in chapter 1. However, data in the context of dengue infection is sparse. Findings presented in this chapter revealed that DENV strongly activates the IRE1α-XBP1 pathway and increased EDEM1 and ERDJ4 mRNA levels downstream. Inhibition of the endonuclease activity of IRE1α resulted in reduced secretion of infectious and total virus levels suggesting a proviral role for this pathway. Activation of ERAD accelerates diversion of misfolded and unfolded proteins to ubiquitination and proteasome degradation pathways and it is obvious that inhibition of ERAD could result in persistence of viral proteins. Thus, it is not clear how the IRE1α-XBP1 pathway increases DENV secretion and possibly replication. It is possible that activated XBP1s has an unknown pro-viral activity. Activation of IRE1α-XBP1 was also found to be pro-inflammatory as seen by a reduction of secreted TNFα levels by inhibition of the IRE1α endonuclease activity and XBP1 splicing by 4μ8c treatment. The mechanism of TNFα stimulation by the IRE1α-XBP1 pathway during DENV infection is not well

established. There is evidence that stimuli that activate IRE1α-XBP1 could increase production of TNFα, IFNβ and IL-6 in non-viral conditions. One example is production of TNFα and IL-6 in an IRE1α-XBP1 dependent manner by the toll-like receptor-4 (TLR-4) activator, lipopolysaccharide (LPS) in murine macrophages [69]. Macrophages deficient in XBP1 did not elicit an optimum TNFα or IL-6 response to pathogen infection [69]. Experiments in murine macrophages have shown that IRE1α endonuclease activity regulates TNFα gene expression and IRE1α as well as XBP1 deficiency impairs TNFα response to inflammatory stimuli [70]. However, there are no previous reports that describe an IRE1α-XBP1 mediated DENV-induced TNFα production. Data in this chapter supports that DENV utilizes this pathway to maintain viral secretion and secretion of TNFα. Despite many DENV proteins having been implicated in activating XBP1 splicing in reporter systems, comparison of the fold induction achieved by these proteins in reporter assays with whole virus infection studies suggest that these DENV proteins combine to activate the pathway rather than acting on their own [53]. It is not clear which proteins of the virus activate XBP1-TNFα induction. All data taken together reveal the important role of the IRE1α-XBP1 pathway during DENV infection of macrophages which seems to maintain a pro-viral milieu for the virus in addition to producing TNFα. IFNα levels were also reduced by inhibition of endonuclease activity of IRE1α. IFNβ induction has been linked to XBP1 activation in mouse macrophages in response to pathogen pattern recognition receptor stimulation [166]. However, secretion of IFNα has not been linked to the IRE1α-XBP1 pathway.

The PERK-eIF2α-ATF4 pathway is not activated by DENV in primary macrophages

The PERK-eIF2α-ATF4 pathway was not significantly activated in THP-1 cells or primary macrophages following DENV infection. The marginal increase of the ATF4 level seen at 24 hours p.i. in THP-1 cells and 12 hours p.i. in primary macrophages was not a significant

elevation and the lack of an increase in ATF4 mRNA levels further supports this observation. It could be due to a DENV-specific inhibition of PERK-eIF2α-ATF4. Studies suggest that DENV suppresses eIF2α phosphorylation and thereby downstream activation and that the UPR signature is mainly limited to IRE1α and ATF6. Data in this thesis in a more physiologically relevant cell line supports a similar IRE1α activation by DENV in macrophages. PERK-eIF2α activation results in attenuation of protein translation as phosphorylated eIF2α inhibits the first step of protein translation. It is presumed that this global reduction in protein translation would affect processing of viral proteins necessary for virion assembly. In addition, selective translation of ATF4 helps to maintain redox balance and helps to regulate amino acid metabolism. The inhibition of the kinase activity of PERK by the pharmacological kinase inhibitor GSK2606414, did not significantly change the level of secreted infectious virus. There was a reduction in genome copies detected in the culture supernatant but the overall data might support that secreted virus is infectious in the absence of PERK activation and given the non-significant effect of DENV on the PERK arm of the UPR, it could be assumed that there is no significant effect on the infectivity of DENV by this arm. The lack of a pro-viral nature of this UPR arm is interesting given that virus does not activate this pathway. It is likely that virus modulates the UPR for survival and thus takes advantage of the pro-viral IRE1α-XBP1 pathway and it does not activate the PERK arm due to the absence of its effect in enhancing virus secretion. Previous studies have suggested an antiviral role for this PERK-eIF2α pathway in mouse embryonic fibroblasts (MEFs) infected with DENV, where MEFs deficient in PERK showed enhanced DENV virus secretion compared to WT cells [46]. However, it is apparent from data in this thesis that the PERK-eIF2α-ATF4 pathway is not significantly activated in human macrophages by DENV. However, inhibition of PERK activity in the presence of DENV resulted in reduced TNFα secretion. This suggests that despite a negligible effect of the PERK arm on antiviral activity, the PERK arm drives

a TNFα centered inflammatory response in primary macrophages. The increased TNFα, which is independent of viral levels, could be explained by several signaling events following DENV infection. One hypothesis could be PERK-Nrf2 activation leading to CLEC5A mediated TNFα secretion in DENV infection as suggested previously [84]. As such, it would be of interest to investigate the Nrf2 activation and the redox status in macrophages following DENV-infection and 2THO-DNJ treatment.

Effect of 2THO-DNJ on DENV-induced UPR

Data in this chapter demonstrates that 2THO-DNJ does not worsen ER stress despite inhibiting α-glucosidases in the ER and affecting folding of proteins. The lack of a significant increase in ATF4 levels of the PERK arm and XBP1s levels in uninfected but 2THO-DNJ-treated macrophages is reassuring. Furthermore, 2THO-DNJ treatment reduced XBP1s levels and the XBP1t levels in DENV infection. It is interesting that 2THO-DNJ seems to maintain a favourable ER environment following treatment. This effect was mainly seen with the αGluI inhibiting dose of 100 μM. It might be argued that the reduction in XBP1s activity following 2THO-DNJ treatment was apparent due to having fewer infected cells 48 hours p.i. However, the reduction in XBP1 splicing after Tm and 5 mM DTT treatment suggests that the compound has an ability to attenuate excessive activation of the IRE1α-XBP1 pathway. This finding is also supported by the *in vivo* data from the mouse models of DENV infection and M*O*N-DNJ treatment [2]. The XBP1t transcripts in PBMCs and liver tissue were reduced by M*O*N-DNJ treatment of DENV-infected mice. This effect was not seen with Celgosivir treatment suggesting that these iminosugars have significant drug-dependent diversity in their effects [2]. This reduction in XBP1t was not apparent where the IRE1α-XBP1 pathway activation was less, as with 1.25 mM DTT treatment. It could be hypothesized that the reduction of ER stress and thus UPR is achieved by an increase in ERAD as seen by the significant increase in EDEM1 and

ERDJ4 transcript levels following 2THO-DNJ treatment. It would be quite interesting to explore the compounds' ability to modulate ERAD mechanisms since this could unravel further therapeutic options for iminosugars in diseases caused by accumulation of misfolded proteins.

2THO-DNJ does not rely on the UPR for its antiviral activity and reduction of TNFα and IFNα

The iminosugar 2THO-DNJ increased ATF4 levels following DENV infection of macrophages. Given that 2THO-DNJ significantly reduced DENV-induced TNFα levels, and did not increase this cytokine in the absence of PERK activation, it can be assumed that 2THO-DNJ does not rely on the PERK pathway for its TNFα reducing effects. Further data following 2THO-DNJ treatment in the presence of PERK and IRE1α inhibition shows that 2THO-DNJ does not rely on either of these pathways for its antiviral effect. Furthermore, the reduction of LPS-induced TNFα levels was seen to be independent of both IRE1α-XBP1 and PERK-ATF4 pathways in macrophages and the significant reduction of LPS-induced TNFα by 2THO-DNJ was seen to be unchanged with or without UPR inhibitors. These data confirm that 2THO-DNJ has an ability to reduce TNFα independent of the UPR. Evaluation of the ATF6 arm would also be useful in identifying any potential effect of this pathway on 2THO-DNJ induced antiviral and anti-inflammatory effects. Unavailability of a suitable inhibitor to the ATF6 pathway hampers further evaluation of this UPR cascade.

The UPR is modulated by DENV to preferentially activate the pro-viral and pro-inflammatory IRE1α arm and 2THO-DNJ treatment attenuates this activation while increasing ERAD chaperones and activating PERK arm. The differences in activation of the UPR seen in THP-1 cells and primary macrophages highlight the cell-specific

differences in this response. The IRE1-XBP1 arm was significantly activated by 2THO-DNJ treatment alone in uninfected as well as DENV-infected THP-1 cells. The response seen in primary macrophages was different with no activation seen by the 2THO-DNJ drug. THP-1 cell line is a malignant cell line and it is plausible that these cells have a rapid turnover of proteins with high protein burden on the ER at the basal state. Therefore, it is possible that 2THO-DNJ treatment which inhibits protein folding could result in further ER stress and activation of the UPR. Although THP-1 cells are a good model to investigate the effects of viral infection, the malignant nature of these cells could influence the study results. Primary cells are resting cells at basal state and would be a better model to investigate the effects of viral infection and drug treatment. Major disadvantage is the significant donor variability that occurs with the use of primary immune cells which again influence the final interpretation. It would be useful to have a primary human UPR-knockout cell culture model to investigate and understand this complex cascade of events in DENV-infection. The current available knockout cells are murine embryonic fibroblasts and the cell-type specific differences in DENV-induced UPR activation warrant a more physiological human cell culture model to be used for better understanding of the UPR in viral infections.

VI

Identification of novel markers of dengue disease severity in a patient cohort

Identification of a marker that could predict DENV disease severity has been an ongoing quest. Evaluation of UPR transcripts in the peripheral blood monocytes of dengue-infected patients revealed XBP1s mRNA levels to be significantly elevated in severe dengue disease (SD) at the onset of illness compared to non-severe dengue disease (NSD)

with a reduction in DDIT3 and HSPA5 transcripts. These transcripts correlated with haematological parameters of the patients. In addition, tandem mass tag mass spectrometry identified 163 peptides differentially regulated in DENV-infected cell lysates compared to healthy controls. Proteins involved in innate immune response and host defence pathways were upregulated while platelet activation/degranulation and exocytosis pathways were down-regulated in DENV-infected samples. Comparison of DHF patient samples with DF revealed 167 peptides to be differentially regulated. Humoral immune response pathways, neutrophil degranulation and IRE1-mediated UPR pathways were upregulated in DHF samples compared to DF while proteins involved in platelet activation/degranulation, blood coagulation, regulation of body fluids were down-regulated. Potential markers of disease severity such as histones, PRG2 and reduced levels of SAMHD1 were identified in the DHF lysates prior to development of severe manifestations which will need further validation in larger samples in the future. These data presented in this chapter provide a foundation to identify markers of DENV disease severity.

6.1 Introduction

Dengue infection can range from an asymptomatic illness, mild febrile episode to severe disease with circulatory collapse and death [29]. The biggest obstacles in management include not having a licenced antiviral drug for therapy and inability to triage patients at the onset of the disease. This results in difficulty in identifying patients developing severe disease early during the course of their illness. Therefore, stringent monitoring needs to be adopted which requires significant human resources and infrastructure facilities. Hospital admissions increase during dengue outbreaks since it is impossible to predict patients which patients will suffer only a mild illness not requiring admission. Availability of a sensitive and specific disease severity marker would help to avoid these unnecessary admissions and allow health care personnel to focus on those patients who will develop severe disease and related complications. Identifying an early marker of disease severity has been an ongoing quest without much success. Understanding the disease pathogenesis is crucial to investigate potential markers in dengue disease.

Researchers have investigated potential markers to predict severe disease manifestations in dengue fever (reviewed in [167]). Some of these markers are based on the inflammatory response elicited by DENV. Many cytokines have been associated with development of severe disease [29]. Studies report elevated levels of cytokines such as IFNγ, IL-1β, IL-4, IL-6, IL-10, IL-13, IL-7 and chemokines in severe dengue fever in various combinations [168-175] and increased levels of soluble cytokine receptors [176]. Flores-Mendoza *et al*. showed that IL-10, TNFα and suppressors of cytokine signalling 3 (SOCS 3) were higher in the blood of patients with dengue haemorrhagic fever than those with dengue fever [171]. There was no difference in IL-4, IFNγ or IL-6 values between severe and non-severe dengue groups. However, the patients were recruited at 6-7 days of illness and it would not be the ideal early marker to triage patients in a clinical setting. The use of serum TNFα

as a marker is hampered by the broad range of values detected in patients, the significant influence of the timing of taking on the serum levels and the influence of TNFα genetic polymorphisms [171]. Some studies report that polymorphism of the TNFα gene in the position -308 of the promoter region (substitution of a guanine by an adenine) results in significantly increased production of TNFα levels and susceptibility to DHF [177]. However, the risk or the protective effect of these polymorphisms vary with the ethnicity of the population studied resulting in difficulty to generalize the findings [178]. A meta-analysis performed on pooled data from studies on TNFα genetic polymorphisms have not seen a consistent association [179]. Any variation among patient populations in different regions will likely influence the results and the effect on TNFα levels due to these polymorphisms render this pro-inflammatory cytokine unsuitable as a marker of disease severity. A study conducted in primary dengue infection reported reduced serum levels of cytokines (IFNγ, IL-4, IL-1β, IL-17, G-CSF, IP-10) in dengue haemorrhagic fever patients in comparison with dengue fever, suggesting that the cytokine profile and the immune response could be different in primary versus secondary dengue infection [180]. This reduction is in contrast to studies reporting a higher value of cytokines in severe dengue disease compared to non-severe dengue patients in secondary dengue infection. This is a further problem in using cytokine-based markers of disease severity when using diagnostic tests in endemic settings comprising of both primary and secondary dengue infected cases.

A few studies have reported the use of clinical and laboratory parameters either alone or in combination with cytokine levels to predict disease severity [181, 182]. Apoptosis markers have been evaluated in studies to identify the differential expression in severe dengue disease compared to mild infection. Arias *et al*. found that soluble TNF-related apoptosis inducing ligand (TRAIL) was significantly lower in patients who developed

severe disease or dengue with warning signs compared to dengue fever without warning signs [176]. Similarly, serum TRAIL levels were significantly reduced in patients with severe dengue compared to dengue without warning signs in a paediatric population [183]. It is plausible that DENV inhibits apoptotic pathways to enhance survival in the infected cells.

Data shown in this thesis describe the effect of the UPR during DENV replication and virus secretion from primary monocyte-derived macrophages. Our data shows that the IRE1α-XBP1 pathway is activated by DENV infection and this pathway behaves in a pro-viral and pro-inflammatory manner in monocyte-derived macrophages. ER stress and the resulting activation of the UPR occurs during high protein turnover in the cell and are likely to occur during the viraemic phase of dengue illness in a human infection. Therefore, we hypothesized that ER stress and the UPR should be up-regulated during early dengue infection. Given the pro-viral nature of certain pathways of the UPR such as the IRE1α-XBP1 arm, we postulated that patients who develop severe dengue disease could potentially activate these arms in the viraemic phase ultimately leading to higher viraemia and a robust inflammatory response causing severe manifestations. In a human dengue infection, virus replicates in infected cells and produce viraemia from the incubation period up to the febrile symptomatic phase. Then the immune response clears the virus load but result in severe disease manifestations in certain individuals which coincide with the inflammatory response. So, we hypothesised that the UPR markers should be activated early during the symptomatic phase or even possibly during the incubation period of the virus infection. But the cascade of events activated by the UPR could have effects later in the course of illness during the critical phase when fever subsides. This is the first study comprehensively evaluating the expression of UPR markers in clinical dengue infections. Our hypothesis was further supported by a transcriptomic analysis by Simmons *et al.* of whole blood in dengue-infected patients

which revealed transcript abundance of ER associated genes in patients who developed dengue haemorrhagic fever [184]. Further evaluation of UPR associated genes revealed that they were overrepresented in dengue-infected patients [184]. We evaluated selected UPR transcripts in peripheral blood monocytes (PBMCs) of dengue-infected patients in early dengue-infection and during defervescence. PBMCs were selected as they contain the cell lines important for DENV replication and development of virus mediated immune responses.

6.2 Results

Patient categorisation to dengue fever (DF) and dengue haemorrhagic fever (DHF) was based on the WHO classification, 1997[20]. The WHO classification in 1997 focuses on fluid leakage from capillary endothelium that occurs as a result of increased vascular permeability leading to severe dengue manifestations. This group has been categorised separately from the dengue fever patients without leakage to identify patients at risk of dengue shock. Local management guidelines on administering fluid to maintain organ perfusion and prevent target organ damage is based on the presence or absence of fluid leakage thus presence/absence of a critical phase. Therefore, the 1997 classification was adopted in this study to identify this group of patients who had evidence of fluid leakage and who were at risk of dengue shock if not treated. It is important to note that dengue shock syndrome (DSS) is rare in patients being managed in a hospital due to proper management of these patients based on the local management guidelines. All patients with dengue fever were recruited during the first three days of illness (febrile phase) and blood was collected at recruitment and 24 hours following resolution of fever (defervescence) to identify UPR markers which might be differentially expressed in DHF versus DF. Fever duration was identified as accurately as possible from the patient by asking for the first time of noticing fever. Patients were only recruited if first contact of the recruiter with the patient either at the outpatient department or the ward was within the first 72 hours of noticing fever. All patients were admitted to the hospital during the course of their illness according to local admission policy. Blood was collected from 13 healthy volunteers to compare as a control. Defervescence denotes the recovery period of DF patients and the onset of the critical phase of the DHF patients. Defervescence was defined as documented temperature $\leq 37^0$c persistent for at least 4 hours without any temperature spikes. Blood was collected during the first 24 hours of reaching this temperature for the defervescence sample. This varied among individuals as blood

sample was collected at 10:00 every day while performing venepuncture for routine investigations.

During the study period, there were increased number of dengue-infected patients being self-referred to the IDH (Infectious disease hospital) or referred by the family practitioners. The local practice is to perform a full blood count (FBC) during the first 72 hours of illness and to repeat daily if fever persists. Patients will be admitted either due to persistent symptoms or emergence of thrombocytopaenia. Patients presenting to hospital were screened by me to identify the likelihood of having a viral illness as opposed to other infections/conditions. Only patients with a high likelihood of dengue fever were further investigated with rapid dengue NS1 antigen and recruited to the study.

During the first phase of the study, samples were collected from 13 healthy volunteers and 15 dengue-infected patients. The dengue-infected patients had either DF (10 patients) or DHF (5 patients) during the course of their illness (Figure 6.1). DHF occurred at carrying time points in these patients following recruitment as expected. All of the patients entered critical phase after 48-72 hours of recruitment. Patients having features of fluid leakage on first contact were excluded as this group represented a delayed presentation. These patients had twice daily FBC, daily ultrasonography to look for evidence of fluid leakage. Liver transaminases were performed on admission and during the critical phase. All patients were monitored according to the charts adopted by the Ministry of health which required 4 hourly measurement of vital parameters and PCV twice daily. Once they were detected to have fluid leakage, they were transferred to a special ward with intense monitoring facilities and hourly measurement of parameters and regular PCV were performed.

All samples collected from study participants were processed in duplicate. PBMCs were isolated and RNA extracted as described in the methods section (chapter 3.11). UPR transcripts were selected to represent the three arms of the cascade (XBP1s, ATF4, ATF6). In addition, DDIT3, EDEM1 and HSPA5 were selected due to the important role played by these markers during ER stress. The transcript Nrf2 was selected to identify the antioxidant pathway activation downstream of PERK-ATF4. The transcripts were quantified during the acute febrile phase (within 72 hours of fever) and during defervescence. Serum sample was used to identify the dengue NS1 antigen using the rapid kit and dengue-specific IgM levels were measured by an ELISA method. The serum was also used to extract RNA and a multiplex qRT-PCR was performed to quantify the serum dengue viral load. The infecting DENV serotype was also identified during the qRT-PCR. The stored serum will be used to measure dengue-specific IgG by a direct ELISA to further identify the immune status of these patients in a subsequent analysis.

Phase I:

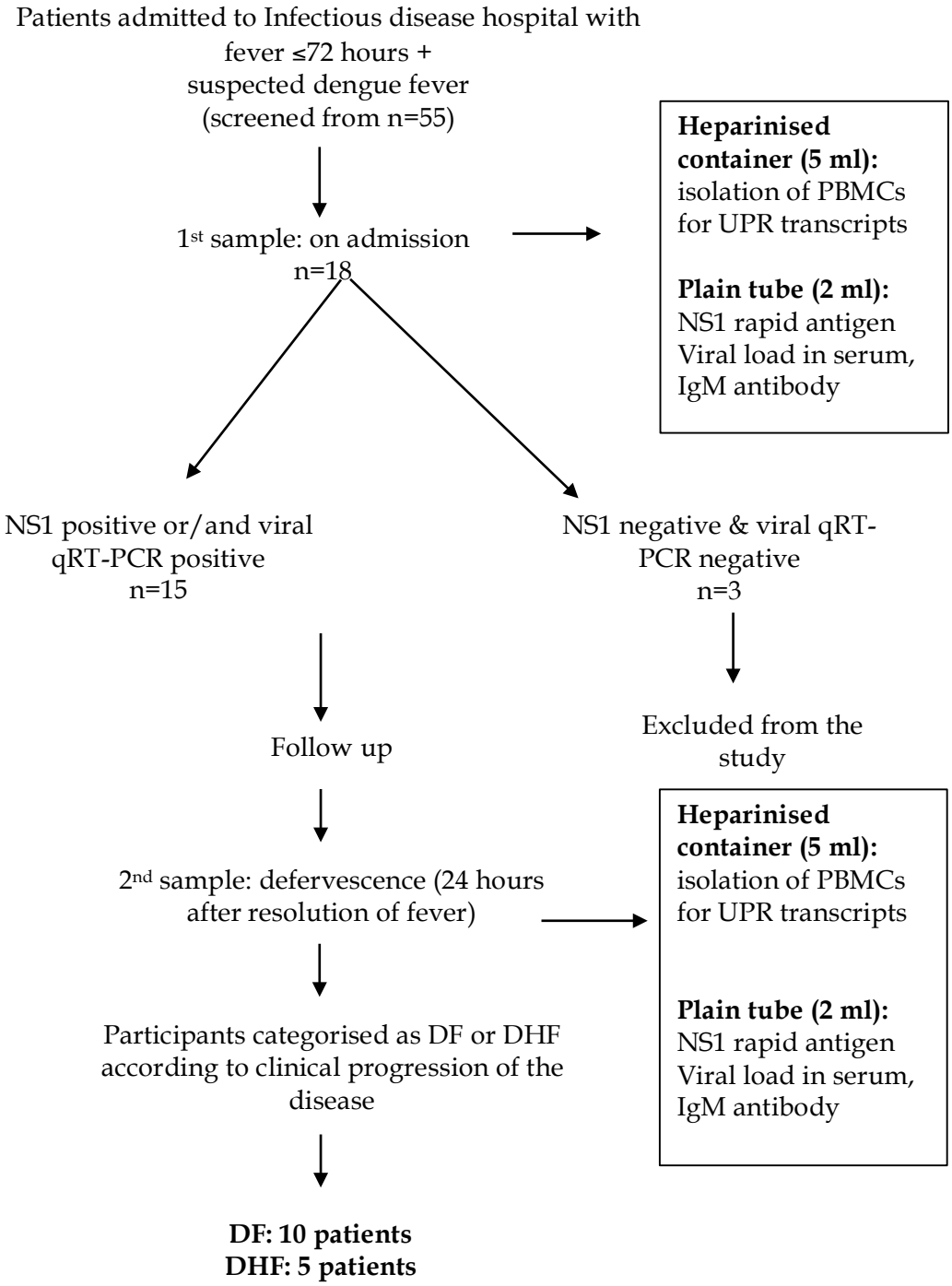

Figure 6.1: A schematic presentation of Phase I of the study. This flowchart shows the recruitment of the participants and the experiments performed on the samples during the study period.

There were only two female patients in phase I of the study population with most patients (86.67%) being male. Comparison of the baseline characteristics and haemodynamic parameters revealed that DHF group patients had lower platelet counts and higher packed cell volumes than the DF patients during the course of their illness and during defervescence (Table 6.1). The liver enzymes (SGOT and SGPT) were also higher in the DHF group than the DF group in the study. However, this difference was not statistically significant (Table 6.1). Rapid dengue NS1 test was positive in 07 (out of 15) patients while positive dengue IgM antibody was detected in 07 patients (Table 6.2). All patients had detectable DENV in the serum as determined by viral qRT-PCR.

The phase II of the study was conducted to identify UPR-related and unrelated proteins that might be differentially regulated during dengue infection. There were 25 patients recruited to the study which included 08 DHF and 17 DF patients (Figure 6.2). Samples were collected on admission (within 72 hours of fever) and defervescence similar to phase I. PBMCs were lysed in RIPA buffer and serum was used for viral load quantification, IgM measurement and NS1 detection. We performed a mass spectrometry experiment following tandem mass tag (TMT) labelling on 08 of these samples (04 DF and 04 DHF) collected during Phase II of the study. Samples collected during the acute febrile phase was used for this experiment and 02 healthy PBMC lysates were used as controls. The used samples were selected based on the protein concentration and samples with the highest protein concentrations were used for this proteomic analysis.

Phase II

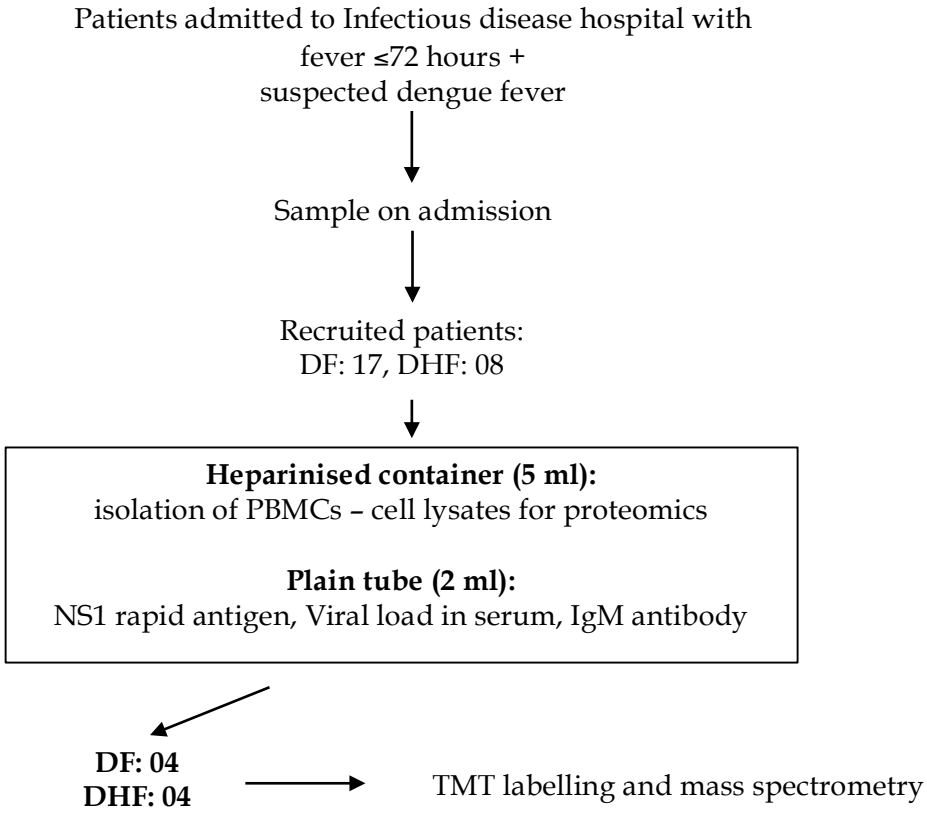

Figure 6.2: A schematic presentation of Phase II of the study. This flowchart shows the recruitment of the participants and the experiments performed on the samples during the study period.

6.2.1. Phase I: Identification of UPR markers by qRT-PCR in PBMCs of dengue fever patients:

PBMCs were isolated from collected blood as described in chapter 3.1.1 and qRT-PCR was performed to identify seven UPR markers in the healthy samples and dengue fever patient samples following optimisation. The markers ATF6, EDEM1 and NFE2L2 could not be identified in sufficient quantities in the samples to perform accurate analysis. The XBP1s, DDIT3 (CHOP), HSPA5 (BiP) and ATF4 transcripts were quantified relative to the house-keeping control RPLP2 transcripts (Figure 6.3). Results revealed that XBP1s was significantly higher during the febrile phase in DHF patients compared to DF fever ($p<0.01$). Although the ATF4 transcripts were higher in the DHF group compared to the DF group, the difference was not statistically significant. Both XBP1s and ATF4 levels reduced back to the baseline in dengue patients during defervescence. Interestingly, DDIT3 and HS5A5 levels were suppressed in DHF patients during the first three days of illness and these transcripts increased to similar levels as the control group when fever subsided (Figure 6.4).

Table 6.1: The baseline characteristics and investigation results in patients recruited to the Phase I study

Variable	DF (n=10)	DHF (n=05)	Significance
Age, mean (SD)	33 (10.88)	33 (12.33)	1.0
Sex			
Males, n (%)	08 (61.54)	05 (38.46)	0.001*
Females, n (%)	02 (100)	0	
Laboratory investigations in acute febrile stage			
WCC	4.17 (1.27)	3.78(1.05)	0.574
Platelets	130.11 (29.86)	105.4 (14.03)	0.112
PCV	39.467 (5.07)	44.02 (2.46)	0.087
Laboratory investigations to show the lowest/highest values over the course of illness			
Lowest WCC	3.22 (1.09)	2.90 (1.04)	0.603
Lowest platelets	104.67 (39.22)	30.60 (31.66)	0.004*
Highest PCV	40.944 (4.52)	48.2 (1.92)	0.005*
Laboratory investigations in defervescence			
Lowest WCC	3.91(1.75)	4.47 (2.64)	0.667
Lowest platelets	126 (35.5)	43.40 (27.41)	0.001*
Highest PCV	38.69 (5.95)	46.14 (3.14)	0.03*
SGOT[a], median (IQR)	44 (24.6-63.4)	103.35 (58.6-191)	0.083
SGPT[b], median (IQR)	37 (20.3-54.0)	70.65 (66.8- 106.9)	0.06
Haemodynamic parameters on admission			
Pulse rate			
SBP[c]	103.89 (12.69)	120 (21.21)	0.097
Pulse pressure	36.11 (6.97)	42 (8.37)	0.183
Haemodynamic parameters during the course of illness			
Highest Pulse rate	84.89 (6.72)	89.2 (10.54)	0.364
Lowest SBP	98.33 (9.35)	104 (16.73)	0.425
Lowest pulse pressure	32.22 (4.47)	32.0 (6.67)	0.898

[a] SGOT; serum glutamic oxaloacetic transaminase, [b]SGPT; serum glutamic pyruvic transaminase, [c] SBP: systolic blood pressure. Values represent mean and standard deviation unless otherwise specified.

Table 6.2: Diagnosis of dengue fever in patients recruited to the study

Variable	DF (n=10)	DHF (n=05)
Diagnosis of dengue		
Positive rapid NS1, n (%)	04 (40)	03 (60)
Positive dengue IgM, n (%)	03 (30)	04 (80)
Detectable viraemia, n (%)	10 (100)	05 (100)
Serotype of dengue		
DENV 1	01 (10)	0
DENV 2	09 (90)	05 (100)
Evidence of fluid leakage		
Pleural effusion, n (%)	0	05 (100)
Ascites, n (%)	0	01 (20)

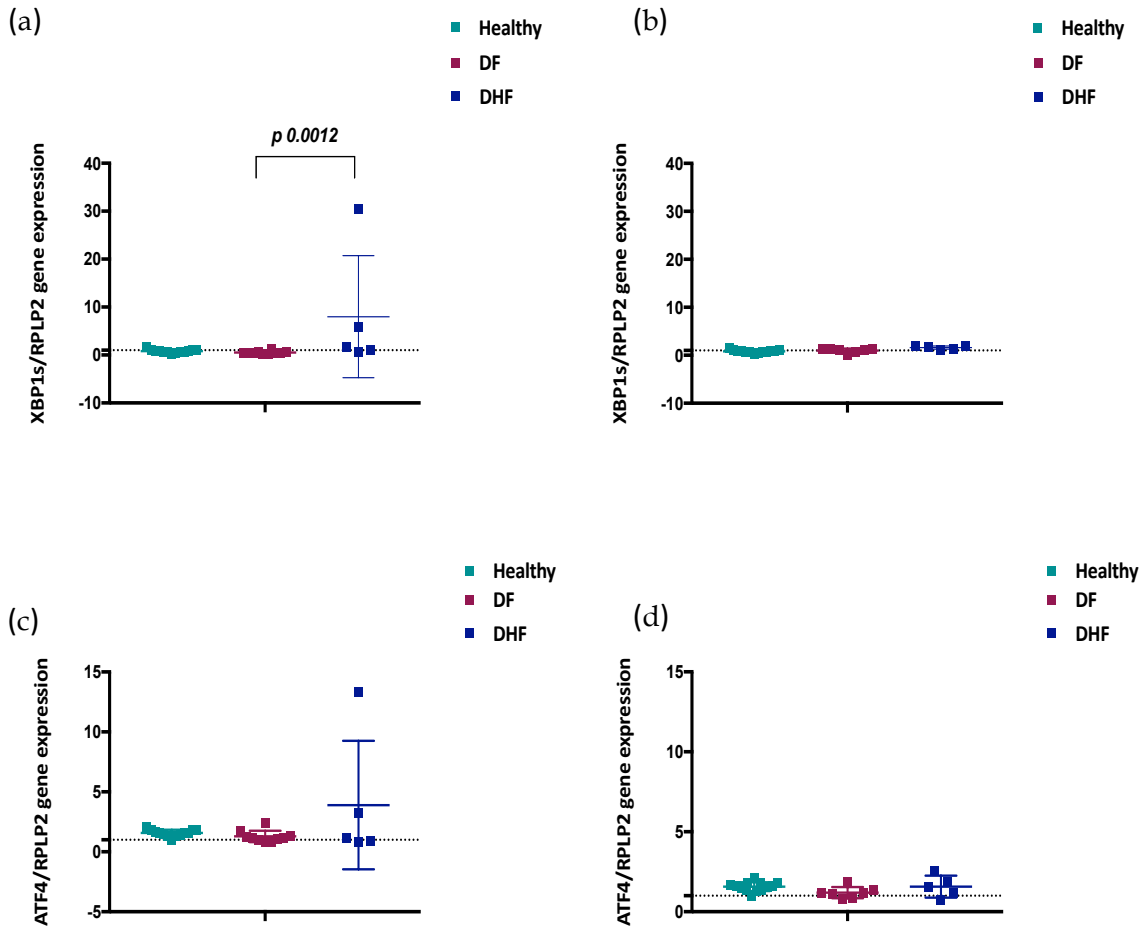

Figure 6.3: Expression levels of XBP1s and ATF4 transcripts in PBMCs of patients with dengue fever. PBMCs were isolated as described in Chapter 3 from patients with dengue infection during the first 3 days of illness (febrile phase) and 24 hours after fever subsided (defervescence phase). A multiplex qRT-PCR was performed to identify XBP1s (a) and (b) and ATF4 (c) and (d) transcripts as described in chapter 3 and normalised to the RPLP2 housekeeping gene transcripts. Figures show mean values from 13 healthy, 10 DF and 5 DHF samples in duplicate. Error bars denote standard deviation. DF; dengue fever, DHF; dengue haemorrhagic fever, ns; non-significant. Analysed by one-way ANOVA.

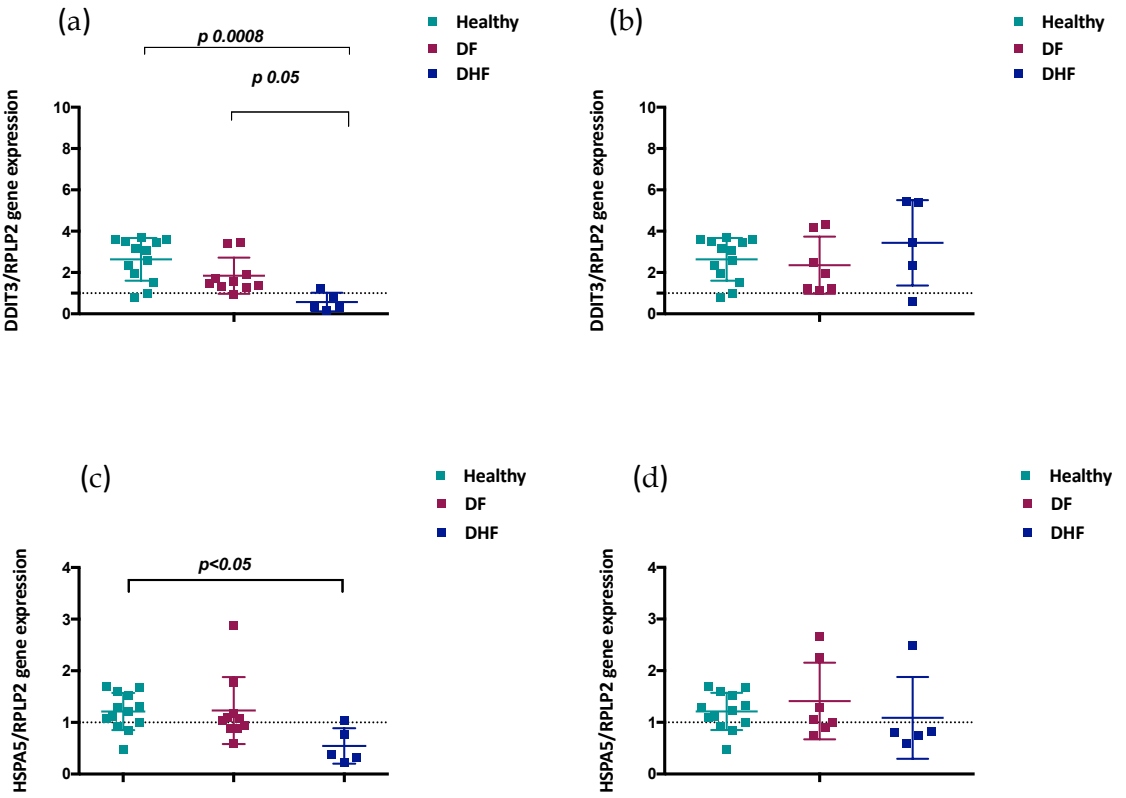

Figure 6.4: Expression levels of DDIT3 and HSPA5 transcripts in PBMCs of patients with dengue fever. PBMCs were isolated as described in chapter 3 from patients with dengue infection during the first 3 days of illness (febrile phase) and 24 hours after fever subsided (defervescence phase). A multiplex qRT-PCR was performed to identify DDIT3 (a) and (b) and HSPA5 (c) and (d) transcripts as described in chapter 3 and normalised to the RPLP2 housekeeping gene transcripts. Figures show mean values from 13 healthy, 10 DF and 5 DHF samples in duplicate. Error bars denote standard deviation. DF; dengue fever, DHF; dengue haemorrhagic fever, ns; non-significant. Analysed by one-way ANOVA.

Overall, these qRT-PCR data show that the IRE1α-XBP1s pathway which is pro-viral (Chapter 5) is upregulated during the early phase of dengue infection in patients developing severe dengue disease. In addition, DDIT3 and HSPA5 are suppressed in these patients. Since suppression of the pro-apoptotic marker, DDIT3 was observed in severe dengue patients, the viral load was quantified in the serum to see whether these patients had higher viraemia compared to non-severe dengue patients (Figure 6.5). However, the serum viral load was not significantly different in the two groups during the febrile phase or when the fever subsided.

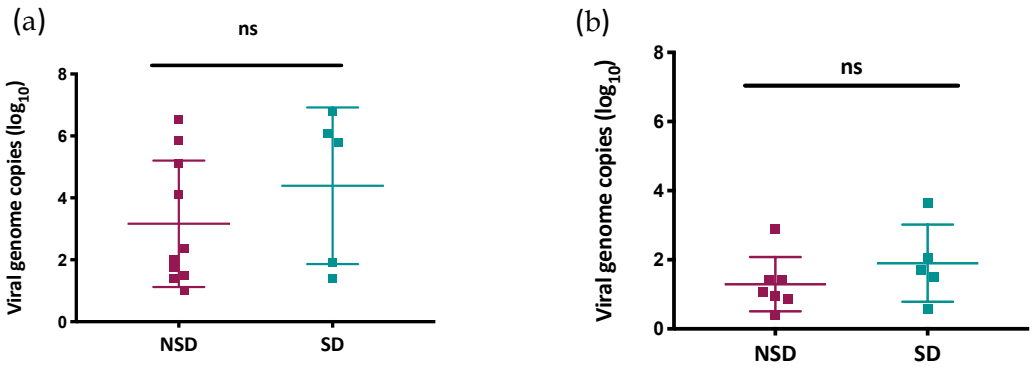

Figure 6.5: Serum viral load measured by qRT-PCR in patients with dengue fever. RNA was isolated from serum as described previously and viral RNA load was quantified by qRT-PCR and compared to a standard curve during (a) febrile phase and (b) 24 hours after fever subsided. Samples included 10 DF and 5 DHF patients during febrile phase and 7 DF and 5 DHF patients during defervescence. DF; dengue fever, DHF; dengue haemorrhagic fever, ns; non-significant. Analysed by Mann-Whitney U

Since patients who developed DHF had lower platelets and higher packed cell volume (PCV) values, further analysis was performed to find a potential correlation between expression of the UPR transcripts during the febrile phase of illness and the clinical parameters during the course of illness. The platelet number in dengue patients on admission to the hospital and the lowest platelet count observed during the course of illness positively correlated with the expression of DDIT3 and HSPA5 transcript levels (Figures 6.6 and 6.7). There was no correlation observed between XBP1s, ATF4 and platelet number (Figures 6.6 and 6.7). There was no significant correlation between UPR transcripts and the platelet number during defervescence (data not shown).

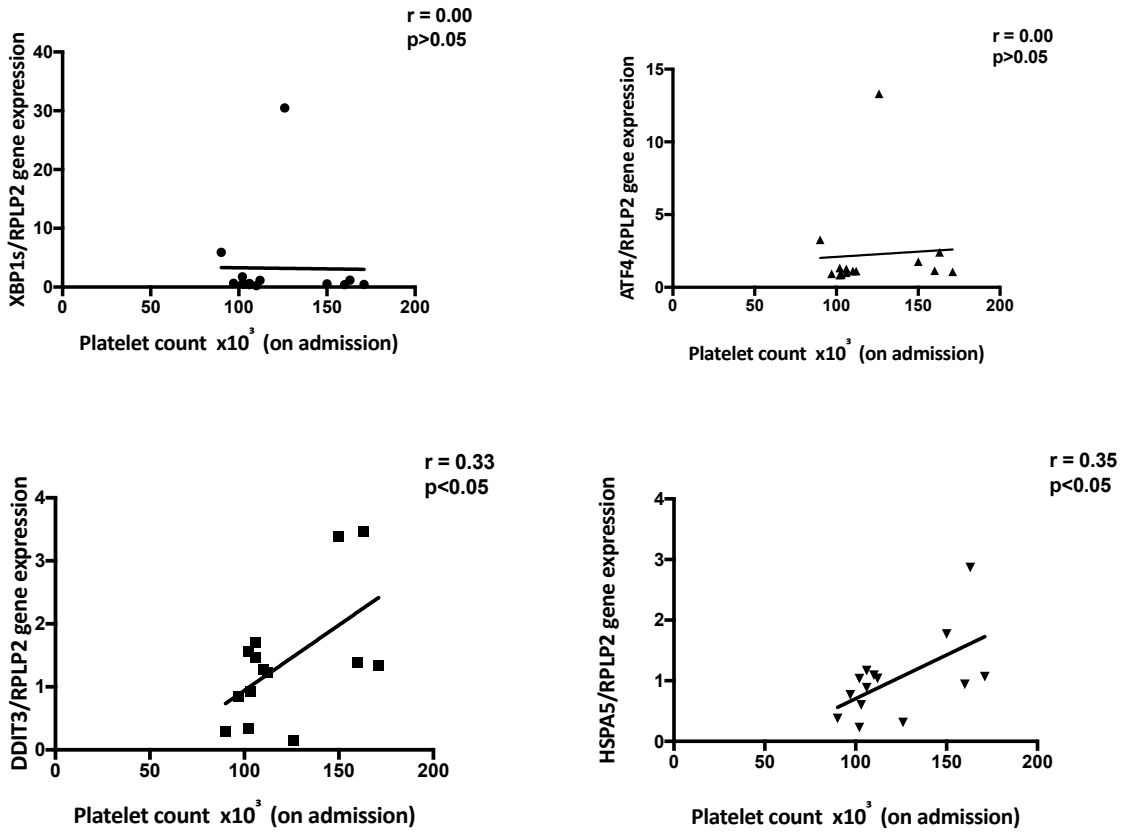

Figure 6.6: Correlation of UPR transcripts in PBMCs with the platelet count on admission. The UPR transcript level was plotted against the platelet count of the patient documented on admission to hospital. Correlation was measured by Spearman r non-parametric testing.

Analysis of the white cell number on admission and the lowest white cells reported during the illness revealed that these values did not correlate with the UPR transcripts in the PBMCs (Figures 6.8 and 6.9).

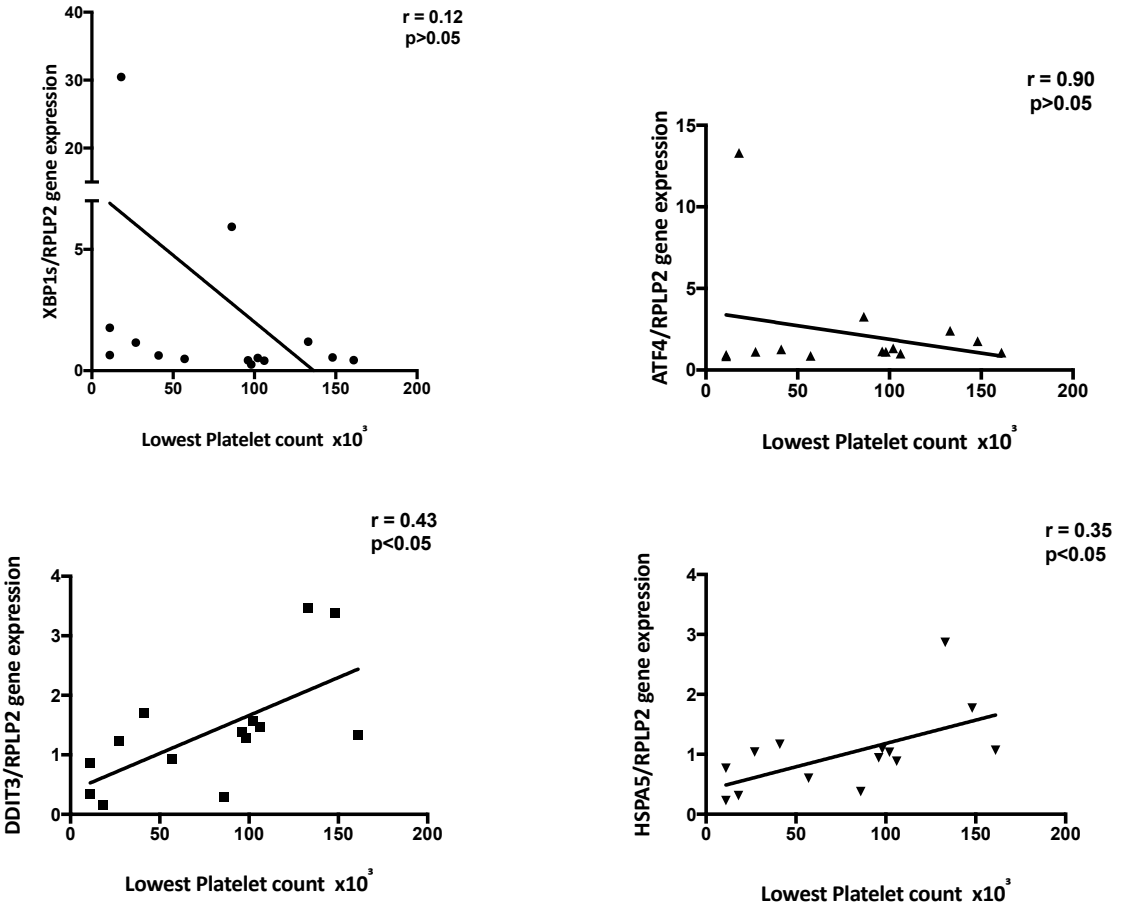

Figure 6.7: Correlation of UPR transcripts in PBMCs with the lowest platelet count. The UPR transcript level was plotted against the lowest platelet count of the patient documented during the hospital stay. Correlation was measured by Spearman r non-parametric testing.

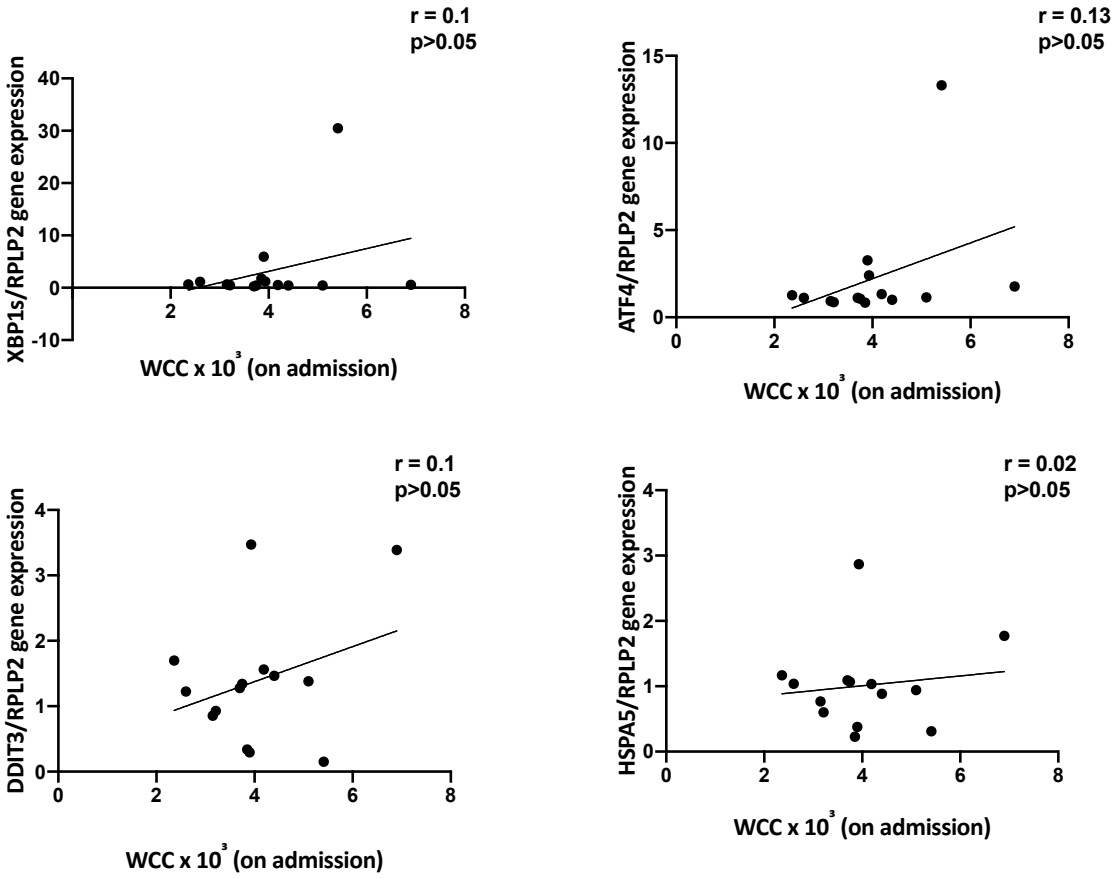

Figure 6.8: Correlation of the UPR transcripts in PBMCs with the white cell count (WCC) on admission. The UPR transcript level was plotted against the white cell number of the patient documented on admission. Correlation was measured by Spearman r non-parametric testing.

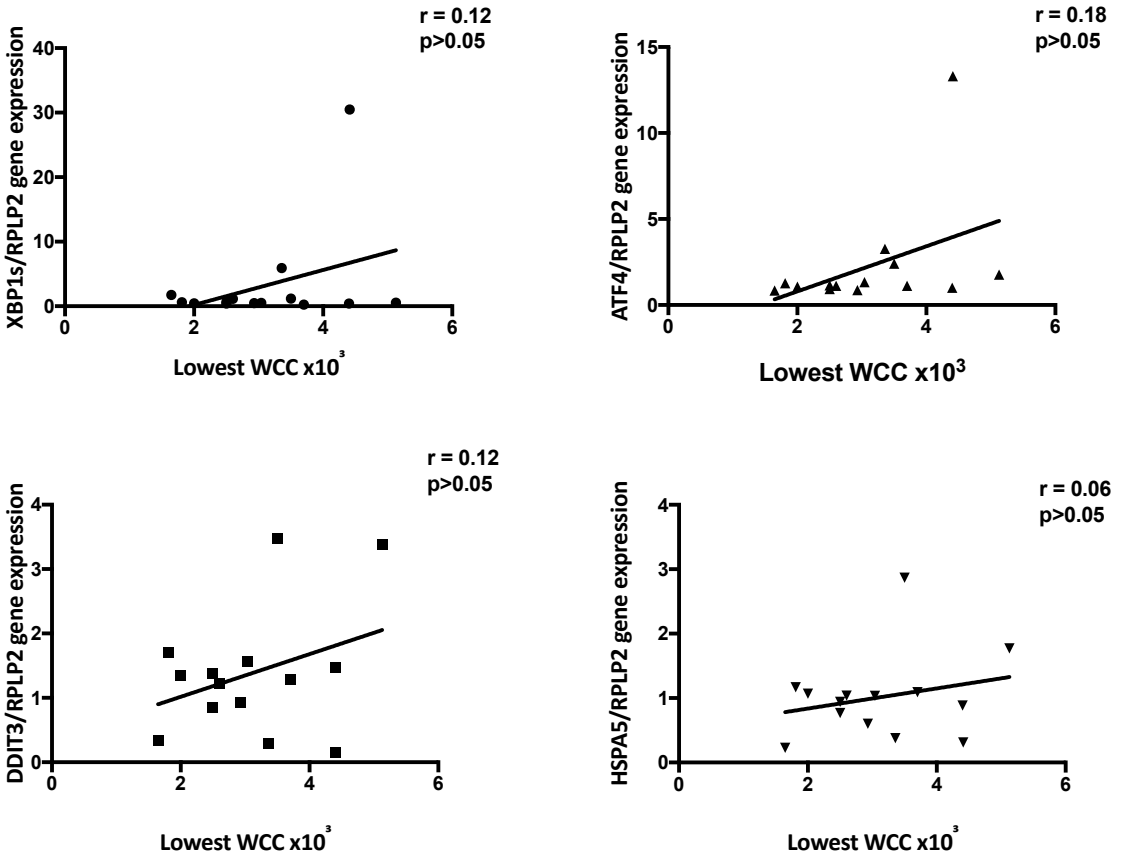

Figure 6.9: Correlation of the UPR transcripts in PBMCs with the lowest white cell count. The UPR transcript level was plotted against the lowest white cell number of the patient documented during hospital stay. Correlation was measured by Spearman r non-parametric testing.

I further analysed the relationship between the PCV on admission and the highest recorded PCV of the patient with the UPR transcripts. Only DDIT3 a significant negative correlation with the highest PCV documented during the course of illness (figures 6.10 and 6.11).

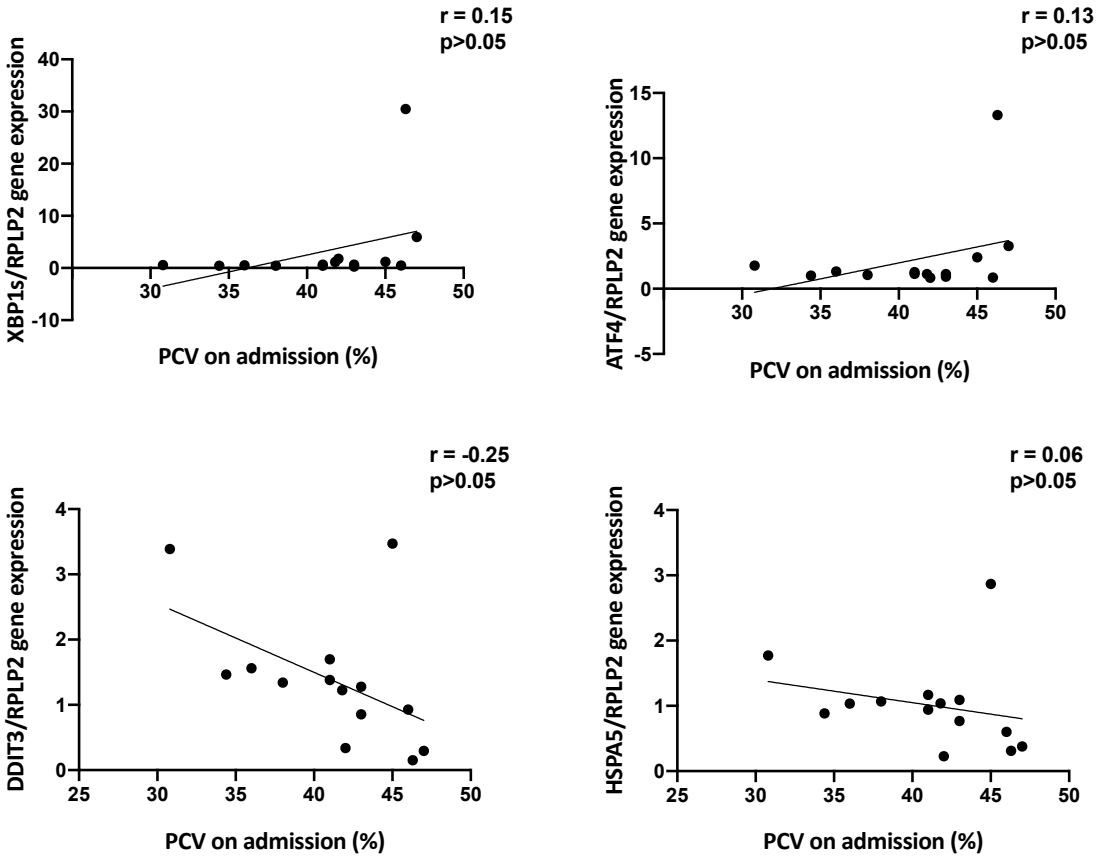

Figure 6.10: Correlation of UPR transcripts in PBMCs with the PCV on admission. The UPR transcript level was plotted against the PCV of the patient documented on admission. Correlation was measured by Spearman r non-parametric testing.

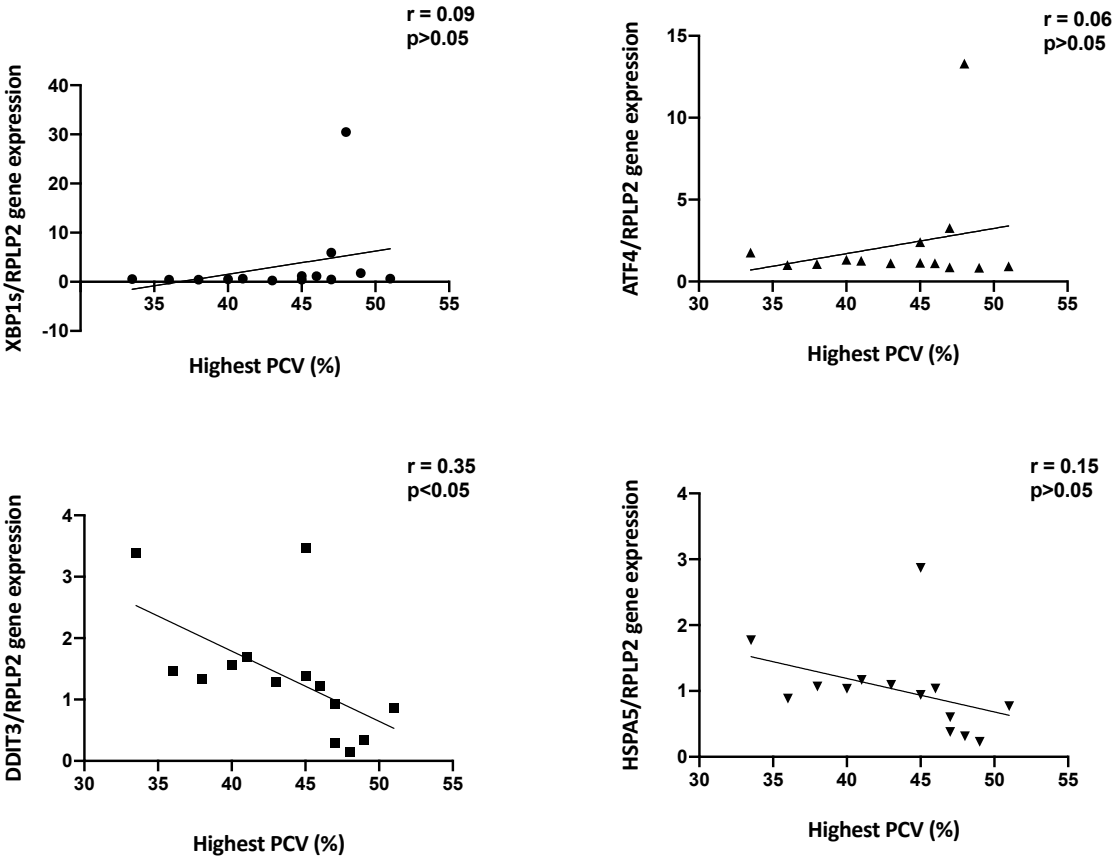

Figure 6.11: Correlation of the UPR transcripts in PBMCs with the highest PCV. The UPR transcript level was plotted against the highest PCV of the patient documented during hospital stay. Correlation was measured by Spearman r non-parametric testing.

6.2.2. Phase II: Identification of protein markers of disease severity in the PBMCs of dengue patients:

We performed mass spectrometry following TMT labelling on 8 PBMC lysates from patients with dengue fever. These were compared to 2 TMT labelled healthy control PBMC lysates. Protein levels and the total peptide concentrations following digestion were quantified and normalized among samples prior to the experiment. Mass spectrometry identified 1058 proteins constituting of 7353 peptide sequences. The mean amount of these peptides were compared among the healthy samples and the dengue-infected samples (pooled DF and DHF samples). Peptides with a mean fold change of more than 2 were identified and further analyzed. There were 163 peptides differentially expressed with a fold change more or less than 2 in the dengue-infected patient PBMCs compared to the healthy controls. Among these peptides, 109 were up-regulated while 54 peptides were down-regulated in the infected samples compared to healthy cell lysates. The top 20 differentially expressed proteins are given in Table 6.3 (top 10 up-regulated peptides and the 10 down-regulated peptides). The differentially expressed peptides were analyzed further by the STRING software to identify pathways implicated in dengue-infected patients compared to the healthy group (Figure 6.10).

Pathway analysis revealed that the main up-regulated biological processes (Gene Ontology, GO) were related to immune response and defense against organisms/viruses (Supplementary table 1). Proteins related to type 1 interferon pathway were also identified in addition to those constituting stress response. The down-regulated proteins were mainly involved in exocytosis, platelet degranulation and activation, cell activation and cell-matrix adhesion (Supplementary table 2).

Table 6.3: The top 20 differentially expressed proteins in dengue-infected PBMCs

Proteins	Function	Healthy sample mean (SD)	Dengue-infected samples mean (SD)
Proteins up-regulated in dengue infected PBMCs			
IFIT3	Antiviral response	1.07 (0.07)	8.8 (4.72)
ISG15	Innate immunity	0.89 (0.10)	5.33 (2.06)
PERM	Host defense in PMN	0.96 (0.04)	4.35 (4.9)
MX1	**Interferon-induced antiviral activity**	**1.11 (0.11)**	**5.03 (1.97)**
IFIT2	Antiviral activity	1.02 (0.02)	4.30 (1.48)
LBP	DNA-binding transcription factor activity	1.24 (0.24)	5.17 (3.21)
ALBU	Antioxidant activity and chaperone binding	0.57 (0.43)	2.36 (2.89)
OAS2	Cellular innate antiviral response	1.09 (0.09)	4.51 (1.22)
MYH9	Actin binding and cytokinesis	0.79 (0.21)	3.13 (1.84)
ACAD9	Required for mitochondrial complex 1 assembly	1.02 (0.02)	3.96 (7.69)
Proteins down-regulated in dengue infected PBMCs			
SAMHD1	**Host restriction factor**	**0.69 (0.31)**	**0.22 (0.12)**
K1H1	Structural constituent of cytoskeleton	1.11 (0.11)	0.37 (0.17)
F13A	Stabilizes fibrin clot	1.27 (0.27)	0.43 (0.22)
ODO1	2-oxoglutarate metabolic process	1.32 (0.32)	0.50 (0.06)
SIAS	Carbohydrate biosynthetic process	0.72 (0.27)	0.27 (0.08)
RAB8A	Intracellular membrane trafficking	0.9 (0.1)	0.34 (0.13)
GTPB1	GTP metabolic process	3.02 (2.02)	1.17 (0.34)
URP2	Role in cell adhesion	1.32 (0.32)	0.53 (0.19)
CO3	Activation of complement system	0.93 (0.06)	0.38 (0.10)
PRKDC	Molecular sensor for DNA damage	0.74 (0.25)	0.31 (0.13)

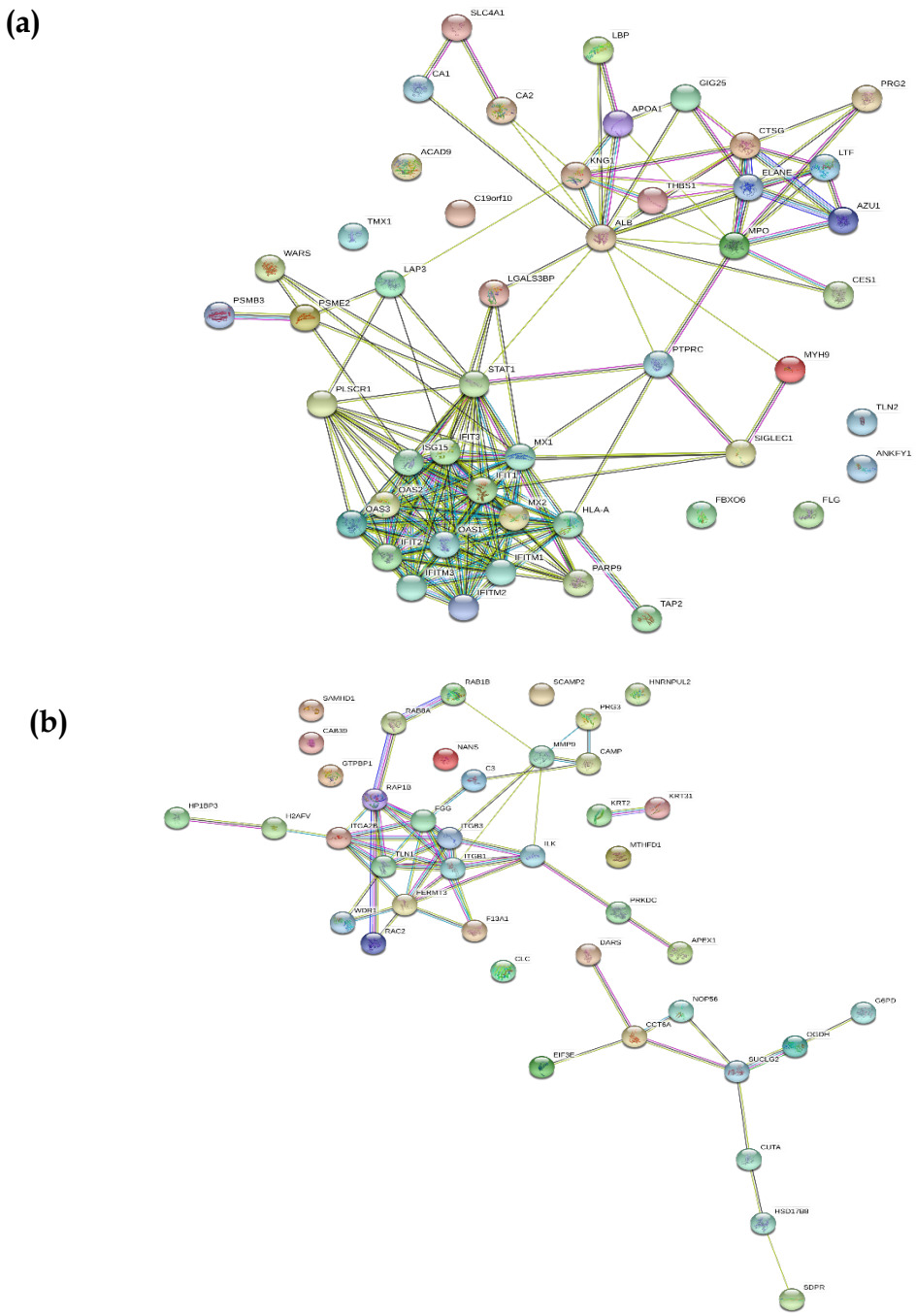

Figure 6.12: Pathways differentially regulated in dengue infected PBMCs compared to healthy controls. (a) Up-regulated proteins, (b) down-regulated proteins in dengue infection. The STRING software was used to identify the functional pathways associated with the proteins differentially regulated in dengue infection. The nodes represent the proteins and the network shows possible interactions among the identified proteins.

Following identification of proteins differentially expressed in dengue infection, the DHF and DF categories were compared to identify proteins in these groups. There were 167 proteins differentially regulated among DHF patients compared to DF. From these proteins, 77 were up-regulated in DHF while 90 proteins were down-regulated compared to the DF group (Supplementary table 3). The top 10 up-regulated and down-regulated proteins are shown in Table 6.4. Further analysis of the possible pathways enriched by these proteins revealed that the major pathways up-regulated in DHF (in comparison with DF) were the defence responses to organisms including humoral immune response, neutrophil degranulation, exocytosis and response to stress (Supplementary appendix 3, table S4). Interestingly, the IRE1-mediated UPR pathway was upregulated in DHF compared to DF with 2 proteins (MYDGF and TLN1) matching in the network analysis (False detection rate 0.0477). The network of proteins is schematically shown in Figure 6.11. These 2 peptides are shown in table S3 (Appendix 3), pages …… and ……. respectively and highlighted in bold. Although both MYDGF and TLN1 were not seen in the top 20 differentially regulated proteins in DHF compared to DF, these proteins are of interest given the important role of IRE1-XBP1 pathway in *in vitro* dengue infection as sown in chapter 5. Therefore, the possible role of these peptides in DHF is further discussed in detail in 6.3.

The down-regulated proteins were involved in 354 pathways. Important pathways were platelet degranulation and activation, exocytosis, regulation of blood coagulation, regulation of body fluids and cytoskeleton organization networks (Supplementary appendix 3, table S5). Regulation of endothelial cell apoptosis and apoptotic signalling pathways were also a function of the down-regulated proteins FGA, FGB, FGG, THBS1, ACAA2, GSN, SRC and YWHAH.

Table 6.4: Top 20 differentially regulated proteins in dengue haemorrhagic fever (DHF) compared to dengue fever (DF)

Proteins	Function	DF Sample, mean (SD)	DHF Sample, mean (SD)
Proteins up-regulated in PBMCs from DHF patients			
ACAD9	Required for mitochondrial complex 1 assembly	1.04 (0.11)	6.88 (10.01)
PRG2	Cytotoxin & induces histamine release from basophils	0.79 (0.08)	4.7 (5.7)
ELNE	Modifies function of NK cells, monocytes and granulocytes	0.86 (0.13)	4.55 (5.12)
ALBU	Antioxidant activity and chaperone binding	0.75 (0.29)	3.67 (2.9)
H2B1K	Transcription regulation, DNA repair, DNA replication and chromosomal stability	0.46 (0.29)	2.14 (2.5)
B3AT	Anion exporter and structural protein	0.63 (0.21)	2.71 (3.39)
PERM	Host defense in PMN	0.66 (0.16)	2.79 (1.52)
H2A proteins	Transcription regulation, DNA repair, DNA replication and chromosomal stability	0.45 (0.21)	1.77 (1.69)
CAH1	Carbonic anhydrase activity	0.81 (0.24)	2.93 (3.16)
H2B proteins	Transcription regulation, DNA repair, DNA replication and chromosomal stability	0.64 (0.28)	2.24 (2.39)
Proteins down-regulated in PBMCs from DHF patients			
SRC	Non-receptor protein tyrosine kinase	4.16 (4.45)	0.95 (.27)
HNRL2	RNA binding	0.59 (0.36)	0.15 (0.06)
PTPRC	T-cell activation	3.39 (4.09)	0.94 (0.25)
MIC60	Mitochondrial membrane protein	3.43 (2.98)	1.06 (0.18)
K2C6B	Structural constituent of cytoskeleton	1.54 (1.62)	0.52 (0.13)
KNG1	Role in blood coagulation	5.24 (5.6)	1.81 (0.52)
TLN1	Cell-cell junction assembly	1.1 (0.63)	0.39 (0.03)
GELS	Actin-binding protein	3.33 (3.1)	1.21 (0.44)
MX1	Interferon-induced antiviral activity	3.62 (4.46)	1.33 (0.48)
ITB3	Cell-adhesion molecular binding	2.17 (1.75)	0.81 (0.27)

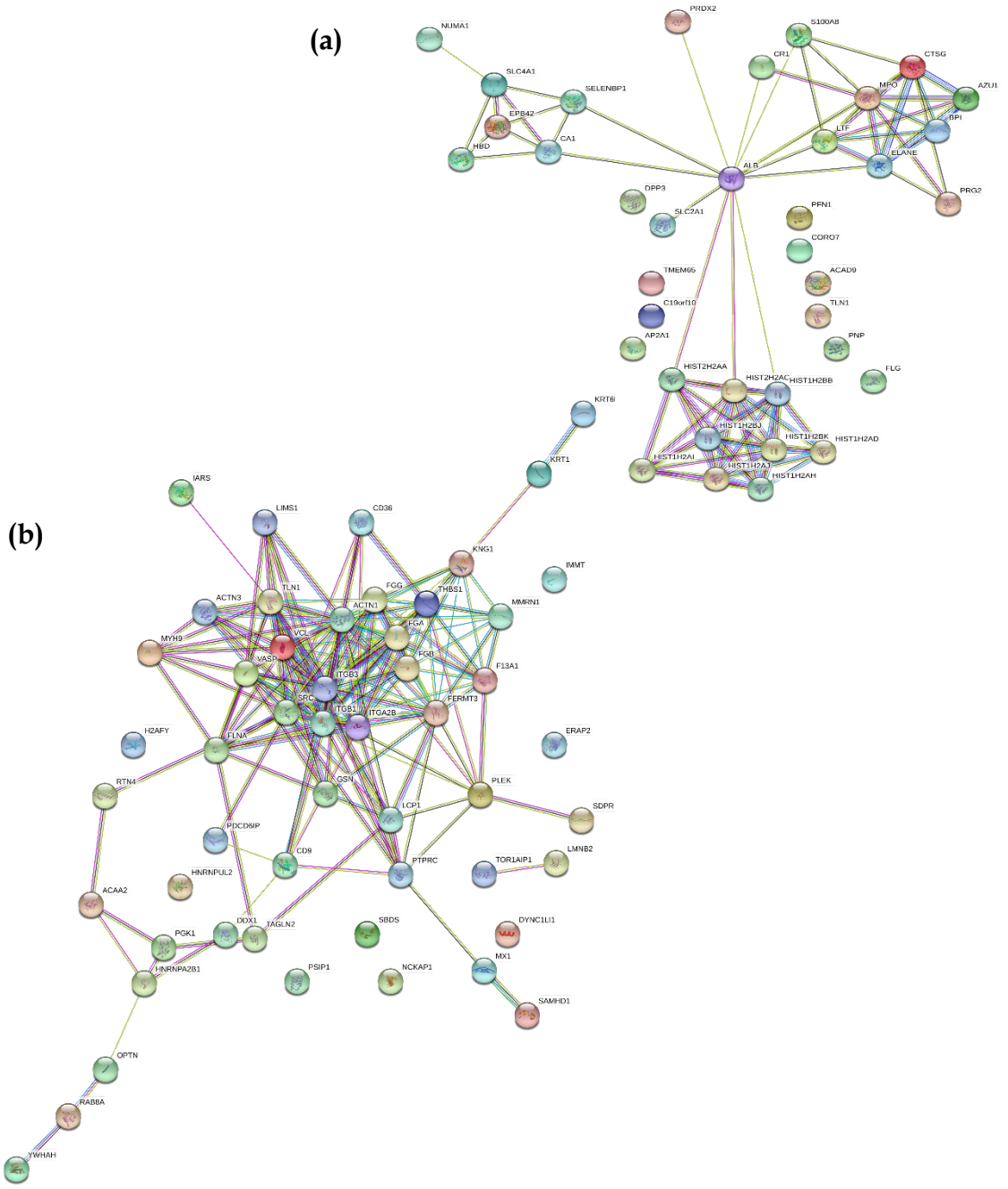

Figure 6.13: Pathways differentially regulated in DHF patient PBMCs compared to DF PBMCs. (a) Up-regulated proteins, (b) down-regulated proteins in severe dengue disease. The STRING software was used to identify the functional pathways associated with the proteins differentially regulated in dengue infection. The nodes represent the proteins and the network shows potential interactions among the identified proteins.

6.3 Discussion

Identification of biomarkers that could accurately predict disease severity in dengue fever has been an ongoing research question. However, variable and non-reproducible results have been a problem in utilizing inflammatory mediators as potential markers as published previously. Currently, there are no approved biomarkers that could be used to triage patients in early disease.

6.3.1 UPR chaperones identified as markers of severe dengue manifestations

I sought to identify host factors that could indicate DHF in peripheral blood monocytes. The basis for investigating the UPR-related markers was based on the understanding of the effect of the UPR on virus secretion and inflammatory mediator secretion from cultured human monocyte-derived macrophages. As described previously in chapter 5, UPR pathways were differentially regulated in the presence of dengue infection. Namely, the IRE1α-XBP1 pathway was pro-viral in monocyte-derived macrophages and it was associated with increased secretion of TNFα and IFNα from these cells. I questioned whether this pathway could be differentially regulated in patients who develop severe disease during the early phase of their illness leading ultimately to increased viraemia and a dysregulated inflammatory response. The UPR has complex interactions with host inflammatory pathways, apoptosis and autophagy mechanisms [33]. All these host responses have been identified to be relevant in dengue infection. In addition, previous studies investigating the cellular transcriptome in patients who developed severe dengue infection have suggested upregulation of UPR-related genes [177]. The clinical observation that patients who have obesity and diabetes develop more severe manifestations and fluid leakage also suggests that host-viral interactions might be responsible [185]. The UPR is known to be activated in the liver, pancreas and the adipose tissue of patients with a metabolic phenotype (reviewed in [186]). All these associations

and the previous literature reports linking the UPR and obesity prompted us to investigate the possible association between the UPR and dengue disease severity in clinical samples. This study provides the first comprehensive analysis of the UPR in early dengue infection of patients who later developed either DHF or DF.

The most interesting finding was a significant increase in XBP1s transcripts during the initial phase of the illness, in patients who later developed DHF compared to the DF category. This data suggest that IRE1α-XBP1 pathway could be an important host response determining the outcome of dengue infection. The proteomic analysis performed with the PBMC lysates identified 2 peptides associated with the IRE1-mediated UPR pathways. These were myeloid derived growth factor (MYDGF, C19Orf10, page 169 supplementary table S3) and Talin-1 (TLN1, page 171, supplementary table S3) according to the "reactome" pathway analysis database the two genes that are chaperones of XBP1.

MYDGF is located in the ER lumen [187] and secreted [188]. A study identified this protein in the bone marrow cells (monocyte/macrophage origin) in patients with acute myocardial infarction involved in myocardial repair [189]. In addition, MYDGF was found in the liver of hepatocellular carcinoma and it was thought to be responsible for accelerating tumour growth [188]. MYDGF was also identified in the synovium of patients with inflammatory arthritis [190]. We report MYDGF for the first time in peripheral blood monocytes where it may be potentially implicated in severe dengue disease. Patients with DHF had higher MYDGF protein expressed in the PBMCs compared to DF patients (fold change 2.1, supplementary table S3). Although the exact function of this protein is not clear in dengue disease pathogenesis, further experiments could provide much needed information on its role in dengue infection. In addition, quantification of the secreted

MYDGF in serum might provide a marker for identifying DHF patients early in the course of illness.

The second differentially regulated protein reported in the reactome database as a XBP1 chaperone was TLN1. Many peptides derived from TLN1 protein were identified and one of these peptides was up-regulated while another peptide was down-regulated in DHF infection (Figure 6.11) making further interpretation difficult. TLN1 is a cytoskeletal protein important in cell-cell contact. Database search reveals that TLN1 is a XBP1 chaperone. Although TLN1 has not being implicated in dengue before, another study found TLN1 to act as a virus restriction factor in HIV infection [191]. It would be interesting to further investigate the role of TLN1 in DENV pathogenesis.

The second interesting finding is reduced expression of DDIT3 (CHOP) transcripts in the PBMCs of DHF patients. DDIT3 is a pro-apoptotic marker activated by ER stress downstream of the PERK-ATF4 pathway. In addition to DDIT3 transcripts, pathway analysis of down-regulated proteins in DHF PBMC lysates revealed inhibition of apoptotic signalling pathways compared to the DF patient group. Previous *in vitro* studies have shown inhibition of apoptosis by DENV to maintain its survival in infected cells [40]. It is possible that inhibition of apoptotic pathways by DENV ensures viral replication in affected cells in DHF patients which ultimately leads to higher ER stress and possibly increased inflammatory mediator secretion. The HSPA5 (BiP) transcripts were also suppressed in early dengue infection in DHF patients, compared to the DF group, which later increased during the defervescence. Interestingly, reduced DDIT3 and HSPA5 levels had a significant correlation with thrombocytopaenia and DDIT3 had a significant correlation with increased PCV. Patients who had lower DDIT3 and HSPA5 levels developed lower platelet counts and patients with lower DDIT3 had higher PCV than the

rest. However, patients with DHF did not have a significantly higher virus load in serum compared to DF group. It raises the question whether patients who developed DHF infection and higher XBP1s transcripts respond differently to the same viral load compared to the DF patients. Do these patients develop higher ER stress in PBMCs in response to DENV? Or would the intracellular viral load be different if quantified in these patients despite not having a significant difference in the serum virus load? Answers to these questions could provide further insight into the pathogenesis of severe dengue disease in human infections. Overall, data in this chapter provides evidence that UPR is an important host response and suggest that it is possible to utilize them as disease markers in early infection to identify patients developing severe disease.

6.3.2 Non-UPR proteins differentially expressed in DHF infection

Several protein networks were differentially expressed in patients with DHF compared to DF. Of note, histones were highly expressed in DHF lysates which comprised of H2A and H2B histone proteins. Histones are involved in the structural assembly of the nucleosome [192]. DENV capsid protein is known to bind histones in liver cells and inhibit formation of the nucleosomes and this study also suggests that DENV infection increases the levels of core histones in the nucleus [193]. Interestingly, a proteomic analysis of platelets during DENV infection showed increased levels of histone proteins (mainly H2A histones) in patients with severe dengue infection compared to DF [194]. The levels correlated with serum histones in these patients. Despite sequestering histones in platelets of DHF patients, histones were not produced in platelets in response to DENV infection [194]. It was postulated that histones were produced in higher amounts by the infected megakaryocytes or platelets sequestered histones from the circulation. Our data reveal that PBMCs of DHF patients expressed increased amounts of H2A and H2B histones suggesting that the source of serum histones may be derived from circulating monocytes.

SAM domain and HD domain-containing protein 1 (SAMHD1) was down-regulated in dengue-infected PBMCs compared to healthy controls. The fold change of SAMHD1 peptide levels was also lower in DHF patients (Figure 6.14) compared to DF (fold change -2.01). This deoxynucleotide triphosphate (dNTP) hydrolase maintains the dNTP pool within the cell appropriate for DNA repair and replication [195]. Its antiviral role has been investigated in HIV, hepatitis B and Herpes simplex virus-1 (HSV-1) infection (reviewed in [195]). Data in this chapter suggest a possible role of SAMHD1 in severe dengue disease. The lower expression of this protein in patients with DHF suggest that DENV inhibits this restriction factor to overcome the replication block. However, the viral load was not significantly different among DHF and DF groups suggesting a different role for this protein. Quantification of the intracellular viral load would provide more accurate details in this regard.

Another interesting protein up-regulated in DHF PBMCs was Proteoglycan 2 (PRG2) (Figure 6.14). PRG2 is a cytotoxin in addition to stimulating release of histamine from mast cells. Mast cells, residing in the skin encounter DENV early during infection and studies have found mast cells to secrete histamine, Chymase, vascular endothelial growth factor (VEGF), serotonin, cytokines and chemokines in response to DENV infection (reviewed in [196]). Severe dengue infection has been associated with high urinary histamine levels among other mediators [167]. Histamine causes vasodilatation and it is implicated in severe manifestations of dengue fever. The observation of high PRG2 in DHF lysates raises the question whether PRG2 secreted by PBMCs plays a role in mediating histamine release from mast cells during severe dengue infection.

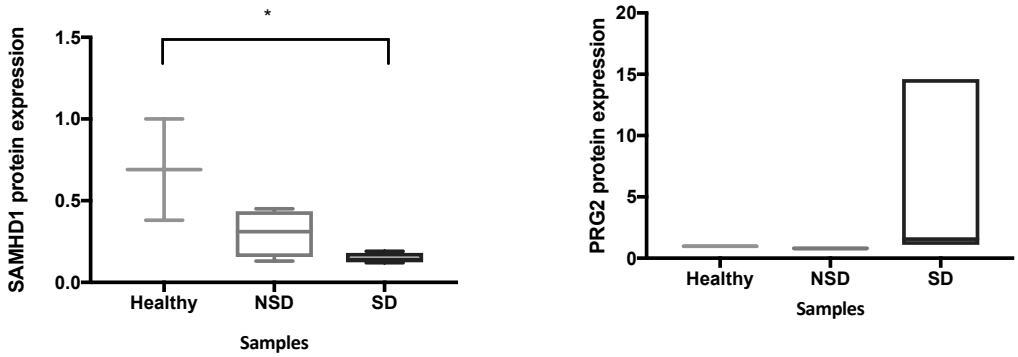

Figure 6.14: Expression of SAMHD1 and PRG2 proteins in the PBMC lysates. Proteins were quantified in the PBMC lysates of 02 healthy, 04 DF and 04 DHF patient samples by TMT mass spectrometry. Protein expression is shown. Analysed by one-way ANOVA. *$p<0.05$

Overall, protein expression in PBMCs of DHF patients reveals up-regulation of several proviral proteins and networks and reduction of antiviral factors. Platelet degranulation, activation and aggregation was also down-regulated in DHF lysates compared to the DF group. It is important to quantify these markers identified from this study in a larger population to confirm the possibility of using them as markers of disease severity. In addition, mechanistic studies could help to understand the role of these markers in dengue disease pathogenesis. This study could potentially provide a foundation to identify a marker to assess dengue disease severity.

Several limitations were encountered during this study. One such issue was the variable viraemia expected during the course of illness. Although all the samples were pooled together when analysing the viral load in the febrile and defervescence phases, it is important to understand that the level could be significantly influenced by the day of

illness as well as the serotype and immune status. Further data on this regard is necessary to have a better interpretation.

VII

The effect of iminosugar treatment on DENV-induced oxidative stress and antioxidant levels

Viral infection induces reactive oxygen species (ROS) in infected cells to combat infection and to mount an innate immune response. DENV-infection induces NADPH oxidase (NOX)-dependent ROS in dendritic cells. The effect of redox balance on the DENV

replication and the close association of ROS levels and the inflammatory signaling cascade warrant investigation of the effect of iminosugars on redox balance in DENV infection. Results in this chapter show that DENV infection induced ROS and increased the total antioxidant capacity (TAC) in infected primary macrophages. Treatment with 2THO-DNJ and M*O*N-DNJ resulted in attenuation of DENV-induced ROS. In addition, treatment with the two DNJ-derived iminosugars reduced the compensatory TAC levels in DENV-infection while increasing the TAC in uninfected cells. The increase in the TAC levels of uninfected cells was not associated with an increase in oxidative stress suggesting that these compounds could potentially increase antioxidant capacity independent of ROS in cells.

7.1 Introduction

DENV infection, similar to other viruses, induces free radical formation in infected cells [65]. The Nrf2-mediated antioxidant mechanisms try to mitigate excessive free radical stress and maintain a redox balance. The ROS production and the implications for disease severity in DENV infection is described in detail in chapter 1.

Iminosugars elicit antiviral effects in DENV-infected cells by reducing viral secretion and infectivity. But the effect of iminosugars on redox status in the context of viral infection is unknown. Previous transcriptomic work on DENV-infected macrophages in our lab revealed that MON-DNJ upregulated the Nrf2 pathway suggesting that this compound could potentially modulate the antioxidant pathways [2]. The reduction of TNFα seen in iminosugar-treated DENV-infected macrophages (chapter 5) and DCs (chapter 4) as well the reduction of TNFα in LPS-treated macrophages (chapter 5), raises the question of the role of ROS in mediating these effects. This chapter discusses the effect of 2THO-DNJ and MON-DNJ on DENV-induced oxidative stress and their effect on the antioxidant capacity in primary macrophages.

7.2 Results

Primary macrophages were infected with DENV2 at MOI 1 and the reactive oxygen species (ROS) were measured using CellRox Green detection reagent as described in chapter 3.7.1. It was known from literature that the optimal time point for ROS detection was 18 hours p.i.. Analysis of the geometric mean fluorescence data revealed a significant increase in ROS levels in DENV-infection compared to uninfected samples (Figure 7.1a). However, the difference observed was minimal suggesting that cells were able to quench the ROS levels by the compensatory mechanisms. Therefore, the total antioxidant capacity (TAC) was measured which showed an increase in TAC levels following DENV-infection (Figure 7.1b) which was dependent on the MOI of infection.

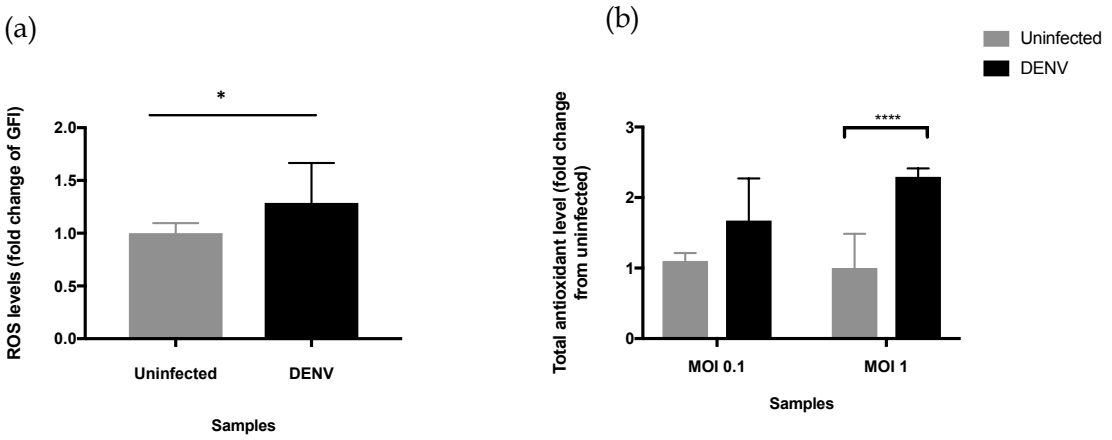

Figure 7.1. Reactive oxygen species and total antioxidant capacity in DENV-infected monocyte-derived macrophages. (a) Primary macrophages were infected with DENV2 at MOI 1. At 18 hours p.i. cells were harvested and ROS detected by flow cytometry. Analysed by t-test. (b) Primary macrophages were infected with DENV2 at MOI 0.1 or MOI 1 for 18 hours and then lysed to quantify the total antioxidant capacity. Analysed by 2-way ANOVA. All data represent pooled values from 3 independent donors. *$p<0.05$, ****$p<0.0001$.

Having observed an induction of ROS and a compensatory increase in TAC levels following DENV infection, the effect of iminosugar treatment was evaluated. Two DNJ-derived iminosugars were used for these experiments. The compound 2THO-DNJ was used as the main drug investigated in this thesis. MON-DNJ was used to validate changes seen in the transcriptomic research carried out in our group previously. Both 2THO-DNJ and MON-DNJ were used at concentrations that inhibited αGluI. The GluI inhibition was observed at doses exceeding 10 μM MON-DNJ treatment and 31.6 μM 2THO-DNJ treatment. For the following experiments we decided to administer drug in a single dose at a concentration that was 3-times higher than the IC_{50} for the respective drug, i.e. 25 μM MON-DNJ and 80 μM 2THO-DNJ. Treatment with both iminosugars reduced DENV-induced ROS levels significantly. There was no increase in ROS levels in uninfected controls following iminosugar treatment suggesting that the compound does not increase oxidative stress in cells despite inhibiting α-glucosidases and disrupting protein folding.

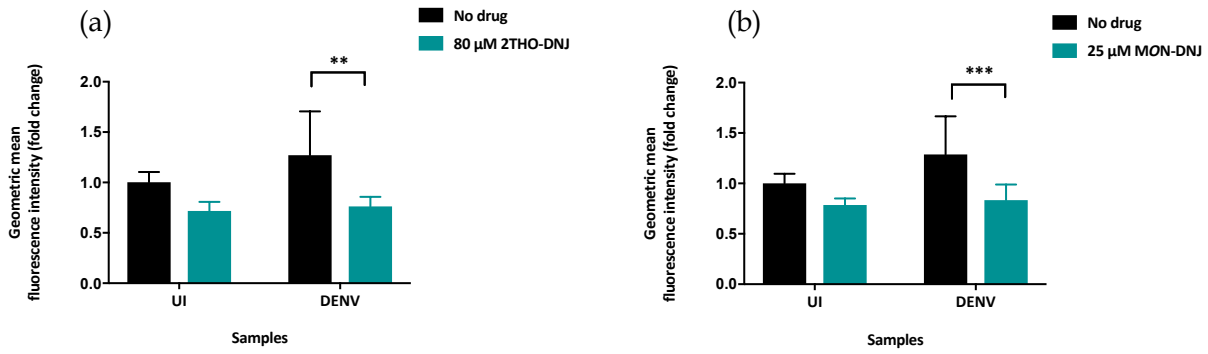

Figure 7.2. Reactive oxygen species in DENV-infected and iminosugar-treated monocyte-derived macrophages. Primary macrophages were infected with DENV2 at MOI 1 and treated with (a) 80 μM 2THO-DNJ, (b) 25 μM MON-DNJ. At 18 hours p.i. cells were harvested and ROS detected by flow cytometry. All data represent pooled values from 3 independent experiments. Analysed by 2-way ANOVA. $^{**}p<0.01$, $^{***}p<0.001$.

The effect of iminosugar treatment on the TAC was also evaluated. Treatment with 2THO-DNJ and MON-DNJ reduced DENV-induced TAC, which likely reflects a reduced ROS-mediated antioxidant response (Figure 7.3). Interestingly, treatment of the uninfected macrophages with the two compounds resulted in an increase in TAC levels. This suggests that the iminosugars have the ability to induce an antioxidant response independent of oxidative stress.

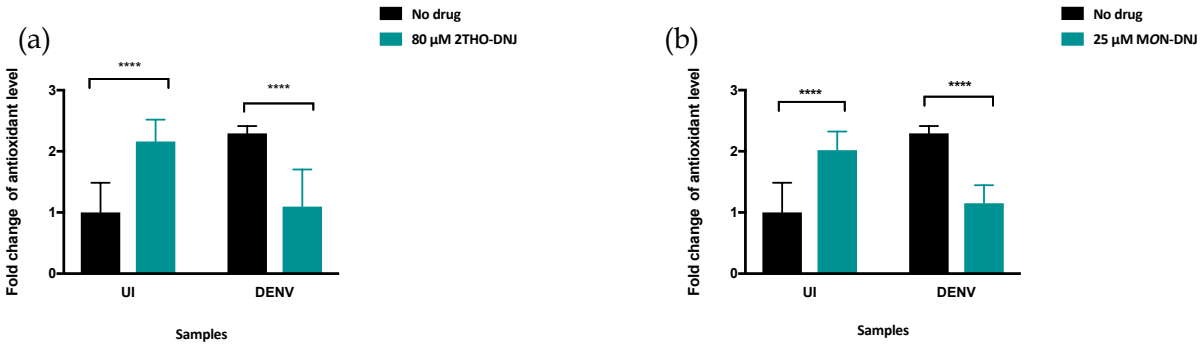

Figure 7.3. TAC in DENV-infected and iminosugar-treated monocyte-derived macrophages. Primary macrophages were infected with DENV2 at MOI 1 and treated with (a) 80 µM 2THO-DNJ, (b) 25 µM MON-DNJ. At 18 hours p.i. cells were lysed and TAC quantified. All data represent pooled values from 3 independent experiments. Analysed by 2-way ANOVA. ****$p<0.0001$.

7.3 Discussion

The iminosugars MON-DNJ and 2THO-DNJ reduce DENV secretion and DENV and LPS-induced TNFα levels in primary cells. Data in chapter 5 show that 2THO-DNJ modulates the DENV-induced UPR in a favourable manner for the virus. The UPR and cellular oxidative stress can affect many cellular signaling events such as autophagy and apoptosis [65, 197]. In addition, both crosstalk with each other and the inflammatory pathways of the cell [63, 85]. Given the ability of iminosugars to reduce TNFα levels induced by replicating and non-replicating pathogens, it is of interest to understand the effect of iminosugars on cellular redox status.

DENV infection induces ROS in primary macrophages as shown in this chapter and similar to previously published literature in Mo-DCs [65]. The low level of ROS induction following DENV infection is explained by the ability of the cells to quench the free radicals by increasing the antioxidant capacity. The antioxidant capacity in the DENV-infected cells was significantly increased at 18 hours p.i., which was greater at MOI 1 of infection compared to MOI 0.1, suggesting that the antioxidant responses correlate with the degree of DENV-infection. The TAC levels were likely higher following DENV infection as a compensatory response to the DENV-induced ROS and the reduction of these levels in 2THO-DNJ and MON-DNJ treatment could be due to the reduced ROS levels seen in these conditions. However, treatment with the two iminosugars in uninfected cells resulted in an increase TAC, despite not having an increase in ROS. This results suggests that treatment with the iminosugars could potentially increase antioxidant levels in the cells independent of producing oxidative stress. The increase in TAC levels could be Nrf2 driven. Previous transcriptomics data in our lab revealed that MON-DNJ could upregulate the Nrf2 signature and its downstream mediators [2]. It would be of interest to look at the Nrf2 protein levels following MON-DNJ and 2THO-DNJ treatment to

identify whether the increase in TAC is Nrf2-mediated in macrophages. However, detection of Nrf2 protein was challenging and a protein band could not be detected by western blots with confidence despite several attempts (data not shown). Future experiments to observe nuclear translocation of Nrf2 by confocal microscopy, following co-staining of the nucleus, might overcome this issue. A possible increase in Nrf2 activity can be explained by a PERK-dependent pathway. The increased activation of PERK transmembrane protein phosphorylates the cytoplasmic Nrf2 which results in dissociation of this molecule from the Keap complex and nuclear translocation. Once translocated, Nrf2 could activate ARE to induce antioxidant related genes. It is plausible that the increase in PERK arm activity observed following 2THO-DNJ treatment in DENV-infected and uninfected cells (Fig 5.6 c-d) could potentially activate an Nrf2-driven antioxidant response.

The reduction of DENV-induced ROS levels by iminosugar treatment could be due to there being fewer infected cells at 18 hours p.i. due to the antiviral effect of the compound. However, a viral independent effect cannot be completely excluded. It would be interesting to conduct a 2-colour flow cytometry experiment to understand whether the reduction in overall ROS levels was achieved by a reduction in the number of DENV antigen expressing cells or by a reduction of ROS in infected cells or both. If the ROS attenuation is seen to be unrelated to reducing DENV-infected cells, it could be a potential mechanism for the TNFα reduction observed with these drugs in both replicating and non-replicating inducers of inflammation.

VIII

Conclusions & Future work

8.1 Overview

This thesis attempted to answer two main questions. Firstly, the objective was to understand the effect of DENV infection on the host UPR in primary monocyte-derived macrophages *in vitro* and identify the expression of UPR transcripts in clinical dengue infections. The second objective was to understand the effect of iminosugar treatment on the host UPR in the presence of DENV infection in an attempt to describe how this interaction may contribute to the antiviral and anti-inflammatory effects observed with iminosugar treatment.

Chapter 4 shows the effect of iminosugar treatment on DENV-infected imDCs for the first time. Data shows that three DNJ-derived iminosugars but not *N*N-DGJ, reduce secretion of virus and the infectivity of secreted virus particles in a dose dependent manner. In addition, these drugs also reduced DENV-induced TNFα secretion from primary monocyte-derived imDCs. These results confirm that iminosugars elicit antiviral effects in immune cells other than macrophages. It would also be of interest in the future to understand how these drugs could affect T-cell mediated effects in DENV infection.

Data presented in this thesis reveal the pro-viral nature of the IRE1α-XBP1 UPR pathway in dengue infection and the preferential activation of this arm of the UPR by dengue infection *in vitro.* Interestingly, XBP1s transcripts and the IRE1α mediated UPR proteins were up-regulated in the PBMCs of patients developing severe dengue infection further providing evidence of the importance of the IREα pathway in dengue pathogenesis. These changes were observed during the early viraemic phase of clinical infections raising the possibility of potentially using IREα pathway mediators as a predictor of severe dengue disease with or without the combination of other UPR markers. Suppression of DDIT3 in

DHF raise further questions about the role of apoptosis in severe dengue manifestations. Measuring a combination of these transcript levels could provide a test to be used in early dengue disease to identify patients developing fluid leakage and severe manifestations during the course of illness. This thesis provides the foundation for developing a UPR-based disease biomarker to triage patients likely develop DHF at the onset of the disease.

The proteomic data from patient PBMC lysates also revealed potential non-UPR proteins contributing to dengue disease pathogenesis. Some identified factors differentially expressed in DHF patients are Sterile Alpha Motif and HD Domain-containing protein 1 (SAMHD1), Proteoglycan 2 (PRG2), ELNE (Neutrophil Elastase precursor) and MX1 (Interferon-induced GTP binding protein). SAMHD1 is a viral restriction factor which was significantly down-regulated in DHF patients early in the course of illness prior to development of severe disease manifestations compared to DF and the healthy controls. SAMHD1 is an interferon-inducible protein and it catalyzes deoxynucleotide triphosphates (dNTPs) in the cell thus maintaining a lower dNTP pool to restrict viral replication[195, 198, 199]. The role of SAMHD1 in restricting HIV-1 replication in monocytes and dendritic cells is well studied and cells deficient in SAMHD1 are highly susceptible to HIV-1 infection [198]. The role of this protein in viral infection, innate immunity and cancer has been reviewed extensively [195, 199, 200]. However, there are no studies on the role of SAMHD1 in DENV replication or disease pathogenesis. The down-regulation of SAMHD1 and also the other interferon-related antiviral protein MX1 suggests a possible suppression of interferon-related innate immune mechanisms in patients with DHF. We did not observe a significant difference in the viral load in serum of patients with DHF versus DF. However, it remains a possibility that the intracellular viral load is still different in these two groups. Further investigation to quantify the

intracellular viral load and continuation of the study to have a larger sample size might provide the answer to this particular question.

Investigation into other mediators differentially expressed in DHF would also provide new insight into dengue disease pathogenesis. One such protein is PRG2, known to increase release of histamine from basophils in allergic diseases. Severe dengue is associated with fluid leakage and one of the mediators implicated in this situation is histamine. Although the exact source of histamine in dengue disease is not clear, it is assumed that mast cells may play a role in secreting histamine in dengue infections [167]. PRG2 that is secreted from one of the components of PBMCs could be the culprit mediator inducing release of histamine from mast cells during dengue infection. Apart from understanding the pathogenesis, measurement of PRG2 in serum might be a good marker to differentiate DHF from DF in early dengue disease.

The effect of iminosugar treatment on the UPR was studied *in vitro*. An important question pertaining to iminosugar treatment was to identify how the UPR was modulated by iminosugars and identify whether this change contributed to the antiviral and anti-inflammatory effects observed with iminosugars. The results reveal that iminosugars dampened the dengue-mediated activation of the IRE1α-XBP1 pathway and up-regulated ERAD genes. Iminosugars had a minimal effect on the PERK arm in the human macrophage infection model used and the iminosugar 2THO-DNJ did not require the UPR for its antiviral or its TNFα dampening effects. However, the reduction in ROS levels observed with iminosugar treatment could potentially be the link to reduction of inflammatory mediators. It would be interesting to explore this further and to identify the effects of 2THO-DNJ mediated reduction of reactive species.

8.2 Limitations

It is important to consider study limitations when interpreting the results of this thesis. The major limitation of the data presented in chapters IV, V and VII is the extent to which this *in vitro* results could be interpolated to a human clinical infection. Dengue infection is complex and in a human infection, many host and viral responses, cell-cell interactions influence the final outcome. Therefore, the results should be interpreted with caution. However, primary immune cells (dendritic cells and macrophages) provide a better cell culture model than cell lines in this context and the attempt was to use the better model for the *in vitro* studies.

The data from the iminosugar antiviral effects on primary dendritic cells provide us information on how effective these DNJ-derived drugs are in a DENV-infected dendritic cell population. comparison of the IC50 and selectivity index among these drugs give us useful information before proceeding with human studies. Although these values help us to make assumptions on the effects of these drugs in reducing viral output from infected cells, the effects might be quite different in a clinical trial and this is further affected by the individual variability seen in treated subjects and how they react to drugs. Same consideration should be given when translating the effects of iminosugars on the UPR and the reactive oxygen species. Although the effects of individual arms of the UPR need to be evaluated in vitro, crosstalk between these arms as well with other host responses might elicit different effects in drug-treated individuals.

Chapter V contain data on the effect of DENV and 2THO DNJ on the UPR. The ATF6 pathway was not evaluated during these experiments and it is possible that ATF6 pathway might have many interactions with IRE1-XBP1 and PERK arm. Therefore, it is a limitation of these experiments. In addition, some of the downstream targets were

evaluated by looking at the RNA. This was due to unavailability of antibodies to detect these proteins. It is plausible that some of these RNAs will not be translated and as such redundant. Detection of these proteins will help understand some of these cascades better. This is mostly relevant to EDEM1 and ERDJ4 transcripts as XBP1 splicing was seen to be inhibited by 2THO-DNJ treatment but enhancing the downstream EDEM1 and ERDJ4 transcripts. It would be useful to detect ERDJ4 and EDEM1 proteins in this regard.

The data from clinical samples done during the dengue outbreak in Sri Lanka has provided interesting findings to follow on. The major drawback is the low number of samples in the experiment. Getting the target sample size is always a challenge in diseases such as dengue. The number of samples collected will heavily depend on the outbreak. Increasing the sample size to detect UPR transcripts in further patient PBMCs would give valuable information. since dengue serotypes behave differently, it would be interesting to see any effects of the serotype. Current data contained 14 DENV-2 samples and 1 DENV-1 sample. Further patient PBMCs to have more of DENV-1 and other serotypes (if present during an outbreak) would be useful. And analyzing the data based on the serotype will give further information about pathogenesis. On the other hand, if such a transcript is to be used as a marker of disease severity, it is important that such a marker is useful in all 4 serotypes. Other important parameter to look at is the immune status of the individual. Performing DNEV-specific direct IgG to calculate the IgM:IgG ratio will be helpful to categorize these patients in to primary Vs secondary infection and will help understand the role of the UPR in these situations. In addition, how clinical parameters are defined can pose problems during analysis.

The proteomics analysis of the PBMC lysates have revealed interesting peptides differentially regulated in DHF and DF. Since the sample size is only 04, it is important to

validate some of these proteins by doing mass spectrometry in a larger sample and possibly in serum.

8.3 Future work

Identification of the role of the IRE1α-XBP1 arm in mediating severe dengue manifestations is of interest given the findings in our clinical cohort described in chapter 6 and the data in cultured macrophages. Our *in vitro* data is derived from infection of monocyte-derived macrophages and the effects of this UPR pathway was evaluated using the chemical inhibitor 4μ8c. However, the incomplete inhibition of this arm at non-toxic doses of 4μ8c requires a better cell culture model to evaluate and understand this pathway. Data in this thesis also showed that immortal cell lines such as THP-1 monocytic cells behave differently to primary cell models in the presence of dengue infection and that the UPR signature could be different to that observed in primary cells. Therefore, a good option would be to have a CRISPR knockout (KO) cell line in iPSCs (induced pluripotent stem cells) which could be differentiated into macrophages, hepatocytes or neural cells to investigate the effects of the UPR more comprehensively. The initial steps for this CRISPR KO work were initiated to produce PERK, IRE1α, ATF6 and XBP1 knockouts (Appendix 4).

The iPSC clones were infected with DENV-2 to identify the best clones susceptible to infection by the virus. A double nicking strategy was adopted to knockout the genes of interest using guide RNAs (gRNAs). The method of initial steps of iPSC generation is given in supplementary appendix 4. Establishment of the UPR knockouts in iPSCs would provide the first available UPR knockouts in a human cell line and it would provide a

model to investigate the effects of UPR in infections and other relevant diseases (e.g. non-alcoholic fatty liver disease, diabetes).

The findings from the patient data in this thesis open up interesting questions about dengue disease pathogenesis. Identification of a marker of disease severity in dengue infected patients is needed urgently. Therefore, the future work should involve expanding the sample size of the fieldwork presented in chapter 6 in this thesis to identify the best combination of UPR marker transcripts that could be used to identify patients with severe disease. If such a combination could be identified which has good specificity and sensitivity, this could be used to triage patients during early disease in combination with the rapid NS1 testing. In addition, follow up from the proteomics data should also lead to identification of markers in serum of dengue fever patients that could potentially serve as markers of severe dengue infection. These proteins could also expand our knowledge on the disease pathogenesis and it would be important to validate some of these identified proteins in a larger cohort of dengue disease. These future studies would provide many unanswered questions in dengue viral infections.

Appendix 1

The gBlock DNA fragments used as the standard curve for qRT-PCR reaction in measuring serum viral load:

DENV 1 (5′-3′)

GGAAAGGCAAAAGGAAGTCGTGCAATATGGTACATGTGGTTGGGAGCACGCTTT

TTAGAGTTTGAAGCCCTTGGTTTCATGAATGAAGATCATTGGTTCAGCAGAGAG

AATTCACTCAGTGGAGT

DENV 2 (5′-3′)

TTAAAGTAACACCACAGAGTTCCATTACAGAAGCAGAACTGACAGGCTATGGC

ACTGTCACGATGGAATGCTCTCCGAGAACGGGCCTCGACTTCAATGAGATGGTG

TTGCTGCAGATGGAAAAC

DENV 3 (5′-3′)

TGTCGGCATGGGACTGGACACACGCACCCAAACCTGGATGTCGGCTGAAGGAG

CTTGGAGACAAGTCGAGAAGGTAGAGACATGGGCCCTTAGGCACCCAGGGTTC

ACCATACTAGCCCTATTTCT

DENV 4 (5′-3′)

GCGAACTGTCTTCTTTGTCCTAATGATGCTGGTCGCCCCATCCTACGGAATGCGA

TGCGTAGGAGTAGGAAACAGAGACTTTGTGGAAGGAGTCTCAGGTGGAGCATG

GGTCGACCTGGTGCTAGA

Appendix 2

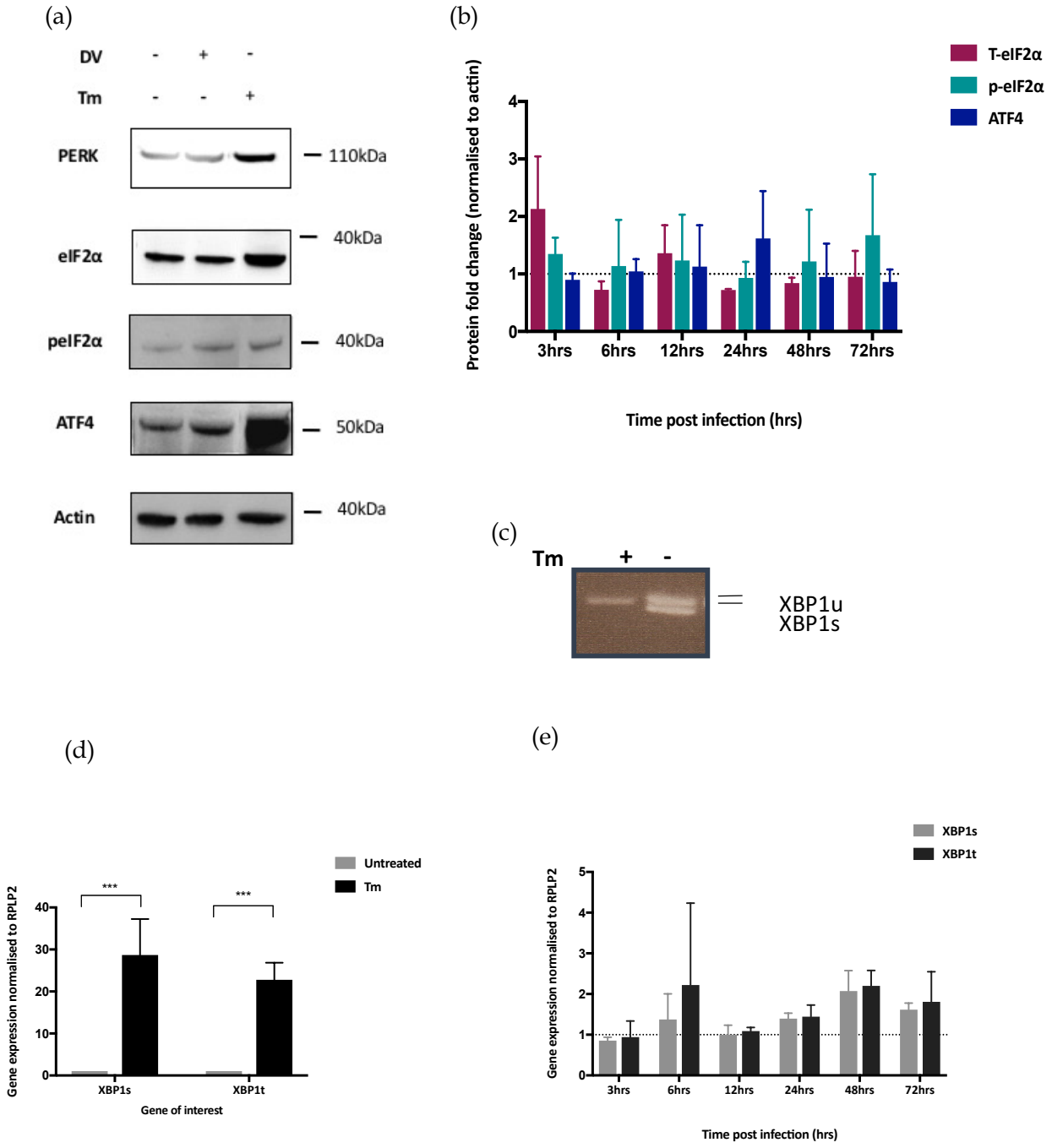

Figure S1: Activation of the PERK-eIF2α-ATF4 pathway and the XBP1 splicing in THP-1 cells. THP-1 cells were infected with DENV (MOI 5), left uninfected or treated with 1 μg/ml Tm for 6 hours. (a) Western blots were performed on cell lysates for PERK, total eIF2α (T-eIF2α, phosphorylated eIF2α (p-eIF2α) and ATF4. Actin was used as the housekeeping control. A representative blot is given. (b) Quantification of proteins in western blots by densitometry at 3, 6, 12, 24, 48 and 72 hours p.i. (n=3). (c) PCR gel image showing Tm induced splicing of XBP1. (d) qRT-PCR data showing an increase in XBP1t and XBP1s mRNA in response to Tm treatment (n=3). (e) qRT-PCR data showing the trend of XBP1t and XBP1s mRNA in DENV-infected THP-1 cells (n=3). All data are given as mean and error bars represent standard error of the mean. ****p<0.001*

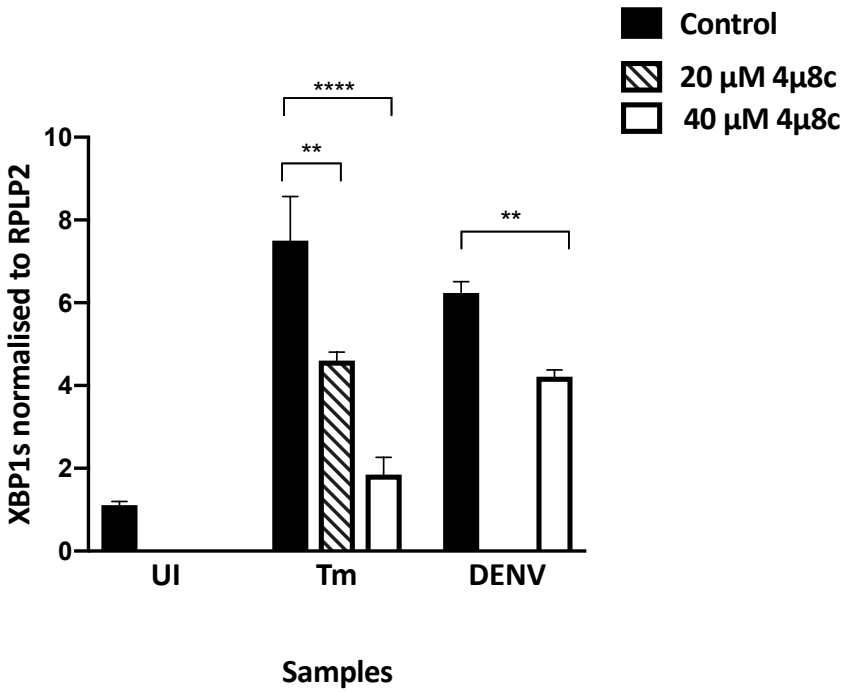

Figure S2: XBP1s levels in Tm and DENV following 4µ8c treatment. Primary macrophages were treated with 1 µg/ml Tm for 8 hours or infected with DENV at MOI 1 for 48 hours. Cells were either treated with 20 µM, 40 µM 4µ8c or left untreated. XBP1s levels were quantified by qRT-PCR and normalised to the RPLP2 housekeeping gene. Values represent mean and the error bar shows the standard deviation. ** $p<0.01$, **** $p<0.0001$

Appendix 3

Supplementary tables:

Table S1: GO processes upregulated in PBMC lysates of dengue-infected patients compared to healthy controls

GO process	Description	False detection rate (FDR)
GO:0098542	defense response to other organism	5.07E-21
GO:0002252	immune effector process	6.83E-19
GO:0060337	type I interferon signaling pathway	6.83E-19
GO:0051607	defense response to virus	2.37E-18
GO:0051707	response to other organism	5.10E-18
GO:0006952	defense response	1.80E-17
GO:0009615	response to virus	2.52E-17
GO:0051704	multi-organism process	9.40E-17
GO:0006955	immune response	5.94E-16
GO:0043901	negative regulation of multi-organism process	7.88E-16
GO:0043903	regulation of symbiosis, encompassing mutualism through parasitism	6.90E-15
GO:0002376	immune system process	5.65E-14
GO:0045071	negative regulation of viral genome replication	2.25E-13
GO:0009605	response to external stimulus	4.78E-13
GO:0048525	negative regulation of viral process	9.34E-13
GO:0043687	post-translational protein modification	1.01E-12
GO:0043900	regulation of multi-organism process	1.28E-12
GO:0006950	response to stress	8.18E-12
GO:0035455	response to interferon-alpha	1.43E-10
GO:0044419	interspecies interaction between organisms	1.52E-10
GO:0044403	symbiont process	3.13E-10
GO:0019221	cytokine-mediated signaling pathway	3.40E-10
GO:0045087	innate immune response	5.16E-10
GO:0045055	regulated exocytosis	7.00E-10
GO:0016579	protein deubiquitination	2.01E-09
GO:0034097	response to cytokine	4.02E-09
GO:0006508	proteolysis	6.11E-09
GO:0016192	vesicle-mediated transport	8.63E-09
GO:0071345	cellular response to cytokine stimulus	8.63E-09
GO:0046903	secretion	5.16E-08
GO:0030163	protein catabolic process	1.22E-07
GO:0002275	myeloid cell activation involved in immune response	1.58E-07
GO:0051603	proteolysis involved in cellular protein catabolic process	2.06E-07
GO:0035456	response to interferon-beta	6.68E-07
GO:0043312	neutrophil degranulation	7.00E-07
GO:0010033	response to organic substance	8.97E-07
GO:0050896	response to stimulus	1.00E-06
GO:0070887	cellular response to chemical stimulus	1.33E-06
GO:0042742	defense response to bacterium	1.90E-06
GO:0034341	response to interferon-gamma	1.92E-06

GO:0016032	viral process	3.11E-06
GO:0009057	macromolecule catabolic process	3.21E-06
GO:0044265	cellular macromolecule catabolic process	3.83E-06
GO:0044130	negative regulation of growth of symbiont in host	4.35E-06
GO:0001775	cell activation	6.02E-06
GO:0045321	leukocyte activation	7.28E-06
GO:0042221	response to chemical	8.05E-06
GO:0051883	killing of cells in other organism involved in symbiotic interaction	8.05E-06
GO:0031640	killing of cells of other organism	8.72E-06
GO:0070647	protein modification by small protein conjugation or removal	1.26E-05
GO:0071310	cellular response to organic substance	1.65E-05
GO:0006810	transport	2.48E-05
GO:0019941	modification-dependent protein catabolic process	2.64E-05
GO:0070944	neutrophil mediated killing of bacterium	2.95E-05
GO:0032101	regulation of response to external stimulus	3.00E-05
GO:0019538	protein metabolic process	3.18E-05
GO:0002682	regulation of immune system process	4.06E-05
GO:0060333	interferon-gamma-mediated signaling pathway	5.10E-05
GO:0007166	cell surface receptor signaling pathway	5.36E-05
GO:0002576	platelet degranulation	5.48E-05
GO:0031347	regulation of defense response	8.60E-05
GO:0048519	negative regulation of biological process	8.60E-05
GO:0019730	antimicrobial humoral response	9.39E-05
GO:0009617	response to bacterium	9.98E-05
GO:0006464	cellular protein modification process	0.00012
GO:0042535	positive regulation of tumor necrosis factor biosynthetic process	0.00015
GO:0050776	regulation of immune response	0.00015
GO:0001818	negative regulation of cytokine production	0.00016
GO:0002684	positive regulation of immune system process	0.00016
GO:0006511	ubiquitin-dependent protein catabolic process	0.00016
GO:0009987	cellular process	0.00018
GO:0035457	cellular response to interferon-alpha	0.00018
GO:0050829	defense response to Gram-negative bacterium	0.00019
GO:0042035	regulation of cytokine biosynthetic process	0.0002
GO:0098657	import into cell	0.0002
GO:1901575	organic substance catabolic process	0.0002
GO:0001817	regulation of cytokine production	0.00021
GO:0044267	cellular protein metabolic process	0.00021
GO:0019731	antibacterial humoral response	0.00024
GO:0051179	localization	0.00024
GO:0044248	cellular catabolic process	0.00026
GO:0050832	defense response to fungus	0.00027
GO:0009056	catabolic process	0.00028
GO:1901564	organonitrogen compound metabolic process	0.00028
GO:0006897	endocytosis	0.00029
GO:0051817	modification of morphology or physiology of other organism involved in symbiotic interaction	0.00029
GO:0032102	negative regulation of response to external stimulus	0.00031
GO:0046597	negative regulation of viral entry into host cell	0.00044

GO:0042108	positive regulation of cytokine biosynthetic process	0.00047
GO:0051716	cellular response to stimulus	0.00094
GO:0051851	modification by host of symbiont morphology or physiology	0.00097
GO:0002526	acute inflammatory response	0.0011
GO:0006954	inflammatory response	0.0012
GO:0034369	plasma lipoprotein particle remodeling	0.0012
GO:0080134	regulation of response to stress	0.0012
GO:0002697	regulation of immune effector process	0.0013
GO:0048878	chemical homeostasis	0.0019
GO:0001819	positive regulation of cytokine production	0.002
GO:0031348	negative regulation of defense response	0.0026
GO:0050691	regulation of defense response to virus by host	0.0031
GO:0002683	negative regulation of immune system process	0.0033
GO:0003374	dynamin family protein polymerization involved in mitochondrial fission	0.0036
GO:0060700	regulation of ribonuclease activity	0.0036
GO:0065008	regulation of biological quality	0.0038
GO:0050778	positive regulation of immune response	0.0041
GO:0015701	bicarbonate transport	0.0042
GO:0042592	homeostatic process	0.0042
GO:0050830	defense response to Gram-positive bacterium	0.0042
GO:0006953	acute-phase response	0.0043
GO:0046719	regulation by virus of viral protein levels in host cell	0.0043
GO:0051791	medium-chain fatty acid metabolic process	0.0043
GO:0002698	negative regulation of immune effector process	0.0044
GO:0032680	regulation of tumor necrosis factor production	0.0046
GO:0019885	antigen processing and presentation of endogenous peptide antigen via MHC class I	0.005
GO:0043062	extracellular structure organization	0.0057
GO:0034145	positive regulation of toll-like receptor 4 signaling pathway	0.0059
GO:0043086	negative regulation of catalytic activity	0.0065
GO:0001878	response to yeast	0.0069
GO:0045073	regulation of chemokine biosynthetic process	0.0069
GO:0050790	regulation of catalytic activity	0.0069
GO:0002831	regulation of response to biotic stimulus	0.007
GO:0045088	regulation of innate immune response	0.0075
GO:0002523	leukocyte migration involved in inflammatory response	0.0078
GO:0050777	negative regulation of immune response	0.0079
GO:0045637	regulation of myeloid cell differentiation	0.0091
GO:0051336	regulation of hydrolase activity	0.0094
GO:0052548	regulation of endopeptidase activity	0.0111
GO:0001959	regulation of cytokine-mediated signaling pathway	0.0112
GO:0007165	signal transduction	0.012
GO:0001911	negative regulation of leukocyte mediated cytotoxicity	0.0135
GO:0034375	high-density lipoprotein particle remodeling	0.0135
GO:0051246	regulation of protein metabolic process	0.0138
GO:0032642	regulation of chemokine production	0.0142
GO:0044092	negative regulation of molecular function	0.0146

GO:0000266	mitochondrial fission	0.0159
GO:0061025	membrane fusion	0.0159
GO:0051240	positive regulation of multicellular organismal process	0.016
GO:0048661	positive regulation of smooth muscle cell proliferation	0.017
GO:0051346	negative regulation of hydrolase activity	0.0172
GO:0045778	positive regulation of ossification	0.0184
GO:0098581	detection of external biotic stimulus	0.0184
GO:0007154	cell communication	0.0195
GO:0006909	phagocytosis	0.0204
GO:0030155	regulation of cell adhesion	0.0212
GO:0043032	positive regulation of macrophage activation	0.0212
GO:0050920	regulation of chemotaxis	0.0212
GO:0045639	positive regulation of myeloid cell differentiation	0.0215
GO:0016477	cell migration	0.0226
GO:0001914	regulation of T cell mediated cytotoxicity	0.0239
GO:0002479	antigen processing and presentation of exogenous peptide antigen via MHC class I, TAP-dependent	0.0239
GO:0002230	positive regulation of defense response to virus by host	0.0255
GO:0043534	blood vessel endothelial cell migration	0.0255
GO:0060334	regulation of interferon-gamma-mediated signaling pathway	0.0255
GO:0050727	regulation of inflammatory response	0.0275
GO:0008152	metabolic process	0.0299
GO:0065007	biological regulation	0.0299
GO:0045648	positive regulation of erythrocyte differentiation	0.03
GO:0061844	antimicrobial humoral immune response mediated by antimicrobial peptide	0.0333
GO:0006911	phagocytosis, engulfment	0.0335
GO:0051241	negative regulation of multicellular organismal process	0.0384
GO:0050801	ion homeostasis	0.0385
GO:0045785	positive regulation of cell adhesion	0.0406
GO:0030501	positive regulation of bone mineralization	0.0412
GO:0050728	negative regulation of inflammatory response	0.0413
GO:0061024	membrane organization	0.0437
GO:0034976	response to endoplasmic reticulum stress	0.0439
GO:0050922	negative regulation of chemotaxis	0.0444
GO:0001936	regulation of endothelial cell proliferation	0.0448
GO:0010951	negative regulation of endopeptidase activity	0.0448
GO:0051239	regulation of multicellular organismal process	0.0448
GO:0043170	macromolecule metabolic process	0.0454
GO:0001937	negative regulation of endothelial cell proliferation	0.0456
GO:0002707	negative regulation of lymphocyte mediated immunity	0.0456
GO:0007162	negative regulation of cell adhesion	0.0456
GO:0065009	regulation of molecular function	0.0456
GO:0030162	regulation of proteolysis	0.0458
GO:0071704	organic substance metabolic process	0.047
GO:0002687	positive regulation of leukocyte migration	0.0477

GO:0044238	primary metabolic process	0.0477
GO:0030003	cellular cation homeostasis	0.0483
GO:0006695	cholesterol biosynthetic process	0.0499
GO:0042116	macrophage activation	0.0499

Table S2: GO processes down-regulated in PBMC lysates of dengue-infected patients compared to healthy controls

GO Process	Description	FDR
GO:0006887	exocytosis	6.07E-07
GO:0045055	regulated exocytosis	9.51E-07
GO:0002576	platelet degranulation	5.64E-06
GO:0016192	vesicle-mediated transport	6.99E-06
GO:0001775	cell activation	0.00022
GO:0031589	cell-substrate adhesion	0.00029
GO:0007160	cell-matrix adhesion	0.0011
GO:0032879	regulation of localization	0.0011
GO:0071840	cellular component organization or biogenesis	0.0011
GO:0016043	cellular component organization	0.0022
GO:0070527	platelet aggregation	0.0038
GO:0007229	integrin-mediated signaling pathway	0.0045
GO:0048468	cell development	0.0045
GO:0065008	regulation of biological quality	0.0045
GO:0002376	immune system process	0.0056
GO:0002446	neutrophil mediated immunity	0.0078
GO:0006104	succinyl-CoA metabolic process	0.0083
GO:0034446	substrate adhesion-dependent cell spreading	0.0083
GO:0044085	cellular component biogenesis	0.0099
GO:0007159	leukocyte cell-cell adhesion	0.0134
GO:0022607	cellular component assembly	0.0139
GO:0033622	integrin activation	0.0162
GO:0098609	cell-cell adhesion	0.0162
GO:0030335	positive regulation of cell migration	0.0225
GO:0030198	extracellular matrix organization	0.0235
GO:0052803	imidazole-containing compound metabolic process	0.0235
GO:0055086	nucleobase-containing small molecule metabolic process	0.0246
GO:0017157	regulation of exocytosis	0.0248
GO:0045321	leukocyte activation	0.0248
GO:0048518	positive regulation of biological process	0.0248
GO:0043312	neutrophil degranulation	0.0249
GO:0072376	protein activation cascade	0.0258

GO:0000904	cell morphogenesis involved in differentiation	0.0262
GO:0002252	immune effector process	0.0262
GO:0051049	regulation of transport	0.0269
GO:0033627	cell adhesion mediated by integrin	0.0275
GO:0051179	localization	0.0275
GO:0043933	protein-containing complex subunit organization	0.0291
GO:0044281	small molecule metabolic process	0.0298
GO:0048522	positive regulation of cellular process	0.0303
GO:0030334	regulation of cell migration	0.0306
GO:0065003	protein-containing complex assembly	0.031
GO:0010927	cellular component assembly involved in morphogenesis	0.0333
GO:0014912	negative regulation of smooth muscle cell migration	0.0364
GO:0044283	small molecule biosynthetic process	0.0364
GO:0043648	dicarboxylic acid metabolic process	0.0367
GO:0009117	nucleotide metabolic process	0.0369
GO:0097435	supramolecular fiber organization	0.0369
GO:0051247	positive regulation of protein metabolic process	0.0383
GO:0016477	cell migration	0.0387
GO:0009888	tissue development	0.0423
GO:0048333	mesodermal cell differentiation	0.0423
GO:0048646	anatomical structure formation involved in morphogenesis	0.0423
GO:0051248	negative regulation of protein metabolic process	0.0423
GO:0072378	blood coagulation, fibrin clot formation	0.0429
GO:0001704	formation of primary germ layer	0.044
GO:0001932	regulation of protein phosphorylation	0.044
GO:0006950	response to stress	0.044
GO:0007155	cell adhesion	0.044
GO:0019752	carboxylic acid metabolic process	0.044
GO:0034113	heterotypic cell-cell adhesion	0.044
GO:0051173	positive regulation of nitrogen compound metabolic process	0.044
GO:0071375	cellular response to peptide hormone stimulus	0.044
GO:0050776	regulation of immune response	0.046
GO:0006099	tricarboxylic acid cycle	0.0482
GO:0006163	purine nucleotide metabolic process	0.0482
GO:0019221	cytokine-mediated signaling pathway	0.0482
GO:0040011	locomotion	0.0482
GO:0048660	regulation of smooth muscle cell proliferation	0.0482
GO:0051246	regulation of protein metabolic process	0.0482
GO:0051291	protein heterooligomerization	0.0482
GO:0070887	cellular response to chemical stimulus	0.0482
GO:1901564	organonitrogen compound metabolic process	0.0482

Table S3: Peptides differentially expressed (>2 fold change) in PBMC lysates of DHF patients compared to DF patients

Protein	Accession	Fold change
Q9H845	ACAD9	6.60
P13727	PRG2	5.93
P08246	ELNE	5.27
P02768	ALBU	4.92
P02768	ALBU	4.84
O60814	H2B1K	4.69
P02730	B3AT	4.32
P05164	PERM	4.25
P02730	B3AT	3.96
P0C0S8	H2A1	3.93
Q6FI13	H2A2A	3.93
P20671	H2A1D	3.93
Q16777	H2A2C	3.93
Q99878	H2A1J	3.93
Q96KK5	H2A1H	3.93
P0C0S8	H2A1	3.81
Q6FI13	H2A2A	3.81
P20671	H2A1D	3.81
Q16777	H2A2C	3.81
Q99878	H2A1J	3.81
Q96KK5	H2A1H	3.81
P00915	CAH1	3.62
P05164	PERM	3.59
P33778	H2B1B	3.52
P06899	H2B1J	3.52
P32119	PRDX2	3.31
P00915	CAH1	3.25
A0M8Q6	IGLC7	3.24
P0C0S8	H2A1	3.24
Q6FI13	H2A2A	3.24
P20671	H2A1D	3.24
Q16777	H2A2C	3.24
Q99878	H2A1J	3.24
Q96KK5	H2A1H	3.24
P05164	PERM	3.22
P02788	TRFL	3.03
P02788	TRFL	3.03
P02788	TRFL	3.01
P00491	PNPH	2.89
P02730	B3AT	2.87
P02788	TRFL	2.84
P20930	FILA	2.84
P32119	PRDX2	2.81
P05109	S10A8	2.77
P33778	H2B1B	2.74
P06899	H2B1J	2.74

Q14980	NUMA1	2.64
P32119	PRDX2	2.60
P05164	PERM	2.58
P05164	PERM	2.48
P16452	EPB42	2.46
P08311	CATG	2.37
P02730	B3AT	2.34
P0DOX5	IGG1	2.32
P02042	HBD	2.29
P11166	GTR1	2.23
P17213	BPI	2.21
O95782	AP2A1	2.21
P02788	TRFL	2.19
P05164	PERM	2.18
P57737	CORO7	2.16
P02788	TRFL	2.15
P13727	PRG2	2.15
P05164	PERM	2.15
P02788	TRFL	2.14
P01861	IGHG4	2.14
P17927	CR1	2.14
Q13228	SBP1	2.14
Q9NY33	DPP3	2.13
P20160	CAP7	2.12
Q969H8	**MYDGF**	**2.12**
Q9Y490	TLN1	2.12
P20930	FILA	2.11
P05109	S10A8	2.10
P05164	PERM	2.07
P07737	PROF1	2.04
Q6PI78	TMM65	2.03
P02675	FIBB	-2.00
P35579	MYH9	-2.01
P22626	ROA2	-2.01
P35579	MYH9	-2.01
P35579	MYH9	-2.02
Q9Y3A5	SBDS	-2.02
P05556	ITB1	-2.02
Q9Y3Z3	SAMH1	-2.03
P13796	PLSL	-2.04
Q86UX7	URP2	-2.04
P02675	samh1	-2.04
P02671	FIBA	-2.04
P18206	VINC	-2.05
P02679	FIBG	-2.05
P61006	RAB8A	-2.05
Q08043	ACTN3	-2.05
O95810	CAVN2	-2.05
Q13201	MMRN1	-2.06
O75475	PSIP1	-2.06
P02679	FIBG	-2.07
Q5JTV8	TOIP1	-2.08

P35579	MYH9	-2.09
P02679	FIBG	-2.10
O75367	H2AY	-2.11
Q96CV9	OPTN	-2.11
P02675	FIBB	-2.12
P21926	CD9	-2.13
P12931	SRC	-2.14
P02671	FIBA	-2.14
P05106	ITB3	-2.15
Q9Y490	TLN1	-2.15
P12814	ACTN1	-2.16
P00488	F13A	-2.18
P35579	MYH9	-2.18
Q6P179	ERAP2	-2.18
P02679	FIBG	-2.20
P02675	FIBB	-2.20
P07996	TSP1	-2.20
P50552	VASP	-2.21
P02671	FIBA	-2.21
P21926	CD9	-2.21
P05106	ITB3	-2.22
P21333	FLNA	-2.22
P41252	SYIC	-2.23
P02675	FIBB	-2.24
Q13201	MMRN1	-2.24
P35579	MYH9	-2.24
P05556	ITB1	-2.24
P21333	FLNA	-2.25
P16671	CD36	-2.25
P02671	FIBA	-2.26
P05106	ITB3	-2.28
P00488	F13A	-2.28
P08514	ITA2B	-2.29
Q03252	LMNB2	-2.29
P42765	THIM	-2.30
P04264	K2C1	-2.30
P08567	PLEK	-2.30
P21926	CD9	-2.31
Q9Y2A7	NCKP1	-2.38
P05106	ITB3	-2.38
Q92499	DDX1	-2.38
P05106	ITB3	-2.39
P35579	MYH9	-2.40
P48059	LIMS1	-2.40
P02675	FIBB	-2.40
P00558	PGK1	-2.40
Q8WUM4	PDC6I	-2.41
P08514	ITA2B	-2.43
P37802	TAGL2	-2.45
P02679	FIBG	-2.47
P35579	MYH9	-2.47
P02679	FIBG	-2.55

P00488	F13A	-2.55
Q9Y6G9	DC1L1	-2.56
Q9NQC3	RTN4	-2.58
P35579	MYH9	-2.62
P08514	ITA2B	-2.64
Q04917	1433F	-2.67
P05106	ITB3	-2.70
P20591	MX1	-2.71
P12931	SRC	-2.74
P06396	GELS	-2.76
Q9Y490	**TLN1**	**-2.84**
P01042	KNG1	-2.89
P04259	K2C6B	-2.96
Q16891	MIC60	-3.24
P08575	PTPRC	-3.62
Q1KMD3	HNRL2	-3.93
P12931	SRC	-4.39

Table S4: GO processes up-regulated in PBMC lysates of DHF patients compared to DF patients

GO Term	Description	FDR
GO:0042742	defense response to bacterium	4.64E-08
GO:0006959	humoral immune response	2.12E-07
GO:0019730	antimicrobial humoral response	2.12E-07
GO:0019731	antibacterial humoral response	2.12E-07
GO:0031640	killing of cells of other organism	2.12E-07
GO:0050829	defense response to Gram-negative bacterium	2.12E-07
GO:0045055	regulated exocytosis	5.39E-07
GO:0043312	neutrophil degranulation	1.95E-06
GO:0006342	chromatin silencing	2.53E-06
GO:0051883	killing of cells in other organism involved in symbiotic interaction	2.98E-06
GO:0050832	defense response to fungus	3.00E-06
GO:0070944	neutrophil mediated killing of bacterium	1.27E-05
GO:0044419	interspecies interaction between organisms	2.34E-05
GO:0016192	vesicle-mediated transport	4.00E-05
GO:0051817	modification of morphology or physiology of other organism involved in symbiotic interaction	6.43E-05
GO:0061844	antimicrobial humoral immune response mediated by antimicrobial peptide	6.43E-05
GO:0044130	negative regulation of growth of symbiont in host	9.34E-05
GO:0006325	chromatin organization	0.00011
GO:0051704	multi-organism process	0.00013
GO:0006952	defense response	0.00026
GO:0051851	modification by host of symbiont morphology or physiology	0.00026
GO:0002227	innate immune response in mucosa	0.0003
GO:0051234	establishment of localization	0.00036
GO:0006955	immune response	0.00038

GO:0044403	symbiont process	0.0005
GO:0006950	response to stress	0.00064
GO:0006810	transport	0.0009
GO:0002376	immune system process	0.0011
GO:0050830	defense response to Gram-positive bacterium	0.0011
GO:0016043	cellular component organization	0.0016
GO:0009605	response to external stimulus	0.0018
GO:0048519	negative regulation of biological process	0.003
GO:0032496	response to lipopolysaccharide	0.0041
GO:0001878	response to yeast	0.0044
GO:0045073	regulation of chemokine biosynthetic process	0.0044
GO:0002523	leukocyte migration involved in inflammatory response	0.0049
GO:0006996	organelle organization	0.005
GO:0043901	negative regulation of multi-organism process	0.0052
GO:0097006	regulation of plasma lipoprotein particle levels	0.0053
GO:0019430	removal of superoxide radicals	0.0054
GO:0048523	negative regulation of cellular process	0.0071
GO:0043903	regulation of symbiosis, encompassing mutualism through parasitism	0.0086
GO:0098869	cellular oxidant detoxification	0.0088
GO:0032717	negative regulation of interleukin-8 production	0.0099
GO:0006895	Golgi to endosome transport	0.0105
GO:0042744	hydrogen peroxide catabolic process	0.0105
GO:0042035	regulation of cytokine biosynthetic process	0.0113
GO:0001818	negative regulation of cytokine production	0.0154
GO:0034369	plasma lipoprotein particle remodeling	0.0172
GO:0032680	regulation of tumor necrosis factor production	0.0175
GO:0065007	biological regulation	0.0208

GO:0042743	hydrogen peroxide metabolic process	0.021
GO:0051240	positive regulation of multicellular organismal process	0.0238
GO:0006334	nucleosome assembly	0.0269
GO:0051235	maintenance of location	0.0343
GO:0015701	bicarbonate transport	0.0378
GO:0043062	extracellular structure organization	0.0421
GO:0065008	regulation of biological quality	0.0425
GO:0051239	regulation of multicellular organismal process	0.0431
GO:1903556	negative regulation of tumor necrosis factor superfamily cytokine production	0.0457
GO:0060071	Wnt signaling pathway, planar cell polarity pathway	0.047
GO:0010558	negative regulation of macromolecule biosynthetic process	0.0471
GO:0036498	IRE1-mediated unfolded protein response	0.0477
GO:0043933	protein-containing complex subunit organization	0.0493
GO:0050778	positive regulation of immune response	0.0493

Table S5: GO processes down-regulated in PBMC lysates of DHF patients compared to DF patients

GO process	Description	FDR
GO:0002576	platelet degranulation	1.53E-22
GO:0006887	exocytosis	9.99E-16
GO:0045055	regulated exocytosis	1.18E-15
GO:0016192	vesicle-mediated transport	5.66E-14
GO:0016043	cellular component organization	1.75E-13
GO:0051179	localization	1.93E-11
GO:0031589	cell-substrate adhesion	1.88E-10
GO:0030193	regulation of blood coagulation	2.61E-10
GO:0050878	regulation of body fluid levels	3.24E-10
GO:0051234	establishment of localization	4.08E-10
GO:1903034	regulation of response to wounding	1.49E-09
GO:0007596	blood coagulation	2.16E-09
GO:0022607	cellular component assembly	2.90E-09
GO:0007160	cell-matrix adhesion	5.22E-09
GO:0006810	transport	5.80E-09
GO:0034329	cell junction assembly	1.32E-08
GO:0034330	cell junction organization	1.39E-08
GO:0042060	wound healing	1.90E-08
GO:0065008	regulation of biological quality	2.18E-08
GO:0051130	positive regulation of cellular component organization	2.85E-08
GO:0001775	cell activation	5.42E-08
GO:0002376	immune system process	1.10E-07
GO:0030168	platelet activation	1.14E-07
GO:1903035	negative regulation of response to wounding	1.91E-07
GO:0007155	cell adhesion	2.39E-07
GO:0030029	actin filament-based process	3.81E-07
GO:0030195	negative regulation of blood coagulation	3.81E-07
GO:0030155	regulation of cell adhesion	4.50E-07
GO:0030036	actin cytoskeleton organization	7.24E-07
GO:0070527	platelet aggregation	7.94E-07
GO:0010638	positive regulation of organelle organization	1.09E-06
GO:0072378	blood coagulation, fibrin clot formation	1.09E-06
GO:0032879	regulation of localization	1.48E-06
GO:0051128	regulation of cellular component organization	1.50E-06
GO:1900026	positive regulation of substrate adhesion-dependent cell spreading	2.10E-06
GO:0010810	regulation of cell-substrate adhesion	2.17E-06
GO:0031639	plasminogen activation	2.69E-06
GO:0072376	protein activation cascade	3.00E-06

GO:0050896	response to stimulus	3.06E-06
GO:0006996	organelle organization	3.12E-06
GO:0007229	integrin-mediated signaling pathway	5.66E-06
GO:0007010	cytoskeleton organization	5.73E-06
GO:0022603	regulation of anatomical structure morphogenesis	6.23E-06
GO:0006950	response to stress	6.67E-06
GO:0065003	protein-containing complex assembly	8.32E-06
GO:0045216	cell-cell junction organization	1.44E-05
GO:0061024	membrane organization	1.48E-05
GO:0042730	fibrinolysis	1.95E-05
GO:0010811	positive regulation of cell-substrate adhesion	2.10E-05
GO:0048522	positive regulation of cellular process	2.10E-05
GO:0048584	positive regulation of response to stimulus	2.25E-05
GO:0006909	phagocytosis	2.45E-05
GO:0000904	cell morphogenesis involved in differentiation	2.51E-05
GO:0044089	positive regulation of cellular component biogenesis	2.51E-05
GO:0032102	negative regulation of response to external stimulus	2.85E-05
GO:0048585	negative regulation of response to stimulus	3.00E-05
GO:0030198	extracellular matrix organization	4.05E-05
GO:0033043	regulation of organelle organization	4.36E-05
GO:0098609	cell-cell adhesion	4.87E-05
GO:0006955	immune response	5.51E-05
GO:0048518	positive regulation of biological process	5.51E-05
GO:0010770	positive regulation of cell morphogenesis involved in differentiation	5.94E-05
GO:0034097	response to cytokine	7.11E-05
GO:0022604	regulation of cell morphogenesis	7.34E-05
GO:0032989	cellular component morphogenesis	7.63E-05
GO:0051716	cellular response to stimulus	7.63E-05
GO:1904035	regulation of epithelial cell apoptotic process	7.63E-05
GO:0032101	regulation of response to external stimulus	8.51E-05
GO:0032880	regulation of protein localization	9.43E-05
GO:0051258	protein polymerization	9.43E-05
GO:0090066	regulation of anatomical structure size	9.74E-05
GO:0031334	positive regulation of protein complex assembly	0.0001
GO:0048468	cell development	0.00014
GO:0080134	regulation of response to stress	0.00014
GO:0071345	cellular response to cytokine stimulus	0.00015
GO:0010769	regulation of cell morphogenesis involved in differentiation	0.00016
GO:0065007	biological regulation	0.00016
GO:0045785	positive regulation of cell adhesion	0.00017
GO:0006897	endocytosis	0.00018
GO:0007166	cell surface receptor signaling pathway	0.00018

GO:0008104	protein localization	0.00018
GO:0051764	actin crosslink formation	0.00018
GO:0070887	cellular response to chemical stimulus	0.00018
GO:0097435	supramolecular fiber organization	0.00018
GO:0032501	multicellular organismal process	0.00019
GO:0051704	multi-organism process	0.0002
GO:2000351	regulation of endothelial cell apoptotic process	0.0002
GO:2001233	regulation of apoptotic signaling pathway	0.0002
GO:0002253	activation of immune response	0.00021
GO:0034116	positive regulation of heterotypic cell-cell adhesion	0.00021
GO:0034622	cellular protein-containing complex assembly	0.00022
GO:0048519	negative regulation of biological process	0.00022
GO:2001237	negative regulation of extrinsic apoptotic signaling pathway	0.00022
GO:0071801	regulation of podosome assembly	0.00029
GO:0044087	regulation of cellular component biogenesis	0.00031
GO:0006952	defense response	0.00032
GO:0007165	signal transduction	0.00032
GO:0010941	regulation of cell death	0.00032
GO:0042221	response to chemical	0.00032
GO:0007015	actin filament organization	0.00033
GO:0048583	regulation of response to stimulus	0.00033
GO:0051270	regulation of cellular component movement	0.00036
GO:0031532	actin cytoskeleton reorganization	0.00039
GO:1902041	regulation of extrinsic apoptotic signaling pathway via death domain receptors	0.00039
GO:1903036	positive regulation of response to wounding	0.00041
GO:0071404	cellular response to low-density lipoprotein particle stimulus	0.00042
GO:0009967	positive regulation of signal transduction	0.00048
GO:0030335	positive regulation of cell migration	0.00048
GO:0042981	regulation of apoptotic process	0.00049
GO:2001234	negative regulation of apoptotic signaling pathway	0.00049
GO:0002252	immune effector process	0.0005
GO:0002757	immune response-activating signal transduction	0.00052
GO:0050793	regulation of developmental process	0.00052
GO:1903827	regulation of cellular protein localization	0.00055
GO:0071310	cellular response to organic substance	0.00064
GO:1903923	positive regulation of protein processing in phagocytic vesicle	0.00068
GO:0006928	movement of cell or subcellular component	0.00069
GO:0048869	cellular developmental process	0.0007
GO:0009987	cellular process	0.00079
GO:0016477	cell migration	0.00079
GO:0007162	negative regulation of cell adhesion	0.0008
GO:0002682	regulation of immune system process	0.00084

GO:0010954	positive regulation of protein processing	0.00084
GO:0022407	regulation of cell-cell adhesion	0.00084
GO:0034332	adherens junction organization	0.00084
GO:0048523	negative regulation of cellular process	0.00084
GO:0051239	regulation of multicellular organismal process	0.00084
GO:0007043	cell-cell junction assembly	0.00088
GO:0030194	positive regulation of blood coagulation	0.0009
GO:0010033	response to organic substance	0.00092
GO:0051707	response to other organism	0.00092
GO:0009888	tissue development	0.00093
GO:0045921	positive regulation of exocytosis	0.00093
GO:0009605	response to external stimulus	0.00095
GO:2000352	negative regulation of endothelial cell apoptotic process	0.001
GO:0003018	vascular process in circulatory system	0.0011
GO:0043277	apoptotic cell clearance	0.0011
GO:0002758	innate immune response-activating signal transduction	0.0012
GO:0017157	regulation of exocytosis	0.0012
GO:0030866	cortical actin cytoskeleton organization	0.0012
GO:0050776	regulation of immune response	0.0012
GO:0002224	toll-like receptor signaling pathway	0.0013
GO:0002684	positive regulation of immune system process	0.0013
GO:0006911	phagocytosis, engulfment	0.0013
GO:0010543	regulation of platelet activation	0.0013
GO:0021943	formation of radial glial scaffolds	0.0013
GO:0030154	cell differentiation	0.0013
GO:0034333	adherens junction assembly	0.0014
GO:0044419	interspecies interaction between organisms	0.0014
GO:0045907	positive regulation of vasoconstriction	0.0014
GO:0051094	positive regulation of developmental process	0.0014
GO:0051641	cellular localization	0.0014
GO:1902905	positive regulation of supramolecular fiber organization	0.0015
GO:0016032	viral process	0.0016
GO:0016479	negative regulation of transcription by RNA polymerase I	0.0017
GO:0031032	actomyosin structure organization	0.0017
GO:0050794	regulation of cellular process	0.0017
GO:1902042	negative regulation of extrinsic apoptotic signaling pathway via death domain receptors	0.0017
GO:0030334	regulation of cell migration	0.0018
GO:0098542	defense response to other organism	0.0018
GO:0051240	positive regulation of multicellular organismal process	0.0019
GO:0032502	developmental process	0.002
GO:0034446	substrate adhesion-dependent cell spreading	0.002
GO:0040011	locomotion	0.002

GO:0048856	anatomical structure development	0.002
GO:0001952	regulation of cell-matrix adhesion	0.0021
GO:0033625	positive regulation of integrin activation	0.0021
GO:0043152	induction of bacterial agglutination	0.0021
GO:0070374	positive regulation of ERK1 and ERK2 cascade	0.0021
GO:0007044	cell-substrate junction assembly	0.0022
GO:0009968	negative regulation of signal transduction	0.0022
GO:0051495	positive regulation of cytoskeleton organization	0.0023
GO:0048539	bone marrow development	0.0026
GO:0050789	regulation of biological process	0.0026
GO:0060627	regulation of vesicle-mediated transport	0.0029
GO:0032970	regulation of actin filament-based process	0.003
GO:0070613	regulation of protein processing	0.003
GO:0010035	response to inorganic substance	0.0033
GO:0019221	cytokine-mediated signaling pathway	0.0033
GO:0051017	actin filament bundle assembly	0.0033
GO:0070201	regulation of establishment of protein localization	0.0035
GO:0120036	plasma membrane bounded cell projection organization	0.0036
GO:0014891	striated muscle atrophy	0.0037
GO:0033622	integrin activation	0.0037
GO:0045184	establishment of protein localization	0.0038
GO:0050865	regulation of cell activation	0.0038
GO:0045087	innate immune response	0.0039
GO:0045088	regulation of innate immune response	0.0039
GO:0045595	regulation of cell differentiation	0.0039
GO:0045937	positive regulation of phosphate metabolic process	0.0039
GO:0031349	positive regulation of defense response	0.004
GO:0051592	response to calcium ion	0.004
GO:0097746	regulation of blood vessel diameter	0.004
GO:0110053	regulation of actin filament organization	0.004
GO:0022409	positive regulation of cell-cell adhesion	0.0041
GO:0051639	actin filament network formation	0.0041
GO:1990000	amyloid fibril formation	0.0041
GO:0008015	blood circulation	0.0043
GO:0009306	protein secretion	0.0044
GO:0009893	positive regulation of metabolic process	0.0044
GO:0051049	regulation of transport	0.0044
GO:0010634	positive regulation of epithelial cell migration	0.0045
GO:0031623	receptor internalization	0.0045
GO:0051893	regulation of focal adhesion assembly	0.0045
GO:0061564	axon development	0.0045
GO:0071803	positive regulation of podosome assembly	0.0046
GO:0090331	negative regulation of platelet aggregation	0.0046

GO:0009966	regulation of signal transduction	0.0047
GO:0045321	leukocyte activation	0.0047
GO:0051241	negative regulation of multicellular organismal process	0.0048
GO:0010646	regulation of cell communication	0.005
GO:0018149	peptide cross-linking	0.005
GO:0023051	regulation of signaling	0.0055
GO:0051127	positive regulation of actin nucleation	0.0058
GO:0051235	maintenance of location	0.006
GO:0009615	response to virus	0.0064
GO:0048534	hematopoietic or lymphoid organ development	0.0065
GO:0034613	cellular protein localization	0.0066
GO:0048010	vascular endothelial growth factor receptor signaling pathway	0.0067
GO:0051897	positive regulation of protein kinase B signaling	0.0069
GO:1902117	positive regulation of organelle assembly	0.007
GO:0051895	negative regulation of focal adhesion assembly	0.0071
GO:1902533	positive regulation of intracellular signal transduction	0.0071
GO:0008064	regulation of actin polymerization or depolymerization	0.0072
GO:1902115	regulation of organelle assembly	0.0085
GO:0032506	cytokinetic process	0.0087
GO:0033627	cell adhesion mediated by integrin	0.0087
GO:0050900	leukocyte migration	0.0089
GO:0001525	angiogenesis	0.009
GO:0002366	leukocyte activation involved in immune response	0.009
GO:0035239	tube morphogenesis	0.009
GO:0051223	regulation of protein transport	0.0094
GO:2000811	negative regulation of anoikis	0.0094
GO:0048731	system development	0.0098
GO:0090559	regulation of membrane permeability	0.0098
GO:0030220	platelet formation	0.0102
GO:0051129	negative regulation of cellular component organization	0.0102
GO:0030838	positive regulation of actin filament polymerization	0.0104
GO:0048646	anatomical structure formation involved in morphogenesis	0.011
GO:0007049	cell cycle	0.0117
GO:0034394	protein localization to cell surface	0.0119
GO:0051493	regulation of cytoskeleton organization	0.0119
GO:0009653	anatomical structure morphogenesis	0.0125
GO:0031325	positive regulation of cellular metabolic process	0.0125
GO:0043312	neutrophil degranulation	0.0127
GO:0010942	positive regulation of cell death	0.0128
GO:0043066	negative regulation of apoptotic process	0.013
GO:0032535	regulation of cellular component size	0.0135
GO:1902531	regulation of intracellular signal transduction	0.0135

GO:0008219	cell death	0.014
GO:0010256	endomembrane system organization	0.014
GO:0031347	regulation of defense response	0.014
GO:0010038	response to metal ion	0.0143
GO:0048041	focal adhesion assembly	0.0144
GO:0090277	positive regulation of peptide hormone secretion	0.0147
GO:0045185	maintenance of protein location	0.015
GO:0007409	axonogenesis	0.0151
GO:0022402	cell cycle process	0.0151
GO:1902745	positive regulation of lamellipodium organization	0.0151
GO:0043410	positive regulation of MAPK cascade	0.0153
GO:0051050	positive regulation of transport	0.0153
GO:1902532	negative regulation of intracellular signal transduction	0.0155
GO:0043534	blood vessel endothelial cell migration	0.0158
GO:0048333	mesodermal cell differentiation	0.0158
GO:0030260	entry into host cell	0.0161
GO:0003008	system process	0.0163
GO:0040007	growth	0.0163
GO:0045597	positive regulation of cell differentiation	0.0163
GO:0048729	tissue morphogenesis	0.0163
GO:0032369	negative regulation of lipid transport	0.0164
GO:0050849	negative regulation of calcium-mediated signaling	0.0164
GO:0030097	hemopoiesis	0.0166
GO:1903532	positive regulation of secretion by cell	0.0175
GO:0007275	multicellular organism development	0.0184
GO:0010743	regulation of macrophage derived foam cell differentiation	0.0184
GO:0034113	heterotypic cell-cell adhesion	0.0184
GO:0043085	positive regulation of catalytic activity	0.0191
GO:0001934	positive regulation of protein phosphorylation	0.0198
GO:0030032	lamellipodium assembly	0.0217
GO:0019220	regulation of phosphate metabolic process	0.0222
GO:0050714	positive regulation of protein secretion	0.0231
GO:1904951	positive regulation of establishment of protein localization	0.0242
GO:0048675	axon extension	0.0249
GO:1901698	response to nitrogen compound	0.0254
GO:1903522	regulation of blood circulation	0.0258
GO:0007006	mitochondrial membrane organization	0.026
GO:0007051	spindle organization	0.026
GO:0010907	positive regulation of glucose metabolic process	0.026
GO:0032570	response to progesterone	0.026
GO:0042742	defense response to bacterium	0.026
GO:0031647	regulation of protein stability	0.0261
GO:0006959	humoral immune response	0.0264

GO:0042325	regulation of phosphorylation	0.027
GO:1904037	positive regulation of epithelial cell apoptotic process	0.027
GO:0044093	positive regulation of molecular function	0.0271
GO:0120031	plasma membrane bounded cell projection assembly	0.0273
GO:0006904	vesicle docking involved in exocytosis	0.028
GO:0010604	positive regulation of macromolecule metabolic process	0.028
GO:0045124	regulation of bone resorption	0.028
GO:1905952	regulation of lipid localization	0.0285
GO:0014003	oligodendrocyte development	0.029
GO:0043065	positive regulation of apoptotic process	0.0291
GO:0048002	antigen processing and presentation of peptide antigen	0.0299
GO:0032270	positive regulation of cellular protein metabolic process	0.0301
GO:0010675	regulation of cellular carbohydrate metabolic process	0.0302
GO:0043297	apical junction assembly	0.0311
GO:0051271	negative regulation of cellular component movement	0.0317
GO:0010883	regulation of lipid storage	0.0322
GO:0012501	programmed cell death	0.0322
GO:0031648	protein destabilization	0.0322
GO:0022008	neurogenesis	0.0327
GO:0002474	antigen processing and presentation of peptide antigen via MHC class I	0.0334
GO:0008154	actin polymerization or depolymerization	0.0334
GO:0071456	cellular response to hypoxia	0.0334
GO:1901028	regulation of mitochondrial outer membrane permeabilization involved in apoptotic signaling pathway	0.0334
GO:0045765	regulation of angiogenesis	0.034
GO:0060429	epithelium development	0.034
GO:0019730	antimicrobial humoral response	0.0354
GO:0002040	sprouting angiogenesis	0.0369
GO:0010677	negative regulation of cellular carbohydrate metabolic process	0.0369
GO:0051248	negative regulation of protein metabolic process	0.0369
GO:0070555	response to interleukin-1	0.0373
GO:1903829	positive regulation of cellular protein localization	0.0373
GO:0001666	response to hypoxia	0.0375
GO:0001954	positive regulation of cell-matrix adhesion	0.0377
GO:0010821	regulation of mitochondrion organization	0.0377
GO:0035722	interleukin-12-mediated signaling pathway	0.0377
GO:0007417	central nervous system development	0.038
GO:0003012	muscle system process	0.0382
GO:0007159	leukocyte cell-cell adhesion	0.04
GO:0030834	regulation of actin filament depolymerization	0.04
GO:0051972	regulation of telomerase activity	0.04
GO:0006986	response to unfolded protein	0.0401

GO:0014070	response to organic cyclic compound	0.0401
GO:0051173	positive regulation of nitrogen compound metabolic process	0.0401
GO:0051246	regulation of protein metabolic process	0.0409
GO:0070925	organelle assembly	0.0409
GO:0072659	protein localization to plasma membrane	0.0416
GO:0051262	protein tetramerization	0.0421
GO:1903530	regulation of secretion by cell	0.0421
GO:0009719	response to endogenous stimulus	0.0426
GO:0032655	regulation of interleukin-12 production	0.0442
GO:0050867	positive regulation of cell activation	0.0442
GO:2000026	regulation of multicellular organismal development	0.0445
GO:0001932	regulation of protein phosphorylation	0.0453
GO:1905475	regulation of protein localization to membrane	0.0454
GO:0002521	leukocyte differentiation	0.046
GO:0033044	regulation of chromosome organization	0.046
GO:0019058	viral life cycle	0.0472
GO:0060348	bone development	0.0472
GO:0015031	protein transport	0.0487
GO:0061025	membrane fusion	0.0497
GO:0031324	negative regulation of cellular metabolic process	0.0498
GO:0001101	response to acid chemical	0.0499

Appendix 4

Generation of iPSC CRISPR KO cells:

The iPSC clones were infected with DENV-2 to identify the best clones susceptible to infection by the virus. The iPSCs were transfected by electroporation using an RNP delivery method. Transfected cells were subsequently screened for the gene knockout by using screening primers and sequenced to identify and confirm the gene deletion. Two strategies were adopted: Either the gRNAs were designed to have the gene deletion within an exon allowing non-homologous end joining or gene deletion was designed to span the exon-intron junction with the first gRNA in the Exon and the second gRNA in the following intron.

An example of gRNA design and gene deletion is given below for PERK (EIF2AK3) KO cells (Figure 8.1). Screening of the transfected cells revealed successful deletion of the PERK and IRE1α (ERN1) genes in the iPSCs. The ATF6 and XBP1 deletions were not successful and will be attempted by a colleague in the future.

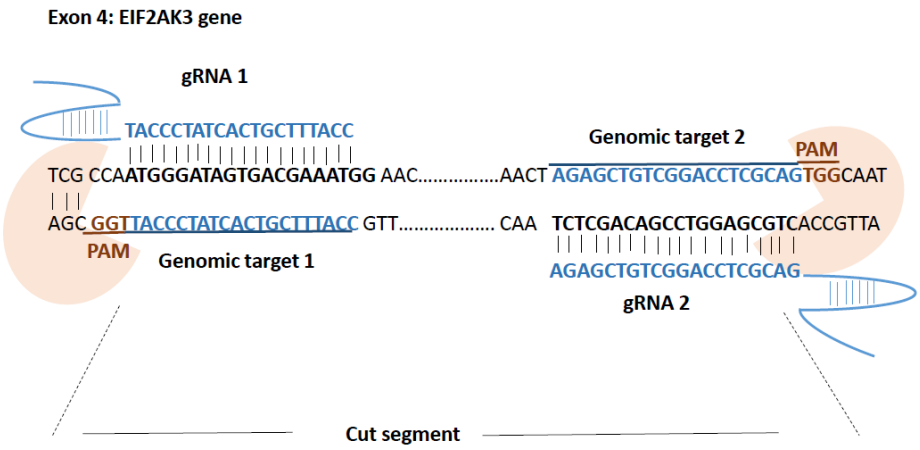

Figure 8.2: The design of gRNAs for PERK (EIF2AK3) gene deletion. Exon 4 was selected as the best site for the gene deletion. The gRNAs were designed to cut a segment of the gene using Cas-9 enzyme. A double nicking strategy was adopted.

References

1. Sayce, A.C., Alonzi D.S., Killingbeck S.S., et al. Iminosugars Inhibit Dengue Virus Production via Inhibition of ER Alpha-Glucosidases--Not Glycolipid Processing Enzymes. *PLoS Negl Trop Dis*. 2016; 10(3): doi:10. 1371/journal.pntd.0004524.

2. Sayce, A.C. Iminosugars as dengue virus therapeutics: Molecular mechanisms of action of a drug entering clinical trials. , in DPhil. University of Oxford. 2014.

3. Guzman M. G., Halstead S.B., Artsob H., et al. Dengue: a continuing global threat. *Nat Rev Microbiol*. 2010; 8(12 0): p. S7–16.

4. Bhatt, S., Gething S.W.,Brady O.J., et al. The global distribution and burden of dengue. *Nature*. 2013; 496(7446): 504-507.

5. Stanaway, J.D., Shepard A.S., Undurraga E.A.,et al., *The global burden of dengue: an analysis from the Global Burden of Disease Study 2013. Lancet Infect Dis.* 2016; 1696): 712-723.

6. Shepard, D.S., Undurraga E.A., Halasa Y.A., et al., *The global economic burden of dengue: a systematic analysis. Lancet Infect Dis*. 2016; 16: 935-41.

7. WHO. *Dengue and severe dengue*. 2018 08/04/2019]; Available from: https://www.who.int/news-room/fact-sheets/detail/dengue-and-severe-dengue.

8. Basu, A. and U.C. Chaturvedi. Vascular endothelium: the battlefield of dengue viruses. *FEMS Immunol Med Microbiol*. 2008; 53: 287-99.

9. Deen, J.A. The Dengue Vaccine Dilemma: Balancing the Individual and Population Risks and Benefits. *PLoS Med*. 2016; 13(11).

10. Meeting of the Strategic Advisory Group of Experts on immunization, April 2016-conclusions and recommendations. *Wkly Epidemiol Rec*. 2016; 27;91(21):266-84.

11. Hadinegoro, S.R., Arredondo-Garcia J.L., Capeding M.R., et al., Efficacy and Long-Term Safety of a Dengue Vaccine in Regions of Endemic Disease. *NEJM* 2015; 373:1195-206.

12. Flasche, S., Jit, M., Rodriguez-Barraquer, I.,et al. The Long-Term Safety, Public Health Impact, and Cost-Effectiveness of Routine Vaccination with a Recombinant, Live-Attenuated Dengue Vaccine (Dengvaxia): A Model Comparison Study. *PLoS Med*. 2016; 13(11): e1002181.

13. https://clinicaltrials.gov/ct2/show/NCT02747927. Accessed on 05/03/2019.

14. Paul, D. and R. Bartenschlager. Flaviviridae Replication Organelles: Oh, What a Tangled Web We Weave. *Annu. Rev. Virol*. 2015; 2: 289-310.

15. Miller, J.L., et al. The Mannose Receptor Mediates Dengue Virus Infection of Macrophages. *PLOS Pathogens*. 2008; 4(2): p. e17.

16. Cruz-Oliveira, C., Freire J.M., Conceicao T.M., et al. Receptors and routes of dengue virus entry into the host cells. *FEMS Microbiol Rev*. 2015; 39(2): 155-70.

17. Fischl, W. and R. Bartenschlager. Exploitation of cellular pathways by Dengue virus. *Curr Opin Microbiol*. 2011; 14(4): p. 470-5.

18. Jain, B., U.C. Chaturvedi, and A. Jain. Role of intracellular events in the pathogenesis of dengue; an overview. *Microb Pathog*. 2014; 69-70: p. 45-52.

19. Guzman, M.G. and E. Harris. Dengue. *Lancet*. 2015; 385: 453-65.20.

20. WHO, *Dengue haemorrhagic fever: diagnosis, treatment, prevention and control.* 1997.

21. WHO, *Dengue: guidelines for diagnosis, treatment, prevention and control.* 2009.

22. Srikiatkhachorn, A., et al., *Dengue – How Best to Classify It.* Clinical Infectious Diseases, 2011. **53**(6): p. 563-567.

23. Malavige, G.A and G.S. Ogg. Pathogenesis of vascular leak in dengue virus infection. *Immunology*. 2017; 151: 261-69.

24. Simmons, C.P., McPherson, K., Van Vinh Chau, N., et al. Recent advances in dengue pathogenesis and clinical management. *Vaccine*. 2015; 33: 7061-68.

25. Halstead, S.B. Dengue. *Lancet.* 2007; 370: 1644-52.

26. Wilder-Smith, A., Ooi, E.E., Horstick, O., et al. Dengue. *Lancet*. 2019; 393: 350-63.

27. Wang, T.T., Sewatanon, J., Memoli, M.J., et al. IgG antibodies to dengue enhanced for FcgammaRIIIA binding determine disease severity. *Science*. 2017; 355(6323): 395-98.

28. Tan, G.K. and S. Alonso. Pathogenesis and prevention of dengue virus infection: state-of-the-art. *Curr Opin Infect Dis*. 2009; 22: 302-308.

29. Rothman, A.L. Immunity to dengue virus: a tale of original antigenic sin and tropical cytokine storms. *Nat Rev Immunol*. 2011; 11(8): 532-43.

30. Rothman, A.L. T lymphocyte responses to heterologous secondary dengue virus infections. *Ann N Y Acad Sci*., 2009; 1171 Suppl 1: E36-41.

31. Rothman, A.L. Immunology and immunopathogenesis of dengue disease. *Adv Virus Res.* 2003; 60:397-419.

32. Jayathilaka, D., et al. Role of NS1 antibodies in the pathogenesis of acute secondary dengue infection. *Nat Commun*. 2018; 9(1): 5242.

33. Perera, N., J. Miller, and N. Zitzmann. The role of the unfolded protein response in dengue virus pathogenesis. *Cellular microbiology*. 2017; 19(5).

34. Jheng, J.R., J.Y. Ho, and J.T. Horng. ER stress, autophagy, and RNA viruses. Front Microbiol. 2014; 5: p. 388.

35. Diwaker, D., K.P. Mishra, and L. Ganju. Effect of modulation of unfolded protein response pathway on dengue virus infection. *Acta Biochim Biophys Sin (Shanghai).* 2015; 47(12): p. 960-8.

36. Diehl, J.A., S.Y. Fuchs, and C. Koumenis. The cell biology of the unfolded protein response. *Gastroenterology.* 2011; 141(1): p. 38-41.

37. Blázquez, A.B., et al. Stress responses in flavivirus-infected cells: activation of unfolded protein response and autophagy. *Front Microbiol*. 2014; 5: p. 266.

38. Smith, J.A. A new paradigm: innate immune sensing of viruses via the unfolded protein response. *Front Microbiol*. 2014; 5: p. 222.

39. Smith, J.A. Regulation of Cytokine Production by the Unfolded Protein Response; Implications for Infection and Autoimmunity. *Front Immunol*. 2018; 9: 422.

40. Celli, J. and R.M. Tsolis. Bacteria, the endoplasmic reticulum and the unfolded protein response: friends or foes? *Nat Rev Microbiol*. 2015; 13(2): p. 71-82.

41. Ron, D. and P. Walter. Signal integration in the endoplasmic reticulum unfolded protein response. *Nat Rev Mol Cell Biol*. 2007; 8(7): p. 519-29.

42. Shen, J., Snapp E.L., Lippincott-Scwartz J., et al. Stable Binding of ATF6 to BiP in the Endoplasmic Reticulum Stress Response. *Mol Cell Biol*. 2005; 25(3): p. 921-32.

43. Bhattacharyya, S. Can't RIDD off viruses. *Front Microbiol*. 2014; 5: p. 292.

44. Chan, S.W. Unfolded protein response in hepatitis C virus infection. *Front Microbiol*. 2014; 5: p. 233.

45. Iranpour, M., Moghadam A.R., Yazdi M., et al. Apoptosis, autophagy and unfolded protein response pathways in Arbovirus replication and pathogenesis. *Expert Rev Mol Med*. 2016; 18: p. e1.

46. Peña, J. and E. Harris. Dengue virus modulates the unfolded protein response in a time-dependent manner. *J Biol Chem*. 2011; 286(16): p. 14226-36.

47. Upton, J.P., Wang L., Han D., et al., IRE1alpha cleaves select microRNAs during ER stress to derepress translation of proapoptotic Caspase-2. *Science*. 2012; 338(6108): p. 818-22.

48. Chen, H., Yang H., Pan L., et al., The molecular mechanisms of XBP-1 gene silencing on IRE1α-TRAF2-ASK1-JNK pathways in oral squamous cell carcinoma under endoplasmic reticulum stress. *Biomedicine & Pharmacotherapy*. 2016; 77: p. 108-113.

49. Grootjans, J., KAser A., Kaufman R.J., et al., The unfolded protein response in immunity and inflammation. *Nat rev Immunol*. 2016; 16(8): 469-84.

50. Yoshida, H., Matsui T., Yamamoto A., et al., XBP1 mRNA Is Induced by ATF6 and Spliced by IRE1 in Response to ER Stress to Produce a Highly Active Transcription Factor. *Cell*. 2001; 107(7): p. 881-891.

51. Umareddy, I., Pluquet O., Wang Q.Y., et al., Dengue virus serotype infection specifies the activation of the unfolded protein response. *Virol J*. 2007; 4: p. 91.

52. Klomporn, P., Panyasrivanit M., Wikan N., et al. Dengue infection of monocytic cells activates ER stress pathways, but apoptosis is induced through both extrinsic and intrinsic pathways. *Virology*. 2011; 409(2): p. 189-97.

53. Yu, C.Y., Hsu Y.W., Liao C.L., et al. Flavivirus infection activates the XBP1 pathway of the unfolded protein response to cope with endoplasmic reticulum stress. *J Virol*. 2006; 80(23): p. 11868-80.

54. Paradkar, P.N., OOi E.E., Hanson B.J., et al. Unfolded protein response (UPR) gene expression during antibody-dependent enhanced infection of cultured monocytes correlates with dengue disease severity. *Biosci Rep*. 2011; 31(3): p. 221-30.

55. Edgil, D., C. Polacek, and E. Harris. Dengue Virus Utilizes a Novel Strategy for Translation Initiation When Cap-Dependent Translation Is Inhibited. *Journal of Virology*. 2006; 80(6): p. 2976-2986.

56. Fraser, J.E., Watanabe S., Wang C., et al. A nuclear transport inhibitor that modulates the unfolded protein response and provides in vivo protection against lethal dengue virus infection. *J Infect Dis*. 2014; 210(11): p. 1780-91.

57. Chen, T.H., Tang P., Yang C.F., et al. Antioxidant defense is one of the mechanisms by which mosquito cells survive dengue 2 viral infection. *Virology*. 2011; 410(2): p. 410-7.

58. Huang, M., Xu A., Wu X., et al. Japanese encephalitis virus induces apoptosis by the IRE1/JNK pathway of ER stress response in BHK-21 cells. *Archives of Virology*. 2016; 161(3): p. 699-703.

59. Tardif, K.D., Mori K., Kaufman R.J., et al., Hepatitis C virus suppresses the IRE1-XBP1 pathway of the unfolded protein response. *J Biol Chem*. 2004; 279(17): 17158-64.

60. Ambrose, R.L. and J.M. Mackenzie. West Nile virus differentially modulates the unfolded protein response to facilitate replication and immune evasion. *J Virol*, 2011; 85(6): p. 2723-32.

61. Saeed, M., Suzuki R., Watanabe N., et al., Role of the endoplasmic reticulum-associated degradation (ERAD) pathway in degradation of hepatitis C virus envelope proteins and production of virus particles. *The Journal of biological Chemistry* 2011; 286(43): 37264-37273.

62. Chang, T.H., Chen S.R., Yu C.Y., et al. Dengue virus serotype 2 blocks extracellular signal-regulated kinase and nuclear factor-kappaB activation to downregulate cytokine production. *PLoS one*. 2012; 7(8): e41635.

63. Valadao, A.L., R.S. Aguiar, and L.B. de Arruda. Interplay between Inflammation and Cellular Stress Triggered by Flaviviridae Viruses. *Front Microbiol*. 2016; 7: 1233.

64. Nasirudeen, A.M., Wong H.H., Thien P., et al. RIG-I, MDA5 and TLR3 synergistically play an important role in restriction of dengue virus infection. *PLoS Negl Trop Dis*. 2011; 5(1): e926.

65. Olagnier, D., Peri S., Steel C., et al. Cellular oxidative stress response controls the antiviral and apoptotic programs in dengue virus-infected dendritic cells. *PLoS Pathog*. 2014; 10(12): p. e1004566.

66. Green, A.M., Beatty P.R., Hadjilaou A., et al. Innate immunity to dengue virus infection and subversion of antiviral responses. *J Mol Biol*. 2014; 426(6): p. 1148-60.

67. Dalrymple, N.A., V. Cimica, and E.R. Mackow. Dengue Virus NS Proteins Inhibit RIG-I/MAVS Signaling by Blocking TBK1/IRF3 Phosphorylation: Dengue Virus Serotype 1 NS4A Is a Unique Interferon-Regulating Virulence Determinant. *MBio*. 2015; 6(3): e00553-15.

68. Jaiyen, Y., Masrinoul P., Kalayanarooj S., et al. Characteristics of dengue virus-infected peripheral blood mononuclear cell death that correlates with the severity of illness. *Microbiol Immunol*. 2009; 53(8): 442-50.

69. Martinon, F., Chen X., Lee A.H., et al. TLR activation of the transcription factor XBP1 regulates innate immune responses in macrophages. *Nat Immunol*. 2010; 11(5): p. 411-8.

70. Kim, S., Joe Y., Kim H.J., et al. Endoplasmic reticulum stress-induced IRE1alpha activation mediates cross-talk of GSK-3beta and XBP-1 to regulate inflammatory cytokine production. *J Imunol*. 2015; 194(9); 4498-506.

71. Walter, P. and D. Ron. The unfolded protein response: from stress pathway to homeostatic regulation. *Science*. 2011; 334(6059): p. 1081-6.

72. Lencer, W.I., SeLuca H., Grey M.J., et al. Innate immunity at mucosal surfaces: the IRE1-RIDD-RIG-I pathway. *Trends Immunol*. 2015; 36(7): 401-9.

73. Tam, A.B., Mercado E.L., Hoffmann A., et al. ER stress activates NF-kappaB by integrating functions of basal IKK activity, IRE1 and PERK. *PLoS One*. 2012; 7(10): e45078.

74. De La Cruz Hernandez, S.I., Puerta-Guardo H., Flores-Aguilar H., et al. A strong interferon response correlates with a milder dengue clinical condition. *J Clin Virol*. 2014; 60(3): 196-9.

75. Medina, F.A., Torres-Malave G., Chase A.J., et al. Differences in type I interferon signaling antagonism by dengue viruses in human and non-human primate cell lines. *PLoS Negl Trop Dis*. 2015; 9(3): e0003468.

76. Singla, M., Kar M., Sethi T., et al. Immune Response to Dengue Virus Infection in Pediatric Patients in New Delhi, India--Association of Viremia, Inflammatory Mediators and Monocytes with Disease Severity. *PLoS Negl Trop Dis*. 2016; 10(3): e0004497.

77. Borsa, M., Ferreira P.L., Petry A., et al. HIV infection and antiretroviral therapy lead to unfolded protein response activation. *Virol J*. 2015; 12: p. 77.

78. Heaton, N.S. and G. Randall. Dengue virus and autophagy. *Viruses*. 2011; 3(8): 1332-41.

79. McLean, J.E., Wudzinska A., Datan E., et al. Flavivirus NS4A-induced autophagy protects cells against death and enhances virus replication. *J Biol Chem*. 2011; 286(25): 22147-59.

80. Ke, P.-Y. and S.S.L. Chen. Autophagy: A novel guardian of HCV against innate immune response. *Autophagy*. 2011; 7(5): p. 533-535.

81. Ke, P.-Y. and S.S.L. Chen. Activation of the unfolded protein response and autophagy after hepatitis C virus infection suppresses innate antiviral immunity in vitro. *The Journal of clinical investigation*. 2011; 121(1): p. 37-56.

82. Cardier, J.E., Marino E., Romano E., et al., Proinflammatory factors present in sera from patients with acute dengue infection induce activation and apoptosis of human microvascular endothelial cells: possible role of TNF-alpha in endothelial cell damage in dengue. *Cytokine*. 2005; 30(6): 359-65.

83. Chakravarti, A. and R. Kumaria, Circulating levels of tumour necrosis factor-alpha & interferon-gamma in patients with dengue & dengue haemorrhagic fever during an outbreak. *Indian J Med Res*. 2006; 123(1): 25-30.

84. Cheng, Y.L., Lin Y.S., Chen C. L., et al. Activation of Nrf2 by the dengue virus causes an increase in CLEC5A, which enhances TNF-alpha production by mononuclear phagocytes. *Sci Rep*. 2016; 6:32000.

85. Malhotra, J.D. and R.J. Kaufman, Endoplasmic reticulum stress and oxidative stress: a vicious cycle or a double-edged sword? *Antioxid Redox Signal*. 2007; 9(12): 2277-93.

86. Soundravally, R., Sankar P., Hot S.L., et al. Oxidative stress induced changes in plasma protein can be a predictor of imminent severe dengue infection. *Acta Trop,*. 2008; 106(3): p. 156-61.

87. Soundravally, R., Hoti S.L., Patil S.A., et al. Association between proinflammatory cytokines and lipid peroxidation in patients with severe dengue disease around defervescence. *Int J Infect Dis*. 2014; 18: p. 68-72.

88. Castro, R., H.S. Pinzon, and N. Alvis-Guzman. A systematic review of observational studies on oxidative/nitrosative stress involvement in dengue pathogenesis. *Colomb Med (Cali)*. 2015; 46(3): p. 135-43.

89. Chandrasena, L.G., Peiris H., Wanigasuriya K.J., et al., Antioxidants in patients with dengue viral infection. *Southeast Asian J Trop Med Public Health*. 2014; 45(5): p. 1015-22.

90. Harijith, A., D.L. Ebenezer, and V. Natarajan. Reactive oxygen species at the crossroads of inflammasome and inflammation. *Front Physiol*. 2014; 5: p. 352.

91. Lin, Y.L., Liu C.C., Chuang J.L., et al. Involvement of oxidative stress, NF-IL-6, and RANTES expression in dengue-2-virus-infected human liver cells. *Virology*. 2000; 276(1): p. 114-26.

92. Yen, Y.T., Chen H.C., Lin Y.D., et al. Enhancement by tumor necrosis factor alpha of dengue virus-induced endothelial cell production of reactive nitrogen and oxygen species is key to hemorrhage development. *J Virol*. 2008; 82(24): 12312-24.

93. D, B. RHS Encyclopedia of Herbs and Their Uses. 2003: Dorling Kindersley.

94. Horne, G., Wilson F.X., Tinsley J., et al. Iminosugars past, present and future: medicines for tomorrow. *Drug Discov Today*. 2011; 16(3-4): 107-18.

95. Dwek, R.A., Butters T.D., Platt F.M., et al. Targeting glycosylation as a therapeutic approach. *Nat Rev Drug Discov*. 2002; 1(1): 65-75.

96. Sayce, A.C., Miller J.L. and N. Zitzmann. Targeting a host process as an antiviral approach against dengue virus. *Trends Microbiol*. 2010; 18(7): 323-30.

97. Kingma, P.J., Menheere P.P., Sels J.P.,et al. alpha-Glucosidase inhibition by miglitol in NIDDM patients. *Diabetes Care*. 1992; 15(4): 478-83.

98. Cox, T., Lachmann R., Hollak C., et al. Novel oral treatment of Gaucher's disease with N-butyldeoxynojirimycin (OGT 918) to decrease substrate biosynthesis. *Lancet.* 2000; 355(9214): 1481-5.

99. Alonzi, D.S., Scott K.A., Dwek R.A., et al. Iminosugar antivirals: the therapeutic sweet spot. *Biochem Soc Trans*. 2017; 45(2): 571-82.

100. Leach MR, Williams.D.B. Calnexin and Calreticulin, Molecular Chaperones of the Endoplasmic Reticulum. Madame Curie Bioscience Database [Internet]. Austin (TX): *Landes Bioscience*. 2000-2013.

101. Wu, S.F., Lee C.J., Liao C.L., et al. Antiviral effects of an iminosugar derivative on flavivirus infections. *J Virol*. 2002; 76(8): 3596-604.

102. Miller, J.L., Lachica R., Sayce A.C., et al. Liposome-mediated delivery of iminosugars enhances efficacy against dengue virus in vivo. *Antimicrob Agents Chemother*. 2012; 56(12): 6379-86.

103. Gu, B., Mason P., Wang L., et al. Antiviral profiles of novel iminocyclitol compounds against bovine viral diarrhea virus, West Nile virus, dengue virus and hepatitis B virus. *Antivir Chem Chemothe*r. 2007; 18(1): 49-59.

104. Mehta, A., Lu X., Block T.M., et al. Hepatitis B virus (HBV) envelope glycoproteins vary drastically in their sensitivity to glycan processing: evidence that alteration of a single N-linked glycosylation site can regulate HBV secretion. *Proc Nati Acad Sci U S A*. 1997; 94(5): 1822-7.

105. Mehta, A., Carrouee S., Conyers B., et al. Inhibition of hepatitis B virus DNA replication by imino sugars without the inhibition of the DNA polymerase: therapeutic implications. *Hepatology*. 2001; 33(6): 1488-95.

106. Qu, X., Pan X., Weidner J., et al. Inhibitors of endoplasmic reticulum alpha-glucosidases potently suppress hepatitis C virus virion assembly and release. *Antimicrob Agents Chemother*. 2011; 55(3): 1036-44.

107. Hussain, S., Miller J.L., Harvey D.J., et al., Strain-specific antiviral activity of iminosugars against human influenza A viruses. *J Antimicrob Chemother*. 2015; 70(1): 136-52.

108. Tyms A.S., Berrie, E.M., Ryder T.A., et al. Castanospermine and other plant alkaloid inhibitors of glucosidase activity block the growth of HIV. *Lancet.* 1987; 2(8566): 1025-6.

109. Warfield, K.L., Plummer E.M., Sayce A.C., et al. Inhibition of endoplasmic reticulum glucosidases is required for in vitro and in vivo dengue antiviral activity by the iminosugar UV-4. *Antiviral res*. 2016; 129:93-98.

110. Perry, S.T., Buck M.D., Plummer E.M., et al. An iminosugar with potent inhibition of dengue virus infection in vivo. *Antiviral Res*. 2013; 98(1): 35-43.

111. Low, J.G., Sung C., Wijaya L., et al., Efficacy and safety of celgosivir in patients with dengue fever (CELADEN): a phase 1b, randomised, double-blind, placebo-controlled, proof-of-concept trial. *Lancet Infect Dis*. 2014; 14(8): 706-15.

112. https://clinicaltrials.gov/ct2/show/NCT02696291. Accessed on 09/04/2019.

113. Warfield, K.L., Plummer E., Alonzi D.S., et al. A Novel Iminosugar UV-12 with Activity against the Diverse Viruses Influenza and Dengue (Novel Iminosugar Antiviral for Influenza and Dengue). *Viruses*. 2015; 7(5): 2404-27.

114. Laue, T., Emmerich P and H. Schmitz, Detection of dengue virus RNA in patients after primary or secondary dengue infection by using the TaqMan automated amplification system. *J Clin Microbiol*. 1999; 37(8): 2543-7.

115. Livak, K.J. and T.D. Schmittgen. Analysis of relative gene expression data using real-time quantitative PCR and the 2(-Delta Delta C(T)). *Methods*. 2001; 25(4): 402-8.

116. Alonzi, D.S., Neville D.C., Lachmann R.H., et al. Glucosylated free oligosaccharides are biomarkers of endoplasmic- reticulum alpha-glucosidase inhibition. *Biochem J*. 2008; 409(2): 571-80.

117. Tricou, V., Vu H.T., Quynh N.V., et al. Comparison of two dengue NS1 rapid tests for sensitivity, specificity and relationship to viraemia and antibody responses. *BMC Infect D*is. 2010; 10: 142.

118. Cheong, C., Matos I., Choi J.H., et al. Microbial stimulation fully differentiates monocytes to DC-SIGN/CD209(+) dendritic cells for immune T cell areas. *Cell.* 2010; 143(3): 416-29.

119. Nakano, H., Lin K.L., Yanagita M., et al. Blood-derived inflammatory dendritic cells in lymph nodes stimulate acute T helper type 1 immune responses. *Nat Immunol.* 2009; 10(4); 394-402.

120. Schmid, M.A. and E. Harris, Monocyte recruitment to the dermis and differentiation to dendritic cells increases the targets for dengue virus replication. *PLoS Pathog*. 2014; 10(12): 21004541.

121. Banchereau, J. and R.M. Steinman. Dendritic cells and the control of immunity. *Nature*. 1998; 392(6673): 245-52.

122. Schmid, M.A., M.S. Diamond, and E. Harris. Dendritic cells in dengue virus infection: targets of virus replication and mediators of immunity. *Front Immunol*. 2014; 5: 647.

123. Fogg, D.K., Sibon C., Miled C., et al. A clonogenic bone marrow progenitor specific for macrophages and dendritic cells. *Science*. 2006; 311(5757): 83-7.

124. Reizis, B., Bunin A., Ghosh H.S., et al. Plasmacytoid dendritic cells: recent progress and open questions. *Annu Rev Immunol*. 2011; 29: 163-83.

125. Auffray, C., Sieweke M.H., and F. Geissmann. Blood monocytes: development, heterogeneity, and relationship with dendritic cells. *Annu Rev Immunol*. 2009; 27: 669-92.

126. Randolph, G.J., Inaba K., Robbiani D.F., et al. Differentiation of phagocytic monocytes into lymph node dendritic cells in vivo. *Immunity*. 1999; 11(6): 753-61.

127. Geissmann, F., Jung S and D.R. Littman. Blood monocytes consist of two principal subsets with distinct migratory properties. *Immunity*. 2003; 19(1): 71-82.

128. Taylor, P.R. and S. Gordon. Monocyte heterogeneity and innate immunity. *Immunity*. 2003; 19(1): 2-4.

129. Santos Souza, H.F., B. da Silva Almeida, and S.B. Boscardin. Early dengue virus interactions: the role of dendritic cells during infection. *Virus Res*. 2016; 223: 88-98.

130. Flipse, J., Torres S., Diosa-Toro M., et al. Dengue tropism for macrophages and dendritic cells: the host cell effect. *J Gen Virol*. 2016; 97(7): 1531-36.

131. Boonnak, K., Slike B.M., Burgess T.H., et al. Role of dendritic cells in antibody-dependent enhancement of dengue virus infection. *J Virol*. 2008; 82(8): 3939-51.

132. Marovich, M., Grouard-Vogel G., Louder M., et al. Human dendritic cells as targets of dengue virus infection. *J Investig Dermatol Symp Proc*. 2001; 6(3): 219-24.

133. Green, S. and A. Rothman. Immunopathological mechanisms in dengue and dengue hemorrhagic fever. *Curr Opin Infect Dis*. 2006; 19(5): 429-36.

134. Srikiatkhachorn, A. and S. Green. Markers of dengue disease severity. *Curr Top Microbiol Immunol*. 2010; 338: 67-82.

135. Hober, D., Poli L., Robin B., et al. Serum levels of tumor necrosis factor-alpha (TNF-alpha), interleukin-6 (IL-6), and interleukin-1 beta (IL-1 beta) in dengue-infected patients. *Am J Trop Med Hyg*. 1993: 48(3): 324-31.

136. Kurane, I. Dengue hemorrhagic fever with special emphasis on immunopathogenesis. *Comparative Immunology, Microbiology and Infectious Diseases*. 2007; 30(5): p. 329-340.

137. Kurane, I., Rothman A.L., Livingston P.G., et al. Immunopathologic mechanisms of dengue hemorrhagic fever and dengue shock syndrome. *Arch Virol Suppl.* 1994; 9: 59-64.

138. Anderson, R., Wang S., Oslowy C., et al. Activation of endothelial cells via antibody-enhanced dengue virus infection of peripheral blood monocytes. *J Virol*. 1997; 71(6): 4226-32.

139. Ho, L.J., Wang J.J., Shaio MF., et al. Infection of human dendritic cells by dengue virus causes cell maturation and cytokine production. *J Immunol*. 2001; 166(3): 1499-506.

140. Hober, D., Delannoy A.S., Benyoucef S., et al. High levels of sTNFR p75 and TNF alpha in dengue-infected patients. *Microbiol Immunol*. 1996; 40(8): 569-73.

141. Green, S., Vaughn D.W., Kalayanarooj S., et al. Early immune activation in acute dengue illness is related to development of plasma leakage and disease severity. *J Infect Dis*. 1999; 179(4): 755-62.

142. Gagnon, S.J., Mori M., Kurane I., et al. Cytokine gene expression and protein production in peripheral blood mononuclear cells of children with acute dengue virus infections. *J Med Virol*. 2002; 67(1): 41-6.

143. Phanthanawiboon, S., Limkittikul K., DSakai Y., et al. Acute Systemic Infection with Dengue Virus Leads to Vascular Leakage and Death through Tumor Necrosis Factor-alpha and Tie2/Angiopoietin Signaling in Mice Lacking Type I and II Interferon Receptors. *PLoS One*. 2016; 11(2): e0148564.

144. Kiappes, J.L., Hill M.L., Alonzi D.S., et al. ToP-DNJ, a Selective Inhibitor of Endoplasmic Reticulum alpha-Glucosidase II Exhibiting Antiflaviviral Activity. *ACS Chem Biol*. 2018; 13(1): 60-65.

145. Mehta, A., Ouzounov S., Jordan R., et al. Imino sugars that are less toxic but more potent as antivirals, in vitro, compared with N-n-nonyl DNJ. *Antivir Chem Chemother*. 2002; 13(5): 299-304.

146. Sallusto, F. and A. Lanzavecchia. Efficient presentation of soluble antigen by cultured human dendritic cells is maintained by granulocyte/macrophage colony-stimulating factor plus interleukin 4 and downregulated by tumor necrosis factor alpha. *J Exp Med*. 1994; 179(4): 1109-18.

147. Fischer, P.B., Collin M., Karisson G.B., et al. The alpha-glucosidase inhibitor N-butyldeoxynojirimycin inhibits human immunodeficiency virus entry at the level of post-CD4 binding. *J Virol*. 1995; 69(9); 5791-7.

148. Schwarz, D.S. and M.D. Blower. The endoplasmic reticulum: structure, function and response to cellular signaling. *Cell Mol Life Sci*. 2016; 73(1): 79-94.

149.. Lee, D.Y., J. Lee, and B. Sugden. The Unfolded Protein Response and Autophagy: Herpesviruses Rule!. *J Virol*. 2009; 83(3): 1168-72.

150.. Su, A., Wang H., Li Y., et al. Opposite Roles of RNase and Kinase Activities of Inositol-Requiring Enzyme 1 (IRE1) on HSV-1 Replication. *Viruses*. 2017; 9(9): p. 235.

151. Isler, J.A., Skalet A.H. and J.C. Alwine, Human cytomegalovirus infection activates and regulates the unfolded protein response. *J Virol*. 2005; 79(1): 6890-9.

152. Kazemi, S., Papadopoulou S., Li S., et al. Control of alpha subunit of eukaryotic translation initiation factor 2 (eIF2 alpha) phosphorylation by the human papillomavirus type 18 E6 oncoprotein: implications for eIF2 alpha-dependent gene expression and cell death. *Mol Cell Biol*. 2004; 24(8): 3415-29.

153. Balakrishnan, B., Sen D., Hareendran S., et al., Activation of the cellular unfolded protein response by recombinant adeno-associated virus vectors. *PLoS One*. 2013; 8(1): p. e53845.

154. Su, H.-L., Liao C.L. and Y.L. Lin. Japanese encephalitis virus infection initiates endoplasmic reticulum stress and an unfolded protein response. *J Virol*. 2002; 76(9): p. 4162-4171.

155. Ke, P.Y. and S.S. Chen. Hepatitis C virus and cellular stress response: implications to molecular pathogenesis of liver diseases. *Viruses*. 2012; 4(10): p. 2251-90.

156. Medigeshi, G.R., Lancaster A.M., Hirsch A.J., et al. West Nile Virus Infection Activates the Unfolded Protein Response, Leading to CHOP Induction and Apoptosis. J Virol. 2007; 81(20): p. 10849.

157. Hassan, I.H.,Zhang M.S., Powers L.S., et al. Influenza A viral replication is blocked by inhibition of the inositol-requiring enzyme 1 (IRE1) stress pathway. *J Biol Chem*. 2012. 287(7): p. 4679-89.

158. Thepparit, C., Khakpoor A., Khongwichit S., et al. Dengue 2 infection of HepG2 liver cells results in endoplasmic reticulum stress and induction of multiple pathways of cell death. *BMC Res Notes*. 2013; 6: p. 372.

159. Lee, Y.R., Kuo S.H., Lin C.Y., et al. Dengue virus-induced ER stress is required for autophagy activation, viral replication, and pathogenesis both in vitro and in vivo. *Scientific Reports.* 2018; 8(1): p. 489.

160. He, B., B. Gross M and B. Roizman. The gamma134.5 protein of herpes simplex virus 1 has the structural and functional attributes of a protein phosphatase 1 regulatory subunit and is present in a high molecular weight complex with the enzyme in infected cells. *J Biol Chem*. 1998; 273(33): 20737-43.

161. Rathore, A.P., Paradkar P.N., Watanabe S., et al. Celgosivir treatment misfolds dengue virus NS1 protein, induces cellular pro-survival genes and protects against lethal challenge mouse model. *Antiviral Res*. 2011; 92(3): p. 453-60.

162. Bosshart, H. and M. Heinzelmann. THP-1 cells as a model for human monocytes. *Ann Transl Med*. 2016; 4(21): 438.

163. Tyrrell, B., Antiviral and immunomodulatory activities of iminosugars: candidate therapeutics for arbovirus infections. Thesis 2019.

164.. Woehlbier, U. and C. Hetz. Modulating stress responses by the UPRosome: a matter of life and death. *Trends Biochem Sci*. 2011; 36(6): p. 329-37.

165. Abdullah, A. and P. Ravanan. The unknown face of IRE1alpha - Beyond ER stress. *Eur J Cell Biol.* 2018; 97(5): 359-368.

166. Smith, J.A., Turner M.J., Delay M.L., et al. Endoplasmic reticulum stress and the unfolded protein response are linked to synergistic IFN-beta induction via X-box binding protein 1. *Eur J Immunol.* 2008; 38(5): 1194-203.

167. John, D.V., Y.S. Lin, and G.C. Perng. Biomarkers of severe dengue disease - a review. *J Biomed Sci*. 2015; 22: 83.

168. Bozza, F.A., Cruz O.G., Zagne S.M., et al. Multiplex cytokine profile from dengue patients: MIP-1beta and IFN-gamma as predictive factors for severity. *BMC Infect Dis*. 2008; 8: 86.

169. Malavige, G.N., Gomes L., Alles L., et al. Serum IL-10 as a marker of severe dengue infection. *BMC Infect Dis*. 2013; 13: 341.

170. Nguyen, T.H., Lei H.Y., Nguyen T.L., et al. Dengue hemorrhagic fever in infants: a study of clinical and cytokine profiles. *J Infect Dis*. 2004; 189(2): 221-32.

171. Flores-Mendoza, L.K., Estrada-Jimenez T., Sedeno-Monge V., et al. IL-10 and socs3 Are Predictive Biomarkers of Dengue Hemorrhagic Fever. *Mediators Inflamm*. 2017; 2017: 5197592.

172. Butthep, P., Chunhakan S., Yoksan S., et al. Alteration of cytokines and chemokines during febrile episodes associated with endothelial cell damage and plasma leakage in dengue hemorrhagic fever. *Pediatr Infect Dis J*. 2012; 31(12): e232-8.

173. Abhishek, K.S., Chakravarti A., Baveja C.P., et al. Association of interleukin-2, -4 and -10 with dengue severity. *Indian J Pathol Microbiol*. 2017; 60(1): 66-69.

174. Her, Z., Kam Y.W., Gan V.C., et al. Severity of Plasma Leakage Is Associated With High Levels of Interferon gamma-Inducible Protein 10, Hepatocyte Growth Factor, Matrix Metalloproteinase 2 (MMP-2), and MMP-9 During Dengue Virus Infection. *J Infect Dis*. 2017; 215(1): 42-51.

175 Yong Y.K., Tan H.Y., Jen S.H., et al. Aberrant monocyte responses predict and characterize dengue virus infection in individuals with severe disease. *J Transl Med*. 2017; 15(1): 121.

176. Arias, J., Valero N., Mosquera J., et al. Increased expression of cytokines, soluble cytokine receptors, soluble apoptosis ligand and apoptosis in dengue. *Virology*. 2014; 452-453: 42-51.

177. Fernando, A.N., MAlavige G.N., PereraK.L., et al. Polymorphisms of Transporter Associated with Antigen Presentation, Tumor Necrosis Factor-alpha and Interleukin-10 and their Implications for Protection and Susceptibility to Severe Forms of Dengue Fever in Patients in Sri Lanka. *J Glob Infect Dis*. 2015; 7(4): 157-64.

178. Pabalan, N., Chaisri S., Tabunhan S., et al. Associations of tumor necrosis factor-alpha-308 polymorphism with dengue infection: A systematic review and meta-analysis. *Acta Trop*. 2017; 173: 17-22.

179. Naing, C., Htet N.H., Siew tung W., et al. Association of tumour necrosis factor-alpha (TNF-alpha) gene polymorphisms (-308 G>A and -238 G>A) and the risk of severe dengue: A meta-analysis and trial sequential analysis. *PLoS One*. 2018; 13(10): e0205413.

180. Kumar, Y., Liang C., Bo Z., et al. Serum proteome and cytokine analysis in a longitudinal cohort of adults with primary dengue infection reveals predictive markers of DHF. *PLoS Negl. Trop Dis*. 2012; 6(11): e1887.

181. Brasier, A.R., Ju H., Garcia J., et al. A three-component biomarker panel for prediction of dengue hemorrhagic fever. *Am J Trop Med Hyg*. 2012; 86(2): 341-8.

182. Cavailler, P., Tarantola A., Leo Y.S., et al. Early diagnosis of dengue disease severity in a resource-limited Asian country. *BMC Infect Dis*. 2016; 16(1): 512.

183. Limonta, D., Torrentes-Carvalho A., Marinho C.F., et al. Apoptotic mediators in patients with severe and non-severe dengue from Brazil. *J Med Virol*. 2014; 86(8): 1437-47.

184. Simmons, C.P., Popper S., Dolocek C., et al. Patterns of host genome-wide gene transcript abundance in the peripheral blood of patients with acute dengue hemorrhagic fever. *J Infect Dis*. 2007; 195(8): 1097-107.

185. Tan, V.P.K., Ngim C.F., Lee E.Z., et al. The association between obesity and dengue virus (DENV) infection in hospitalised patients. *PLoS One*, 2018. 13(7): p. e0200698-e0200698.

186. Lee, J. and U. Ozcan. Unfolded protein response signaling and metabolic diseases. *J biol chem*. 2014; 289(3): p. 1203-1211.

187. Bortnov, V., Annis D.S., Fogerty F.J., et al. Myeloid-derived growth factor is a resident endoplasmic reticulum protein. *J Biol Chem*. 2018; 293(34): 13166-75.

188. Sunagozaka, H., Honda M., Yamshita T., et al. Identification of a secretory protein c19orf10 activated in hepatocellular carcinoma. *Int J Cancer*. 2011; 129(7): 1576-85.

189. Korf-Klingebiel, M., Reboll M.R., Klede S., et al. Myeloid-derived growth factor (C19orf10) mediates cardiac repair following myocardial infarction. *Nat Med*. 2015; 21(2): 140-9.

190. Weiler, T., Du Q., Krokhin O., et al. The identification and characterization of a novel protein, c19orf10, in the synovium. *Arthritis Res Ther*. 2007; 9(2): R30.

191. Brown, C., Morham S.G., Walsh D., et al. Focal adhesion proteins talin-1 and vinculin negatively affect paxillin phosphorylation and limit retroviral infection. *J Mol Biol*. 2011; 410(5): 761-77.

192. Mariño-Ramírez, L., KAnn M.G., Shoemaker B.A., et al. Histone structure and nucleosome stability. *Expert Rev Proteomics*. 2005; 2(5): p. 719-729.

193. Colpitts, T.M., Barthel S., Wang P., et al. Dengue virus capsid protein binds core histones and inhibits nucleosome formation in human liver cells. *PLoS One*. 2011; 6(9): p. e24365-e24365.

194. Trugilho, M.R.O., Hottz E.D., Brunoro G.V.F., et al. Platelet proteome reveals novel pathways of platelet activation and platelet-mediated immunoregulation in dengue. *PLoS Pathog*. 2017; 13(5): e1006385.

195. Mauney, C.H. and T. Hollis. SAMHD1: Recurring roles in cell cycle, viral restriction, cancer, and innate immunity. *Autoimmunity*. 2018; 51(3): p. 96-110.

196. Wan, S.W., Wu-Hsieh B.A., Lin Y.S., et al. The monocyte-macrophage-mast cell axis in dengue pathogenesis. *J Biomed Sci*. 2018; 25(1): 77.

197. Lee, J., S. Giordano, and J. Zhang. Autophagy, mitochondria and oxidative stress: cross-talk and redox signalling. *Biochem J*. 2012; 441(2): p. 523-40.

198. Berger, A., Sommer A.F., Zwarg J., et al. SAMHD1-deficient CD14+ cells from individuals with Aicardi-Goutières syndrome are highly susceptible to HIV-1 infection. *PLoS Pathog*. 2011; 7(12): p. e1002425-e1002425.

199. Antonucci, J.M., C. St. Gelais, and L. Wu. The Dynamic Interplay between HIV-1, SAMHD1, and the Innate Antiviral Response. *Frontiers in Immunology*. 2017; 8: p. 1541.

200. Chen, Z., Zhang L. and S. Ying. SAMHD1: a novel antiviral factor in intrinsic immunity. *Future Microbiol*. 2012; 7(9): 1117-26.